Studies on the synthesis of cyclic building blocks and their application in solid phase polymer synthesis

---

Inaugural-Dissertation

to obtain the academic degree

Doctor rerum naturalium (Dr. rer. nat.)

of the Faculty of Mathematics and Natural Sciences

of the Heinrich Heine University Düsseldorf

submitted by

Robert Horst Johannes Steinfort

born on 09.03.1995 in Bonn

Düsseldorf, May 2023

From the Institute of Organic Chemistry and Macromolecular Chemistry at the Heinrich Heine University Düsseldorf

Published by permission of the

Faculty of Mathematics and Natural Sciences

Heinrich Heine University Düsseldorf

Supervisor: Prof. Dr. Laura Hartmann

Co-supervisor: Prof. Dr. Thomas J. J. Müller

Date of oral examination: 25.10.2023

This thesis was accomplished in the period between October 2019 and March 2023 in the Institute of Organic Chemistry and Macromolecular Chemistry at the Heinrich Heine University in Düsseldorf under supervision of Prof. Dr. Laura Hartmann.

I, Robert Steinfort, hereby declare that the thesis submitted is my own work without making use of impermissible aids, considering the “Rules on the Principles for Safeguarding Good Scientific Practice at Heinrich Heine University Düsseldorf”. All direct or indirect sources used are acknowledged in the bibliography as references. I further declare that I have not submitted this nor a similar thesis at any other examination board in order to obtain a degree.

Düsseldorf,

_____

Robert Steinfort

"Success is not final, failure is not fatal:

it is the courage to continue that counts."

Winston Churchill

Table of Contents:

Publications

Publications that are included in this thesis

Hill, S. A., Steinfort, R., Mücke, S., Reifenberger, J., Sengpiel, T., Hartmann, L., **"Exploring Cyclic Sulfamidate Building Blocks for the Synthesis of Sequence-Defined Macromolecules"** *Macromol. Rapid Commun.*, **2021**, 2100193.

Contribution: First synthesis of building block 1. Coupling experiments with this building block to the solid phase. Synthesis of oligomers 6 and 19. Experiments for linear and branched growth with building block 19. Experiments for coupling building block 1 to the solid phase with different coupling reagents. Experiments for the latent and active strategies. Analytical sample preparation (IR, EA, NMR, LC-MS). Analysis and evaluation of the structures. Work carried out by Sandra Mücke and Josefine Reifenberger under the supervision of Robert Steinfort: Optimization of the synthesis of building block 1. Coupling reactions with building block 1 to the solid phase. Coupling experiments for linear and branched growth with building blocks 1 and 16.

Dr. Stephen Andrew Hill and Robert Steinfort contributed equally to this work.

Steinfort, R., Hill, S. A., Capar, Ö., Hartmann, L., **"Cyclic carbonates as protection group free building blocks in solid phase synthesis of sequence-defined macromolecules"** *paper draft*, **2023**

Contribution: Robert Steinfort: Synthesis of all structures and their analysis. Optimization of the coupling conditions. Collaborative writing of the first paper draft. Collaborative writing of the manuscript.

Other Publications not included in this thesis

Hill, S. A., Steinfort, R., Hartmann, L., **"Progress, challenges and future directions of heterocycles as building blocks in iterative methodologies towards sequence-defined oligomers and polymers"** *Polym. Chem*., **2021**, 10.1039/d1py00425e

Abstract

Nature provides us with a large number of complex macromolecules with highly specific properties and functions, such as deoxyribonucleic acids (DNA) or proteins. In comparison, synthetic macromolecules or polymers are often much less complex and their properties and functions simpler. Nevertheless, synthetic macromolecules play an important role in our everyday life and through advanced synthetic methods such as controlled polymerization more complex synthetic polymers, e.g., multiblock copolymers, have become available. Indeed, the increase in structural complexity has enabled more advanced properties and functions, e.g., of synthetic macromolecules in biomedicine or catalysis. One limitation that remains with polymer synthesis is the control over the dispersity where most polymers are isolated only as mixtures of macromolecules of different chain lengths. An alternative synthetic strategy that has been successfully used to derive both, biological and synthetic macromolecules with absolute control over their chain length and thus dispersity, is the solid phase synthesis. For example, in solid phase peptide synthesis, amino acids carrying protecting groups are successively coupled to a solid-phase resin, thus building up oligomeric structures. After each coupling step, the protecting group is removed, and only then a new building block can be coupled ensuring both, sequence control and monodispersity. Alternatively, synthetic strategies without the use of protecting groups or so-called submonomer approaches have been developed, especially for the solid phase synthesis of non-natural macromolecules such as oligo(amidoamines) e.g., by alternating coupling of diacid and diamine building blocks. In principle, this represents a more atom-efficient approach and potentially allows for an easier upscaling of the synthesis. In recent years, cyclic building blocks have gained increasing attention in this context.

In this thesis, three groups of cyclic building blocks and their possible applications and coupling conditions in solid phase synthesis are studied: a) cyclic sulfamidates which can be coupled either actively with linear or branched chain growth or latently to the solid phase and introduce sulfate groups into the oligomer b) cyclic carbonates which upon ring opening lead to oligohydroxyurethanes in the main chain c) cyclic amines which by ring opening with chloroformates lead to *N*-substituted amide linkages in the oligomer backbone. The coupling reactions of the three groups of building blocks to the solid phase are shown schematically in Figure 1.

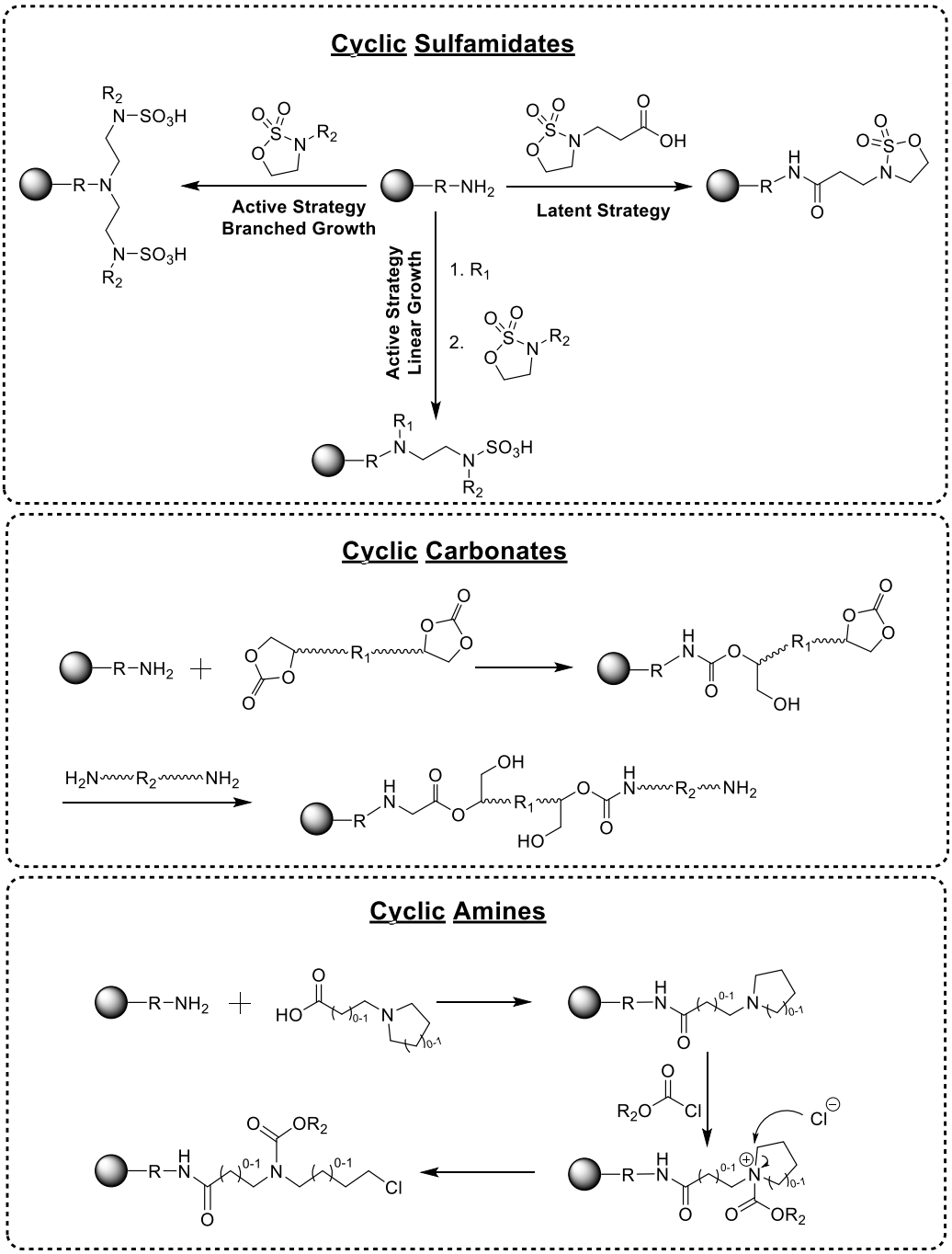

Figure 1: Schematic illustration of the coupling of the three cyclic building block groups to the solid phase investigated for this thesis.

In the first part of this thesis, cyclic sulfamidate building blocks were investigated for their use as building blocks in solid phase synthesis. For this purpose, cyclic sulfamidate building blocks were synthesized which carry the cyclic sulfamidate on one side and a carboxy functionality on the other side of the molecule. Then, two strategies were investigated to couple the building blocks to the solid phase. In the so-called latent strategy, the building blocks are coupled to the solid phase with the carboxy functionality. In the active strategy, the cyclic ring is coupled directly to the oligomer. Since on the solid phase resin the functional end group is

a primary amine, it is able to open two ring building blocks and branched oligomers are formed. If the amine of the solid phase is first reacted with a building block that carries a secondary amine as a functional end group, this also enables the linear structure of oligomers. Thus, sulfate groups were introduced into the side chains of the oligomer.

In the second part of this thesis, the conditions for the coupling of cyclic carbonate building blocks to the solid phase were investigated. For this purpose, a biscyclocarbonate was used which was coupled to the solid phase with one ring in the first step. Coupling was optimized by addition of a lithium triflate/triazabicyclodecen catalyst system, elevated reaction temperature, increased coupling time and equivalents of building blocks used. Subsequently, the second ring was opened with hexamethylenediamine, and the coupling conditions were also optimized for this step. For the further construction of the oligomer, it was crucial to reduce the intra- and intermolecular interactions of the growing oligomer chains on the resin as this drastically reduces coupling efficiency. Therefore, the resulting urethane units, which form upon ring opening, were spaced further apart by adding ethylene glycol spacer units employing previously developed building blocks from the Hartmann lab and the hydroxy groups were capped after each ring opening step. Thus, oligomers with oligohydroxyurethane groups in the backbone were constructed. As another group of cyclic carbonate building blocks, glycerol carbonate-based building blocks were also synthesized and coupled to the solid phase. Different building blocks were synthesized with the cyclic carbonate motif on one side and a carboxy functionality on the other side of the molecule. These building blocks were then coupled to the solid phase and investigated for the formation of oligomeric structures. Although the building blocks were successfully coupled to the solid phase once, they could not be repeatedly incorporated into an oligomer.

In the third and final part of the thesis, cyclic amines were investigated as potential building blocks in solid phase synthesis. For this purpose, cyclic amine building blocks were synthesized which vary in their ring size and in the chain length between the ring and the carboxy functionality in order to investigate the influence of the structure of the building block on the ring opening. The four building blocks prepared were coupled to the solid phase, with the five membered building blocks showing the highest coupling conversions. Subsequently, various chloroformates and acid chlorides were investigated for their ability to open the cyclic amine ring. The best results were achieved with fluorenylmethyloxycarbonyl chloride (Fmoc-Cl), and

this allowed *N*-substituted amide linkages to be introduced into the oligomer backbone. Upon subsequent cleavage of the Fmoc protecting group, intramolecular ring closure was observed, preventing further assembly of the oligomer. Therefore, attempts were made to substitute the terminal chloride by a nucleophile and thus further build up the oligomer. However, these experiments also led to the cleavage of the Fmoc group and thus to a ring closure and no further extension of the chain.

In summary, in this thesis various cyclic building blocks were investigated for their use in solid phase polymer synthesis. The synthesis and subsequent coupling of the building blocks was successful, allowing various functional groups to be introduced into the oligomers. Subsequent attempts to open the cyclic rings on the solid phase were also mostly successful, allowing for chain extension. The greatest challenge was the repeated incorporation of multiple building blocks into oligomers. Further reaction optimization and adaptation of the building blocks themselves will be required in the future to allow for building up oligomers of multiple repeating units from the presented cyclic building blocks.

1 General Introduction

Sequence-defined macromolecules are a class of molecules that play a significant role in biological systems.[1] For example, DNA and ribonucleic acids (RNA) are polymers whose structure enables genetic information to be stored, replicated, and translated into the synthesis of proteins in natural systems.[2] Proteins represent another biologically important class of sequence-defined macromolecules.[3,4]

The synthesis of non-natural macromolecules with well-defined structures is a topic that is currently being explored by many research groups.[1,5] Early approaches in this field focused on sequencing controlled free radical polymerizations to synthesize polymers with controlled low dispersity. In contrast, more recent approaches often resort to iterative synthesis methods, since only in this case monodisperse and sequence-defined macromolecules can be obtained.[1,6,7] Often, the exact position of a functional unit correlates with a specific function of the molecule. Therefore, in order to develop sequence-defined macromolecules for targeted applications, it is critical to be able to precisely control the assembly and structure of the sequence-defined target molecules.[4]

As it stands today, solid phase synthesis is an established method and often the method of choice to ensure sequence-defined monomer sequence of macromolecules.[4,8]

1.1 Solid phase synthesis of non-natural macromolecules

The principle of solid phase synthesis (SPS) was investigated and established by Merrifield in 1963.[9] The development of peptide synthesis at the solid phase was primarily aimed at achieving monodisperse and sequence-defined oligopeptides from single selected amino acids.[9] Nowadays, solid phase synthesis is standardly used for the synthesis of various biomacromolecules such as the peptides and oligonucleotides as well as oligosaccharides.[10,11]

The approach of solid phase synthesis offers many advantages that make this method interesting for the synthesis of other, non-natural substance groups.[12] For example, the Hartmann group developed the synthesis of sequence-defined oligo(amidoamines) as synthetic scaffolds for the presentation of carbohydrates or other selected molecular building blocks.[11,13,14] The synthesis of oligomeric structures using solid-phase resins has been addressed by many research groups,[15] each of which has published standard protocols for the individual reaction steps depending on the substance groups to be synthesized. The coupling steps have been appropriately designed and optimized for each system so that high conversions are achieved.[11] Compared with equivalent methods, reaction times are short and by-products hardly occur.

The workup of each coupling step is simple compared to reactions in solution, as their procedure is technically easier to apply.[4] In SPS, the building blocks bind to polymeric resin beads, while all other reaction components remain in the solvent, so filtration can be used as a separation and washing method. For this purpose, the solid phase beads are washed several times with a solvent to remove all by-products as well as excess reaction components.[16] Recently, Hartmann et al. presented a method for the recovery of the excess building blocks.[17] The growing chain remains on the solid phase resin, which can be separated from by-products and unreacted reagents during filtration. The solid phase resin is then washed with a solvent.[16]

Depending on the desired application, different resins can be used as solid phase materials for solid phase synthesis.[18] The Hartmann working group frequently uses TentaGel® resins,[19] which are hybrid resins consisting of a polystyrene component linked with chain-terminated

polyethylene glycol (PEG). In the example of TentaGel® S RAM, chemically protected amino groups form the functional end groups of the resin surface, linked by a rink amide linker.[16,20]

The building blocks or amino acids are first coupled to the resin during solid phase synthesis. In the first step, an amide bond is formed between the carboxy functionality of the building block and the amino group of the resin with activation reagents.[16] In the subsequent steps, the desired building block sequence is extended toward the *N*-terminus. The building blocks to be used carry a protection group at the *N*-terminus to prevent side and subsequent reactions.[16] Protecting groups are often used to selectively block reactive functional groups on the growing peptide chain. Protecting group strategies are an essential synthetic tool in classical solid-phase synthesis.[21] With the appropriate selection of protecting group strategies for a given molecule, it is possible to synthesize sequence-defined macromolecules with high yields and purities.[22] Several protection groups are presented in the following.

The Fmoc protection group is one of the most widely used protecting groups in solid-phase peptide synthesis.[23] Here the *N*-terminal amino acid is protected with an Fmoc group. The Fmoc group can be selectively cleaved under basic conditions.[23] Cleavage of the Fmoc group can be achieved by the addition of a 20 - 25 vol.-% piperidine in DMF solution to the oligomer bound to the resin.[24] Various coupling reagents can be utilized in combination with the Fmoc protecting group, allowing to synthesize peptides up to over a hundred amino acids in a sequence-defined assembly.[25]

The *tert*-butyloxycarbonyl (Boc) protection group is another commonly used protecting group in solid-phase peptide synthesis.[26] Here the *N*-terminal amino acid is protected with a Boc group, which can be selectively cleaved under acidic conditions.[27] Due to this acidic cleavage conditions the Boc group can be cleaved orthogonally to the Fmoc group, which contributes to the selective protection of certain functionalities in the assembly of oligomeric structures.[28,29] Commonly, the Boc protecting group is used for the synthesis of hydrophobic peptides and peptides containing ester and thioester moieties.[26]

The allyloxycarbonyl (Alloc) protecting group is also used in solid-phase synthesis. Typically functional groups such as alcohols or amines are protected with an Alloc group, which can be selectively cleaved with a palladium catalyst.[30] Due to these cleavage conditions, the Alloc protecting group is stable under the basic conditions of the Fmoc protecting group as well as

the acidic conditions of the Boc protecting group, which makes it an interesting protecting group for the construction of sequence-defined oligomers.[31]

The last protecting group presented here is the benzyl (Bzl) protecting group, which is also used in solid-phase synthesis. Typically hydroxyl groups are protected with Bzl groups, which can be selectively cleaved under strong acidic conditions, e. g. with hydrofluoric acid at 25 °C.[32] An example where the benzyl protecting group was used is in the synthesis of the hormone oxytocin in 1954 which was the first example of a polypeptide hormone synthesis.[33,34] This contributed to Vincent du Vigneaud receiving the Nobel Prize in Chemistry in 1955.[33,35]

The terminal protecting group must be removed before each new coupling step of a building block. In order to couple the building blocks with their carboxy functionality to the amine of the solid phase resin or the terminal building block, different activation and coupling reagents are used. Benzotriazol-1-yl-oxytripyrrolidinophosphonium hexafluorophosphate (PyBOP) and N,N'-diisopropylethylamine (DIPEA) are frequently used in this process.[36] Both the building blocks and the coupling reagents are used in excess to ensure high conversions.[4] The mechanism of carboxylic acid activation by PyBOP and DIPEA is shown in Figure 1.

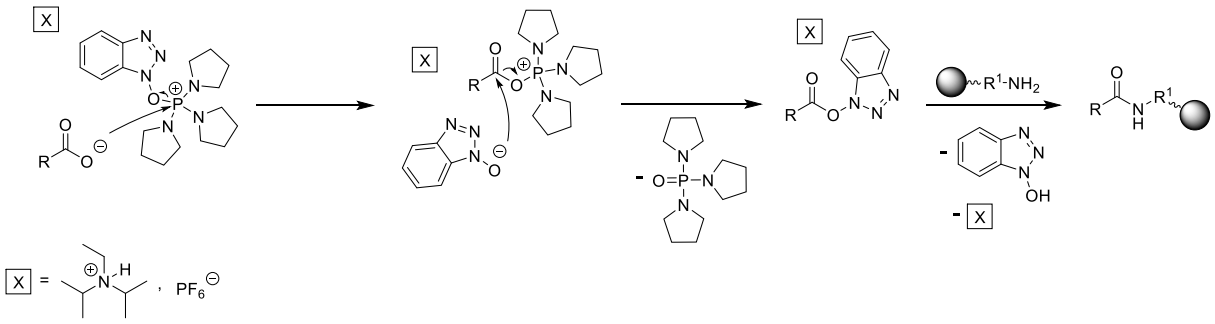

Figure 2: Mechanism of activation of coupling reaction of carboxylic acids with amines by using PyBOP as coupling reagent and DIPEA as base.[36]

The carboxy group of the building block is deprotonated by the base DIPEA. Subsequently, the carboxylate reacts with PyBOP to form a deprotonated form of *N*-hydroxy benzotriazole (OBt^-) and an activated acyl phosphonium species. In the next step, the deprotonated *N*-hydroxy benzotriazole reacts with the acyl phosphonium species and the activated benzotriazole ester of the building block is formed. The driving force of the reaction is the formation of the phosphonium oxide. In the final step, the amide bond is formed as the free amine of the chain end of the resin reacts with the active ester.[37]

In addition to PyBOP and DIPEA, other coupling reagents can also be used to enable the sequence-defined coupling of building blocks to the growing peptide chain. Several coupling reagents are presented in the following. Carbodiimides such as N,N'-Dicyclohexylcarbodiimide (DCC) and 1-Ethyl-3-(3-dimethylaminopropyl)carbodiimide (EDC) are used to activate the carboxy functionality of the amino acid, which then reacts with the amine functionality of the terminal building block on the solid phase resin to form a peptide bond.[38] DCC is often used when a Boc/benzyl strategy is chosen for solid phase coupling.[38] When Fmoc/t-Bu strategies are used, N,N'-Diisopropylcarbodiimide (DIC) is often chosen as a coupling reagent and works in a similar way like DCC. 2-(1H-Benzotriazole-1-yl)-1,1,3,3-tetramethylaminium tetrafluoroborate (TBTU) and Hydroxybenzotriazole (HOBt),[39] as well as (1-cyano-2-ethoxy-2-oxoethylideneaminooxy)dimethylamino-morpholino-carbenium hexafluorophosphate (COMU) and HOBt, are also popular coupling reagent combinations in solid phase synthesis.[40] Various factors influence the choice of coupling reagents such as the length of the peptide chain, the nature of the building block and the desired yield and purity of the final oligomer.[41]

After the building block sequence is fully coupled to the resin, the oligomer is cleaved from the resin (in the case of TentaGel® S RAM) using trifluoroacetic acid (TFA) and triisopropylsilane (TIPS) in dichloromethane (DCM).[4] The mechanism of solid phase synthesis using the Fmoc protection group is summarized in Figure 2.

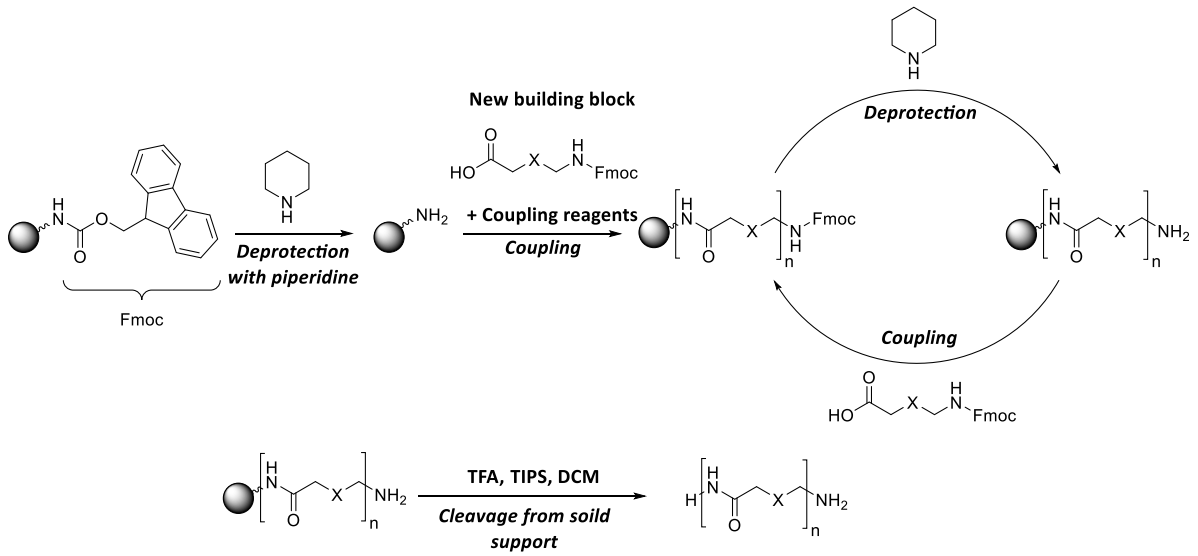

Figure 3: Schema of solid phase synthesis using the Fmoc protection group.[4]

Solid-phase synthesis has been steadily extended by various research groups since its discovery to be applied to natural polymers such as polynucleotides,[42] polypeptides[29,43] and

polysaccharides.[44] The research group Hartmann is working on transferring the solid phase synthesis to oligo(amidoamines).[45] These oligo(amidoamines) are characterized by different properties, such as defined sequences, defined distances between glycosylated residues and monodispersity.[4] Hartmann's working group uses both protected and functionalized amino acids for this purpose, as well as building blocks with diverse properties that have been specially adapted for this purpose. By incorporating these building blocks, success has been achieved in the synthesis of precision glycomacromolecules.[7,46]

Hartmann's working group uses different acyclic building blocks that can be divided into two groups.[11,17,47–50] One is the functional building blocks and the other is the spacer building blocks. A selection of building blocks used in the Hartmann group is shown in Figure 4.

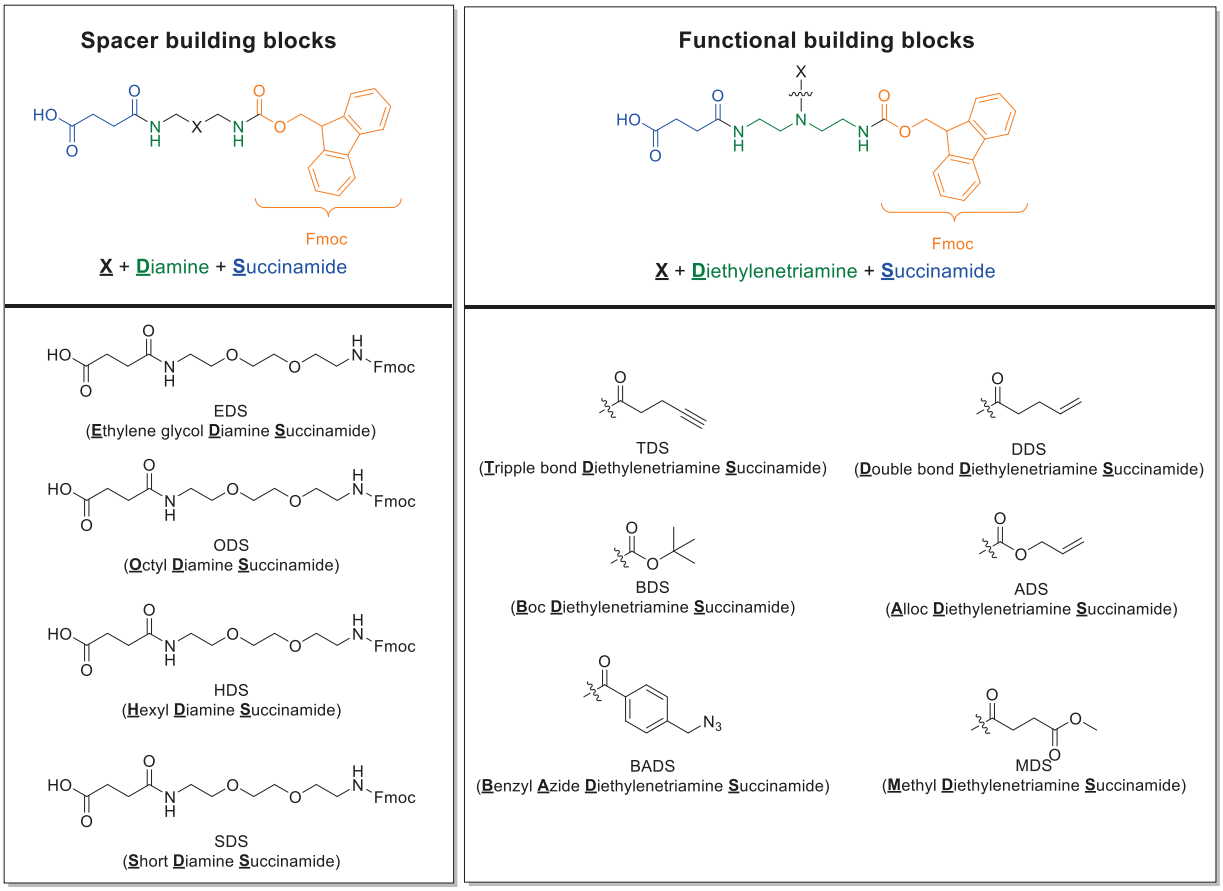

Figure 4: Overview of spacer and functional building blocks used in the Hartmann group.[11,17,47–50]

Spacer building blocks differ in how long the building blocks are and whether they insert polar or non-polar components into the main chain. The functional building blocks allow ligands to be incorporated into the side chain and made usable via functional groups.[4] Two building blocks commonly used in Hartmann's group are EDS and TDS.[11] The EDS building block (Ethylene glycol Diamine Succinamide) is based on the biocompatible ethylene glycol

diamine.[50] The building block is a hydrophilic spacer between different building blocks, which also influences the flexibility and polarity of the oligo(amidoamines). The TDS building block (Triple-bond Diethylenetriamine Succinamide) carries, in addition to the Fmoc-protected amino and the carboxy functionality, a terminal alkyne in the side chain, which can be used for copper-catalyzed azide-alkyne cycloadditions (CuAAC).[50] The TDS building block is also a hydrophilic spacer between different building blocks.

In addition to the acyclic building blocks presented here, cyclic building blocks have also been introduced to solid phase synthesis. These will be discussed in chapter 1.3.

1.2 Submonomer solid phase polymer synthesis

Solid-phase synthesis as presented in chapter 1.1 has certain disadvantages, such as the use of protection groups, the use of coupling reagents and incomplete coupling reactions.[51] To overcome these downsides, a new approach known as submonomer solid-phase synthesis has been developed, which is another method to prepare sequence-defined monodisperse oligomers. This method follows an AB + CD strategy, which involves the coupling of two submonomers, AB and CD, to form sequence-defined macromolecules.[4] The strategy can be used to bypass the use of activated carboxy functionalities, which can lead to more efficient and higher-yielding reactions. An example for the use of an AB + CD strategy is discussed later.

Submonomer solid phase synthesis was first introduced by Zuckermann *et al.* in 1992.[52] The method was used to synthesize the substance class of peptoids (*N*-substituted glycines). The concept was further developed by Zuckermann and other research groups.[1,52,53] In comparison to solid phase synthesis established by Merrifield[9], building blocks are used that do not have to carry protective groups. Working without protecting groups is an atomically more efficient approach, which potentially makes it easier to scale up the synthesis.[1,52] The general reaction scheme is shown in Figure 5.

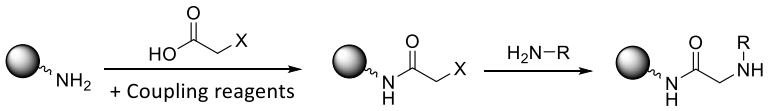

Figure 5: Solid-phase assembly of an N-substituted glycine from two submonomers (X= halogen).[52]

Each addition of a repeating unit consists of two individual steps. The first step is an acetylation, the second a nucleophilic substitution. In both steps, no deprotections have to be carried out, since no protecting group strategy is required due to the orthogonality granted, which is an essential difference to the solid phase synthesis established by Merrifield. Only reactive side chains of the amine need to be protected. The submonomer solid-phase synthesis can be automated and generates the desired functionalized peptoids in high yields and purities.[52,54]

In the first step the acetylation, an amine attached to the resin is reacted with a β-halide carboxylic acid. For example, diisopropylcarbodiimide or other substances capable of activating carboxylates are used as coupling reagents. In the second step, nucleophilic

substitution of the halogen by an excess of primary amines introduces the side chain with a residue. It is possible to use a variety of different primary amines. The group formed by this reaction is called peptoid. This class of substances does not occur in natural form, but can be produced synthetically by this process.[52,54] Peptoids are an important class of biomimetic oligomers that have had a significant impact on the fields of combinatorial drug discovery,[55] gene therapy,[56] drug delivery[57] and biopolymer folding[58] in recent years. Sequence-specific peptoid oligomers are readily prepared from primary amines, via a solid-phase submonomer process[52,54,59].

An application example was presented by the Lutz lab, where an AB + CD approach was used to synthesize eight sequence-defined macromolecules.[60] First, two building blocks were synthesized in which the AB building block carries an acid/alkyne functionality and the CD spacer building block carries an amine/azide functionality. Protection groups are not required, since the acid functionality reacts exclusively with the amine functionality and the alkyne functionality reacts exclusively with the azide functionality. For the AB building block, two different monomers were used, which differ by a methyl group in the side chain and are therefore divided into non-coding (no methyl group) and coding (methyl group) monomers.[60] Through stepwise CuAAC and amide bond linkages, binary encoded sequence-defined macromolecules could be synthesized.[60] Lutz et al. further explored this method and successfully synthesized nucleotide mimetics.[61] Both examples described could then be used for security and encoding technologies, since the sequence-defined macromonomers produced contained either quaternary or binary information that could subsequently be decoded.[60–62]

Another approach to avoid the use of protecting groups in the solid phase is the telechelic strategy where both ends of the building block have the same functional group at the terminal ends.[4] This approach follows an AA + BB strategy using the example of cyclic anhydrides and diamines presented by Hartmann et al. and will be presented in the next chapter.[12,63]

The different pathways to synthesize sequence-defined macromolecules using A) classical solid-phase synthesis with protecting groups (PG) B) an AB + CD approach and C) an AA + BB approach are shown in Figure 6.[64]

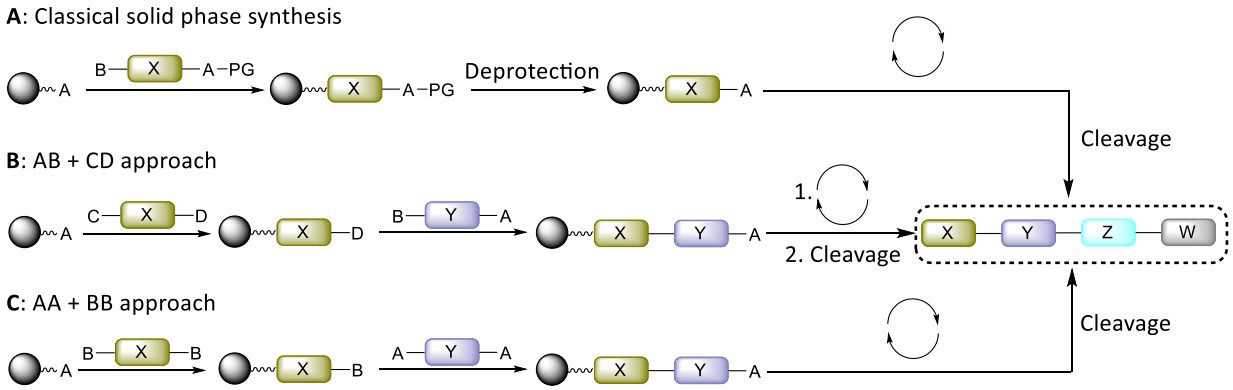

Figure 6: Overview of the different pathways to synthesize sequence-defined macromolecules. A: Classical solid phase synthesis with protection groups (PG). Function A reacts with function B. In the next step the PG is deprotected. B: AB + CD approach. Function A only reacts with function C and function D only reacts with function B. C: AA + BB approach. Function A only reacts with function B.[64]

As in classical solid-phase synthesis, various cyclic building blocks have already been successfully incorporated into submonomer solid-phase synthesis and these are presented in the chapter 1.3. The concept of solid phase submonomer synthesis presented here is used in a similar form in this thesis.

1.3 Cyclic building blocks in solid phase synthesis

Iterative assembly of acyclic building blocks has been the basis for numerous successful syntheses of sequence-defined macromolecules. The use of tailored acyclic building blocks offers several advantages, including the control over backbone length and composition, enabling tuning of hydrophilic or hydrophobic properties and spacing between side-chains.[65] Custom synthesis also enables the creation of toolboxes of acyclic building blocks with appropriate lengths, elemental compositions, and side- and end-groups.[1] Despite the advantages of tailored acyclic building blocks in terms of their ability to provide desired properties, the current trend towards increasing efficiencies in chemical synthesis has led to the investigation of different cyclic building blocks for their use in the solid phase over the past years. This is due to considerations such as atom economy and the time investment required for the multi-step syntheses of the acyclic building blocks.[66] Efforts are being made to address the issue of inefficiencies, especially at a large scale.[67]

In addition to the acyclic building blocks presented in the previous chapter, ring-shaped cyclic building blocks have also been used in solid phase synthesis. Using cyclic building blocks in solid phase synthesis offers different advantages, e. g. that protection group strategies as described in chapter 1.1 can be dispensed. In addition, cyclic building blocks allow the introduction of bi- or multifunctionalities into the oligomer chains and the ring opening of these cyclic building blocks proceed with high regio and/or stereoselectivity.[65] In most cases ring opening of the building blocks can be achieved by a variety of amines. This can also generate branched structures that can subsequently be functionalized or further elongated.[65] Ring opening reactions bring challenges too, as for example cascade or side reactions and the formation of product mixtures.[65,68]

Various cyclic building blocks have already been used in solid phase synthesis. The building blocks presented below are selected to demonstrate how cyclic building blocks can be used in solid phase synthesis to incorporate different functional groups and specific functions into sequence-defined macromolecules. Some of the building blocks presented here were recently described in a review by Hartmann et al. on the use of heterocyclic building blocks and their applications for the assembly of sequence-defined oligomers and polymers.[65]

The Du Prez working group investigated different cyclic building blocks for their use in solid phase synthesis. These include thiolactones, cyclic peptides[69] and cyclic sulfonamides[70]. Thiolactones are cyclic esters of mercapto-acids and their chemical activity is similar to that of lactones except that the endocyclic oxygen is replaced by a sulphur atom.[71] When thiolactones are ring-opened by amines, an amide bond is formed and a thiol group is revealed which can then be functionalized in a further step. Thiolactone aminolysis enables the introduction of two separate residual groups with high atom efficiency, in some cases with full retention of all atoms.[71] By means of a thiol-Michael addition, Du Prez et al. were able to use thiolactones for the construction of sequence-defined oligomers on solid phase.[72]

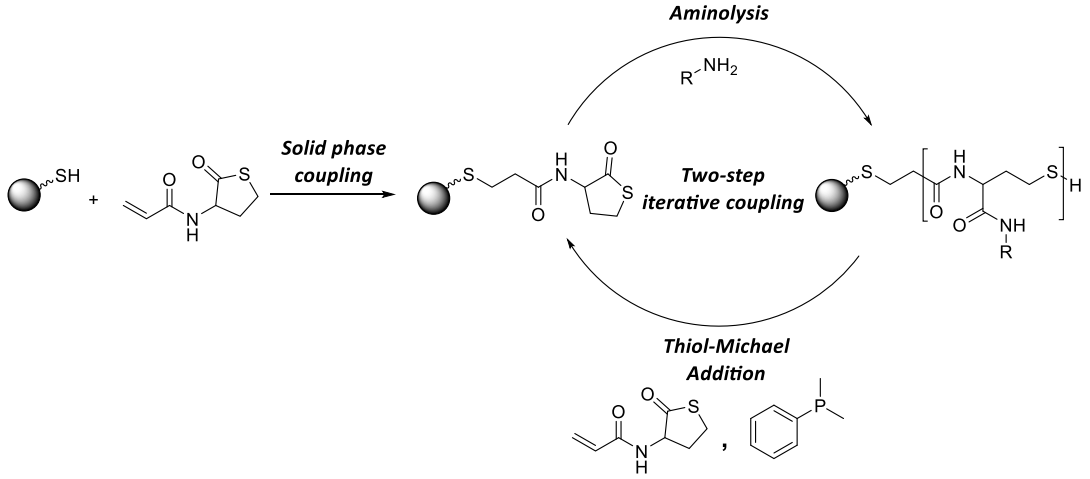

Figure 7: Coupling of a thiolactone to the solid phase. Subsequent two-step iterative coupling by means of aminolysis and thiol-Michael addition.[72]

Subsequently, the thiolactone rings were ring-opened by aminolysis and different side chains could be introduced resulting in tri-, tetra- and pentameric structures with molecular weights up to 1700 g/mol.[72] By the combination of thiolactone chemistry with the Passerini three-component reaction, sequence-defined oligomers could be synthesized at gram scale with molecular weights of up to 4 kDa.[73]

Epoxides have also been used in solid phase synthesis. Epoxides are three-membered rings with an oxygen atom in the ring. With an epoxide bound to the solid phase, oxazolidinones could be synthesized in high yields and purity via cycloaddition reaction with isocyanates.[74] Furthermore Sauleau et al. were able to synthesize epoxides on the solid phase by using alkenoic acids. Subsequently, the epoxides were ring-opened with thiophenols or sodium azide and then cleaved from the solid-phase resin. This allowed γ- and δ-lactones to be synthesized in high yields and purities.[75]

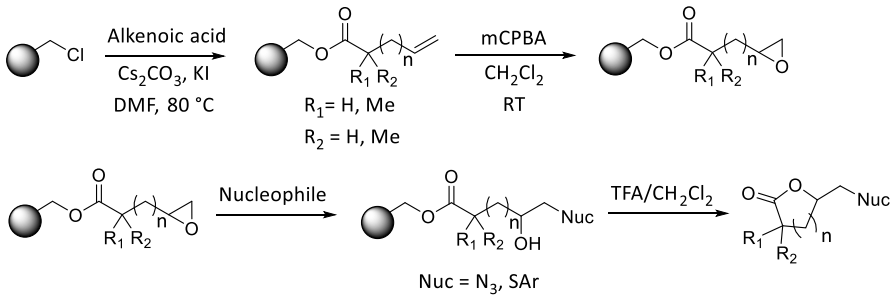

Figure 8: Coupling of alkenoic acids to the solid phase to obtain epoxides. Subsequent ring opening of the epoxides with nucleophiles. Finally cleavage from the solid phase resin to obtain γ- and δ-lactones.[75]

Maleimides are imides of maleic acid substituted on the nitrogen atom with an alkyl group or aryl group and have also been used as cyclic building blocks in solid phase synthesis. Their reactions in chemistry are widely used in Diels-Alder cycloadditions, Michael additions and double-bond polymerizations.[76] The thiol-maleimide coupling is an often used method due to the rapid reaction rates, high selectivity and relative stability of the conjugate products.[77] Thiol-maleimide click reactions have been performed by the Zhang group in creating defined macromolecules.[78] They have used an iterative exponential growth protocol to produce sequence-defined macromolecules, with iterated splitting, orthogonal deprotection, and active coupling leading to sequence-defined macromolecules on gram scale.[79] The Zhang group has developed a method to synthesize sequence-defined digital dendrimers that encode information into the primary sequence and then decode it using tandem mass spectrometry (MS/MS) techniques.[80] Another example is that maleimides were reacted with alpha-amino esters and hydroxybenzaldehydes in a 1,3-dipolar cycloaddition to synthesize highly substituted pyrrolidines.[81]

Houghten et al. were able to obtain cyclic ureas and thioureas by the reduction of acylated dipeptides followed by treatment with carbonyldiimidazole or thiocarbonyldiimidazole affords the corresponding cyclic urea or thiourea in high yield and high purity.[82] In addition, bis-cyclic ureas, bis-cyclic thioureas, and bis-cyclic diketopiperazines could be synthesized.[83]

Lim et al. have shown in their studies how cyclic peptides can be cleaved from the solid phase resin by cyanogen bromide and at the same time ring-opened, which is described as a one-pot ring-opening/cleavage strategy.[84]

Cyclic anhydrides have also been used in solid-phase synthesis. Cyclic anhydrides are ring-shaped molecules in which two acyl groups are linked by an oxygen atom. They are often 5- or 6-membered rings, e.g., maleic, succinic and glutaric anhydrides.[65] Various reactions to bring cyclic anhydrides to ring open with amines have been studied.[85] For example, the reaction of maleic acid and amines can synthesize the maleimides described above.[86] Hartmann et al. have presented an AA + BB approach in which succinic anhydride is reacted with a diamine which is shown in Figure 9.[12] In a first step, succinic anhydride is coupled to a resin with a terminal amine group. When coupling the succinic anhydride to the resin an amide bond is formed and a carboxy functionality is revealed at the end of the oligomer. In a subsequent step, the carboxy functionality was reacted with a diamine, which again results in an amide bond and leads to a terminal amine to which further sequence-defined succinic anhydride building blocks could be coupled. With this protocol up to 10 repeat units were coupled in a sequence-defined assembly.[12] By using cyclic anhydrides, poly(amidoamines) were synthesized. These were explored as polymer medicinal constructs,[63] e. g. monodisperse, cationic structures were used as non-viral polynucleotide delivery vectors.[87] The scheme for the coupling of succinic anhydrides with diamines is shown in Figure 9.

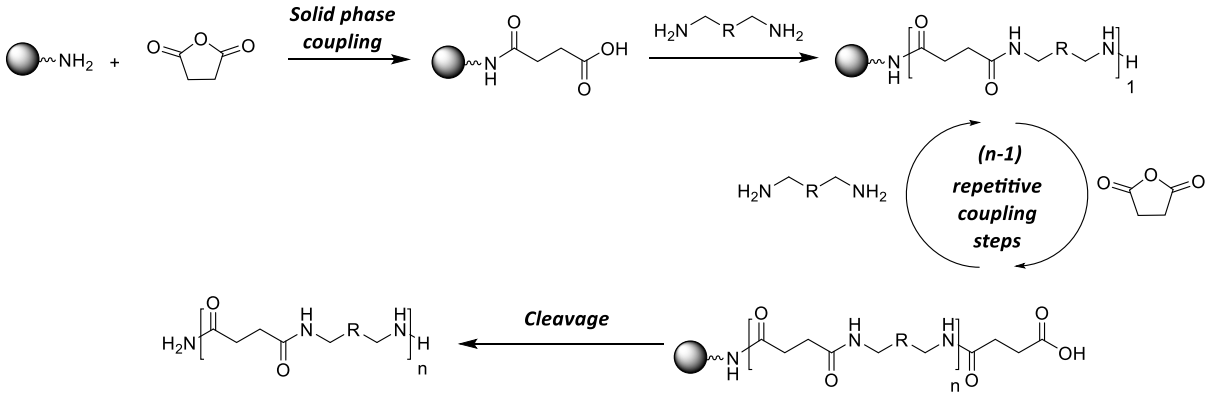

Figure 9: Solid-phase coupling of succinic anhydride to an amine-functionalized resin followed by reaction with a diamine. Subsequent cleavage from the solid-phase resin generates sequence-defined poly(amidoamines).[12]

N-heteroaromatics are another group of cyclic building blocks used in the solid phase which carry a leaving group like chlorides that undergo nucleophilic aromatic substitutions with nucleophiles like amines, alcohols or thiols.[88] An example of an *N*-heteroaromatic is 2,4,6-trichloro-1,3,5-triazine (Trz). With Trz, peptide macrocyclizations could be performed by Wenschuh et al.[89] Other *N*-heteroaromatics were also used e.g., 3,6-dichlooropyridazine was coupled to a thiol bound to the solid phase resulting in aminopyrazidines after aminolysis. In addition, resin-bound amines were reacted with chloropyrimidines in a nucleophilic aromatic

substitution leading to 2,4-diaminopyrimidines after cleavage from the solid phase.[90] Trz-based monomers, which were reacted with thiols or amines prior to coupling them to the solid phase, made it possible to incorporate sequence-defined macromolecules with different side chains.[91] Solid phase coupling then occurs at the second chloride of the Trz building block and the third is reacted with diamines at high temperatures. Additional building blocks can then be coupled via the terminal amine.

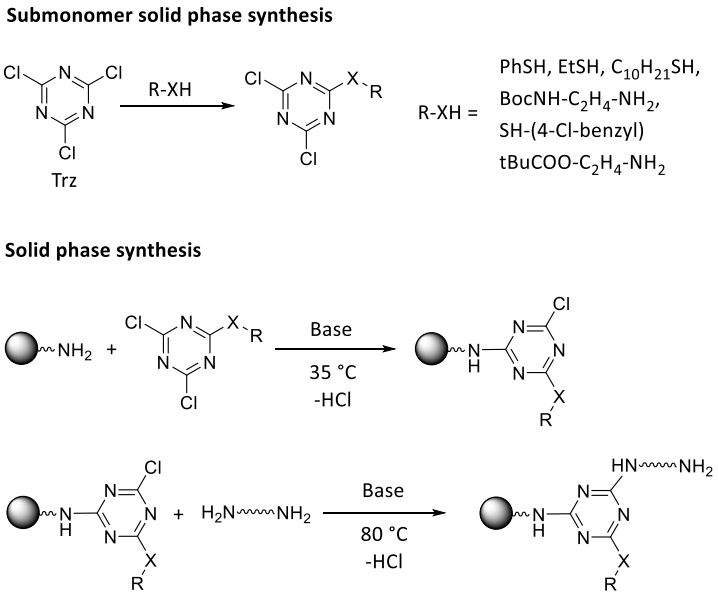

Figure 10: Submonomer solid phase synthesis of a sequence defined macromolecule with triazine-based monomers.[91]

Hexameric oligomers with molecular weights of up to 1400 g/mol and varying side chains could be introduced. Thus, aromatic, alkyl and charged residues oligomers could be introduced and side chain interactions could be studied.[91] By targeting side chain interactions through the formation of foldamer structures and π-π interactions of hydrogen bonds, secondary structures similar to those found in nature could be generated.[92] Photo chemical methods to synthesize sequence-defined macromolecules with *N*-heteroaromatics were carried out by Barner-Kowollik et al.[93]

2. Aims and Outline

In recent years, much progress has been made in the synthesis of sequence-defined synthetic oligomers with absolute control over their monomer sequence and chain length. Such control in synthetic oligomers and polymers can enable the development of new classes and applications of macromolecules, for example, the development of polymeric biomimetics for biomedical applications.[12,91,94]

The aim of this work is to explore different groups of cyclic building blocks for their use in solid phase synthesis and to extend the toolbox for building blocks that can be used in solid phase polymer synthesis. Cyclic sulfamidates, cyclic carbonates and cyclic amines will be explored for their use in solid phase synthesis and will allow for a protecting group free coupling or so-called submonomer strategy. Different cyclic building blocks have already been investigated for the use in solid phase synthesis, e. g. thiolactones by the du Prez group,[71,72,95] maleimides by the Zhang group[96] and epoxides by the Johnson group[97]. The use of cyclic building blocks allows branched structures to be constructed and new functional groups to be inserted in sequence-defined oligomers. In the first step, cyclic building blocks will be designed and subsequently synthesized. The reaction conditions for these syntheses will then be optimized. Subsequently, these building blocks are to be coupled to the solid phase. For this purpose, parameters such as reaction time, reaction temperature, resin loading, reagent stoichiometry, solvents, catalysts and the number of coupling steps per reaction will be investigated.

The first part of this thesis focuses on cyclic sulfamidates and their possible use in solid phase synthesis. Using these building blocks offers the possibility to introduce sulfate groups in the side chain upon ring opening with an amine. Sulfate groups are of special interest in the Hartmann lab, due to the development of polysulfates as antivirals.[98] Building blocks are to be synthesized which carry both the sulfamidate motif and a carboxy functionality with which the building blocks can subsequently be coupled to an amine-functionalised resin. Both the possibility of coupling the ring directly to the solid phase and the variant of first coupling the carboxy functionality to the solid phase are to be investigated. Subsequently, further cyclic sulfamidate building blocks will be coupled to the solid phase and the corresponding coupling conditions will be explored. The possibility to synthesize linear as well as branched structures will also be investigated.

In the second part of this thesis, the cyclic carbonates are investigated for their potential use as building blocks in solid phase synthesis. Cyclic carbonates are an interesting class of building blocks for solid-phase synthesis, as they have gained attention as a green alternative to the classic polyurethane synthesis via the polyaddition of polyisocyanates with polyols.[99,100,101,102] In addition, cyclic carbonates have already been used in solution in the Hartmann group[103] and it is now interesting to explore them for their use in the solid phase. For this purpose, a butyl biscyclocarbonate is chosen as a building block. First, coupling conditions are to be investigated with which it is possible to couple the cyclic carbonate ring to the solid phase. Subsequently, the second ring of the biscyclocarbonate is to be opened by a diamine. The ring opening is expected to lead to the formation of oligohydroxyurethanes, which contain branching hydroxy groups in the main chain. After these coupling conditions have been optimized, further cyclic carbonate building blocks will be coupled to the oligomer and the required coupling conditions will be investigated.

The third and final part of this thesis deals with cyclic amines. Cyclic amines are an interesting class of building blocks for solid phase synthesis, since ring opening creates *N*-substituted amide bonds, which - as is known from peptoids - opens the possibility for the generation of novel peptidomimetics for potential applications in biomedicine.[104] The first step is to synthesize building blocks that vary in both ring size and chain length between the carboxy functionality and the cyclic amine ring. After successful solid phase coupling of these building blocks, the aim is to open the rings of the cyclic amine building blocks with chloroformates bearing protective groups, so that peptoids, with a branching alkyl chloride functionality, can be incorporated into the main chain of the oligomer.[105] Subsequently, the protecting group is to be cleaved off and further building blocks are to be coupled to the secondary amine of the main chain. Alternatively, ways to nucleophilically replace the chloride terminal after ring opening will be explored.

3. Results and Discussion

3.1 Exploring Cyclic Sulfamidate Building Blocks for the Synthesis of Sequence-Defined Macromolecules

Hill, S. A., Steinfort, R., Mücke, S., Reifenberger, J., Sengpiel, T., Hartmann, L., **"Exploring Cyclic Sulfamidate Building Blocks for the Synthesis of Sequence-Defined Macromolecules"** *Macromol. Rapid Commun.*, **2021**, 2100193.

Contribution:

Robert Steinfort: First synthesis of building block 1. Coupling experiments with this building block to the solid phase. Synthesis of oligomers 6 and 19. Experiments for linear and branched growth with building block 19. Experiments for coupling building block 1 to the solid phase with different coupling reagents. Experiments for the latent and active strategies. Analytical sample preparation (IR, EA, NMR, LC-MS). Analysis and evaluation of the structures. Work carried out by Sandra Mücke and Josefine Reifenberger under the supervision of Robert Steinfort: Optimization of the synthesis of building block 1. Coupling reactions with building block 1 to the solid phase. Coupling experiments for linear and branched growth with building blocks 1 and 16.

Stephen Andrew Hill and Robert Steinfort contributed equally to this work.

RESEARCH ARTICLE

Macromolecular Rapid Communications

www.mrc-journal.de

Exploring Cyclic Sulfamidate Building Blocks for the Synthesis of Sequence-Defined Macromolecules

Stephen Andrew Hill, Robert Steinfort, Sandra Mücke, Josefine Reifenberger, Tobias Sengpiel, and Laura Hartmann**

The preparation of sequence-defined macromolecules using cyclic sulfamidates on solid-phase is outlined. The challenges surrounding an AB+CD approach are described with focus on understanding the formation of ring-opened side products when using amide coupling reagents. To avoid undesired side product formation, a strategy of iterative ring-openings of cyclic sulfamidates on solid-phase is explored. Ring-opening on primary and secondary amines is successfully reported, generating both linear and branched chain growth. However, attempts to selectively cleave *N*-sulfate bearing sp^3-hybridized groups cannot be demonstrated, limiting the overall building block scope for this methodology. Consequently, the active ring-opening of cyclic sulfamidates on amine-functionalized oligo(amidoamine) backbones is successfully applied to produce sequence-defined, *N*-sulfated macromolecules.

1. Introduction

The relationship between any molecule's shape and function is fundamental, with shape being governed by molecular composition and the molecule's atomic arrangement. Similarly, a macromolecule's sequence is known to influence its shape with natural examples, like DNA/RNA, proteins and polysaccharides, only functioning properly with the correct atomic or building block (BB) arrangement.[1] The importance of sequence definition is well-understood in biopolymers and attention within the polymer community has turned toward artificial systems over the past decade. The focus on sequence-defined oligomers and polymers has led to many advances in both synthesis and application which have been recently reviewed.[2]

Dr. S. A. Hill, R. Steinfort, S. Mücke, J. Reifenberger, T. Sengpiel, Prof. L. Hartmann
Institute of Organic Chemistry and Macromolecular Chemistry
Heinrich-Heine-University Düsseldorf
Universitätsstraße 1
40225 Düsseldorf, Germany
E-mail: hills@hhu.de; laura.hartmann@hhu.de

The ORCID identification number(s) for the author(s) of this article can be found under https://doi.org/10.1002/marc.202100193

DOI: 10.1002/marc.202100193

In our own work, we have focused on the development of novel peptido- and glycomimetic macromolecules based on sequence-defined oligo(amidoamines) with pendant glycan side chains. We have achieved sequence-definition via the stepwise assembly of tailor-made BBs on solid phase (SP), which offers the chemist many advantages when assembling monodisperse, sequence-defined macromolecules (SDMs). Ever since Merrifield et al. reported the first solid-phase synthesis (SPS) of a tetrapeptide,[3] the versatility and appeal of this synthetic strategy has seen the purification and yield-maximizing benefits being applied to natural polymers, such as polysaccharides,[4] polypeptides,[5] and polynucleotides,[6] as well as non-natural or biomimetic polymers, such as polyurethanes,[7] triazine-,[8] and thioether-based polymers.[9]

Our own work centers around standard peptide coupling strategies for BBs carrying a free carboxylic acid and a Fmoc-protected amine group.[2a] We have developed a toolbox of non-natural building blocks that allows us to vary main and side chain motifs in the final SDM and to site-selectively introduce different motifs, such as hydrophobic units or different glycans. In the recent past, we have looked to expand this toolbox and have become particularly interested in synthesizing glycomacromolecules containing sulfonated or sulfated structures. They are simplified mimetics of glycosaminoglycans (GAGs), densely-sulfated polysaccharides, which often bear other charged functionalities, e.g., amines and carboxylates, and perhaps heparin is the most widely-known example.[10] Heparin/heparan sulfate's *O*- and *N*-sulfation patterns can be highly heterogeneous, nevertheless it is known that specific patterns determine a given GAG's function at the cell, tissue, and organism level influencing processes, such as signal transduction, and development of the nervous and skeletal system.[11] Therefore, it is of high interest to create macromolecules with sequence-defined sulfation patterns and learn more about the correlation between the sequence and resulting biological activity. However, creating such natural or biomimetic sulfated macromolecules with sequence definition is highly challenging. Known synthetic methods include enzymatic modification of natural oligo- and polysaccharides and the use of noncarbohydrate containing polymers and complex protecting group strategies in SPS.[12] In our recently reported work, we have used SPS in two distinct ways to generate sulfonated and

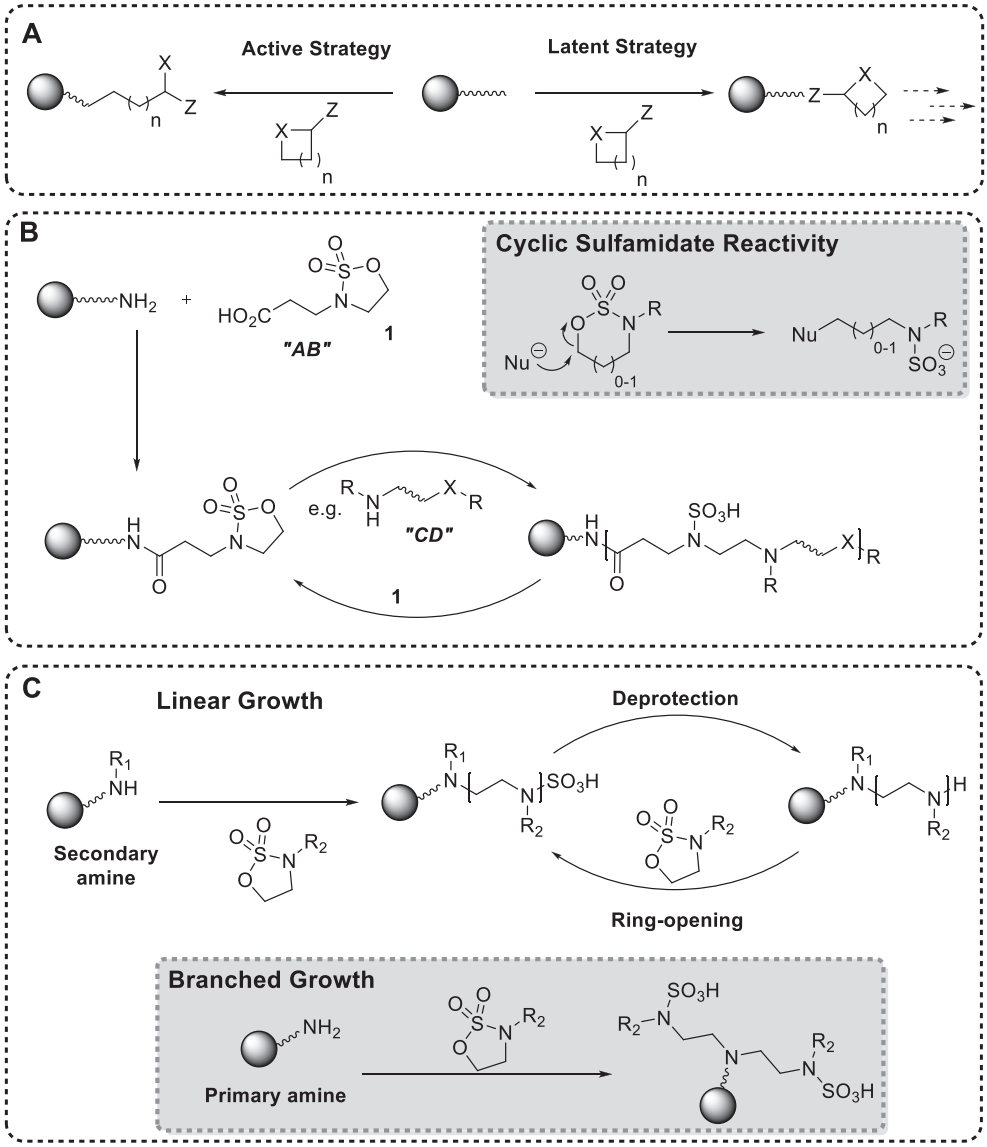

Figure 1. A) General scheme for latent and active SDM chain elongation strategies; Deployment of cyclic sulfamidates on solid phase in either B) latent (inset: cyclic sulfamidate general reactivity) or C) active coupling strategies to generate linear and branched growth.

sulfated SDMs. First, incorporating sulfation patterns onto the desired backbone or architecture on SP prior to cleavage.[13] Alternatively, we reported that a resin-bound SDM may be produced and then cleaved from its support, before the desired sulfation is installed.[14]

In this study, we explore an alternative way to produce *N*-sulfated SDMs that should be compatible with our previously-established SP strategies. Therefore, we identified cyclic sulfamidates (CS) as potential BBs to be added to our toolbox. CSs are a class of heterocycle identified by a N–SO_2–O functionality housed in either a 5 or 6-membered ring. CS reactivity is characterized by a site-selective, ring-opening reaction at the endocyclic C–O bond with a wide variety of nucleophiles including amines, alkoxides, halides, azide, sulfur-, and carbon-centered nucleophiles (**Figure 1**).[15] The use of heterocyclic BBs that can be selectively ring-opened in the stepwise assembly of SDMs has been well-established by Du Prez et al. for thiolactones,[9,16] and by Johnson et al. for epoxides.[17] We envision two strategies for SDM chain elongation using CS BBs which can be categorized as either "latent" or "active" (Figure 1). A latent or active heterocyclic BB strategy describes the outcome of a BB's coupling to a macromolecule. If a strategy is latent then an unreacted heterocyclic functionality remains after SDM incorporation, retaining its reactivity to be used in a subsequent transformation. In contrast, an active strategy utilizes a heterocycle's inherent chemistry in the coupling step. For a latent strategy an "AB+CD" monomer approach, akin to thiolactone examples, would be realized via creating a carboxylic acid-pended CS, e.g., **1** ("AB" monomer). In an initial step **1** would be coupled to an amine-functionalized resin via amide formation. After successful incorporation of the latent CS ring on the resin, treatment with an appropriate bifunctional nucleophile, e.g., diamine, *N*-protected aminol, or aminothiol

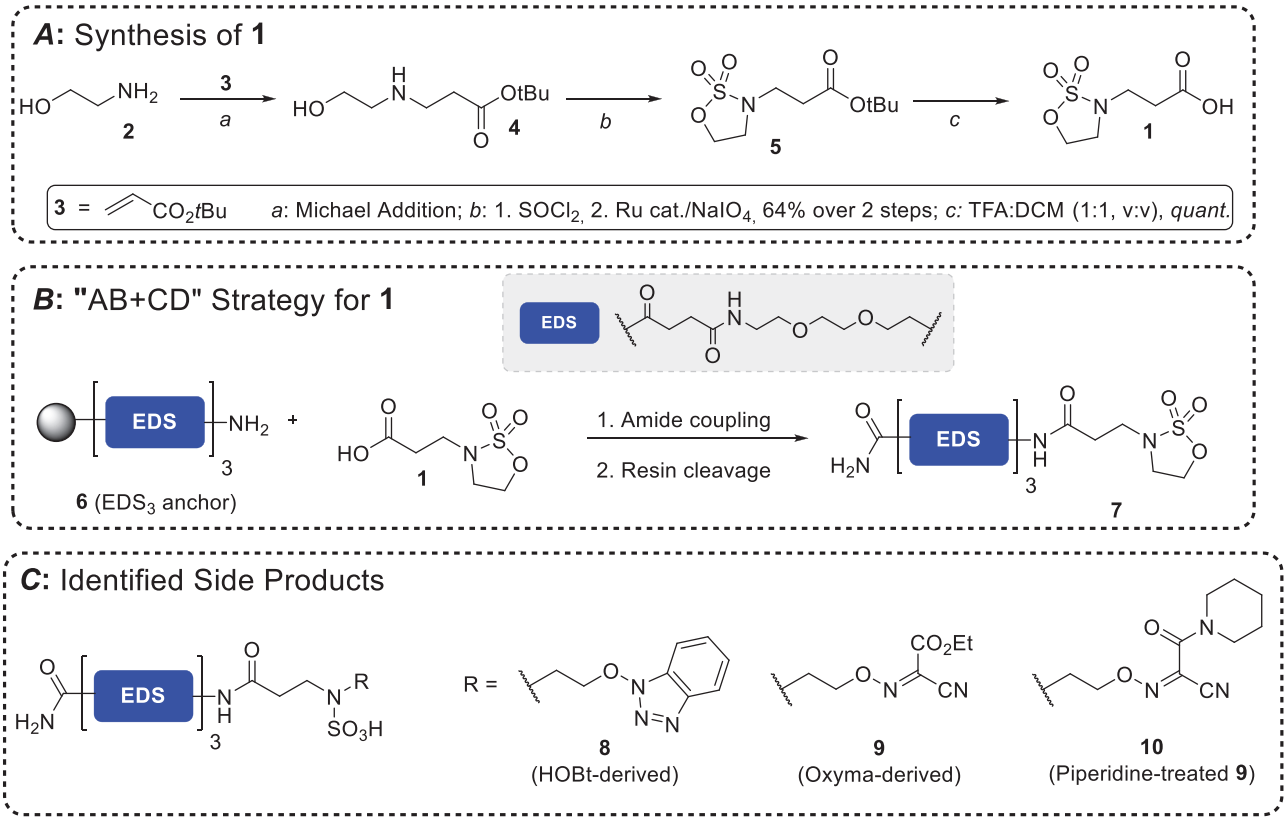

Figure 2. A) Synthesis of **1**; B) Amide coupling of cyclic sulfamidate **1** to resin-bound precursor **6**; and C) the identified ring-opened side products.

("CD" monomer), would afford ring-opening/chain elongation and provide a reactive terminus for further iterative couplings of **1** (Figure 1B).

Alternatively, an active approach would use iterative ring-openings of CS BBs on nucleophile-presenting resins to grow the polymer backbone. Plus, in this approach the revealed *N*-sulfate group could be regarded as a masked protecting group, which after successful deprotection would yield a new amine end-group, primed for further chain elongation (Figure 1C). Secondary amine alkylation would result in linear growth, whereas primary amine termini would afford branching, allowing precise control over architecture. In both examples the role of the N-bound residual group could be: 1) to act as a side-chain (encoding information or additional functionality), or 2) provide an additional reactive group, potentially crucial for future chain elongation. Literature reports of CSs on SP have demonstrated both latent and active approaches but never in an iterated fashion.[18]

2. Results and Discussion

2.1. Latent Coupling Strategy

To begin with, a latent AB+CD monomer approach was investigated and to this end the gram-scale synthesis of novel cyclic sulfamidate **1** was proposed. **1** was synthesized via the Michael addition of ethanolamine (**2**) to *tert*-butyl acrylate (**3**) which afforded key, *N*-alkylated ethanolamine derivative (**4**) in multigram-scale quantities (**Figure 2**A, Supporting Information).[19] Treatment of **4** with thionyl chloride, followed by Ru-catalyzed oxidation afforded CS **5** in 64% over two steps. Deprotection of the *tert*-butyl ester protecting group by exposure to low pH afforded **1** quantitatively. Importantly, this protocol affords the desired building block in high purity and yield, vital for SPS which requires BBs to be used in high excess.

To investigate the stability of **1** tests were conducted. After 14 d bench storage 1H NMR showed degradation due to the presence of a complex set of peaks (Figure S1, Supporting Information). Similarly, **5** was not bench stable after 8 weeks' storage, but it was found that long-term storage at −19 °C was sufficient for **5** (Figure S2, Supporting Information), hence all SP couplings reported herein were conducted with freshly synthesized **1**.

For initial tests an oligomer precursor (**6**) was synthesized on acid-labile resin, forming an oligo(amidoamine) backbone comprising three repeat units of a BB previously developed within our group (Figure 2). The EDS BB (short for **E**thylene glycol—**D**iamine- **S**uccinic acid) is applied in our group to precisely introduce ethylene glycol spacing units into oligo(amidoamine) main chains (Figure 2).[20] **6** allowed reaction progress to be rapidly monitored by reverse phase high-performance liquid chromatography-mass spectrometry (RP-HPLC-MS) following resin cleavage. First coupling experiments were conducted akin to that reported by Cohen et al. using benzotriazol-1-yloxytripyrrolidinophosphonium hexafluorophosphate (PyBOP), *N*-methylmorpholine and dimethylformamide (DMF) (Entry 1, Table S1 and Figure S3, Supporting Information).[18c] Analysis indicated that: 1) 100% conversion of **6** was not achieved, 2) no

evidence of latent electrophile **7** was noted, and 3) unexpected masses were noted, which after extensive consideration were assigned to desulfated-**8** (Figure 2C; and Figures S4–S7, Supporting Information). Side product **8** was likely generated from the ring-opening of resin-bound **7**, as successful PyBOP-mediated amide couplings release deprotonated hydroxybenzotriazole (HOBt), and owing to proximity, likely attacks the electrophilic CS-terminated **7**.[21] It should be noted here that the corresponding desulfated masses can be identified when macromolecules are analyzed by positive mode electrospray ionization mass spectrometry (ESI-MS), as observed in Figure S7 (Supporting Information). Altering the equivalents of BB **1**, PyBOP, base, solvent, or reaction time could not suppress the presence of the mass peaks corresponding to undesired side product **8** (selected conditions are highlighted in Entries 2–3, Table S1, Supporting Information). Due to the requirement for coupling reactions to proceed with high fidelity, alternative reagents were investigated to assess their compatibility for amide couplings with **1**.

Switching the coupling reagent to carbodiimides, e.g., diisopropylcarbodiimide returned only starting material **6** (Entries 4–7, Table S1, Supporting Information), so commercially-available Oxyma-based coupling reagents (OxymaPur, PyOxim and COMU) were then rigorously tested (see selected conditions Entries 7–10, Table S1, Supporting Information). Regardless of the conditions used, Oxyma-based reagents generated ring-opened side product **9** (akin to HOBt-derived **8**), which was identified by RP-HPLC-MS and 1H NMR analysis (Figure 2C; and Figures S8–S10, Supporting Information). On-resin aminolysis by piperidine further indicated the presence of **9** due to the presence of mass peaks corresponding to aminolysed piperidine-adduct **10** (Figure 2; and Figures S11 and S12, Supporting Information). The presence of adducts for PyBOP (**8**) and Oxyma-based reagents (**9**) indicated that amide coupling was successful, but once **7** was established on SP as a latent chain-end undesired, ring-opened side products were produced in significant quantities (Figure 2; and Figure S10, Supporting Information). Such side products, that form while attached to the SP, cannot be separated from the desired product while on-resin transformations continue. Since iterative chain elongation should ideally proceed with high fidelity and yield, this first strategy was abandoned at this point and an alternative approach was undertaken.

2.2. Active Coupling Strategy

Alternatively, an active strategy was pursued via the direct ring-opening of CS BBs on nucleophile-bearing resins to circumvent side products being generated from inadvertent ring-opening. To this end, a small of library of saturated, 5-membered rings CS BBs bearing variable residual (R) groups was synthesized. *N*-ethyl (**14**) and benzyl (**15**) were synthesized from commercially-available ethanolamine starting materials; Boc-protected **16** (synthesized from **2**) and *t*Bu-ester bearing **5** were chosen to investigate BBs with bulky side-chains and which after acidic resin cleavage would reveal new functionality, e.g., unfunctionalized *N*-sulfates (**16**) and carboxylates (**5**). Based upon previous experience it was proposed CS ring-opening could be achieved simply using automation-compatible, non-nucleophilic bases and solvents, e.g., *N*,*N*-diisopropylethylamine (DIPEA) and DMF. Investigations initially focused on linear growth using secondary amine-terminated precursor **11** (bis-alkylation of primary amine-terminated **6** for branching architectures shall be discussed later).

Exploratory CS ring-opening experiments using **11** established a range of solvents, e.g., tetrahydrofuran, dichloromethane and DMF, plus, a range of bases, e.g., pyridine, 1,8-diazabicyclo(5.4.0)undec-7-ene, triethylamine, and DIPEA facilitated ring-opening. Due to their broad SP and automated synthesizer compatibility DMF and DIPEA were taken forward for further investigation (**Figure 3**).

The active ring-opening with benzyl-functionalized CS **15** (25 eq.) proceeded with 100% conversion of **11** and characteristic desulfated masses for **12b** were identified by ESI-MS (Entry 1, Table S2 (Supporting Information), see Figures S13–S16 (Supporting Information) for desulfated oligomer characterization) Indeed, sulfated **12b** was observed by negative mode ESI-MS (Figure S17, Supporting Information). When ring-opening was attempted with ethyl-bearing **14** unreacted starting material **11** was noted (60 min, RT: Entry 2, Table S2 and Figure S13, Supporting Information). Increasing the coupling time fourfold achieved full conversion of **11** (Entry 3, Table S2 and Figure S14, Supporting Information). The reactivity differences between CS BBs were assigned to R group identity, e.g., donating effects via hyperconjugation (ethyl-functionalized **14**) could lower the relative electrophilicity of the CS ring compared to **15**. Further linear growth investigations with **5** and **16** probed reaction time, temperature, and required BB equivalents. It was found that, regardless of reaction time or temperature, a minimum of 10 eq. of BB was necessary to facilitate 100% conversion of **11** (Entries 4–14, Table S2 and see Figures S18–S21, Supporting Information).

Investigations were then undertaken to establish if branched architectures could be synthesized by reacting a primary amine end-group, e.g., EDS_3 precursor **6** with two equivalents of BB (Figure 3). Primary investigations reacted **6** with Boc-protected **16** in 10, 20, 50-fold excess for either 0.5, 2, or 24 h (Entries 15–23, Table S2, Supporting Information). In all cases, 100% conversion of starting materials was observed, but neither the desired bis-alkylated structure (**13c**) nor mono- or bis-desulfated equivalents were directly observed (Figure 3; and Figures S22 and S23, Supporting Information). The same profile was observed with **5** (Entries 24–26, Table S2, Supporting Information). After careful consideration, the masses were assigned to a "diethylamine" end-group akin to **18** (Figure 3). The assignment suggested successful bis-alkylation by **5** and **16** had occurred, but that branched architectures (with poly(ethyleneimine) character) were susceptible to degradation under ESI-MS conditions.[22] Removing formic acid from the eluent still afforded the identical ESI-MS profile (Figures S22 and S23, Supporting Information). MALDI-MS analysis also showed similar degradation patterns (Figure S24, Supporting Information). As similar degradation patterns were not observed from the mono-alkylation of secondary amine-capped **11**, we suggest the observed degradation is indeed architecture dependent. This hypothesis was further bolstered via 1H NMR and ESI-MS analysis of a cleaved **13c** probe dissolved in D_2O. ESI-MS analysis showed **13c** masses for mono- and bis-desulfated **13c**, and mono- and bis-deaminated end-groups, except with deuterium replacing exchangeable protons (Figure S25, Supporting Information). 1H NMR analysis of **13c** did not indicate the presence of expected aminoethyl groups (**18**) and the global

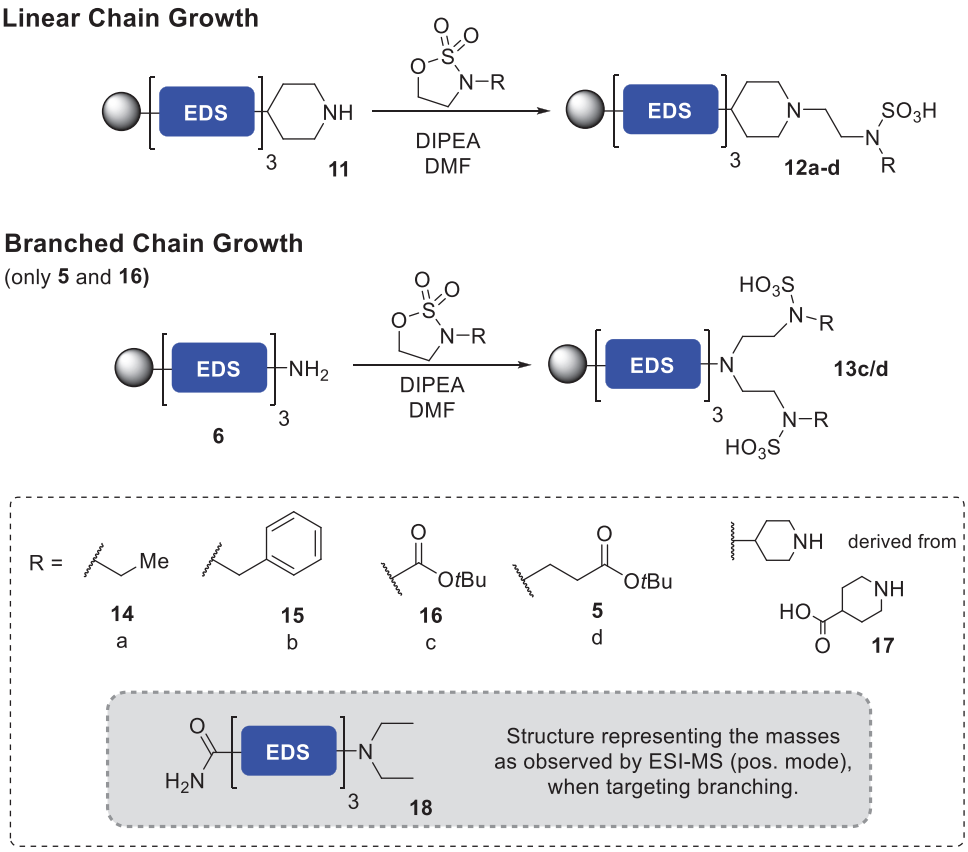

Figure 3. "Active" cyclic sulfamidate coupling investigated using a primary or secondary amine terminated EDS_3 anchor with a range of *N*-functionalized cyclic sulfamidates (inset: the diethyl terminated oligomer **18**, as observed by ESI-MS analysis).

integration of all protons matched the expected proton total (excluding exchangeable and amide protons – Figure S26, Supporting Information). Fourier-transformed infra-red spectroscopy (FTIR) analysis of **13c** indicated the presence of sulfate groups (Figure S27, Supporting Information).[23] These results established that successful chain elongations with a range of CS BBs could be achieved to yield linear and branched architectures, therefore our attentions moved toward regenerating a nucleophilic chain terminus to allow iterative active couplings (Figure 1C).

N-sulfate cleavage following CS ring-opening is typically achieved via acid treatment.[15a,24] The acidic cleavage of carbamate-functionalized *N*-sulfates on SP at elevated temperatures has been demonstrated too.[18a,18b] We envisioned developing an effective deprotection strategy (mild acidic pH/elevated temperatures) that could achieve *N*-sulfate cleavage while not generating resin cleavage. It was evident that low pH conditions required for resin cleavage at room temperature, e.g., 95% trifluoroacetic acid solution did not affect *N*-sulfate cleavage (Figures S12, S17–S19, S21, and S24, Supporting Information). As such, a range of acidic solutions (employing both organic and aqueous mixtures) were tested on SP presenting **13a-c**; microwave irradiation in sealed vials was used to achieved elevated temperatures (50–100 °C, Table S3, Supporting Information). Negative mode ESI-MS after resin cleavage was used to confirm the presence of *N*-sulfate groups and it was discovered that Boc-functionalized *N*-sulfate groups (**13c** generated from **16**) could be deprotected, but alkyl-bearing **13a/b** could not be deprotected regardless of the conditions tested (Table S3, Supporting Information).

With increasing temperature or reducing pH the window between selective *N*-sulfate and resin cleavage shrinks, reducing the favorability of the deprotection conditions. For an iterative SPS of SDMs, conditions should ideally: 1) avoid unwanted resin cleavage to maximize yields and 2) be applicable to a broad range of functionality. As acidic cleavage was not effective for sp3-hybridized *N*-substituents with reasonable, mild conditions this limits the range of CS BBs possible for iterative chain elongations following this strategy. Moreover, we found that exposing deprotected **13c** to a secondary CS BB did not yield the expected chain elongation when the previously optimized conditions were employed. Despite exploring a range of washing protocols at different pH values, with various organic and aqueous solvents, no effective method was discovered allowing a second BB to be employed iteratively. These limitations prevent the effective iterative coupling of CS BBs on SP, so this second strategy was too abandoned, but the successful ring-opening of CS BBs was reapplied to produce *N*-sulfated oligo(amidoamine)s.

2.3. *N*-Sulfated, Sequence-Defined Oligomer Synthesis

Having established that a range of *N*-functionalized CSs could be actively ring-opened on amine-bearing SP, our attentions

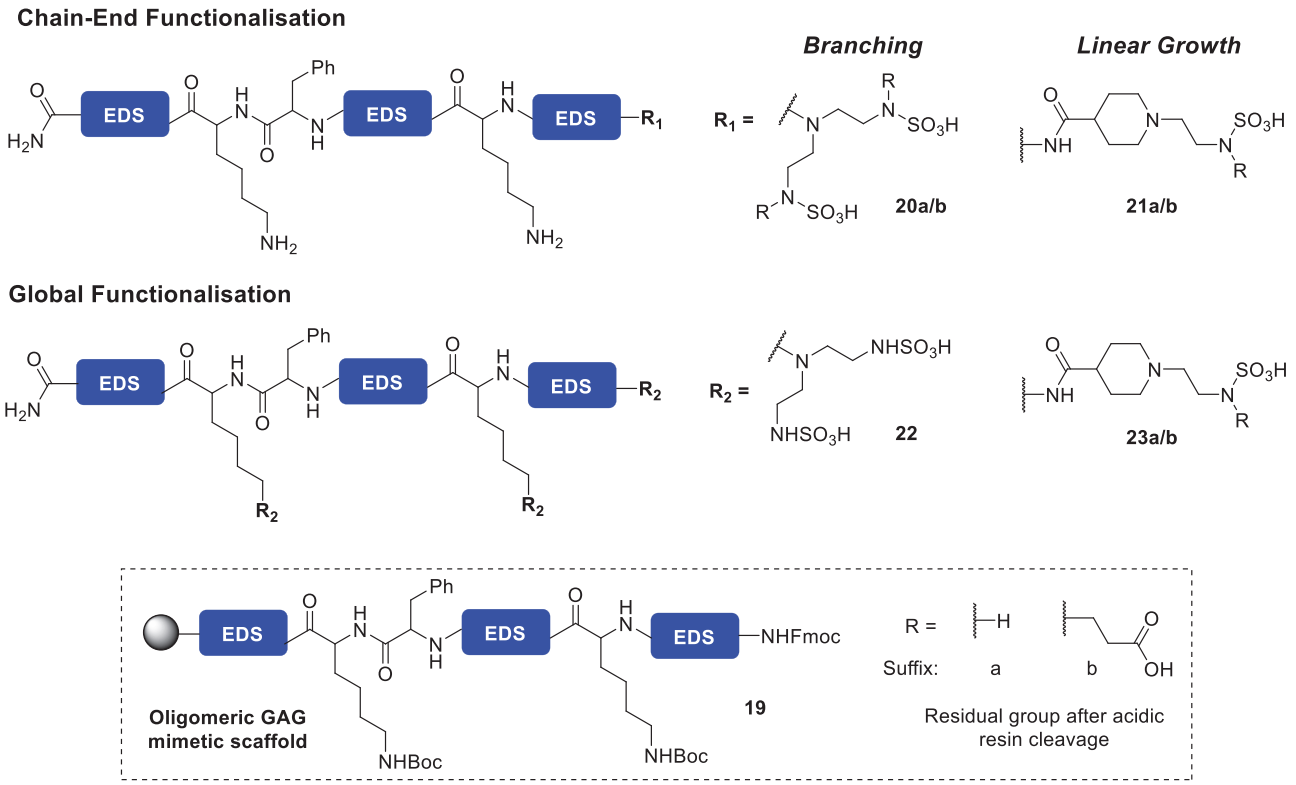

Figure 4. Library of oligomeric GAG mimetics with different charged patterns and architectures.

turned toward generating monodisperse, *N*-sulfated SDMs. We proposed constructing different architectures with varying levels of *N*-sulfation levels to examine the synthetic limitations available on SP, while generating structures of interest for potential GAG mimetic structures. A single backbone (**19**) consisting of three EDS units, phenylalanine and two lysine residues bearing Boc-protected side-chains was assembled on SP (**Figure 4**). From this central scaffold the Fmoc- and Boc-protected amines could be orthogonally manipulated to precisely afford primary or secondary amines. Subsequent functionalization of the primary and secondary amines would target: branched or linear architectures, and variable *N*-sulfation levels. **5** or **16** were employed, as after acidic resin cleavage a carboxylic acid and unsubstituted *N*-sulfate groups would be, respectively, generated. Seven targets, as outlined in Figure 4, were chosen to understand potential synthetic limitations from the interplay of architecture, steric hindrance, and sulfation density. The structures chosen were functionalized either at the backbone terminus or at both backbone and side-chain termini. Terminus functionalization via primary amine bis-alkylation would afford exclusively branching generating bis-sulfated **20a/b** or secondary amine alkylation would afford linear growth and mono-sulfated **21a/b**. Removing both Fmoc and Boc groups would reveal three primary amines which upon global alkylation would afford branched, hexa-sulfated **22** and conversion to secondary amines would generate tris-sulfated **23a/b**.

Having constructed **19** on solid-phase (Figures S28 and S29, Supporting Information) the terminal Fmoc group was removed and the subsequent primary amine was directly reacted with CS BBs **16** or **5** (25 eq. for 2 h) to generate the branching required for **20a/b**. End-group transformation with Fmoc-protected **17** afforded a secondary amine to generate the scaffold for mono-sulfated **21a/b**. For **20a**, no starting material was observed after CS coupling and the ESI-MS mass peak profile corresponded to bis- and mono-desulfated **20a** and the various adducts of a diethylamine end-group, as previously discussed (Figure S30, Supporting Information). A similar profile was observed for **20b** (Figure S30, Supporting Information). ^{1}H NMR, FTIR, and elemental analysis of **20a/b** showed the expect proton counts, presence of sulfate groups and sulfur content (Figures S31–S34 and Table S4, Supporting Information). Having synthesized and cleaved the end-functionalized, mono-sulfated **21a/b** from solid-phase, analysis by ^{1}H NMR, FTIR, ESI-MS and elemental analysis again indicated the desired products (Table S4 and Figure S35–S39, Supporting Information).

To access **22** sequential deprotection of Fmoc and Boc groups afforded a backbone bearing three primary amines, which was then reacted with **16**. ESI-MS analysis identified characteristic peaks corresponding to hexa-desulfated oligomer and the expected branching architecture degradation (Figure S40, Supporting Information). The presence of the desired proton total by ^{1}H NMR analysis (Figure S41, Supporting Information) and the use of FTIR and elemental analysis to indicate sulfur content suggested **22** was successfully generated on SP (Figure S42 and Table S4, Supporting Information). The global functionalization of main- and side chains to generate **23a/b** was similarly achieved using CSs **5** and **16** and analyzed as previously described to show the desired synthesis of these peralkylated, *N*-sulfated

macromolecules (Figure S43–S47 and Table S4, Supporting Information). All targeted structures were produced in good yields (Table S5, Supporting Information) signifying that the ring-opening of CSs for SDM synthesis is an option for future studies when creating functionally diverse *N*-sulfated SDMs, e.g., GAG mimetics.

Given the evidence herein reported for the facile ring-opening of CS BBs, we speculate that the application of CSs to larger oligo- or polymer constructs on solid-phase or in-solution is a viable possibility. Limiting factors likely arising during syntheses would probably be steric hinderance or electronic of either nucleophile or electrophile, which would lower overall reactivity.

3. Conclusion

To the best of our knowledge, this is the first comprehensive study of the use of cyclic sulfamidates for the generation of *N*-sulfated SDMs using latent and active strategies. We have demonstrated the limitations of a latent, AB+CD strategy when an amide bond is used to couple CS BBs to the resin. Alternatively, actively ring-opening cyclic sulfamidates on amine-functionalized resins has been broadly demonstrated with a range of CS BBs on primary- and secondary amine-functionalized oligo(amidoamine) backbones. However, the iterative ring-opening of CS BBs is limited, as acidic *N*-sulfate cleavage was not shown for *N*-sulfate groups bearing sp^3-hybridized residual groups. Therefore, a number of *N*-sulfated SDMs were produced on solid-phase to demonstrate the wide applicability of this method for producing SDMs with variable yet sequence-defined *N*-sulfation levels and architectures. Future work will look to investigate: 1) alternative latent coupling strategies, e.g., click chemistry, 2) alternative *N*-sulfate cleavage methodologies, 3) potential application of CS-based oligo(amidoamine)s as GAG mimetics, and 4) to the best of our knowledge, given no reports exist on either the polymerization of cyclic sulfamidate-based monomers or the postpolymerization functionalization of larger polymers, we will look to expand this methodology.

Supporting Information

Supporting Information is available from the Wiley Online Library or from the author.

Acknowledgements

S.A.H. and R.S. contributed equally to this work. L.H. thanks the DFG for financial support through the FOR2327 (HA 5950/5-2).

Open access funding enabled and organized by Projekt DEAL.

Conflict of Interest

The authors declare no conflict of interest.

Data Availability Statement

Research data are not shared.

Keywords

cyclic sulfamidate, precision oligomers, sequence-definition, solid-phase synthesis

Received: March 26, 2021
Revised: April 20, 2021
Published online: May 4, 2021

[1] a) F. Crick, *Nature* **1970**, *227*, 561; b) H.-J. Gabius, S. André, H. Kaltner, H.-C. Siebert, *Biochim. Biophys. Acta, Gen. Subj.* **2002**, *1572*, 165; c) M. I. Sadowski, D. T. Jones, *Curr. Opin. Struct. Biol.* **2009**, *19*, 357; d) A. V. Guzzo, *Biophys. J.* **1965**, *5*, 809.

[2] a) S. A. Hill, C. Gerke, L. Hartmann, *Chem.- Asian J.* **2018**, *13*, 3611; b) J.-F. Lutz, *Macromol. Rapid Commun.* **2017**, *38*, 1700582; c) M. A. R. Meier, C. Barner-Kowollik, *Adv. Mater.* **2019**, *31*, 1806027; d) P. Nanjan, M. Porel, *Polym. Chem.* **2019**, *10*, 5406; e) R. Aksakal, C. Mertens, M. Soete, N. Badi, F. Du Prez, *Adv. Sci.* **2021**, *8*, 2004038; f) B. Genabeek, B. A. G. Lamers, C. J. Hawker, E. W. Meijer, W. R. Gutekunst, B. V. K. J. Schmidt, *J. Polym. Sci.* **2021**, *59*, 373.

[3] R. B. Merrifield, *J. Am. Chem. Soc.* **1963**, *85*, 2149.

[4] a) A. A. Joseph, A. Pardo-Vargas, P. H. Seeberger, *J. Am. Chem. Soc.* **2020**, *142*, 8561; b) A. Pardo-Vargas, M. Delbianco, P. H. Seeberger, *Curr. Opin. Chem. Biol.* **2018**, *46*, 48.

[5] a) R. Behrendt, P. White, J. Offer, *J. Pept. Sci.* **2016**, *22*, 4; b) D. M. M. Jaradat, *Amino Acids* **2018**, *50*, 39; c) E. Valeur, M. Bradley, *Chem. Soc. Rev.* **2009**, *38*, 606.

[6] S. Roy, M. Caruthers, *Molecules* **2013**, *18*, 14268.

[7] U. S. Gunay, B. E. Petit, D. Karamessini, A. Al Ouahabi, J.-A. Amalian, C. Chendo, M. Bouquey, D. Gigmes, L. Charles, J.-F. Lutz, *Chem* **2016**, *1*, 114.

[8] J. W. Grate, K.-F. Mo, M. D. Daily, *Angew. Chem., Int. Ed.* **2016**, *55*, 3925.

[9] P. Espeel, L. L. G. Carrette, K. Bury, S. Capenberghs, J. C. Martins, F. E. Du Prez, A. Madder, *Angew. Chem., Int. Ed.* **2013**, *52*, 13261.

[10] M. Mende, C. Bednarek, M. Wawryszyn, P. Sauter, M. B. Biskup, U. Schepers, S. Bräse, *Chem. Rev.* **2016**, *116*, 8193.

[11] D. Soares Da Costa, R. L. Reis, I. Pashkuleva, *Annu. Rev. Biomed. Eng.* **2017**, *19*, 1.

[12] a) S. Eller, M. Collot, J. Yin, H. S. Hahm, P. H. Seeberger, *Angew. Chem., Int. Ed.* **2013**, *52*, 5858; b) T. Young, L. L. Kiessling, *Angew. Chem., Int. Ed.* **2002**, *41*, 3449.

[13] T. Freichel, V. Heine, D. Laaf, E. E. Mackintosh, S. Sarafova, L. Elling, N. L. Snyder, L. Hartmann, *Macromol. Biosci.* **2020**, *20*, 2000163.

[14] L. Soria-Martinez, S. Bauer, M. Giesler, S. Schelhaas, J. Materlik, K. Janus, P. Pierzyna, M. Becker, N. L. Snyder, L. Hartmann, M. Schelhaas, *J. Am. Chem. Soc.* **2020**, *142*, 5252.

[15] a) R. E. Meléndez, W. D. Lubell, *Tetrahedron* **2003**, *59*, 2581; b) H. Saeidian, M. Abdoli, Z. Mirjafary, *Synthesis* **2015**, *47*, 1057.

[16] a) K. Bruycker, C. Mertens, F. E. Prez, *J. Polym. Sci., Part A: Polym. Chem.* **2019**, *57*, 322; b) P. Espeel, F. E. Du Prez, *Eur. Polym. J.* **2015**, *62*, 247; c) P. Espeel, F. Goethals, F. E. Du Prez, *J. Am. Chem. Soc.* **2011**, *133*, 1678; d) P. Espeel, F. Goethals, M. M. Stamenović, L. Petton, F. E. Du Prez, *Polym. Chem.* **2012**, *3*, 1007.

[17] a) J. C. Barnes, D. J. C. Ehrlich, A. X. Gao, F. A. Leibfarth, Y. Jiang, E. Zhou, T. F. Jamison, J. A. Johnson, *Nat. Chem.* **2015**, *7*, 810; b) M. R. Golder, Y. Jiang, P. E. Teichen, H. V.-T. Nguyen, W. Wang, N. Milos, S. A. Freedman, A. P. Willard, J. A. Johnson, *J. Am. Chem. Soc.* **2018**, *140*, 1596; c) Y. Jiang, M. R. Golder, H. V.-T. Nguyen, Y. Wang, M. Zhong, J. C. Barnes, D. J. C. Ehrlich, J. A. Johnson, *J. Am. Chem. Soc.* **2016**, *138*, 9369.

[18] a) N. Boutard, A. G. Jamieson, H. Ong, W. D. Lubell, *Chem. Biol. Drug Des.* **2010**, *75*, 40; b) N. Boutard, S. Turcotte, K. Beauregard, C.

Quiniou, S. Chemtob, W. D. Lubell, *J. Pept. Sci.* **2011**, *17*, 288; c) S. B. Cohen, R. L. Halcomb, *J. Am. Chem. Soc.* **2002**, *124*, 2534.

[19] S. Rambharose, R. S. Kalhapure, M. Jadhav, T. Govender, *New J. Chem.* **2018**, *42*, 2232.

[20] a) S. Boden, K. G. Wagner, M. Karg, L. Hartmann, *Polymers* **2017**, *9*, 716; b) M. F. Ebbesen, C. Gerke, P. Hartwig, L. Hartmann, *Polym. Chem.* **2016**, *7*, 7086; c) D. Ponader, F. Wojcik, F. Beceren-Braun, J. Dernedde, L. Hartmann, *Biomacromolecules* **2012**, *13*, 1845.

[21] a) J. Coste, D. Le-Nguyen, B. Castro, *Tetrahedron Lett.* **1990**, *31*, 205; b) B. Castro, J. R. Dormoy, G. Evin, C. Selve, *Tetrahedron Lett.* **1975**, *16*, 1219.

[22] a) E. Altuntaş, K. Knop, L. Tauhardt, K. Kempe, A. C. Crecelius, M. Jäger, M. D. Hager, U. S. Schubert, *J. Mass Spectrom.* **2012**, *47*, 105; b) E. Rivera-Tirado, C. Wesdemiotis, *J. Mass Spectrom.* **2011**, *46*, 876.

[23] a) V. Dubovoy, P. Desai, Z. Hao, C.-y. Cheng, G. Verma, L. Wojtas, T. V. Brinzari, J. M. Boyd, S. Ma, T. Asefa, L. Pan, *Cryst. Growth Des.* **2020**, *20*, 4991; b) D. Dupont, E. Renders, S. Raiguel, K. Binnemans, *Chem. Commun.* **2016**, *52*, 7032; c) J. M. Blackburn, M. A. Short, T. Castanheiro, S. K. Ayer, T. D. Muellers, J. L. Roizen, *Org. Lett.* **2017**, *19*, 6012.

[24] J. F. Bower, J. Rujirawanich, T. Gallagher, *Org. Biomol. Chem.* **2010**, *8*, 1505.

Supporting Information

Exploring cyclic sulfamidate building blocks for the synthesis of sequence-defined macromolecules

Stephen Andrew Hill‡, Robert Steinfort‡, Sandra Mücke, Josefine Reifenberger, Tobias Sengpiel, Laura Hartmann**

Institute of Organic Chemistry and Macromolecular Chemistry, Heinrich-Heine-University Düsseldorf, Universitätsstraße 1, 40225 Düsseldorf, Germany

E-mail: laura.hartmann@hhu.de; hills@hhu.de

Contents

* = corresponding author; ‡ = authors contributed equally to this work

General Experimental

Chemicals

Dichloromethane puriss. p.a., ACS reagent, reag. ISO, ≥ 99.9 % (GC); Ethyl acetate puriss. p.a., ACS reagent, reag. ISO, reag. Ph. Eur., ≥ 99.5 % (GC); Chloroform-d 99.8 atom % D; ethanolamine ACS reagent, ≥ 99.0 %; 2-(ethylamino)ethanol ≥ 98 %; 2-Benzylaminoethanol 95 %; $CDCl_3$, piperidine ReagentPlus®, 99 %; triisopropylsilane 98 %; di-*tert*-butyl dicarbonate ReagentPlus®, ≥ 99 %; Ruthenium(III) chloride hydrate ReagentPlus®; Sodium bicarbonate ACS reagent, ≥ 99.7%; *N,N*'-Diisopropylcarbodiimide(DIC) 99 %; and tetrahydrofuran anhydrous, contains 250 ppm BHT as inhibitor, ≥ 99.9 % were purchased from Sigma Aldrich. Ammonium chloride puriss. p.a.; diethyl Ether, puriss. p.a. ACS Reagent, Honeywell™ Puriss. p.a., contains BHT as inhibitor, ACS Reagent, Reag. ISO, Reag. Ph. Eur., ≥ 99.8 %; and acetonitrile, CHROMASOLV™, for HPLC, gradient grade, ≥ 99.9 %, Honeywell Riedel-de Haën™ were all purchased from Honeywell Riedel-de Haën™. Thionyl chloride, 99.7 % was purchased from ACROS Organics. *tert*-Butyl acrylate, 99 %, stab. with 15 ppm 4-methoxyphenol was purchased from Alfa Aeser. TentaGel® S RAM Resin (0.24 mmol/g) was purchased from Rapp Polymere. *N,N*-Dimethylformamide, high purity (> 99.8 %) for peptide synthesis was purchased from BioSolve. 1,8-Diazabicycloundec-7-ene (DBU) and ruthenium(III) chloride hydrate were purchased from Fluorochem. Triethylamine, ≥ 99.5 %; 1,4-Dioxane, ≥ 99.8 %; sodium periodate, analytical reagent grade; trifluoroacetic acid, ≥ 99.5 %; and pyridine, ≥ 99.5 % were purchased from Fischer Scientific. N-Methylmorpholine, 99 % was purchased from J&K Scientific. Silica Gel 60 M, 0,04 - 0,063 mm was purchased from Machery-Nagel. *N,N*-Diisopropylethylamine (DIPEA) ≥ 99 %, zur Synthese; sodium chloride ≥99,5 %, p.a., ACS, ISO; (Ethylcyano(hydroxyimino)-acetato-O2)tri-1-pyrrolidinylphosphonium-hexafluorphosphat (PyOxim); Celite® 545; and deuterium oxide, 99.8 atom%D were all purchased from Carl Roth. Benzotriazole-1-yl-oxy-tris-pyrrolidino-phosphonium hexafluorophosphat (PyBOP) and N-alpha-(9-Fluorenylmethyloxycarbonyl)-L-phenylalanine (Fmoc-Phe-OH) were purchased from Iris Biotech. Fmoc-Lys(Boc)-OH, 98 %; (1-Cyano-2-ethoxy-2-oxoethylidenaminooxy)dimethylamino-morpholino-carbenium hexafluorophosphate (COMU), 98+%; and Oxyma Pure, 98.57 % were all purchased from BLD Pharamtech. Water was purified with a Milli-Q-system by Millipore with a final resistivity of 18 MΩcm. For anion counter exchange AG® 1-X8 Anion Exchange Resin, analytical grade, 100–200 mesh, acetate form, 500 g #1401443 from BIO-RAD was utilized.

Methods

NMR

^{1}H NMR and ^{13}C NMR spectra were recorded at room temperature with a Bruker AVANCE III 300 (for 300 MHz) and 600 (for 600 MHz). The chemical shifts were reported relative to solvent peaks (chloroform and water) as internal standards and reported as δ in parts per million (ppm). Multiplicities were abbreviated as s for singlet, d for doublet, t for triplet and m for multiplet. For small molecule building block spectra please see Appendix.

FTIR

FT-IR spectra were recorded on Shimadzu IRAffinity-1 (FTIR-8400S), scanning between 600 – 4000 cm^{-1} with a minimum of 25 scans being recorded for a given spectrum (data plotted as %transmission). The samples were measured directly and no further preparation was required. All the data and automatic peak fitting etc. was conducted through IRSolution software.

Reverse Phase – High Performance Liquid Chromatography – Mass Spectrometry (RP-HPLC-MS)

For HPLC and MS analysis, an Agilent 1260 Infinity instrument combined with a variable wavelength detector (VWD) with an adjusted wavelength of 214 nm and a 6120 Quadrupole LC/MS with an electrospray ionization source was used. All measurements were performed in either positive and negative ionization mode in a m/z range of 200 to 2000. For the analysis, a poroshell 120 EC-C18 3.0x50 mm, 2 µm reverse phase (RP) from Agilent was used with the following mobile phases: 95/5 (H_2O/MeCN) (mobile phase A) and 5/95 (H_2O/MeCN) (mobile phase B) both with 0.1 % formic acid. For measurements investigating the branching of primary amines with cyclic sulfamidate building blocks the formic acid component was removed, but the exact same conditions were repeated. The flow rate was set to 0.40 mL/min using a linear gradient starting from 0 % mobile phase B to 50 % mobile phase B in 17 or 30 min with a column temperature of 25 °C. ESI-MS analytics and assignments were informed by ESI-MS adduct calculator.[1] For the assignments of Fmoc-protected **6** and **11** and the cleavage products arising solely from TentaGel® S RAM, please see the Appendix.

Matrix-assisted Laser Desorption Ionisation-Time of Flight (MALDI-TOF)-Mass Spectrometry

MALDI measurements were performed on a Ultraflex I from Bruker Daltonics. Probes were measured in a linear mode using 2,5-dihydroxybenzoic acid (DHB) as MALDI matrix (2:1 ratio against MeCN:H_2O (1:1)).

Elemental Analysis

The ratio of carbon, hydrogen, nitrogen and sulfur were determined using a Vario Micro Cube provided by Analysensysteme GmbH. The theoretical values for oligomeric probes were calculated bearing 3 acetate ions.

Freeze Dryer

Lyophilization (or freeze drying) was performed with an Alpha 1-4 LD instrument provided by Martin Christ Freeze Dryers GmbH. A temperature of –42 °C and a pressure of 0.1 mbar were maintained throughout the freeze-drying process.

General Synthetic Protocols

Building Blocks

Please see below for specific protocols for the cyclic sulfamidates. The synthesis of EDS has been previously reported from our group.[2] The synthesis of Fmoc-protected isonipecotic acid 1**7** was conducted as previously reported by Olsen *et al*.[3] For NMR spectra of the respective building blocks please see the Appendix.

Resin Handling

The SPS resin used for all reaction described was TentaGel® S RAM (0.24 mmol/g, RAPP Polymere) which was into BD syringe reactors containing an inlet frit (10 mL for 0.5 mmol batch sizes). Prior to any reactions, the dry resin was swollen in DCM (2 x 5 mL) for 15 min slots with agitation.

Amide Coupling Strategy

Refers to the amide coupling of EDS, Fmoc-protected isonipecotic acid **17**, Fmoc-Phe-OH, and Fmoc-Lys(Boc)-OH.

For amide coupling steps a 5-fold excess of building block and a 4.9-fold excess of PyBOP was first dissolved in DMF (1.5 mL for 0.005 mmol, 3 mL for 0.05 mmol). Activation was performed by adding a 10-fold excess of DIPEA to the reaction solution with shaking for 3-5 min. The activated solution was taken up into the reaction syringe, and the coupling was performed over a period of 1.5 h while continuously shaking. After coupling, the resin was washed with DMF (10 times) and DCM (3 times) using maximal syringe capacity.

Fmoc Cleavage

Fmoc protecting groups from either the resin or attached building blocks (0.05 mmol scale) were deprotected using 25 % piperidine in DMF (2 x 5 mL) for an initial 10 min and 20 min. Between each treatment with 25 % piperidine in DMF the resin was washed with DMF (3 x 5 mL). After deprotection the resin was additionally washed with DMF (10 x 5 mL) and DCM (3 x 5 mL).

Boc Cleavage

To deprotect Boc groups from lysine side-chains the solid phase was treated with 4 M HCl in dioxane (5 mL) for 5 min and 25 min with agitation. Between the separate treatments, resin was washed with dioxane (3 x 5 mL). The resin was subsequently washed with dioxane (2 x 5 mL) and then alternatively washed with DCM (3 x 5 mL) and 2-propanol (3 x 5 mL). To ensure resin-bound free base amines the resin was exposed to 10 % DIPEA in DCM solution (5 mL) for 10 min. The resin was subsequently washed with dioxane (2 x 5 mL) and then alternatively washed with DCM (3 x 5 mL) and 2-propanol (3 x 5 mL), before re-exposure to 10 % DIPEA in DCM solution (5 mL) for 10 min. The resin was subsequently washed with dioxane (2 x 5 mL) and then alternatively washed with DCM (3 x 5 mL) and 2-propanol (3 x 5 mL); twice washed with DIPEA in DMF (0.2 M) (2 x 5 mL), and finally with DMF (10 x 5 mL).

Cyclic Sulfamidate Amide Coupling Protocol (Latent Coupling Strategy)

Under N_2 atmosphere **1** (0.0625 mmol) was dissolved in DMF (1.5 mL) and the appropriate coupling reagent (0.0625 mmol) was added, followed by DIPEA (66 µL, 0.3125 mmol). The solution was agitated

for 5-10 min prior to being taken up into a reactor syringe containing deprotected, amine-bearing resin (0.0125 mmol). The syringe was agitated for shaken for 60 min and the resin was washed with DMF (12 x 5 mL) and DCM (3 x 5 mL).

Change the equivalents, time, and reagent as appropriate according to Table S1.

Cyclic Sulfamidate Ring-Opening Protocol (Active Coupling Strategy)

To a deprotected, amine-presenting resin (0.05 mmol) was added a solution containing cyclic sulfamidate BB (1.25 mmol: equivalent to 25 eq. per amine) and DIPEA (220 µL, 1.25 mmol) in DMF (10 mL). The reaction syringe was shaken for 60 min and the resin was then washed with DMF (12 x 5 mL) and DMF (3 x 5 mL).

Change the equivalents, time, cyclic sulfamidate building block as appropriate according to Table S3. Reactions at 40 ^{o}C were conducted using a CEM Discoverer Microwave Reactor in a sealed 2-5 mL microwave vial.

Cleavage from solid support

For total cleavage from TentaGel® S RAM an acidic solution (TFA:TIPS:DCM, 95:2.5:2.5) was added to the resin (1 mL for 0.005 mmol, 3 mL for 0.05 mmol). After 60 min agitation at room temperature, the sulfated oligomers were syringed into ice-cold diethyl ether (40 mL) and a precipitate was observed (cloudy solution). The resin was subsequently washed three times alternating between DCM (5 mL) and MeOH (5 mL). The washings were collected, evaporated *in* vacuo and re-dissolved in DCM (3 mL) and were precipitated in ice-cold diethyl ether (20 mL). All the precipitate-containing solutions were centrifuged until the organic phase was clear. The precipitate was then washed with copious amounts of diethyl ether between centrifuging, prior to being dissolved in H_2O (4-5 mL) before freeze-drying (lyophilizing).

The obtained product was then treated with anionic exchange resin to afford acetate counter ions (see below), following freeze-drying the probes were analyzed were possible by ^{1}H NMR, ESI-MS, elemental analysis, and FT-IR. Probes were noted to be hygroscopic/fine oils and so extremely difficult to physically manipulate.

Anionic Exchange Resin

To achieve a global exchange of counter ions for acetate ions was conducted in the following way: resin (1 g resin/0.1 mmol oligomer) was activated by washing with acetic acid solution (3 x 1.6 M and 3 x 0.16 M; *ca.* 90 s per wash). The probe was dissolved in MQ H_2O (*ca*. 2 mL) and exposed to the activated resin in a reactor syringe with shaking for 60 min. The resin was separated from the solution and washed with MQ H_2O (3 x 1.5 mL). All the fractions were collected, and freeze-dried to afford the final product which were analyzed by ^{1}H NMR and FT-IR spectroscopy, ESI-MS, and elemental analysis.

Synthesis

Small Molecule Building Blocks

For NMR spectra – please see Appendix at the end of this document.

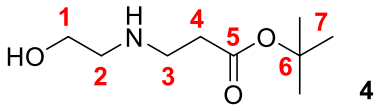

4

In a modified approach from Rambharose *et al*.:[4] To a solution of *tert*-butyl acrylate **3** (135.0 g, 1.05 mol) in methanol (500 mL), ethanolamine **2** (61.0 g, 1.0 mol) was added at RT and stirred for 24 h. Excess reagents and solvent were removed *in vacuo* and 15 g of resulting thick oil residue was purified by flash column chromatography. Initially hexane and ethyl acetate (1:4, v/v) was utilized to remove the double-coupled side product (Rf = 0.65 (Hex:EtOAc, 1:4, v/v)), and then DCM:MeOH (4:1 v/v) was used to elute the desired product **4** (Rf = 0.38 Hex:EtOAc, 1:4, v/v)) (7.17 g, 38 mmol) as a thick colorless oil.

^{1}H NMR (300 MHz, $CDCl_3$): δ = 3.64 (t, J = 5.1 Hz, 2H, **1**), 2.87 (t, J = 6.4 Hz, 2H, **3**), 2.79 (t, J = 5.19 Hz 2H, **2**), 2.44 (t, J = 6.4 Hz, 2H, **4**), 1.44 (s, 9H, **7**) ppm. ^{13}C NMR (75 MHz, $CDCl_3$): δ = 172.1 (**5**), 81.0 (**6**), 60.5 (**1**), 50.8 (**2**), 44.8 (**3**), 35.2 (**4**), 28.2 (**7**). MS (ESI positive mode): m/z calculated for $C_9H_{19}NO_3$: 189.14; found 206.0 $[M+NH_4]^+$ All in accordance with literature.[4] ^{1}H-^{13}C HSQC spectra is shown in Appendix to illustrate full characterization of each methylene in **4**.

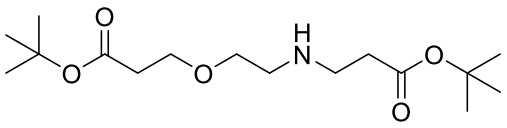

doubly-coupled side product

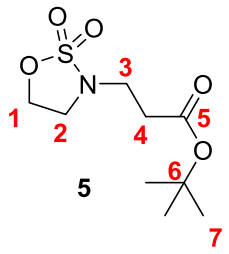

5

Imidazole (18.09 g, 265.2 mmol) was dissolved in DCM (120 mL) and stirred at 0 °C (ice-bath) for 10 min. To this solution thionyl chloride (5.8 mL, 79.5 mmol) in DCM (60 mL) was added dropwise and the reaction mixture was allowed to warm to RT over 60 min. Then the reaction mixture was cooled to -78 °C (dry ice/acetone) before **4** (7.17 g, 38 mmol) dissolved in DCM (120 mL) was added dropwise over 30 min. The reaction mixture was then allowed to stir for 16 h warming to RT. The reaction mixture was filtered over Celite, with DCM washings, and the collected organic phase was washed with H_2O (3 x 100 mL). The phases were separated and the aqueous phase was back-extracted with DCM (100 mL). All organics were combined, dried over $MgSO_4$, filtered, and evaporated *in vacuo* to afford an intermediate (8.61 g).

A portion of the intermediate (4.3 g) was dissolved in MeCN (100 mL) and cooled to 0 °C (ice-bath) and stirred for 10 min. After this time sodium periodate (5.87 g, 18.3 mmol), $RuCl_{3.x}H_2O$ (58 mg) and H_2O (100 mL) were added sequentially and the reaction was stirred for 30 min at 0 °C and allowed to warm to RT over 16 h. The reaction mixture was diluted with Et_2O (100 mL) and the phases separated. The retained organic phase was then sequentially washed with H_2O (2 x 100 mL) and brine (100 mL). Aqueous phases were back-extracted with Et_2O (2 x 100 mL). All organic phases were combined and allowed to stir overnight with active charcoal (2 g) to remove Ru salts. After filtration, the solution was dried over $MgSO_4$, filtered and evaporated *in vacuo* to afford a colorless oil (**5**) (3.05 g, 12 mmol, 66 % over two steps).

^{1}H NMR (300 MHz, $CDCl_3$): δ = 4.53 (t, J = 6.5 Hz, 2H, **1**), 3.60 (t, J = 6.5 Hz, 2H, **2**), 3.38 (t, J = 6.8 Hz, 2H, **3**), 2.60 (t, J = 6.8 Hz, 2H, **4**), 1.47 (s, 9H, **7**) ppm. ^{13}C-NMR (75 MHz, $CDCl_3$): δ = 170.2 (**5**), 81.6 (**6**), 66.7 (**1**), 48.6 (**2**), 43.8 (**3**), 34.5 (**4**), 28.2 (**7**) ppm. MS (ESI positive mode): m/z calculated for $C_9H_{17}NO_5S$: 251.09; found 274.07 [M+Na]; (ESI negative mode): m/z calculated for $C_9H_{17}NO_5S$: 251.0; found 268.0 [M+OH]

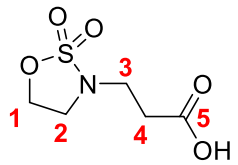

1

5 (250 mg, 1.28 mmol) was dissolved in TFA:DCM (2.5 mL, 1:1, v/v) and allowed to stir for 2.5 h to complete the deprotection. The solution was exposed to a stream of N_2 inert gas for a minimum of 1 h until the solution was completely evaporated. The residual oil was used directly in the coupling to amine-functionalized resins see Table S1.

^{1}H NMR (300 MHz, $CDCl_3$): δ = 4.55l (t, J = 6.48 Hz, 2H, **4**), 3.62 (t, J = 6.54 Hz, 2H, **3**), 3.44 (t, J = 6.69 Hz, 2H, **2**), 2.77 (t, J = 6.63 Hz, 2H, **1**) ppm. ^{13}C-NMR (75 MHz, $CDCl_3$): δ = 176.2 (**5**), 66.8 (**1**), 48.8 (**2**), 43.4 (**3**), 33.0 (**4**) ppm.

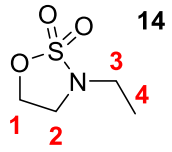

N-ethyl-ethanolamine (3.61 g, 40.5 mmol) was dissolved in DCM (20 mL) and cooled under stirring to -40 ^{o}C (dry ice/MeCN) under N_2 (g). To this solution was added pyridine (6.4 mL, 79 mmol) dropwise and after completion allowed to stir for a further 10 min. Then thionyl chloride (3.6 mL, 50 mmol) in DCM (20 mL) was added dropwise over 30 min. The reaction was stirred at -40 ^{o}C for 60 min. H_2O (50 mL) was subsequently added and stirring continued for a further 10 min. The phases were then separated and the aqueous phase back extracted with DCM (3 x 50 mL). All organics were combined and sequentially washed with 1 M HCl, sat. $NaHCO_3$, and brine; dried over $MgSO_4$, filtered, and evaporated *in vacuo* to afford a colorless oil. This crude oil was dissolved in MeCN (80 mL) and cooled under stirring to 0 ^{o}C (ice-bath). To this solution was sequentially added sodium periodate (12.8 g, 60 mmol), $RuCl_{3.x}H2O$ (10 mg) and H_2O (80 mL), and the reaction mixture was stirred for 60 min at RT. DCM (80 mL) was subsequently added and vigorous stirring continued for 10 min prior to phase separation. The aqueous phase was extracted against DCM (3 x 80 mL). The combined organics were washed against brine, dried over $MgSO_4$, filtered, and evaporated *in vacuo* to afford a colorless oil (1.59 g, 10.5 mmol, 26 %).

^{1}H NMR (300 MHz, $CDCl_3$) δ: 4.51(t, 2H, J = 6.54 Hz, **1**), 3.51 (t, 2H, J = 6.54 Hz, **2**), 3.12 (q, 2H, J = 7.26 Hz, **3**), 1.26 (t, 3H, J = 7.26 Hz **4**). ^{13}C NMR (75 MHz, $CDCl_3$) δ: 66.6 (**1**), 47.5 (**2**), 42.7 (**3**), 12.9 (**4**). MS (ESI negative mode): m/z calculated for $C_4H_9NO_3S$: 151.1; found: 168.0 [M+OH]

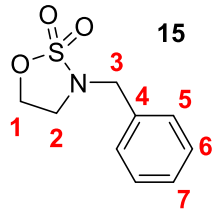

To a stirring solution of N-benzylethanolamine (6.13 g, 40.5 mmol) in DCM (20 mL) cooled to 0 °C (ice-bath) was added pyridine (6.4 mL, 79 mmol), under N_2 (g), which was allowed to stir for 10 min. Then a solution of thionyl chloride (3.6 mL, 50 mmol) in DCM (20 mL) was slowly added dropwise over 20 min. The reaction mixture was stirred for 4 h at 0 °C. H_2O (50 mL) was added and the solution was vigorously stirred for 5 min before the phases were separated. The aqueous phase was back-extracted with DCM (3 x 50 mL), and the combined organics were sequentially washed with 1M HCl, sat. $NaHCO_3$, and brine, dried over $MgSO_4$, filtered, and evaporated *in vacuo* to afford a colorless oil. This oil was then immediately dissolved in MeCN (80 mL) and cooled with stirring to 0 °C (ice-bath). To this solution was sequentially added sodium periodate (12.8 g, 60 mmol), $RuCl_3.xH_2O$ (10 mg) and H_2O (80 mL), and the reaction mixture was stirred for 16 h at RT. DCM (80 mL) was subsequently added and vigorous stirring continued for 10 min prior to phase separation. The aqueous phase was extracted against DCM (3 x 80 mL). The combined organics were washed against brine, dried over $MgSO_4$, filtered, and evaporated *in vacuo*. The resulting oil was crystallized from diethyl ether to afford colorless crystals (4.40 g, 20.6 mmol, 50 %).

^{1}H NMR (300 MHz, $CDCl_3$) δ: 7.37 (m, 5H, **4-7**), 4.51 (t, 2H, J = 6.54 Hz, **1**), 4.23 (s, 2H, **3**), 3.41 (t, 2H, J = 6.54 Hz, **2**). ^{13}C NMR (75 MHz, $CDCl_3$) δ: 134.4 (**4**), 129.0 (**6**), 128.7 (**5**), 128.6 (**7**), 66.8 (**2**), 51.6 (**3**), 47.2 (**1**). MS (ESI negative mode): m/z calculated for $C_9H_{11}NO_3S$: 213.2; found: 230.0 [M+OH]

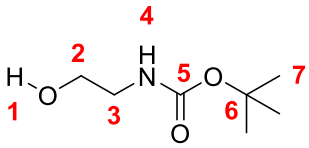

Precursor for **16**

Ethanolamine (8.12 g, 133 mmol) was dissolved in DCM (400 mL) and stirred at 0 °C for 10 min. To this solution was added triethylamine (27.5 mL, 197 mmol), followed by 5 min stirring, and then di-*tert*-butyl-dicarbonate (29.23 g, 134 mmol). The resulting mixture was stirred overnight whilst warming to room temperature. After 24 h stirring sat. NH_4Cl solution (400 mL) was added to the reaction mixture and with vigorous stirring the two phases were thoroughly mixed for 10 min. The phases were separated and the retained aqueous was extracted against EtOAC (3 x 300 mL). Organic phases were combined and washed against brine, dried over MgSO4, filtered and evaporated *in vacuo* to afford a yellow oil (21.3 g, quant.), which was carried forward without purification.

^{1}H NMR (300 MHz, $CDCl_3$) δ: 3.67 (t, 2H, J = 4.89 Hz, **2**), 3.26 (t, 2H, J = 5.28 Hz, **3**), 1.43 (s, 9H, **7**). ^{13}C NMR (75 MHz, $CDCl_3$) δ: 156.8 (**5**), 79.7 (**6**), 62.4 (**2**), 43.2 (**3**), 28.3 (**7**). MS (ESI): m/z calculated for $C_7H_{16}NO_3$: 161.1; found: 162.2 [M+H]. In accordance with literature values.[5]

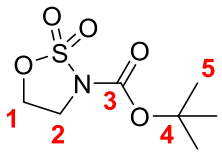

16

To stirring MeCN (100 mL), which was kept under an inert N_2 atmosphere and cooled to -40 °C (Dry ice/MeCN bath) was added thionyl chloride (1.80 mL, 24.8 mmol). This solution was allowed to stir for 10 min, prior to the dropwise addition of N-Boc-ethanolamine (3.22 g, 20 mmol) in MeCN (10 mL). After addition was complete, the solution was allowed to stir for a further 5 min, before pyridine (6.5 mL, 80 mmol) was added dropwise and the reaction allowed to stir for 60 min at -40 °C and a further 60 min at 0 °C (ice-bath). The development of a yellow colour was noted. EtOAc (150 mL) and H_2O (100 mL) was added to the reaction mixture and followed phase separation the organic phase was sequentially extracted against 1 M HCl, sat. $NaHCO_3$, and brine. The combined organics were dried over $MgSO_4$, filtered and evaporated *in vacuo* to afford a yellow-brown oil. The crude oil was immediately dissolved in MeCN (80 mL) and cooled to 0 °C (ice-bath) with stirring. After 15 min stirring, sodium periodate (6.42 g, 30 mmol), $RuCl_3.{}_xH_2O$ (10 mg), and H_2O (80 mL) were added, in that order respectively. The reaction was stirred for 60 min or until all starting material had been consumed (as observed by TLC visualized by $KMnO_4$). Upon completion H_2O (80 mL) and Et_2O (80 mL) were added to the reaction mixture and allowed to mix for 10 min. After separating the phases, the aqueous was further extracted with Et_2O (3 x 100 mL). All organic phases were combined, washed with brine, dried over $MgSO_4$, filtered, and evaporated *in-vacuo* to afford an off-white solid, which was recrystallized either from chloroform or DCM:Et_2O (5:1) to afford a white solid (**16**) (3.70 g, 16.5 mmol, 82 %).

^{1}H NMR (300 MHz, $CDCl_3$) δ: 4.60 (t, 2H, J = 6.51 Hz, **1**), 4.03 (t, 2H, J = 6.42 Hz, **2**), 1.54 (s, 9H, **5**). ^{13}C NMR (75 MHz, $CDCl_3$) δ: 148.6 (**3**), 85.5 (**4**), 65.5 (**1**), 45.2 (**2**), 27.9 (**5**). MS (ESI negative mode): m/z calculated for $C_7H_{13}NO_5S$: 223.24; found: 240.0 [M+OH] Matched literature values.[6]

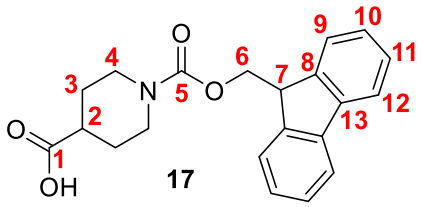

17

In a slightly modified procedure to that published by Olsen *et al.*:[3] To a solution of isonipecotic acid (5 g, 38.7 mmol)), Na_2CO_3 (51.9 g, 194 mmol) in H_2O (200 mL) in a 1 L round-bottomed flask was added 9-Fluorenylmethoxycarbonyl chloride (Fmoc-Cl, 11.0 g, 42.5 mmol) in 1,4-dioxane (200 mL) dropwise under extremely vigorous stirring. A white solid was immediately formed upon solution mixing and the resulting slurry was vigorously stirred for 24 h at RT. H_2O (200 mL) was added to the reaction and the mixture subsequently extracted with Et_2O (4 x 200 mL). The aqueous was acidified with 2M HCl to pH 1-2 and then subsequently extracted with EtOAc (4 x 200 mL). The organics were combined, dried over $MgSO_4$, filtered and concentrated *in vacuo* to yield a yellow/off-white solid (**17**) (12.8 g, 36 mmol, 93 %).

^{1}H NMR (300 MHz, $CDCl_3$): δ = 7.77 (d, J = 7.4 Hz, 2 H, **12**), 7.57 (d, J = 7.3 Hz, 2 H, **9**), 7.40 (t, J = 7.0 Hz, 2H, **11**), 7.32 (t, J = 8.4 Hz, 2H, **10**), 4.44 (br d, 2 H, **6**), 4.24 (t, J = 6.7 Hz, 1H, **7**) 4.15-3.90 (br s, 2 H, **4**), 2.95 (br t, J = 12.0 Hz, 2 H, **4**), 2.51 (complex m, 1H, **2**), 1.91 (br s, 2 H, **3**), 1.65 (br m, 2H, **3**) ^{13}C NMR (75 MHz, $CDCl_3$): δ = 179.4 (**1**), 155.2 (**5**), 143.9 (**8**), 141.3 (**13**), 127.7, 127.0 (**11**, **12**), 124.9 (**10**), 120.0 (**9**), 67.3 (**6**), 47.3 (**7**), 43.1 (**4**), 40.5 (**2**), 27.6 (**3**) MS (ESI positive mode): m/z calculated for $C_{21}H_{21}NO_4$: 351.1; found 352.2 [M+H]. In-line with literature results.[3]

Synthetic Outline for *N*-sulfated oligo(amidoamines) **20-23**

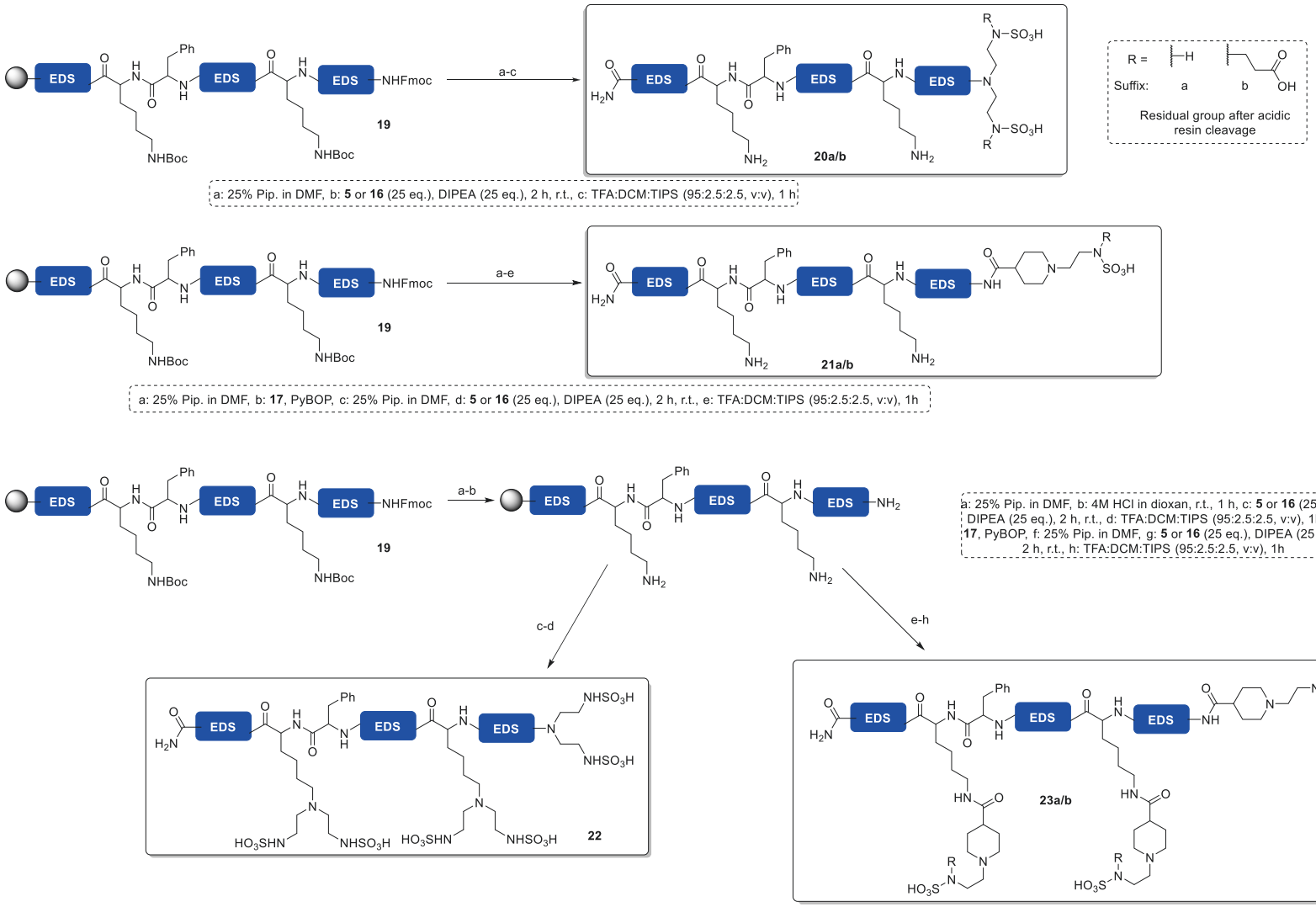

Additional Figures, Schemes and Tables

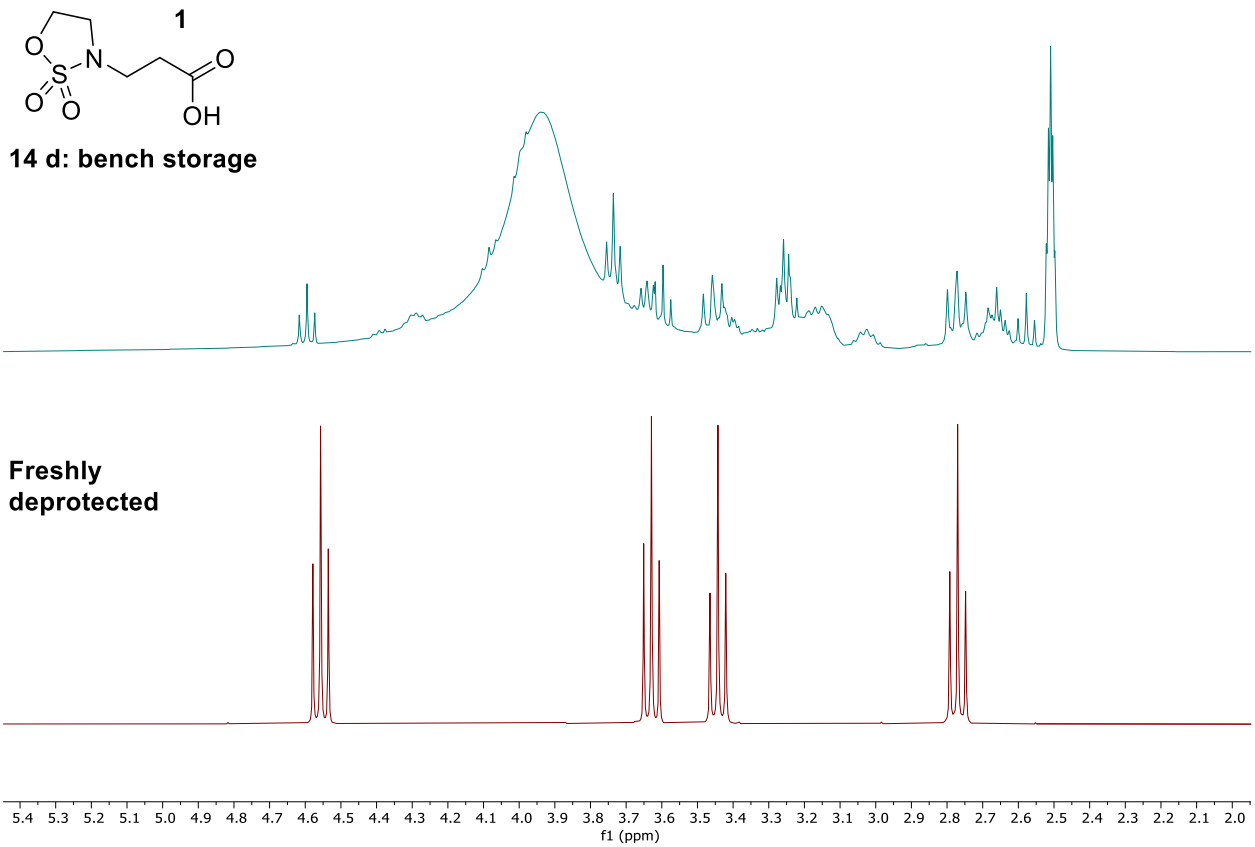

Figure S1: Stacked plot of ^{1}H NMR spectra of **1** measured (below) directly after acidic deprotection and (above) after 14 d storage on the bench

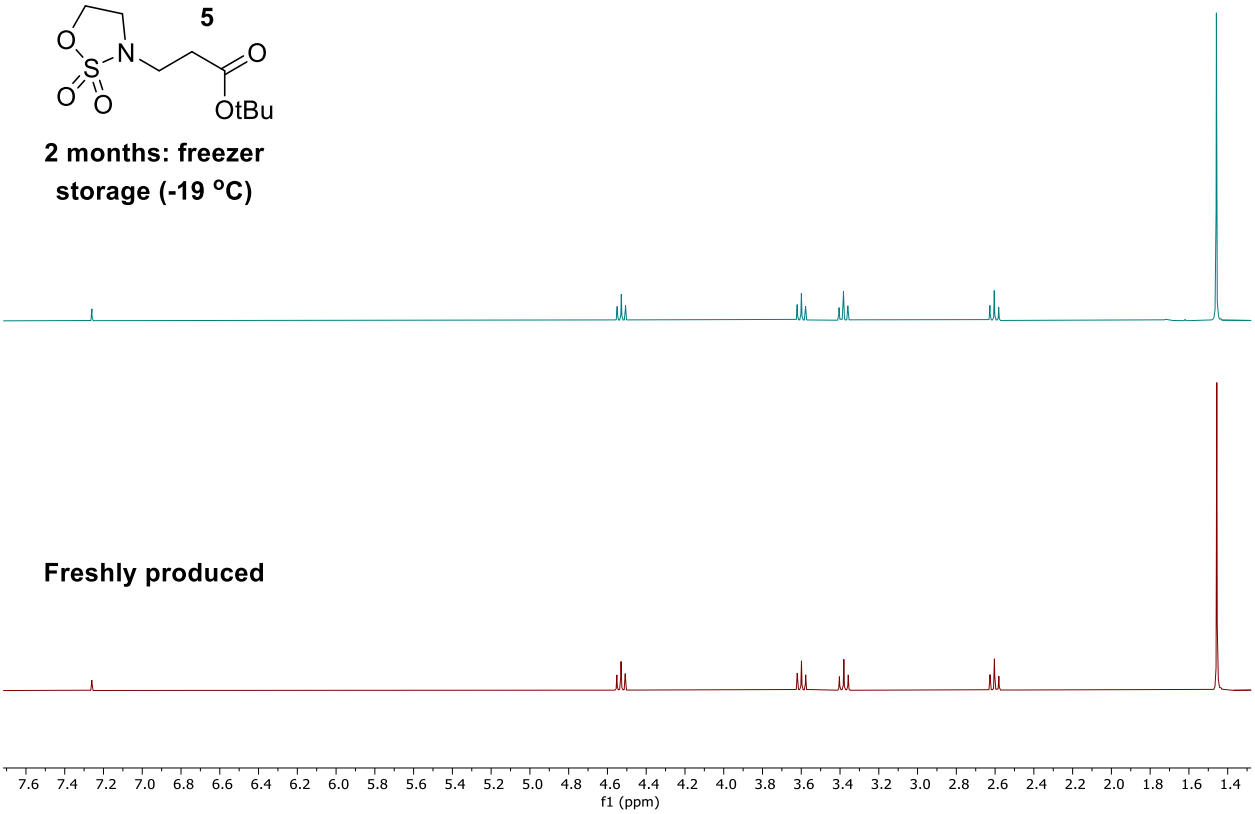

Figure S2: Stacked plot of ^{1}H NMR (300 MHz, $CDCl_3$) spectra of **5** measured (below) directly after synthesis and (above) after 2 months' low temperature (-19 °C) freezer storage

Latent Coupling Strategy Results

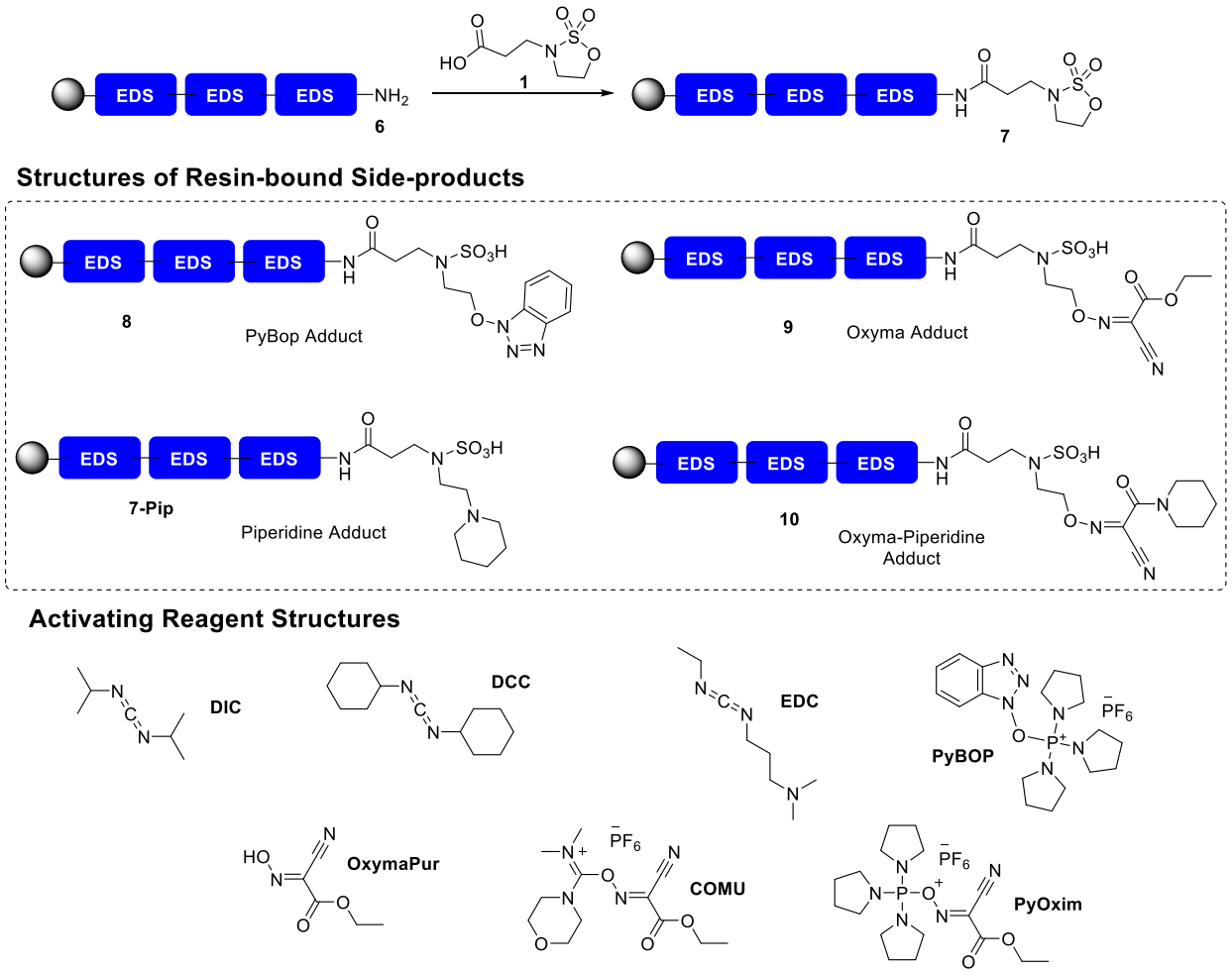

Figure S3: The coupling of **1** to an EDS_3 resin-bound anchor (**6**) with the identified side-products and coupling reagent structures

Table S1: Coupling conditions investigated for the latent coupling strategy of **1**

				Observed Products				
Entry	**Anchor**	**Coupling System (Eq.)**	**Base (Eq.)**	**100% Conversion**	**Coupled Product**	**Piperidine Adduct**	**Coupling System Adduct**	**Oxyma-Pip. Adduct**
1	**6**	PyBOP (5)	NMM (273)	N	-	-	Y	-
2	**6**	PyBOP (5)	DIPEA (25)	N	-	-	Y	-
3	**6**	PyBOP (2)	DIPEA (25)	N	-	-	Y	-
4	**6**	EDC (5)	NMM (273)	N	-	-	-	-
5	**6**	EDC (5)	DIPEA (25)	N	-	-	-	-
6	**6**	DIC (5)	DIPEA (25)	N	-	-	-	-
7	**6**	DCC (5)	DIPEA (25)	N	-	-	-	-
8	**6**	COMU (5)	DIPEA (25)	N	Y	Y	Y	Y
9	**6**	PyOxim (5)	DIPEA (25)	N	Y	Y	Y	Y
10	**6**	OxymaPur-DIC (5)	DIPEA (25)	N	Y	Y	Y	Y

Y = Yes i.e. the corresponding action or product was observed. N = No. Please see below for representative RP-HPLC and ESI-MS evidence from selected conditions from Table S1.

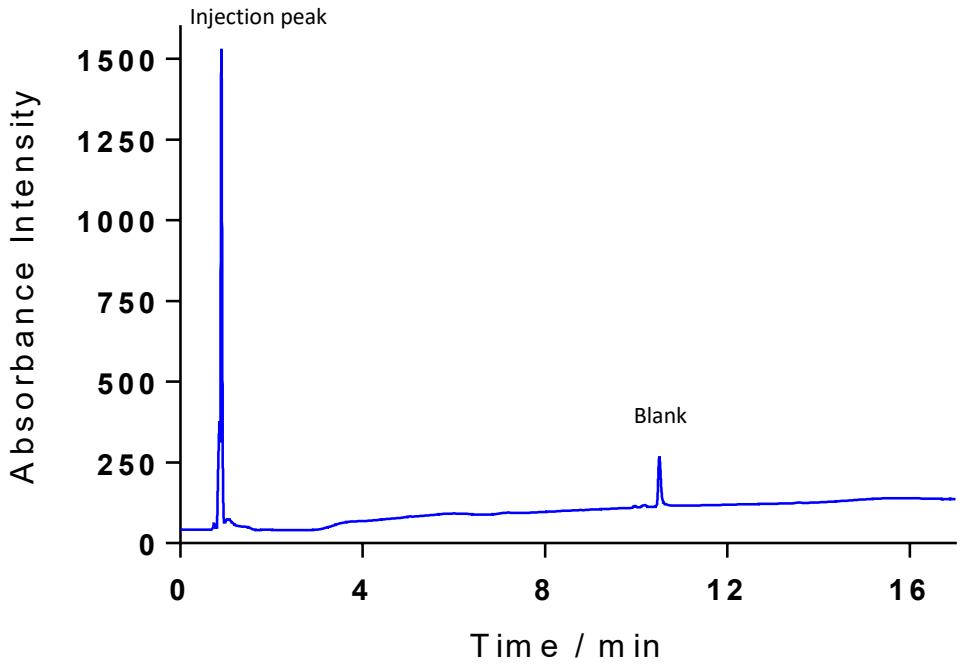

Figure S4: RP-HPLC chromatogram (Gradient 5-95 vol% - MeCN in H_2O (0.1 vol% formic acid) for **6**

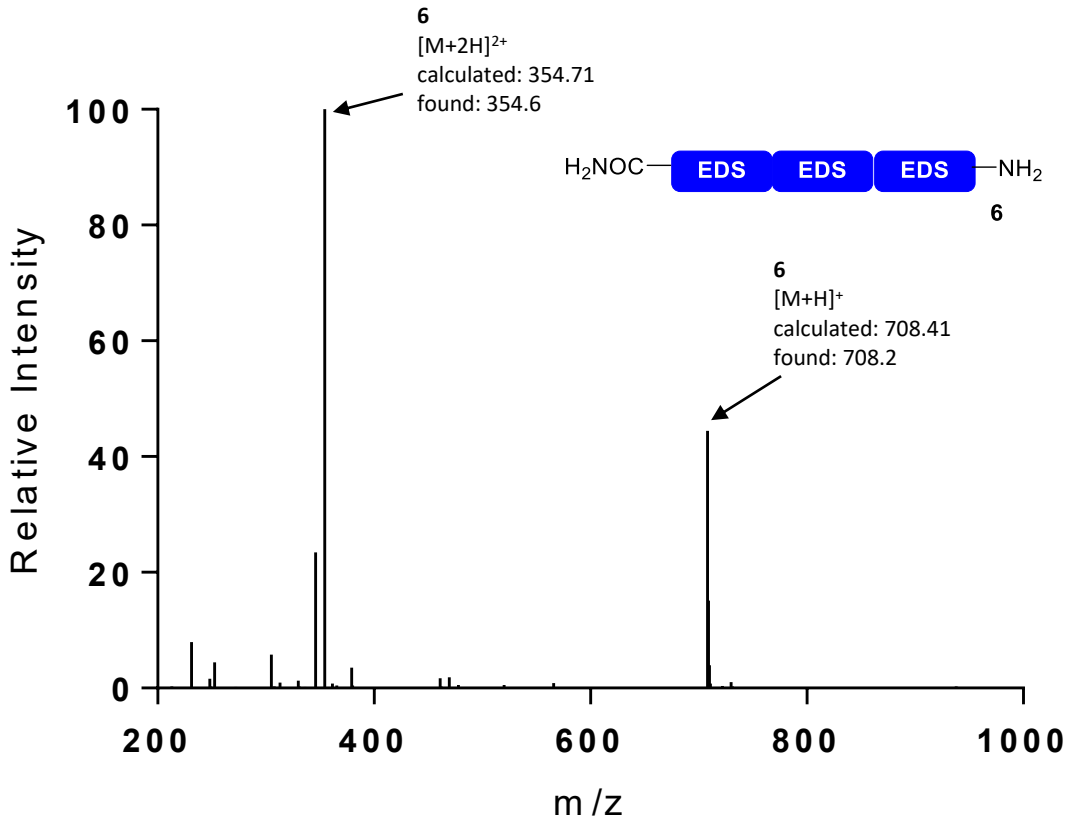

Figure S5: ESI-MS for **6** (injection peak) as showed in Figure S4

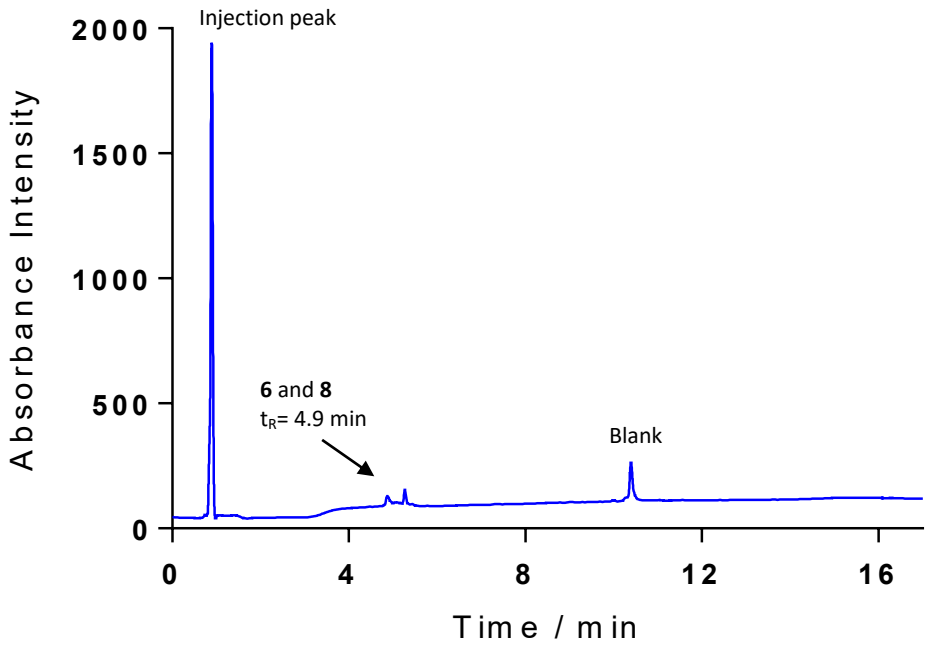

Figure S6: RP-HPLC chromatogram (Gradient 5-95 vol% - MeCN in H_2O (0.1 vol% formic acid) for entry 1, Table S1

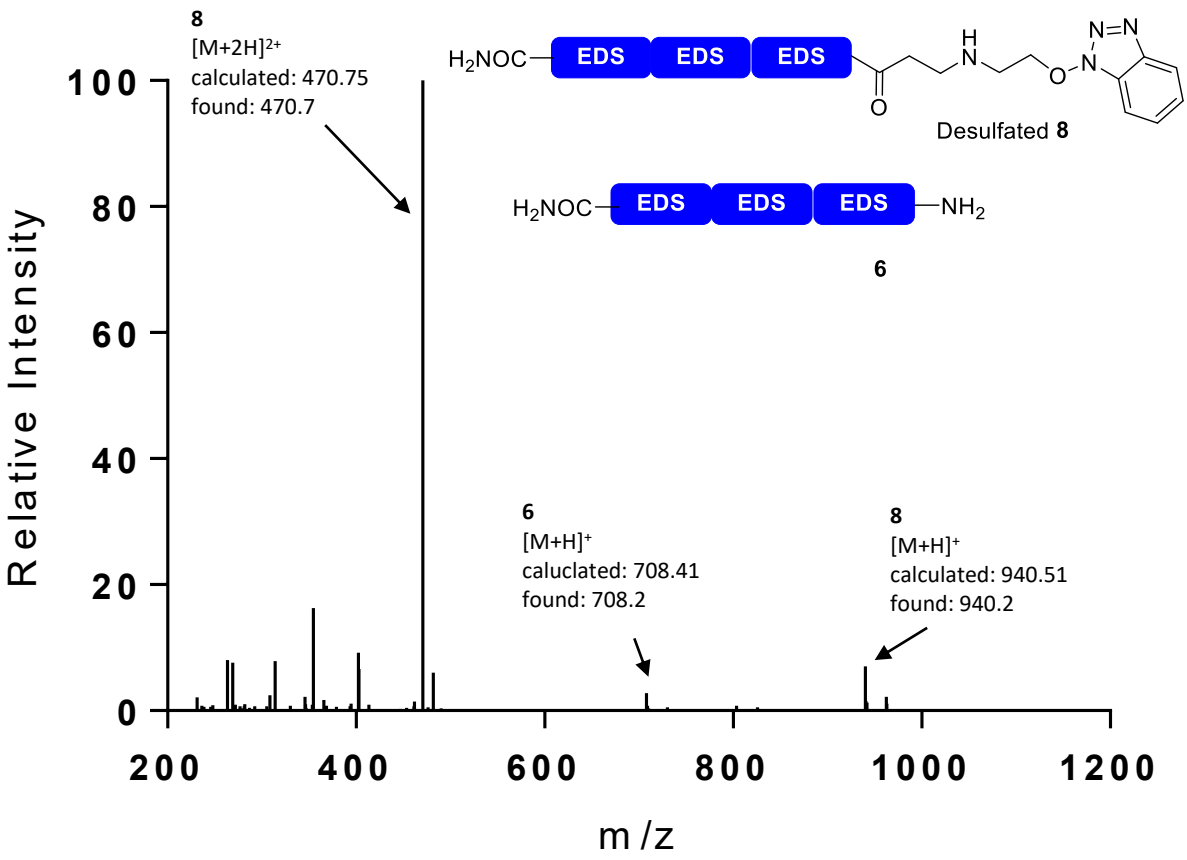

Figure S7: ESI-MS for entry 1, Table S1 showing the presence of **6** and **8**

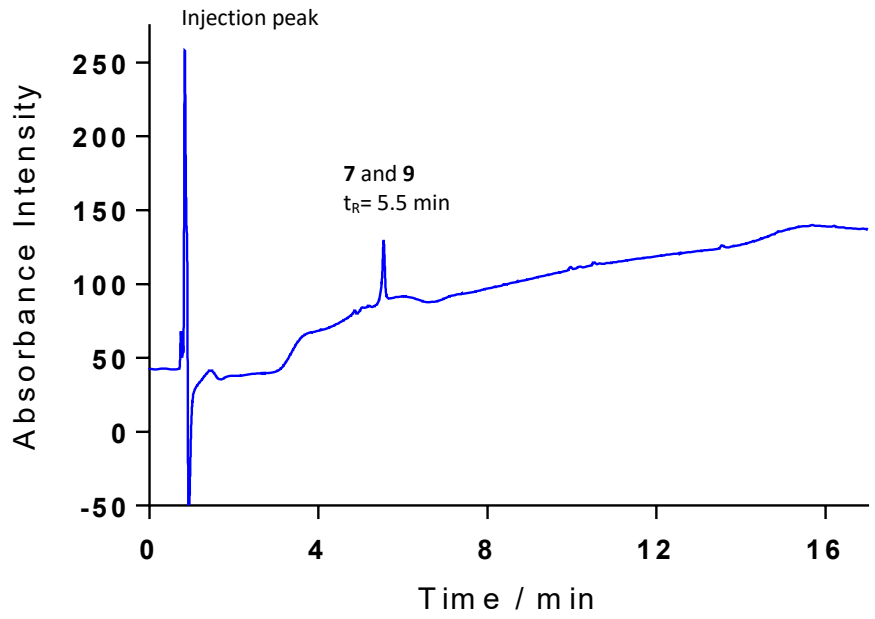

Figure S8: RP-HPLC chromatogram (Gradient 5-95 vol% - MeCN in H_2O (0.1 vol% formic acid) for entry 10, Table S1

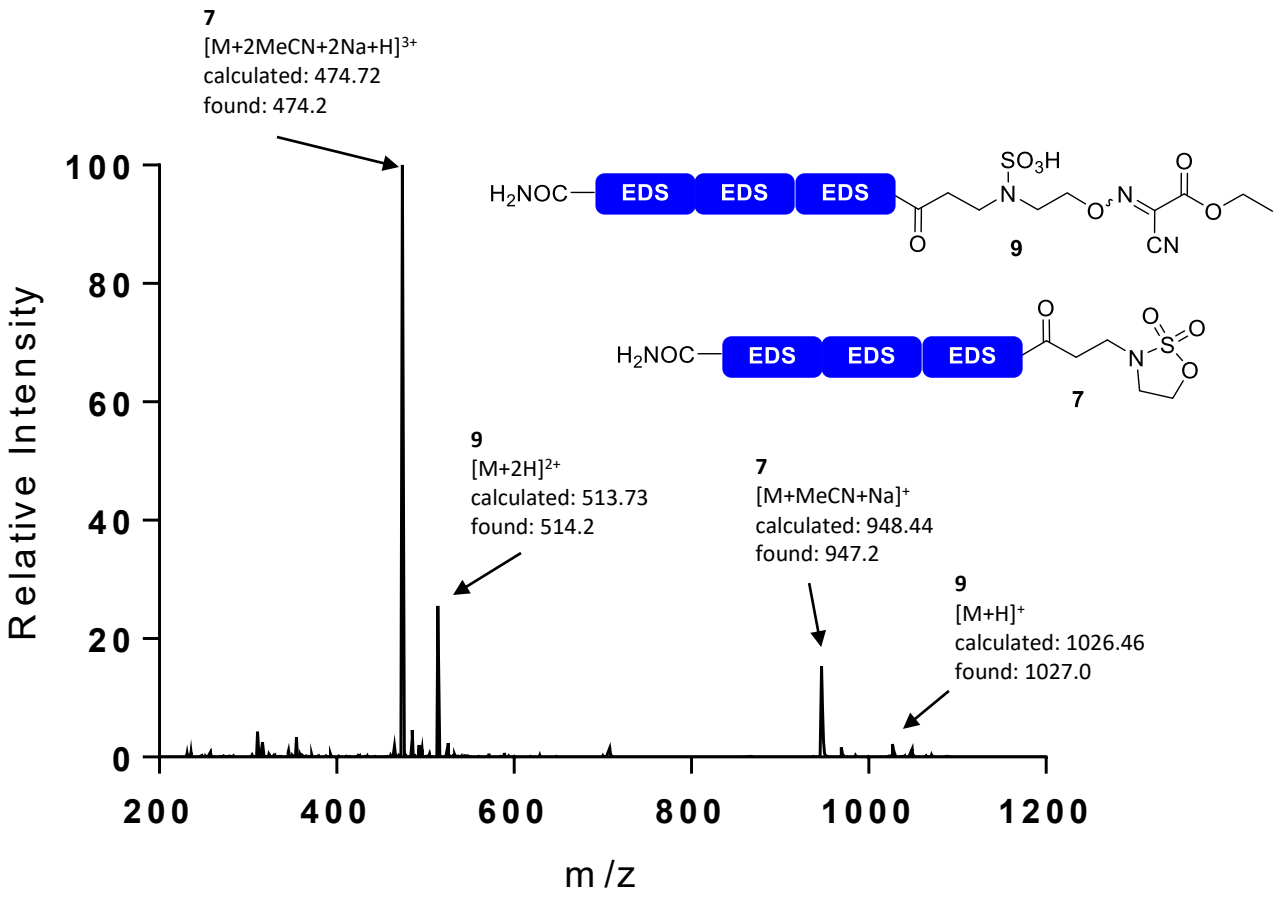

Figure S9: ESI-MS for entry 10, Table S1 (R_t = 5.5 min and injection peak) as shown in Figure S8 showing the presence of **7** and **9**

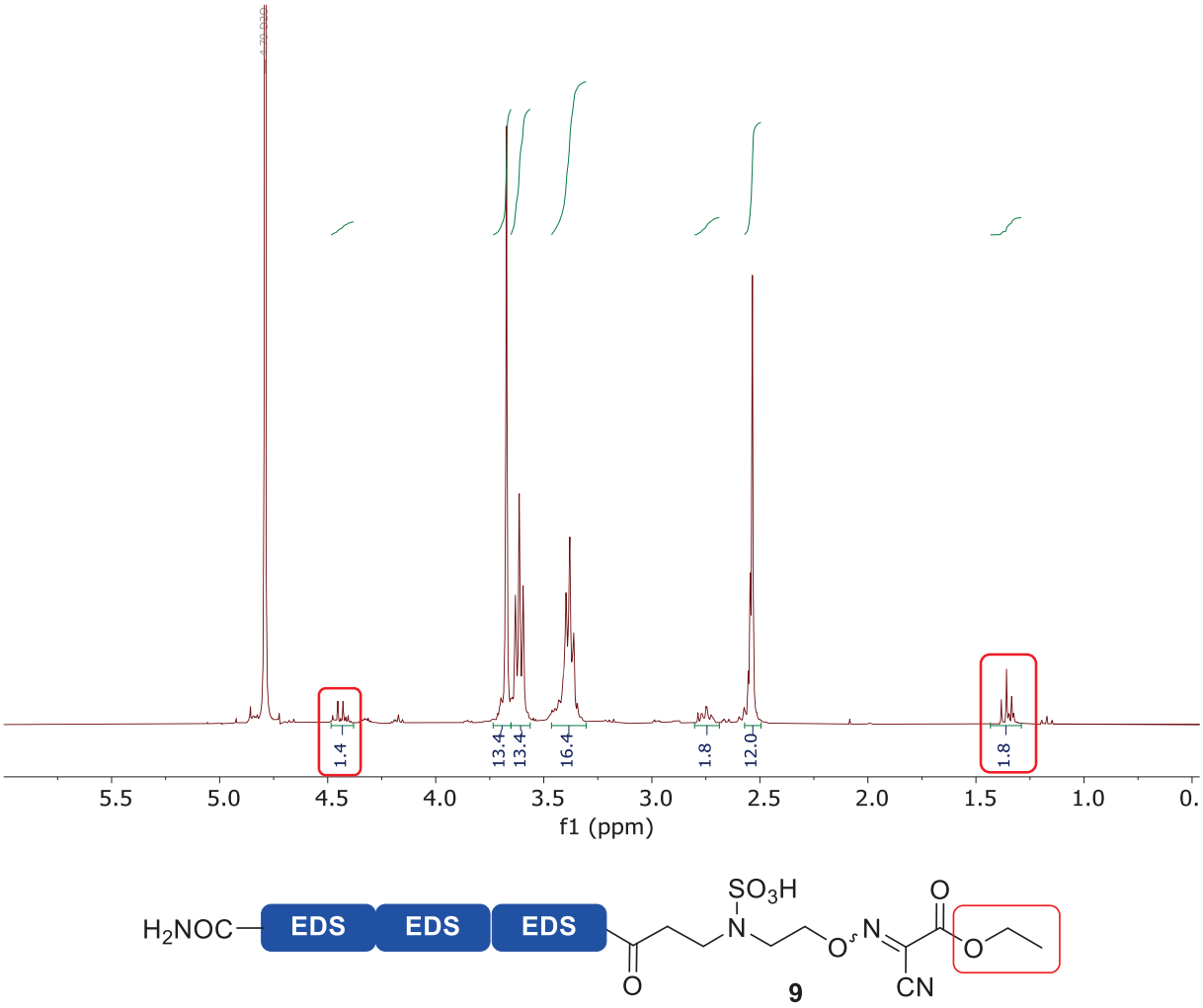

Figure S10: ^{1}H NMR of **9** (entry 9, Table S1) measured in D_2O (300 MHz) with red boxes indicating the presence of ethyl ester peaks. Oxyma-related peaks comprise 60% of the total end-group make-up when integrated against 12 succinate protons (2.55 ppm)

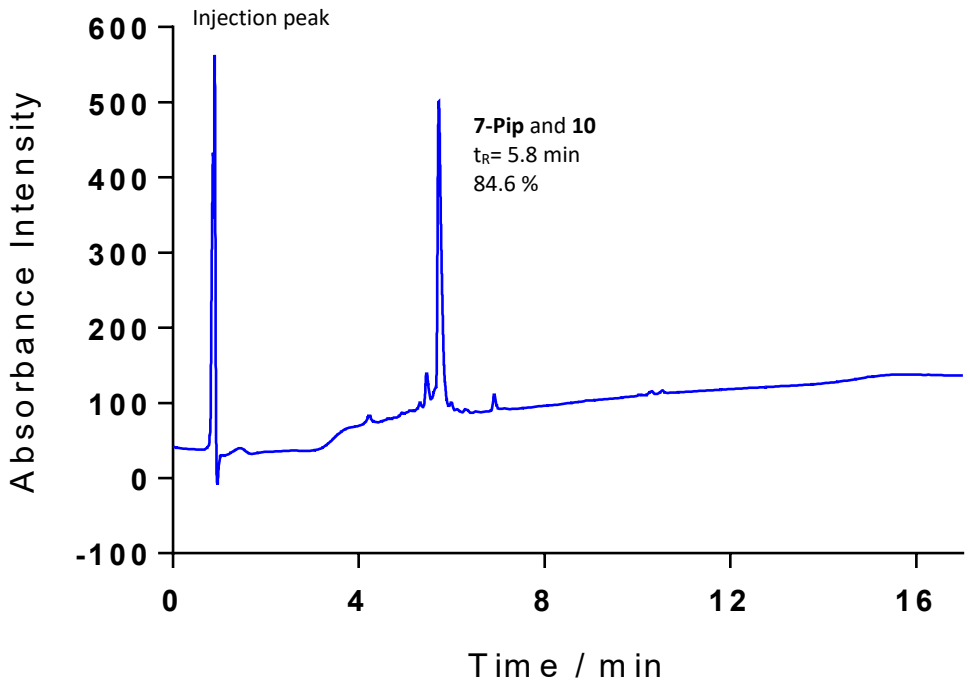

Figure S11: RP-HPLC chromatogram (Gradient 5-95 vol% - MeCN in H_2O (0.1 vol% formic acid) piperidine-treated entry 10, Table S1

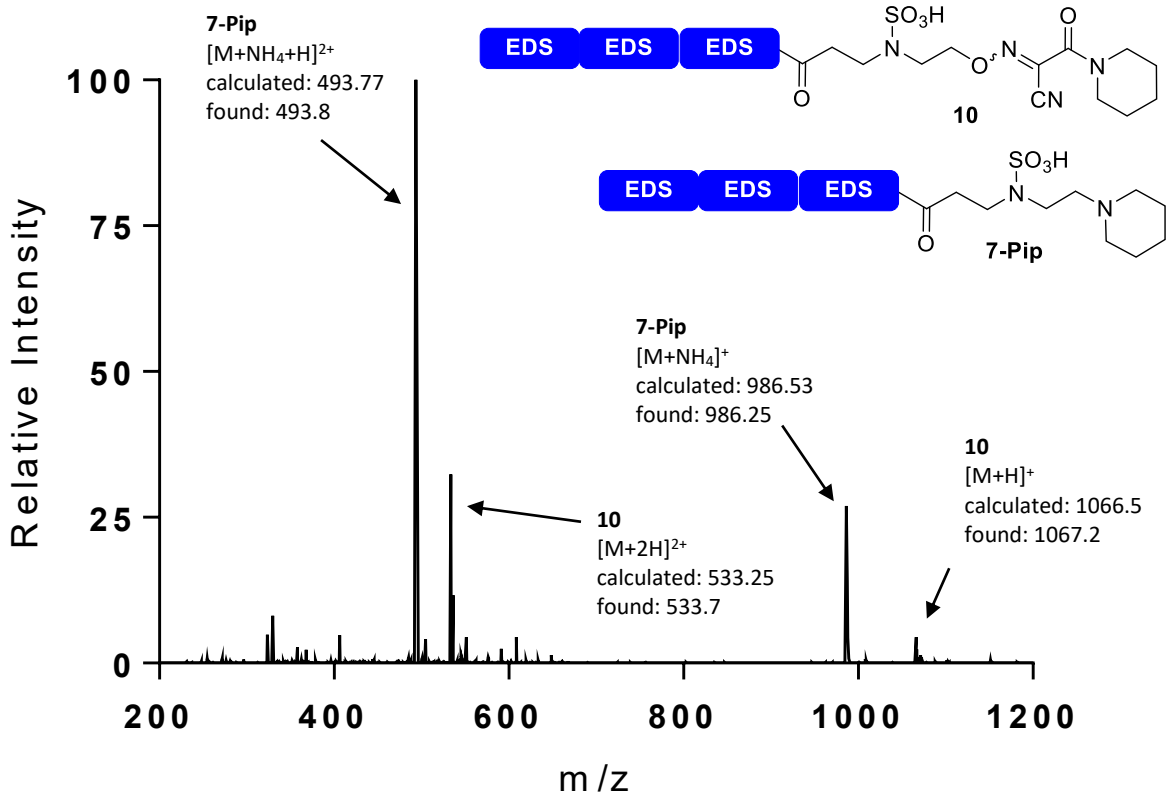

Figure S12: ESI-MS (positive mode) for piperidine-treated entry 10, Table S1 showing the presence of **7-Pip** and **10**

Table S2: Coupling conditions tested for the ring-opening of variably functionalized 5-membered cyclic sulfamidates building blocks

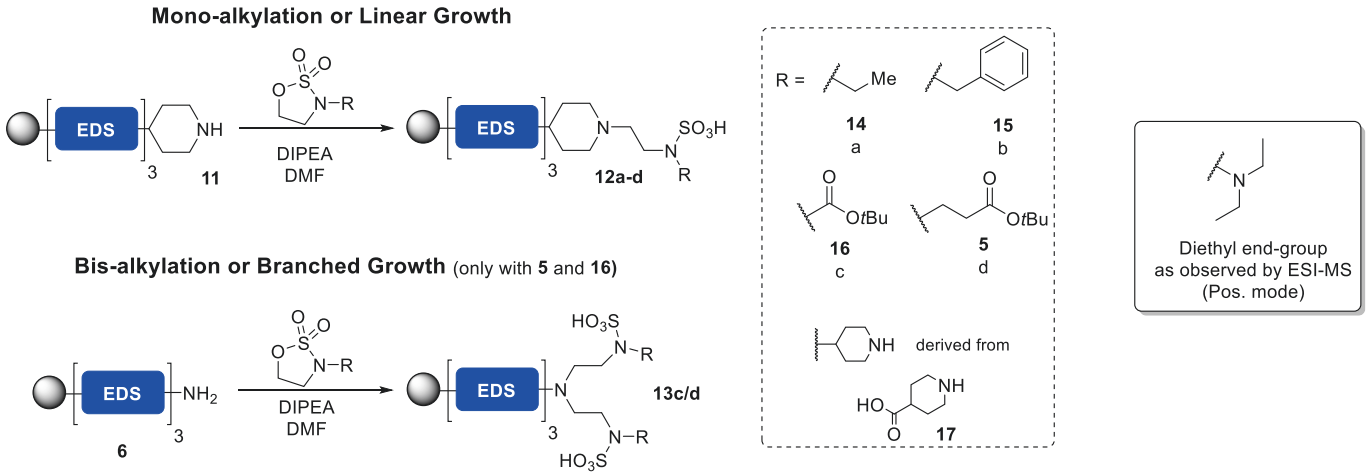

Entry	Resin-bound Anchor	Building Block (Eq.)[a]	Time / min	100% Conversion	Product (P) or Side-product (SP) observed
1	**11**	**15** (25)	60	Y	Y (**12b**)
2	**11**	**14** (25)	60	N	Y (**12a**)
3	**11**	**14** (25)	240	Y	Y (**12a**)
4	**11**	**16** (50)[b]	60	Y	Y (**12c**)
5	**11**	**16** (25)[b]	60	Y	Y (**12c**)
6	**11**	**16** (20)	1440	Y	Y (**12c**)
7	**11**	**16** (20)	120	Y	Y (**12c**)
8	**11**	**16** (20)	30	Y	Y (**12c**)
9	**11**	**16** (5)	1440	N	Y (**12c**)
10	**11**	**16** (5)	120	N	Y (**12c**)
11	**11**	**16** (5)	30	N	Y (**12c**)
12	**11**	**5** (20)	120	Y	Y (**12d**)
13	**11**	**5** (10)	120	Y	Y (**12d**)
14	**11**	**5** (5)	120	N	Y (**12d**)
15	**6**	**16** (50)	1440	Y	**13c** (diethyl end-group)
16	**6**	**16** (20)	1440	Y	**13c** (diethyl end-group)
17	**6**	**16** (10)	1440	Y	**13c** (diethyl end-group)
18	**6**	**16** (50)	120	Y	**13c** (diethyl end-group)
19	**6**	**16** (20)	120	Y	**13c** (diethyl end-group)
20	**6**	**16** (10)	120	Y	**13c** (diethyl end-group)
21	**6**	**16** (50)	30	Y	**13c** (diethyl end-group)
22	**6**	**16** (20)	30	Y	**13c** (diethyl end-group)
23	**6**	**16** (10)	30	Y	**13c** (diethyl end-group)
24	**6**	**5** (50)	120	Y	**13d**(diethyl end-group)
25	**6**	**5** (20)	120	Y	**13d**(diethyl end-group)
26	**6**	**5** (10)	120	Y	**13d**(diethyl end-group)

a: DIPEA equivalents applied in a 1:1 ratio with a given building block; b: reactions conducted at 40 °C used a reactor microwave and were conducted in a sealed microwave vial

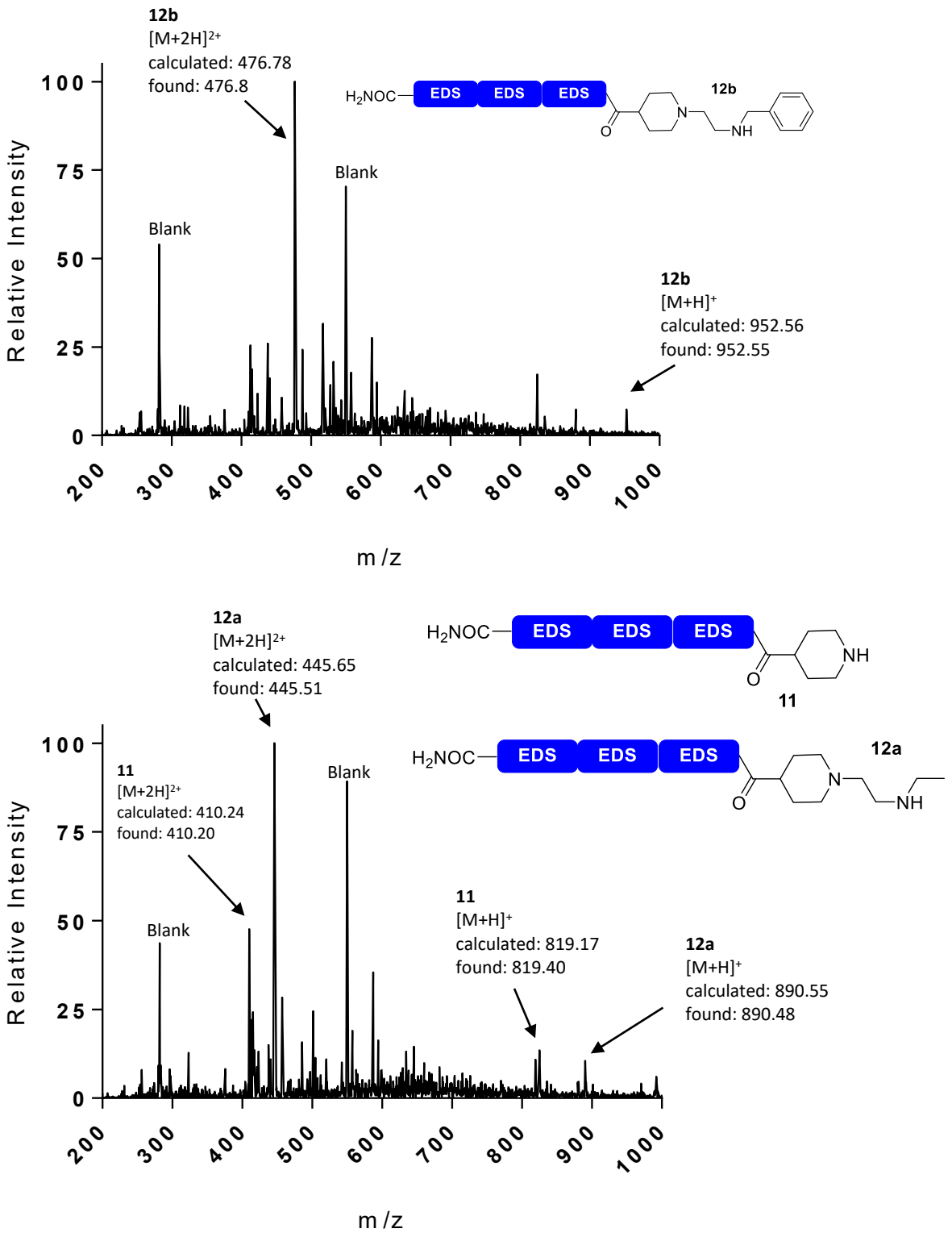

Figure S13: Positive ESI-MS results for (above) entry 1, Table S2 showing mass peaks for **12b** and (below) entry 2, Table S2 showing mass peaks corresponding to **11** and **12a**

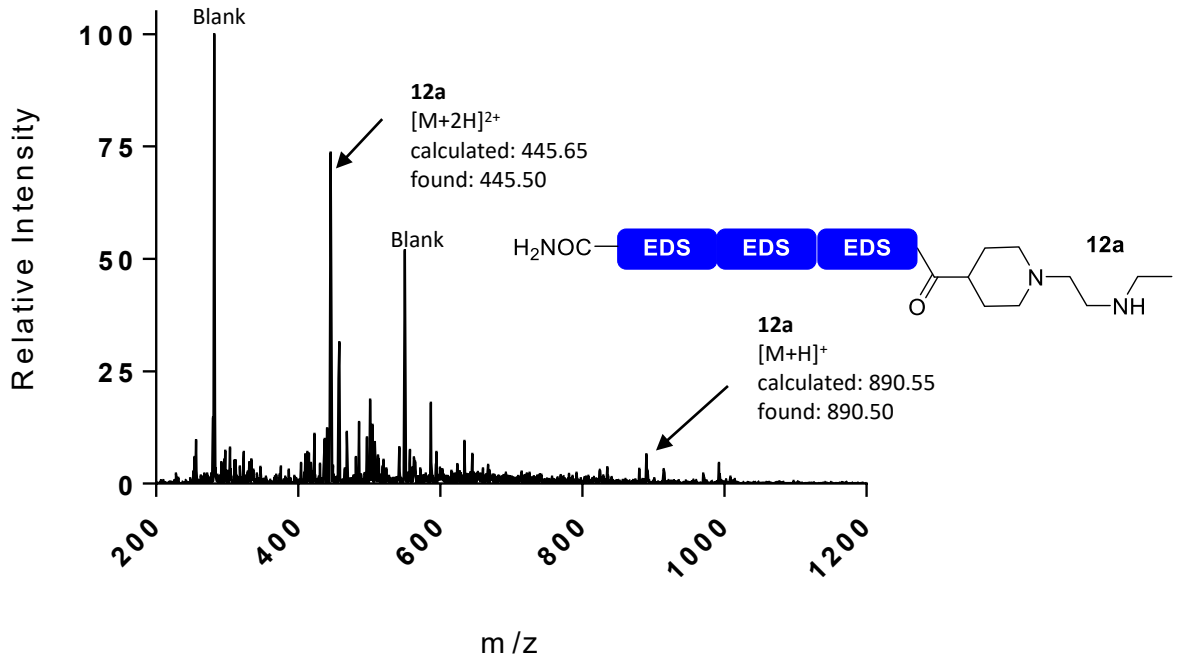

Figure S14: Positive ESI-MS results for entry 2, Table S2 showing mass peaks for **12a** exclusively

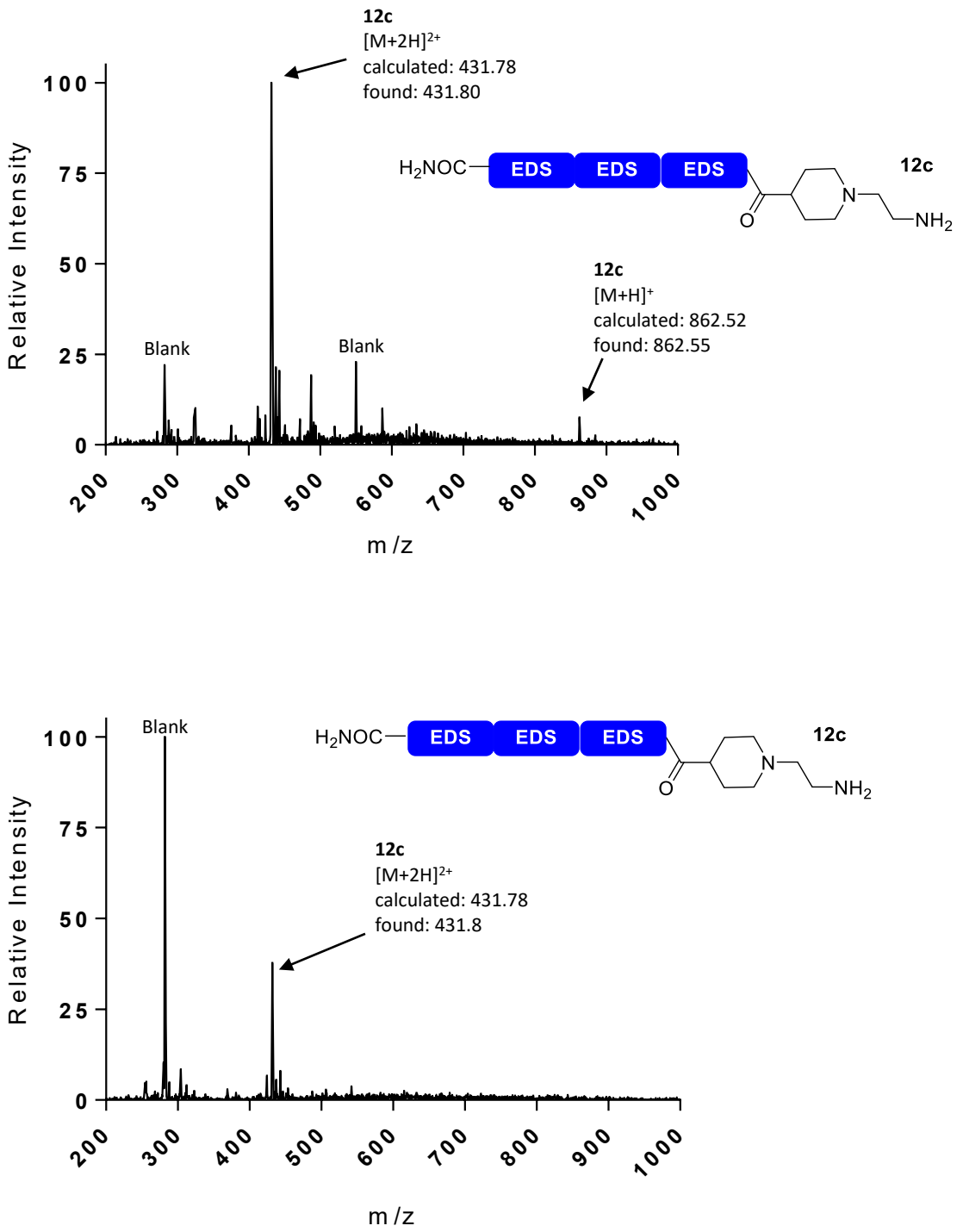

Figure S15: Positive ESI-MS results for (above) entry 4, Table S2 showing mass peaks for **12c** and (below) entry 5, Table S2 showing mass peaks corresponding to **12c**

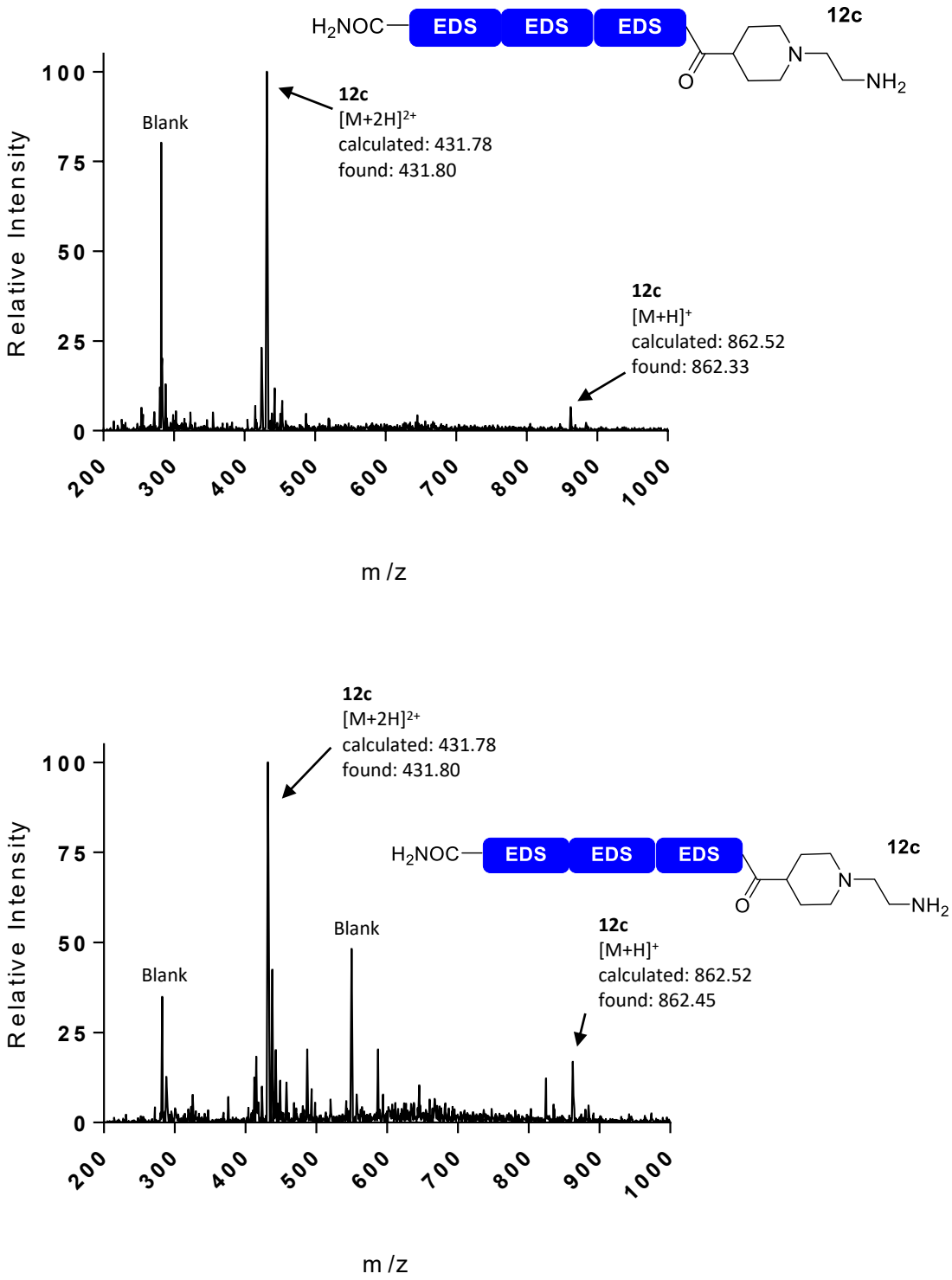

Figure S16: Positive ESI-MS results for (above) entry 6, Table S2 showing mass peaks for **12c** and (below) entry 8, Table S2 showing mass peaks corresponding to **12c**

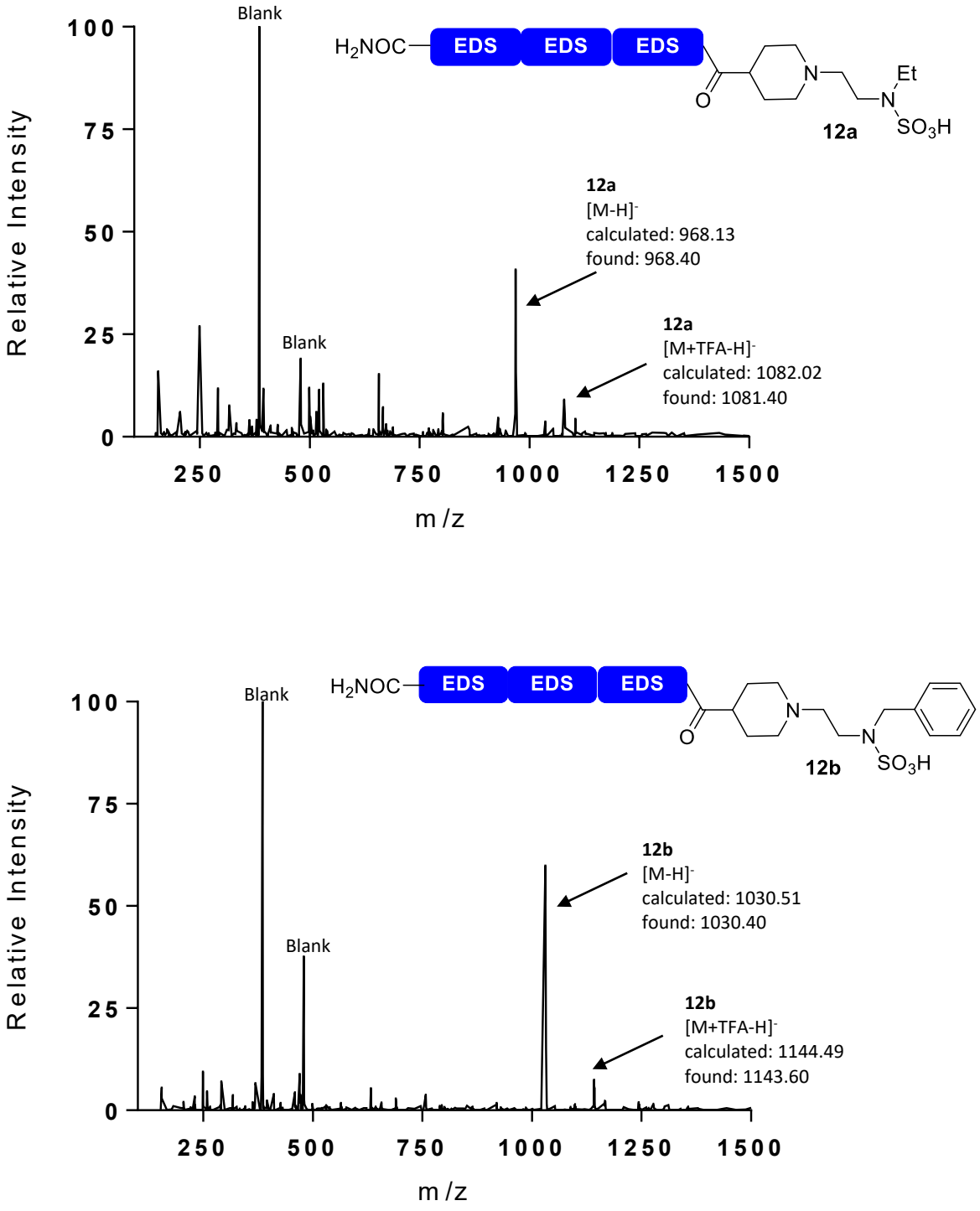

Figure S17: Negative ESI-MS results for (above) entry 2, Table S2 showing mass peaks for **12a** and (below) entry 1, Table S2 showing mass peaks corresponding to **12b**

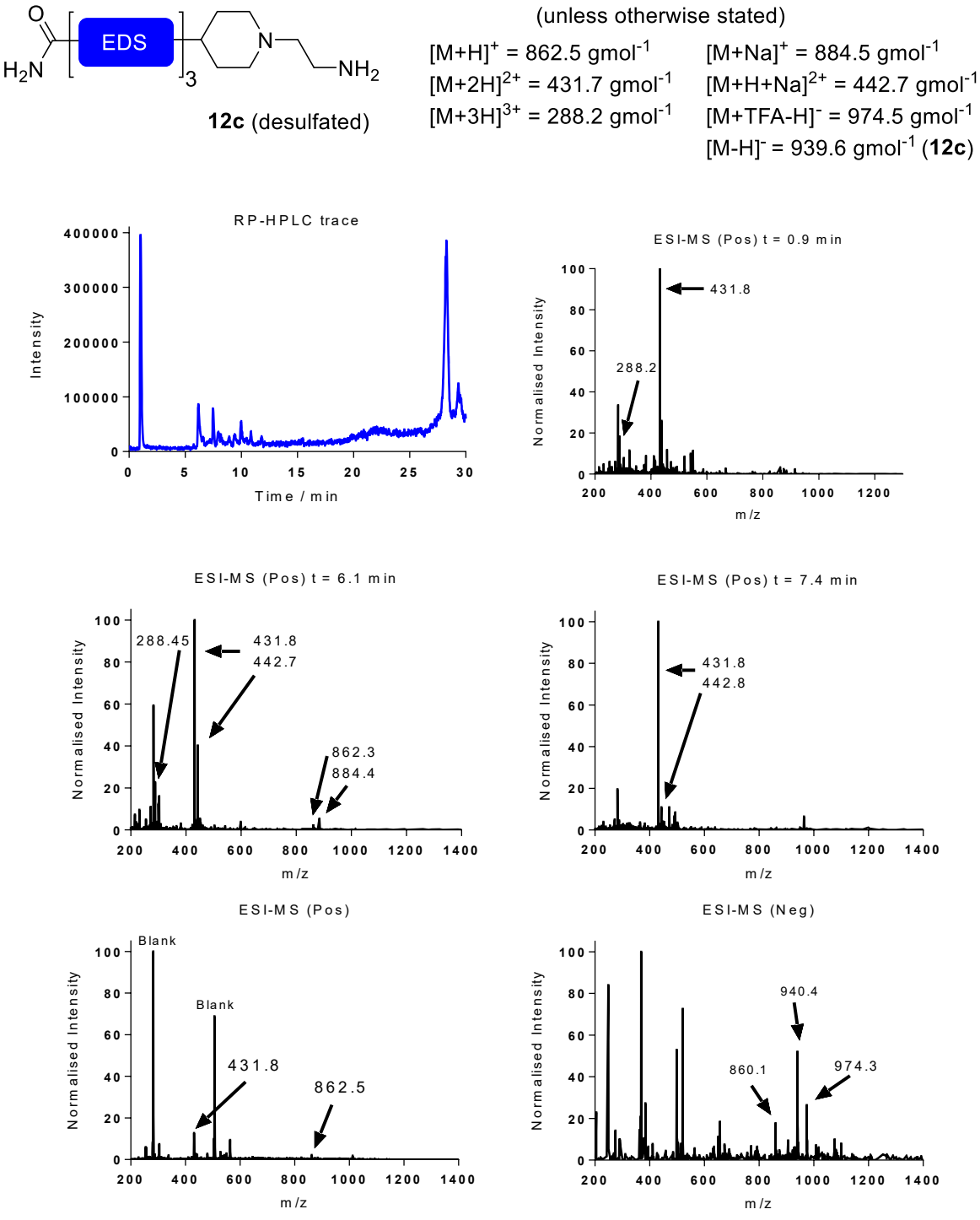

Figure S18: RP-HPLC-MS results for entry 6, Table S2 showing (Top left) RP-HPLC trace ES-MS (pos. mode) for: (top left) at t = 0.9 min, (middle left) t = 6.1 min, and (middle right) t = 7.4 min. Collective ESI-MS: (bottom left) positive and (bottom right) negative mode. All exhibiting masses for **12c**.

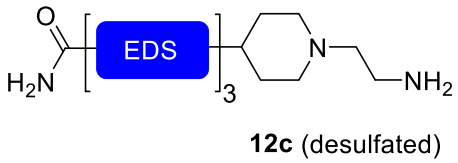

12c (desulfated)

Calculated masses for desulfated **12c**
(unless otherwise stated)

$[M+H]^+$ = 862.5 $gmol^{-1}$
$[M+2H]^{2+}$ = 431.7 $gmol^{-1}$
$[M+3H]^{3+}$ = 288.2 $gmol^{-1}$
$[M+Na]^+$ = 884.5 $gmol^{-1}$
$[M+H+Na]^{2+}$ = 442.7 $gmol^{-1}$
$[M+TFA-H]^-$ = 974.5 $gmol^{-1}$
$[M-H]^-$ = 939.6 $gmol^{-1}$ (**12c**)

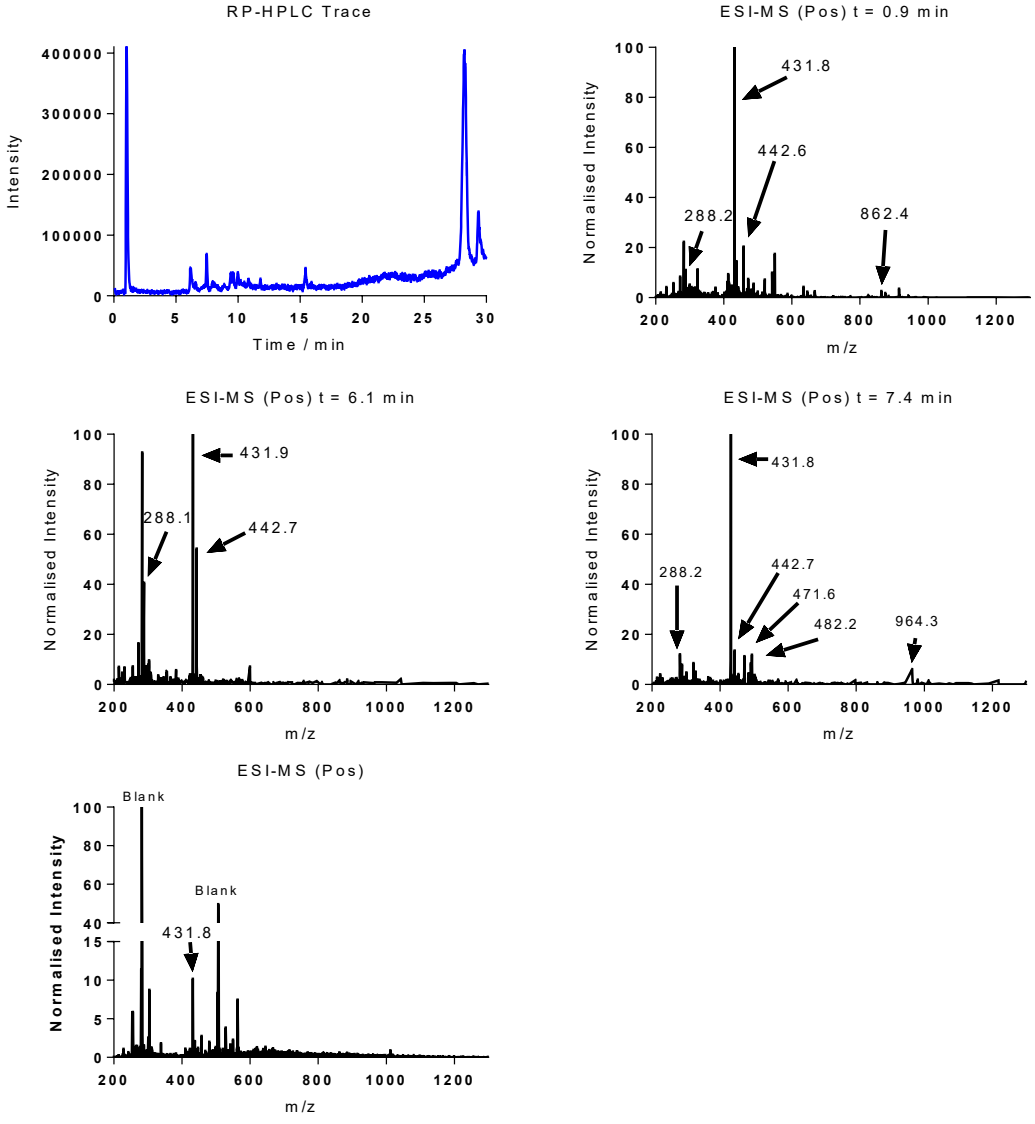

Figure S19: RP-HPLC-MS results for entry 7, Table S2 showing (Top left) RP-HPLC trace ES-MS (pos. mode) for: (top left) at t = 0.9 min, (middle left) t = 6.1 min, and (middle right) t = 7.4 min. Collective ESI-MS: (bottom left) positive mode. All exhibiting masses for **12c**

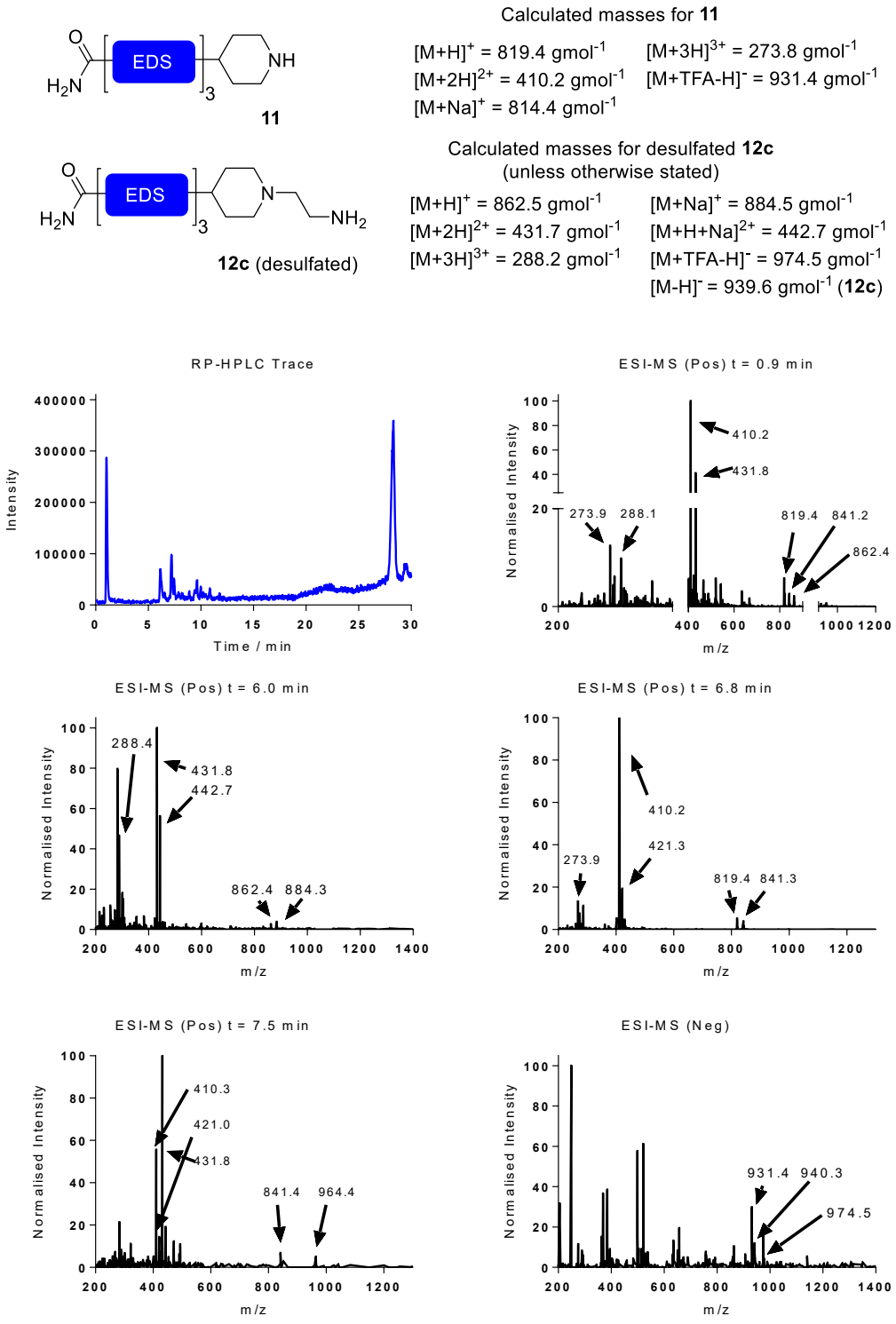

Figure S20: RP-HPLC-MS results for entry 9, Table S2 showing (Top left) RP-HPLC trace ES-MS (pos. mode) for: (top right) at t = 0.9 min, (middle left) t = 6.0 min, (middle right) t = 6.8 min and (bottom left) t = 7.5 min. Collective ESI-MS: (bottom right) negative mode. All exhibiting masses for **11** and **12c**

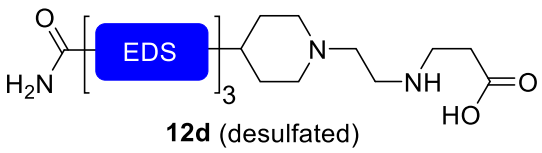

12d (desulfated)

Calculated masses for desulfated **12d**
(unless otherwise stated)

$[M+H]^+$ = 934.5 $gmol^{-1}$
$[M+2H]^{2+}$ = 467.7 $gmol^{-1}$
$[M+3H]^{3+}$ = 312.1 $gmol^{-1}$

$[M+Na]^+$ = 956.5 $gmol^{-1}$
$[M+H+Na]^{2+}$ = 478.7 $gmol^{-1}$
$[M+TFA-H]^-$ = 1046.5 $gmol^{-1}$
$[M-H]^-$ = 932.5 $gmol^{-1}$ (**12d**)

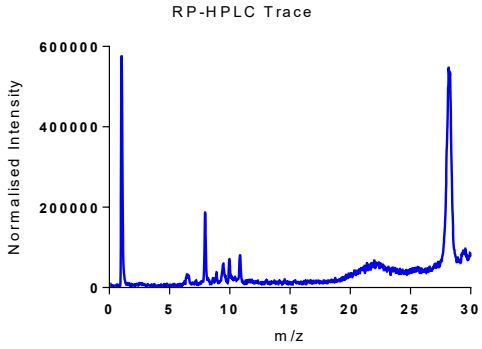

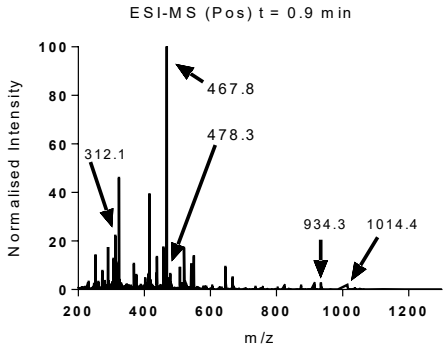

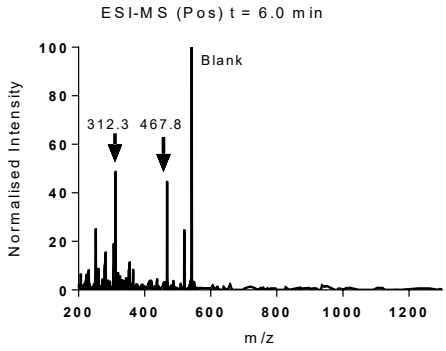

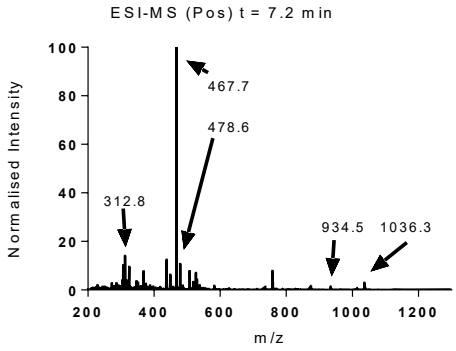

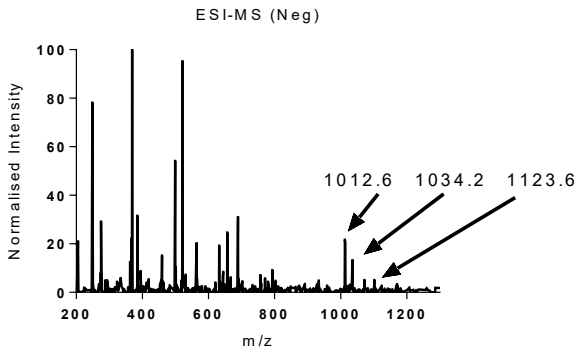

Figure S21: RP-HPLC-MS results for entry 12, Table S2 showing (Top left) RP-HPLC trace ES-MS (pos. mode) for: (top right) at t = 0.9 min, (middle left) t = 6.0 min, (middle right) t = 7.2 min. Collective ESI-MS: (bottom right) negative mode. All exhibiting masses for **12d**

Calculated masses for **13c**, its bis-desulfated equivalent and **18**

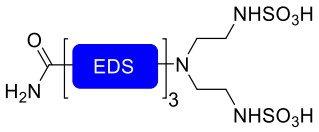

13c

$[M+H]^+$ = 954.4 $gmol^{-1}$
$[M+2H]^{2+}$ = 477.7 $gmol^{-1}$
$[M+3H]^{3+}$ = 318.8 $gmol^{-1}$

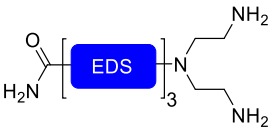

13c (desulfated)

$[M+H]^+$ = 794.4 $gmol^{-1}$
$[M+2H]^{2+}$ = 397.7 $gmol^{-1}$
$[M+3H]^{3+}$ = 265.5 $gmol^{-1}$

18

$[M+H]^+$ = 764.4 $gmol^{-1}$
$[M+2H]^{2+}$ = 382.7 $gmol^{-1}$
$[M+3H]^{3+}$ = 255.4 $gmol^{-1}$
$[M+H+Na]^{2+}$ = 393.7 $gmol^{-1}$
$[M+H+K]^{2+}$ = 401.7 $gmol^{-1}$
$[M+Na+K]^{2+}$ = 413.5 $gmol^{-1}$
$[M+MeOH+H]^+$ = 796.9 $gmol^{-1}$

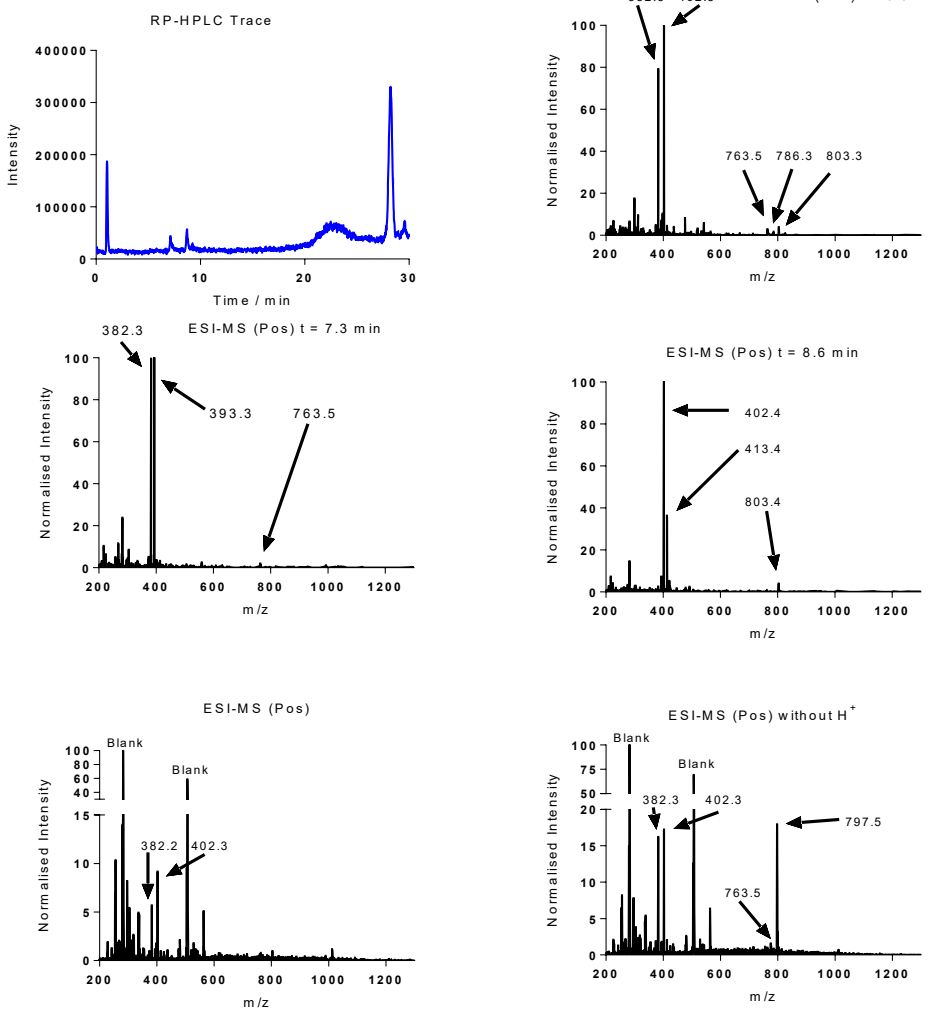

Figure S22: RP-HPLC-MS results for entry 16, Table S2 showing (Top left) RP-HPLC trace ES-MS (pos. mode) for: (top right) at t = 0.9 min, (middle left) t = 7.3 min, (middle right) t = 8.6 min. Collective ESI-MS positive mode: (bottom right) with formic acid in eluent and (bottom right) without formic acid in the eluent. All exhibiting masses for **18,** degradation product of **13c**

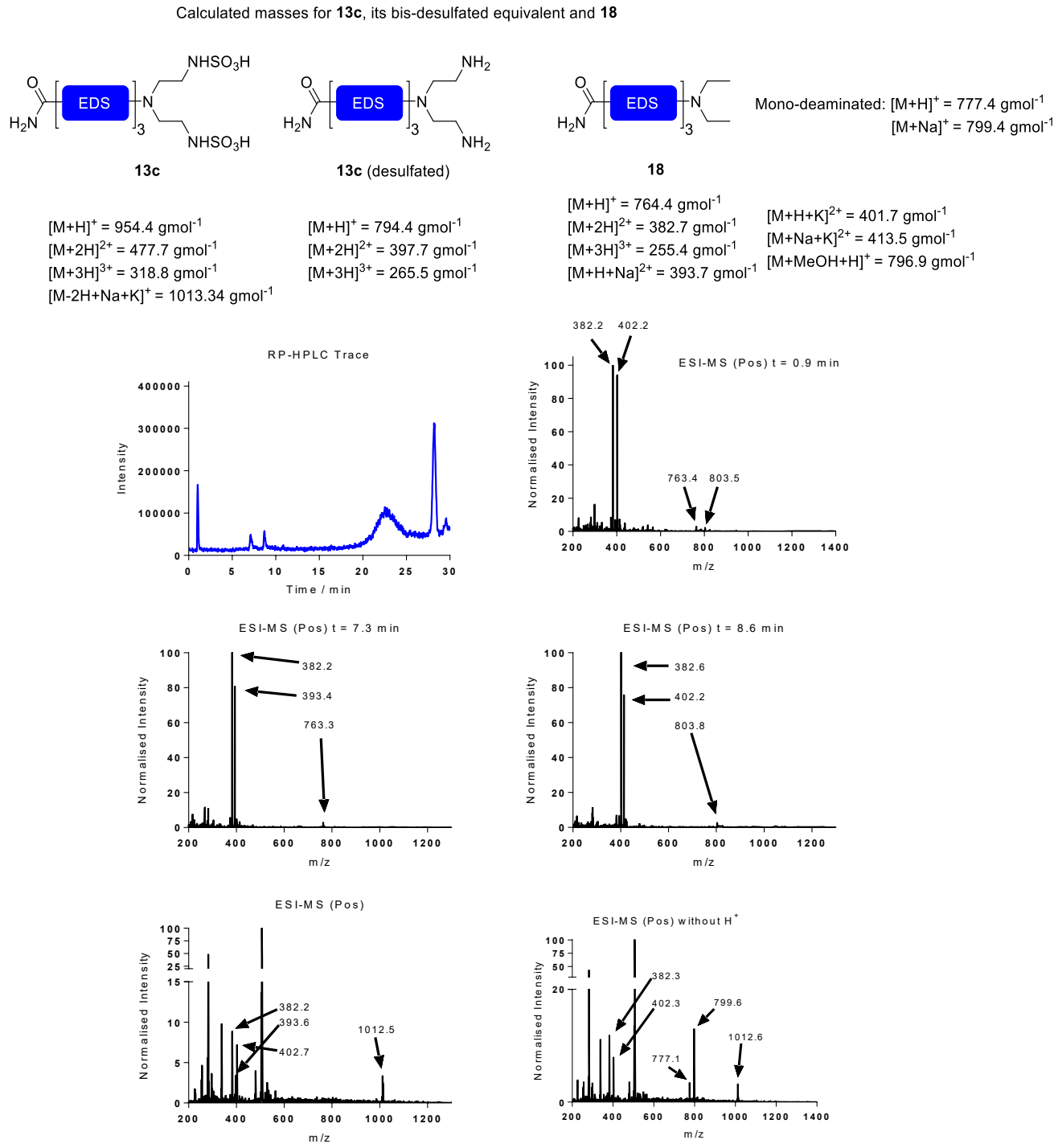

Figure S23: RP-HPLC-MS results for entry 19, Table S2 showing (Top left) RP-HPLC trace ES-MS (pos. mode) for: (top right) at t = 0.9 min, (middle left) t = 7.3 min, (middle right) t = 8.6 min. Collective ESI-MS positive mode: (bottom right) with formic acid in eluent and (bottom right) without eluent. All exhibiting masses for **18,** degradation product of **13c**

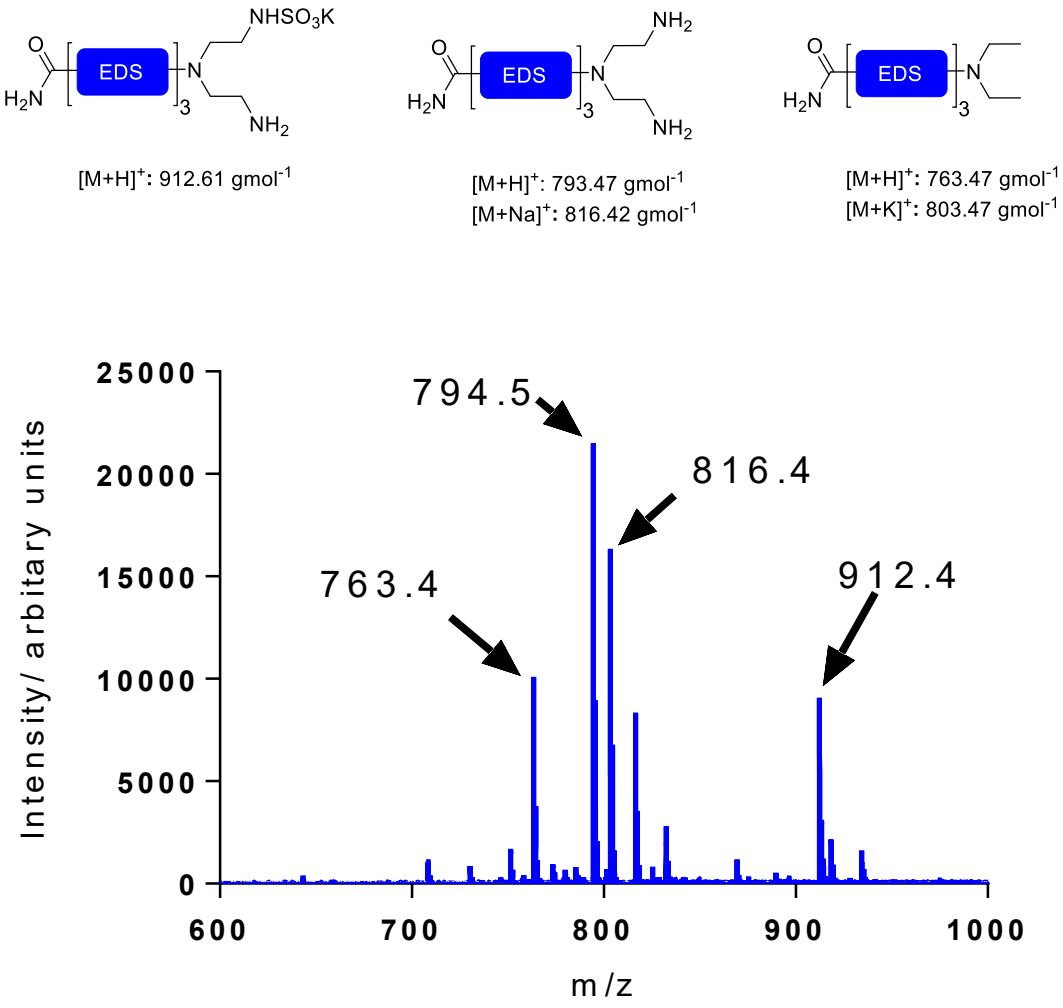

Figure S24: MALDI-MS of **13c** showing the degradation to a desulfated oligomers and **18**

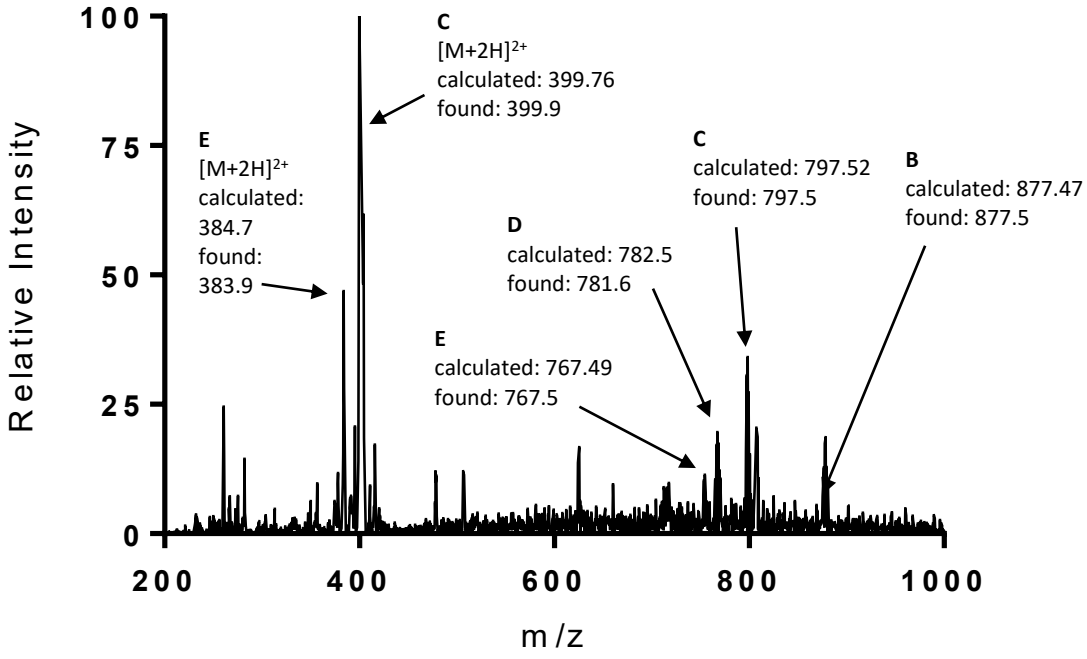

Deuterated variants of **13c**

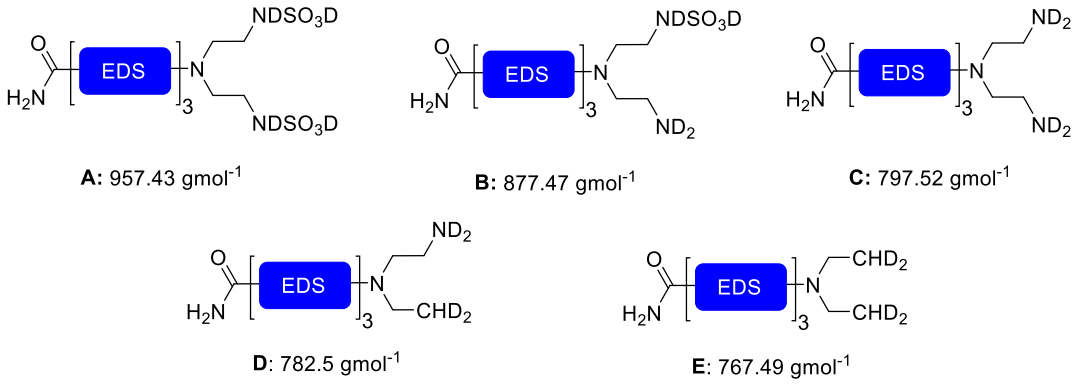

Figure S25: Positive ESI-MS results after solubilizing **13c** in D_2O (24 h immersion) with mass peaks corresponding to various degradation products of **13c**

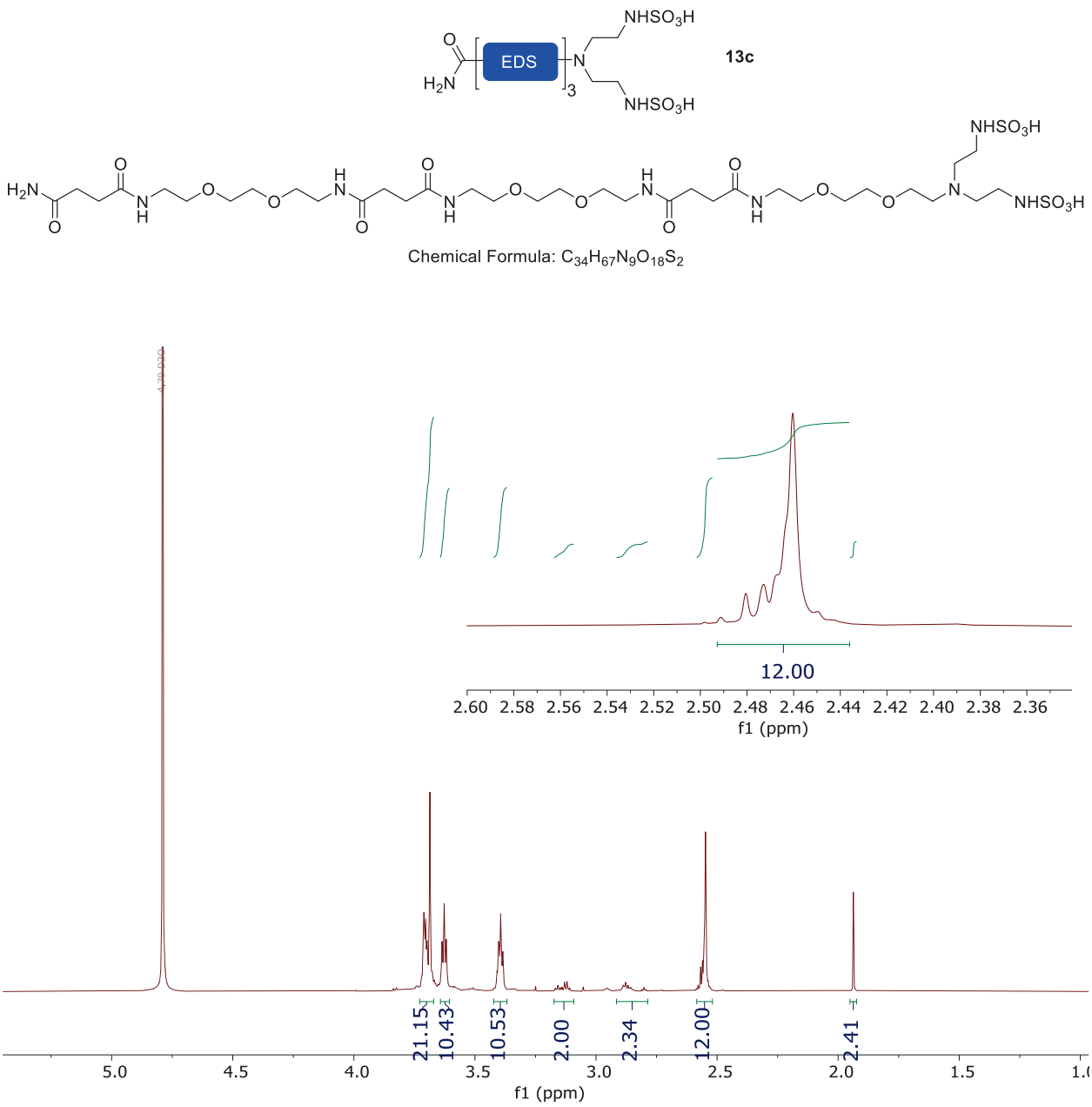

Expected proton count excluding amide and exchangeable protons: **58** **Integrated protons**: **58.45**

Acetate integration: 2.41 = 1 eq.

Figure S26: ^{1}H NMR of **13c** dissolved in D_2O and the integration analysis indicating the proton count (excluding amide and exchangeable protons) and the indicated acetate equivalents

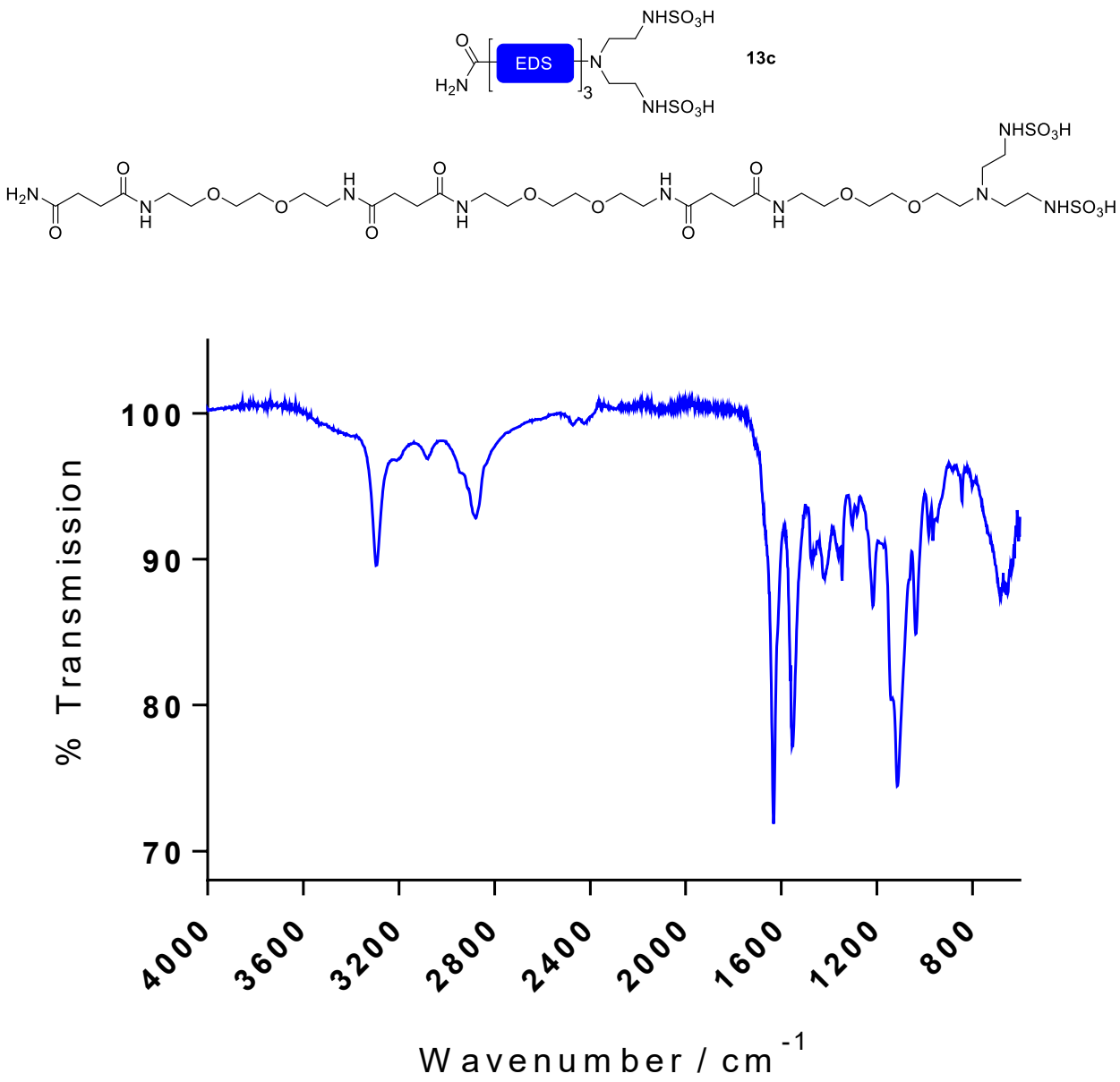

Key peaks: 3292 (N-H/O-H str.), 2877 (C-H sp^3 str.), 1629 (C=O amide), 1548 (N-H amide bend), 1454 (methylene str.) 1415-1342 (S=O str.), 1112 (C-N/C-O) cm^{-1}

Figure S27: FT-IR spectrum of **13c**

Table S3: Selected conditions from the investigations into selective *N*-sulfate cleavage.

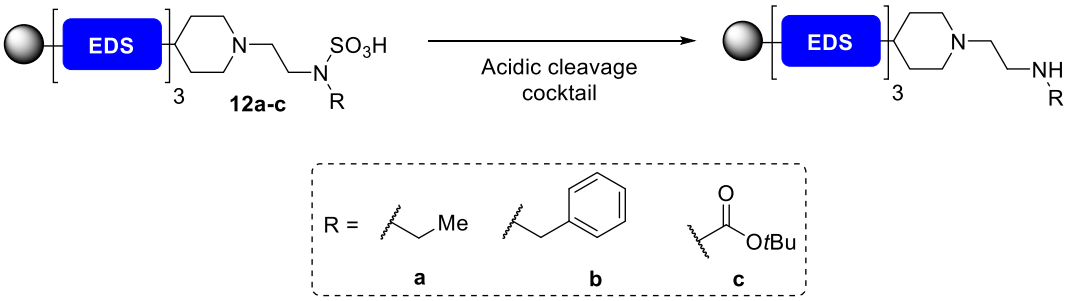

Conditions	pH	Temp. / °C[a]	Time / min	12a cleaved?[b]	12b cleaved?	12c cleaved?
TFA:DCM:TIPS (95:2.5:2.5, v:v)	0	25	30	N	N	N
AcOH:DMSO (5:95, v:v)	5.5	50	10	N	N	Y
AcOH:DMSO (5:95, v:v)	5.5	75	10	N	N	Y
AcOH:DMSO (5:95, v:v)	5.5	100	5	N	N	Y
AcOH:DMSO (5:95, v:v)	5.5	100	10	N	N	Y
AcOH:DMSO (5:95, v:v)	5.5	100	30	N	N	Y
AcOH:DMSO (5:95, v:v)	5.5	100	180	N	N	Y
TFA:DMF (1:99, v:v)	3.5	100	30	N	N	Y
1M HCl in Dioxan	2	50	30	N	N	Y
Formic acid:MeCN:H2O (0.1:95:5, v:v)	4	80	45	N	N	Y
4M HCl in Dioxan	1	25	30	N	N	Y
4M HCl in Dioxan	1	100	30	N	N	Y

a: Elevated temperatures (above 25 °C) was achieved by suspending oligo-bearing resin in the appropriate candidate cleavage cocktail in a sealed microwave vial and heating using a microwave reactor; b: Following cleavage treatment and intentional resin cleavage was the sulfate observed? Y = Yes, the sulfate was cleaved (no signal present in subsequent ESI-MS analysis (negative mode), and N = No, the *N*-sulfate was still observed by ESI-MS (negative mode).

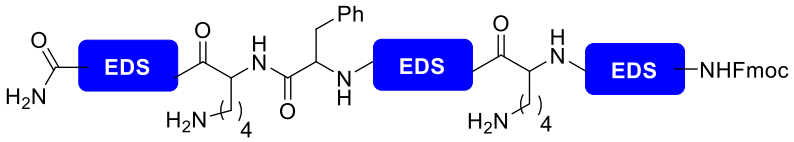

Fmoc-protected **19**

(Boc PGs deprotected on resin cleavage)

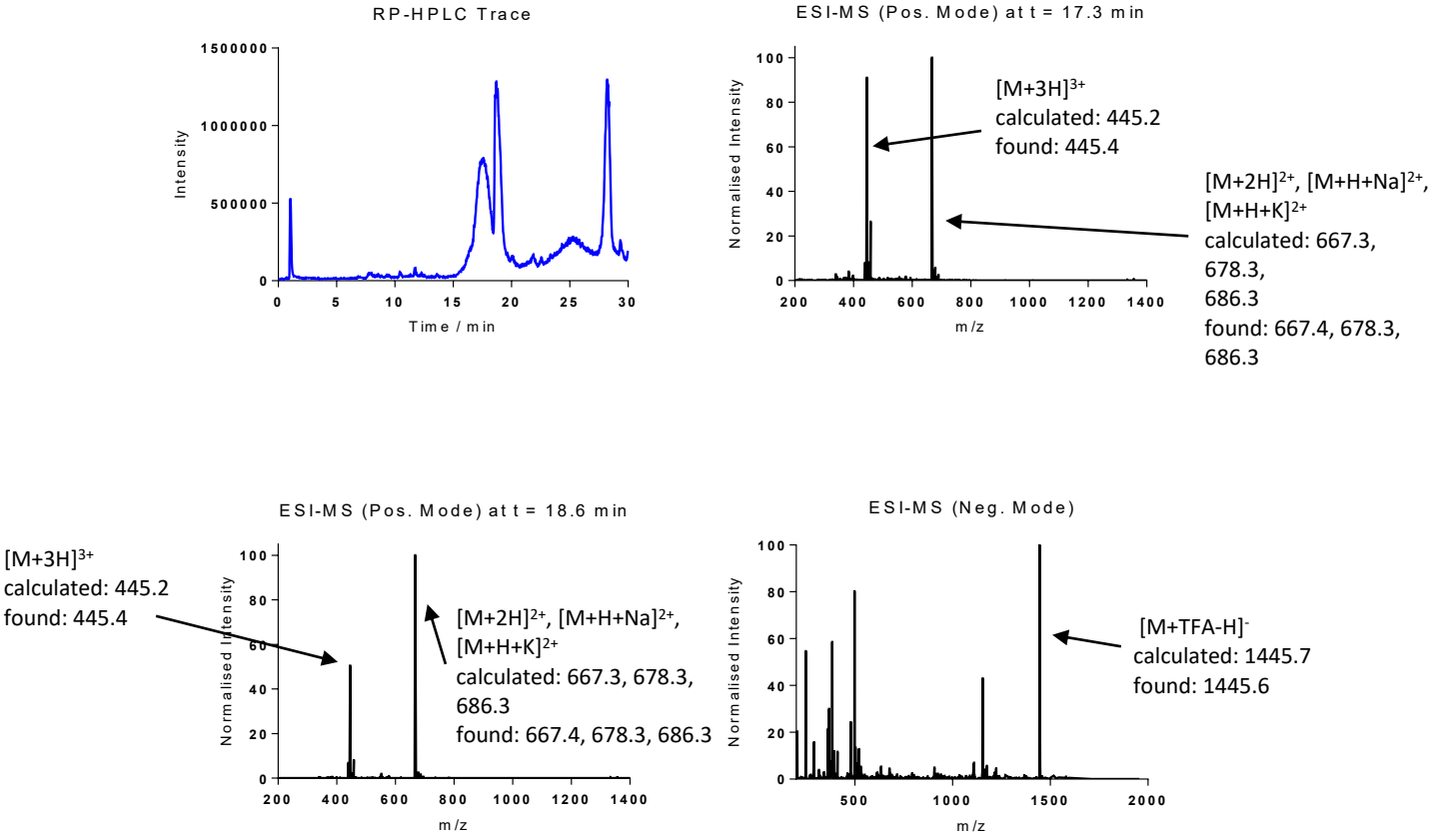

Figure S28: (Top Left) RP-HPLC trace, (Top Right) ESI-MS (Positive mode) at t = 17.3 min, and (Bottom Right) 18.6 min and (Bottom Right) ESI-MS (Negative mode) of Fmoc-protected **19** directly cleaved from solid support

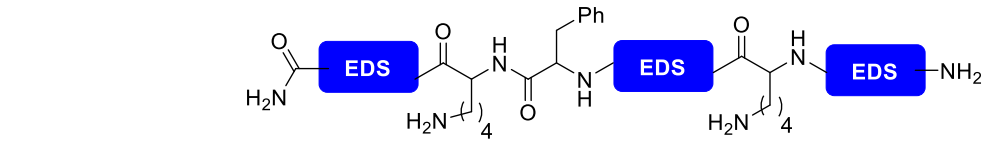

19

(Boc PGs deprotected on resin cleavage)

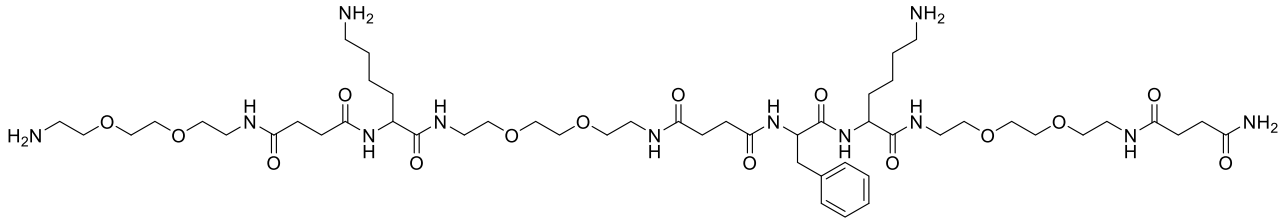

Chemical Formula: $C_{51}H_{90}N_{12}O_{15}$

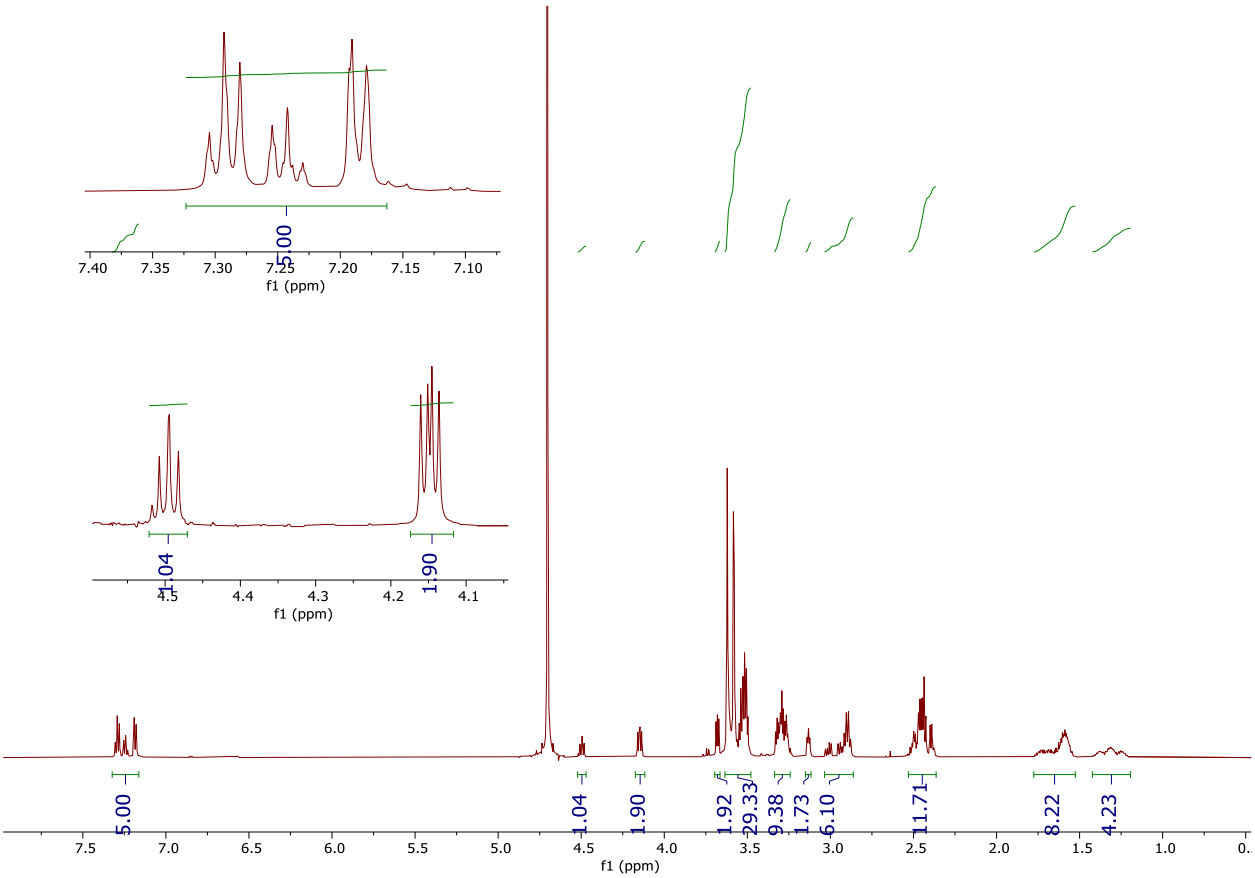

Expected proton count excluding amide protons: 80 **Integrated protons**: **80.55**

Figure S29: ^{1}H NMR of **19** dissolved in D_2O and the integration analysis indicating the proton count (excluding amide protons) and the indicated acetate equivalents

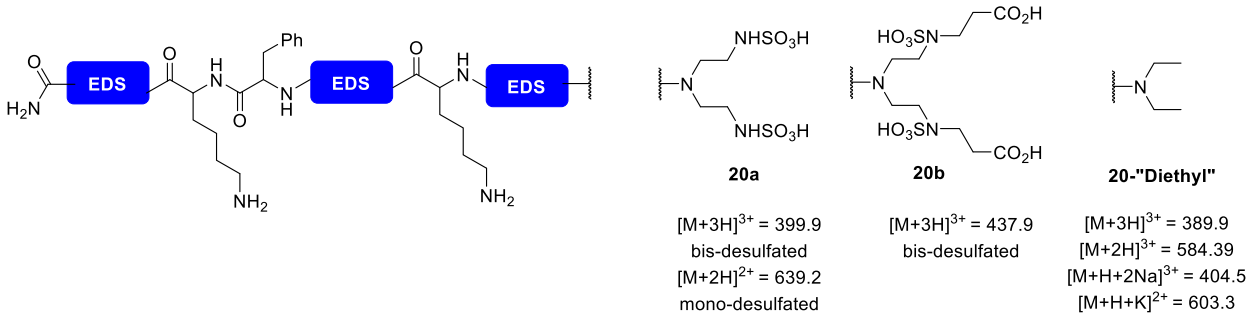

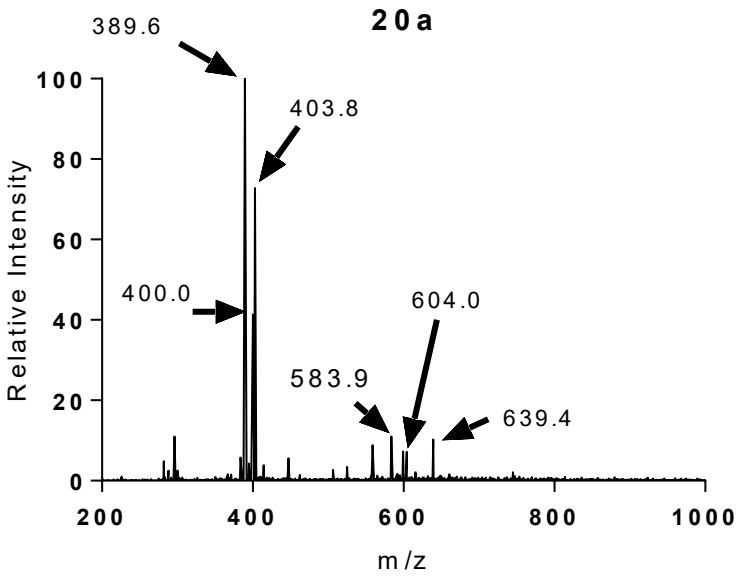

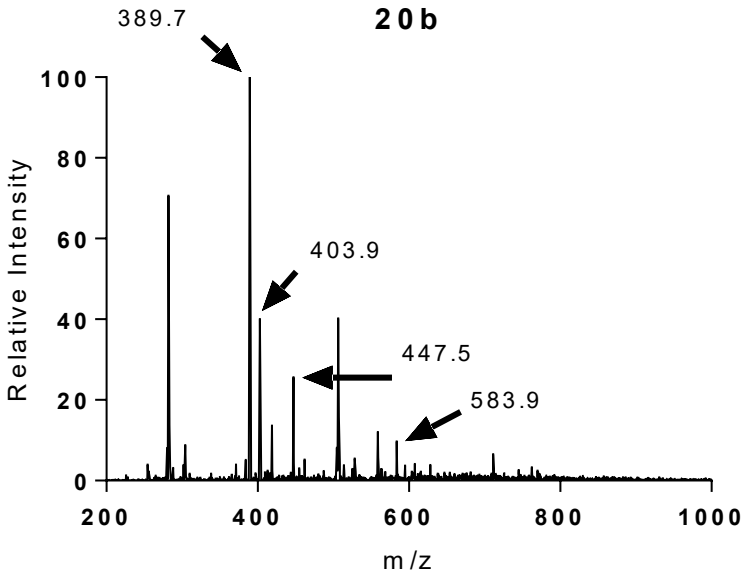

Figure S30: ESI-MS (positive mode) for oligomers **20a-b** with mass peaks identified

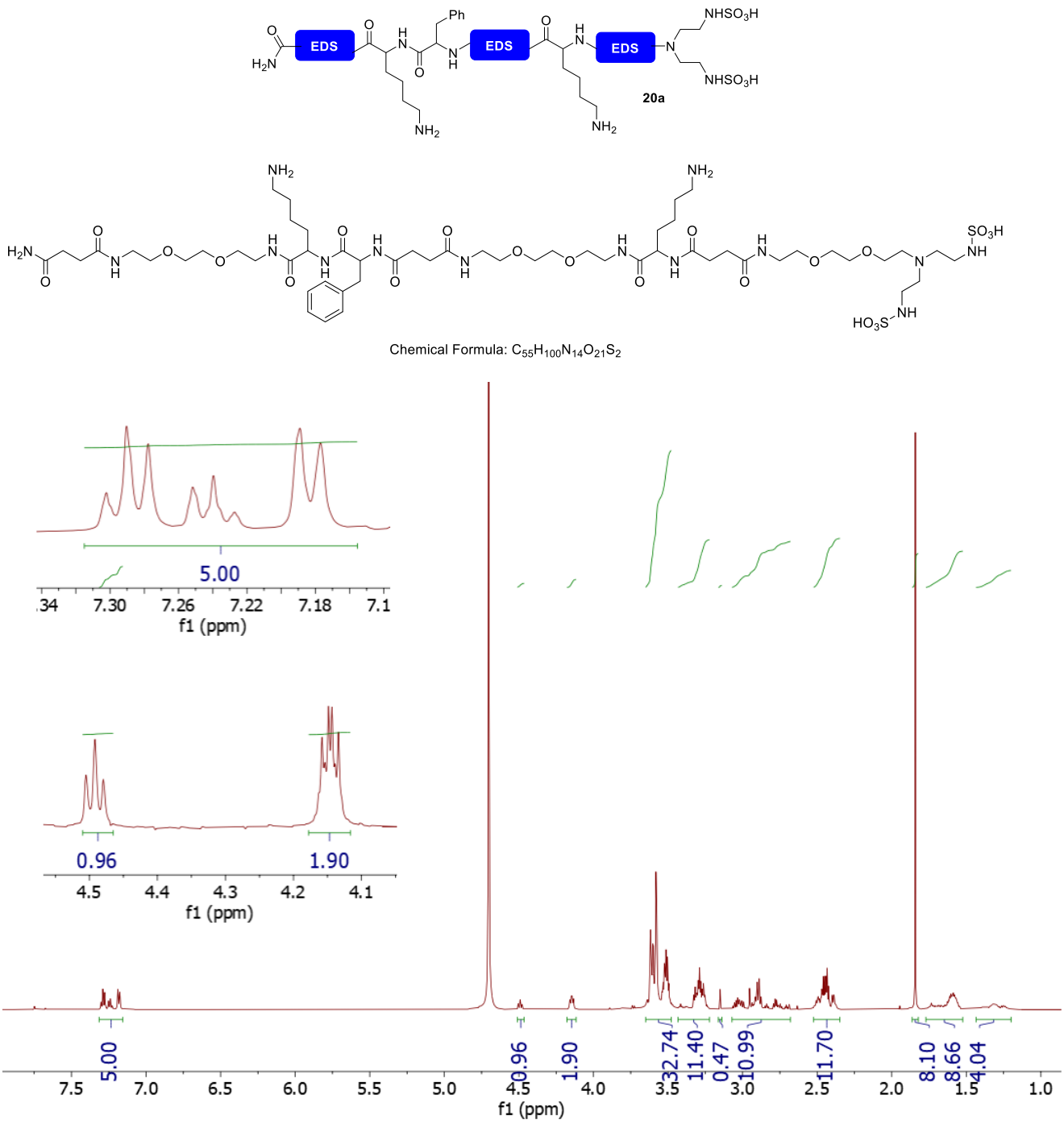

Expected proton count excluding amide and exchangeable protons: **88** **Integrated protons**: **87.86**

Acetate integration: 8.10 = 3 eq.

Figure S31: ^{1}H NMR of **20a** dissolved in D_2O and the integration analysis indicating the proton count (excluding amide and exchangeable protons) and the indicated acetate equivalents

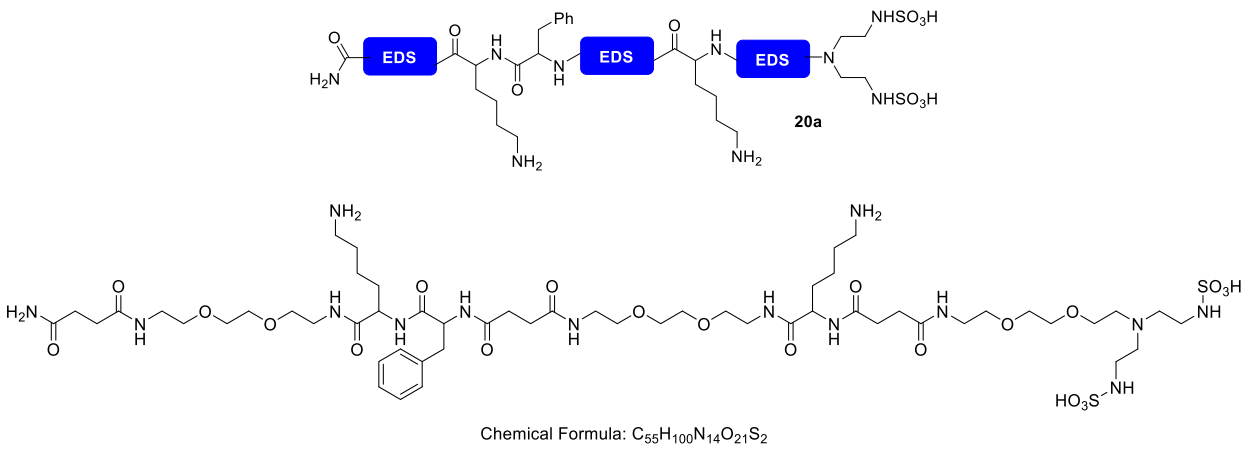

20a

Chemical Formula: $C_{55}H_{100}N_{14}O_{21}S_2$

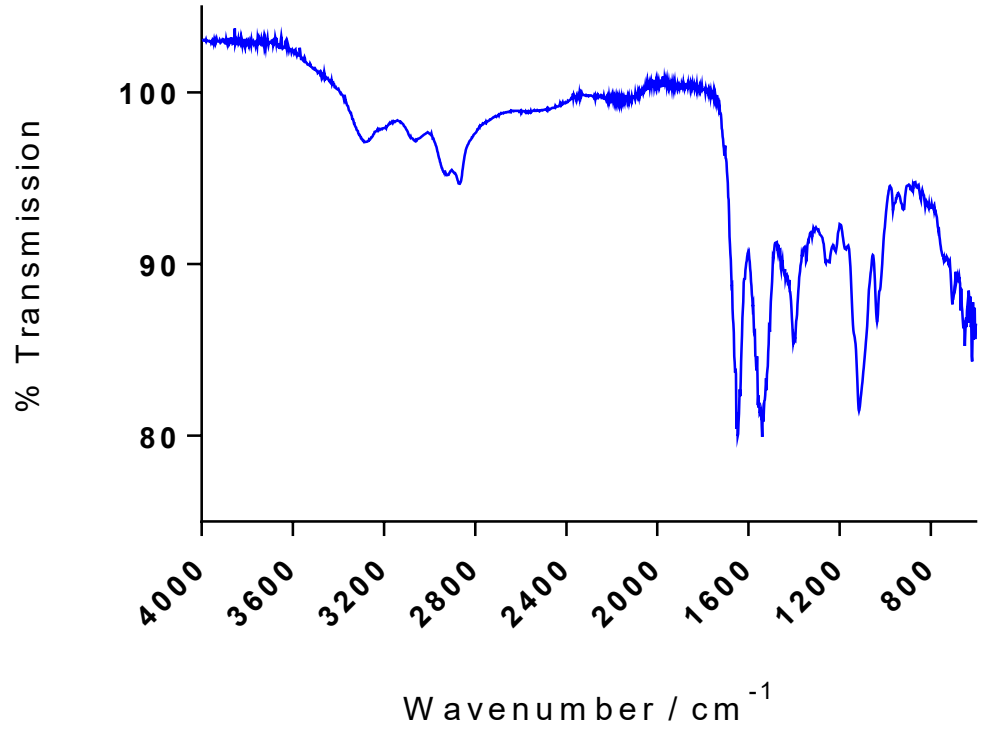

Key peaks: 3261 (N-H/O-H str.), 2866 (C-H sp^3 str.), 1645 (C=O amide), 1531 (N-H amide bend), 1398 (S=O str.), 1113 (C-N/C-O) cm^{-1}

Figure S32: FT-IR spectrum of **20a**

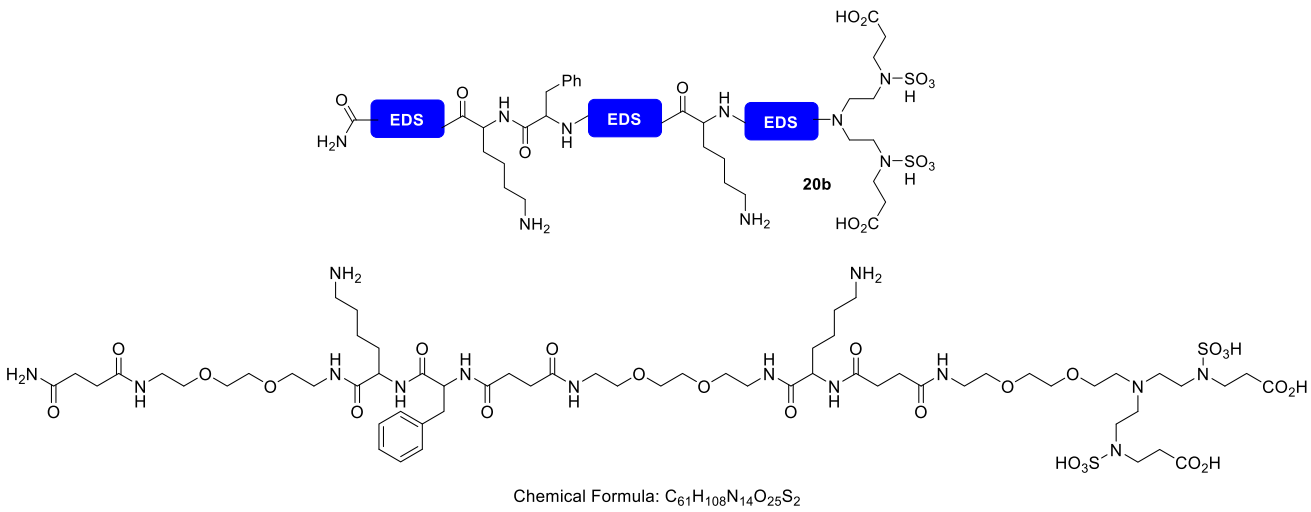

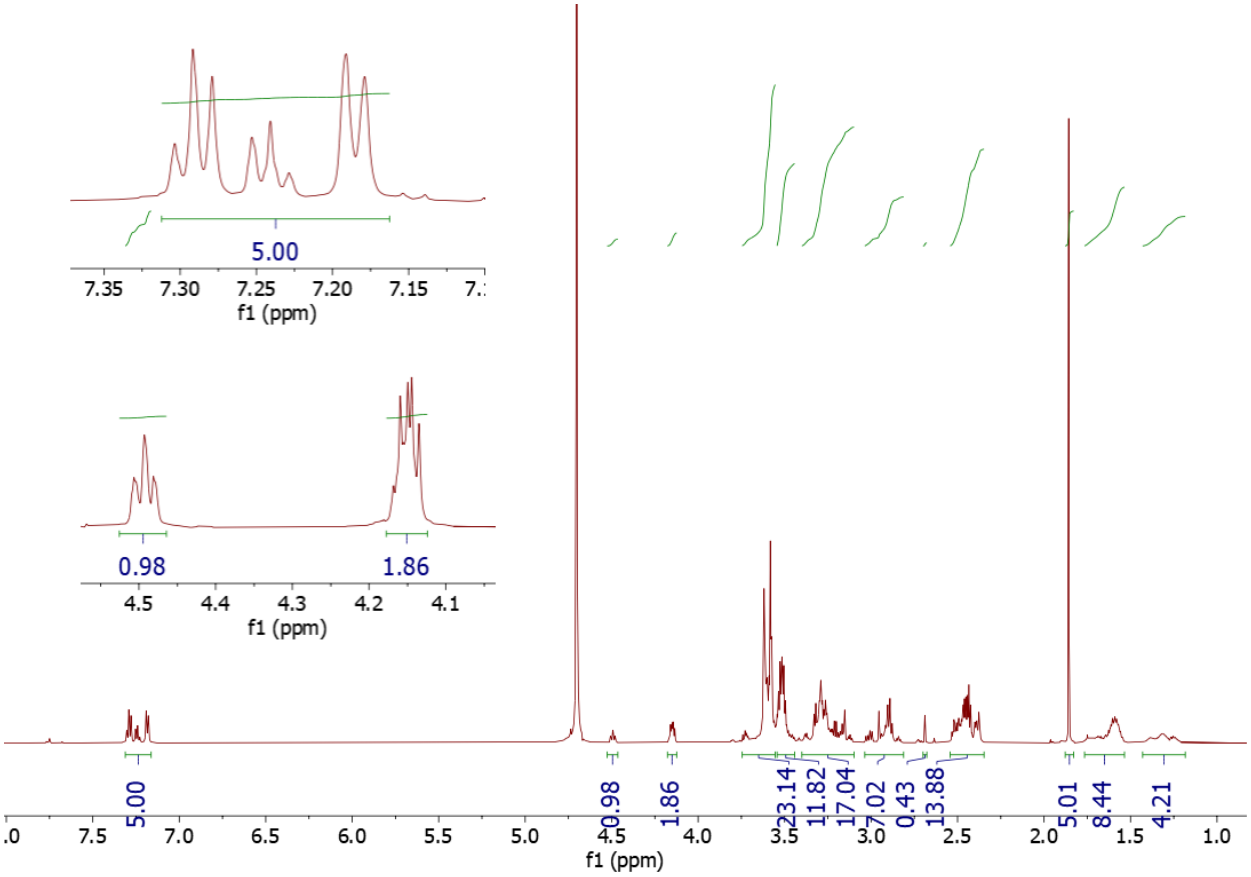

Expected proton count excluding amide and exchangeable protons: **94** **Integrated protons**: **93.83**

Acetate integration: 5.01 = 2 eq.

Figure S33: ^{1}H NMR of **20b** dissolved in D_2O and the integration analysis indicating the proton count (excluding amide and exchangeable protons) and the indicated acetate equivalents

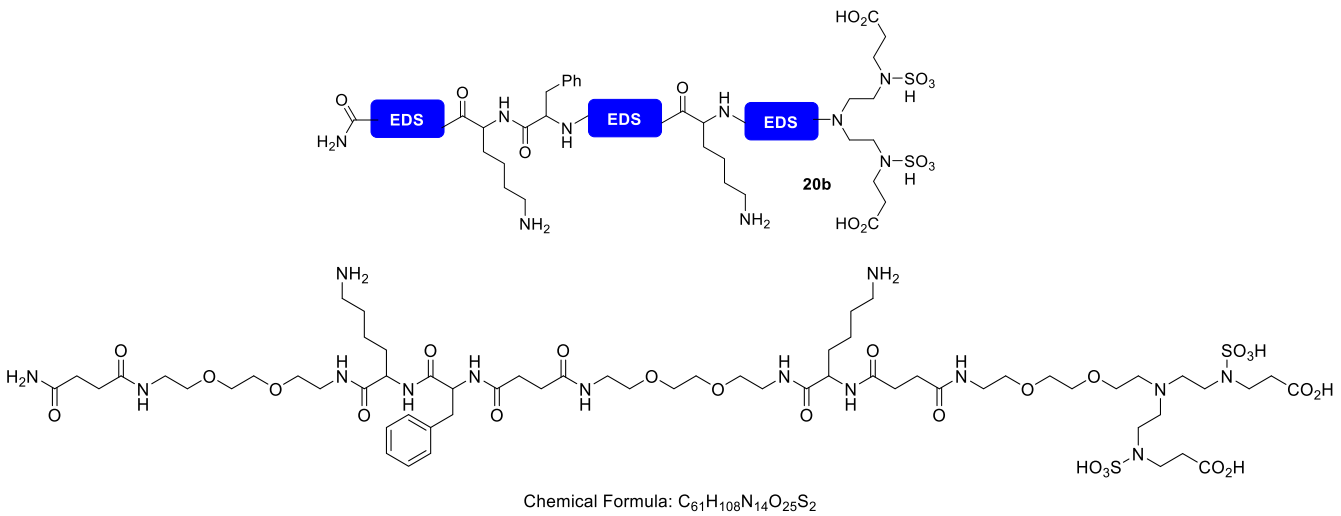

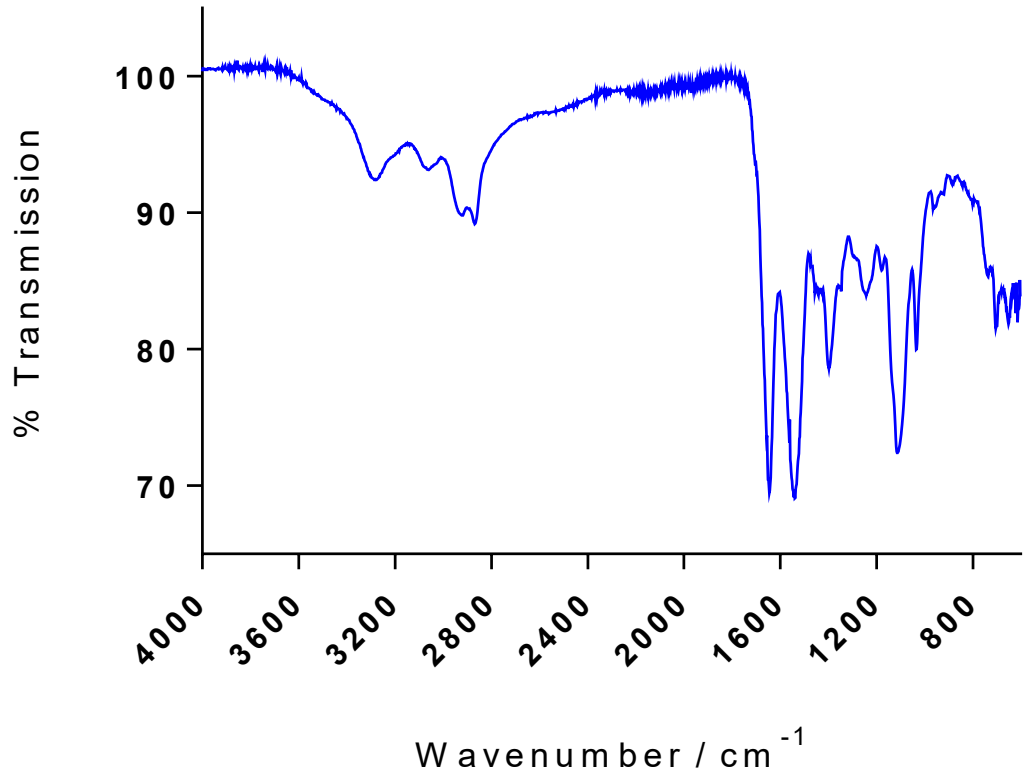

Key peaks: 3267 (N-H/O-H str.), 2868 (C-H sp^3 str.), 1643 (C=O amide), 1537 (N-H amide bend), 1396 (S=O str.), 1110 (C-N/C-O) cm^{-1}

Figure S34: FT-IR spectrum of **20b**

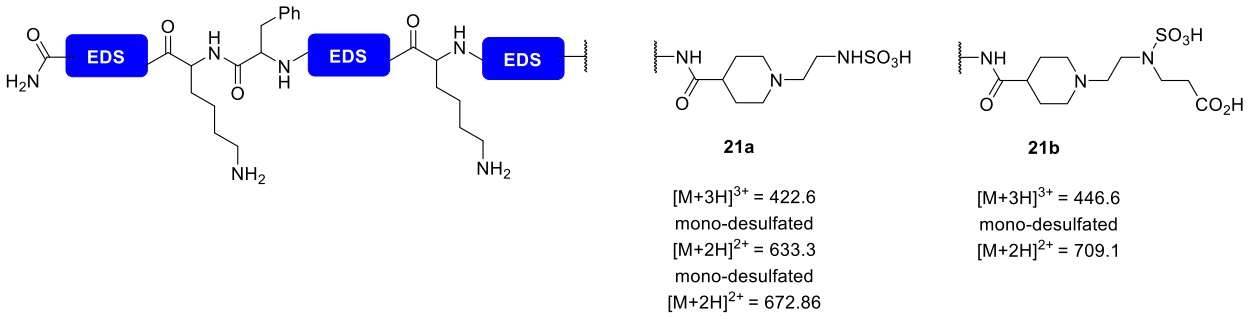

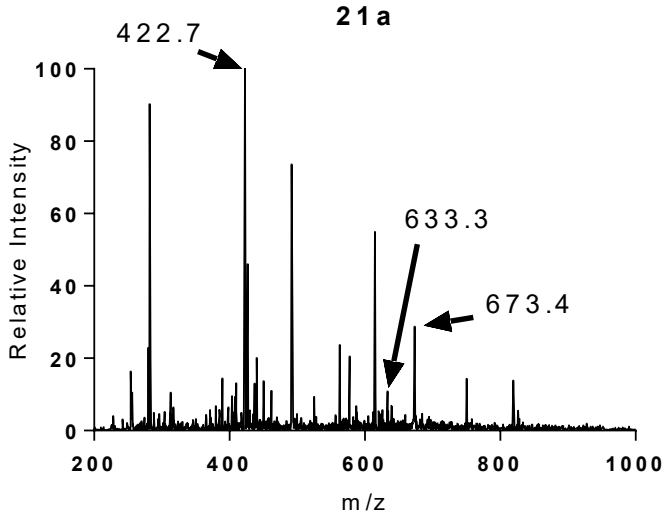

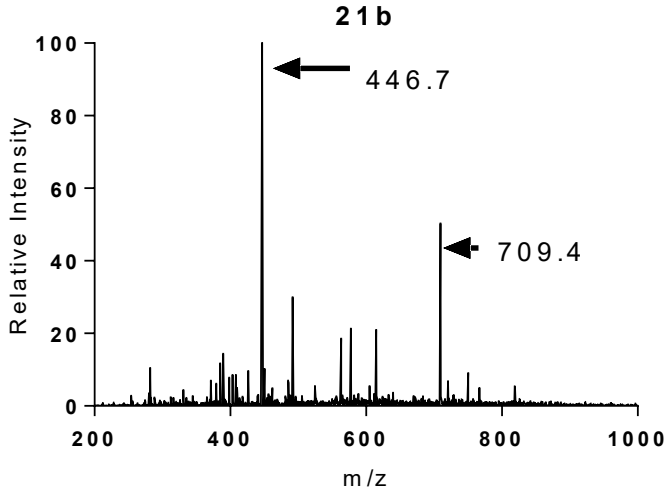

Figure S35: ESI-MS (positive mode) for oligomers **21a-b** with mass peaks identified

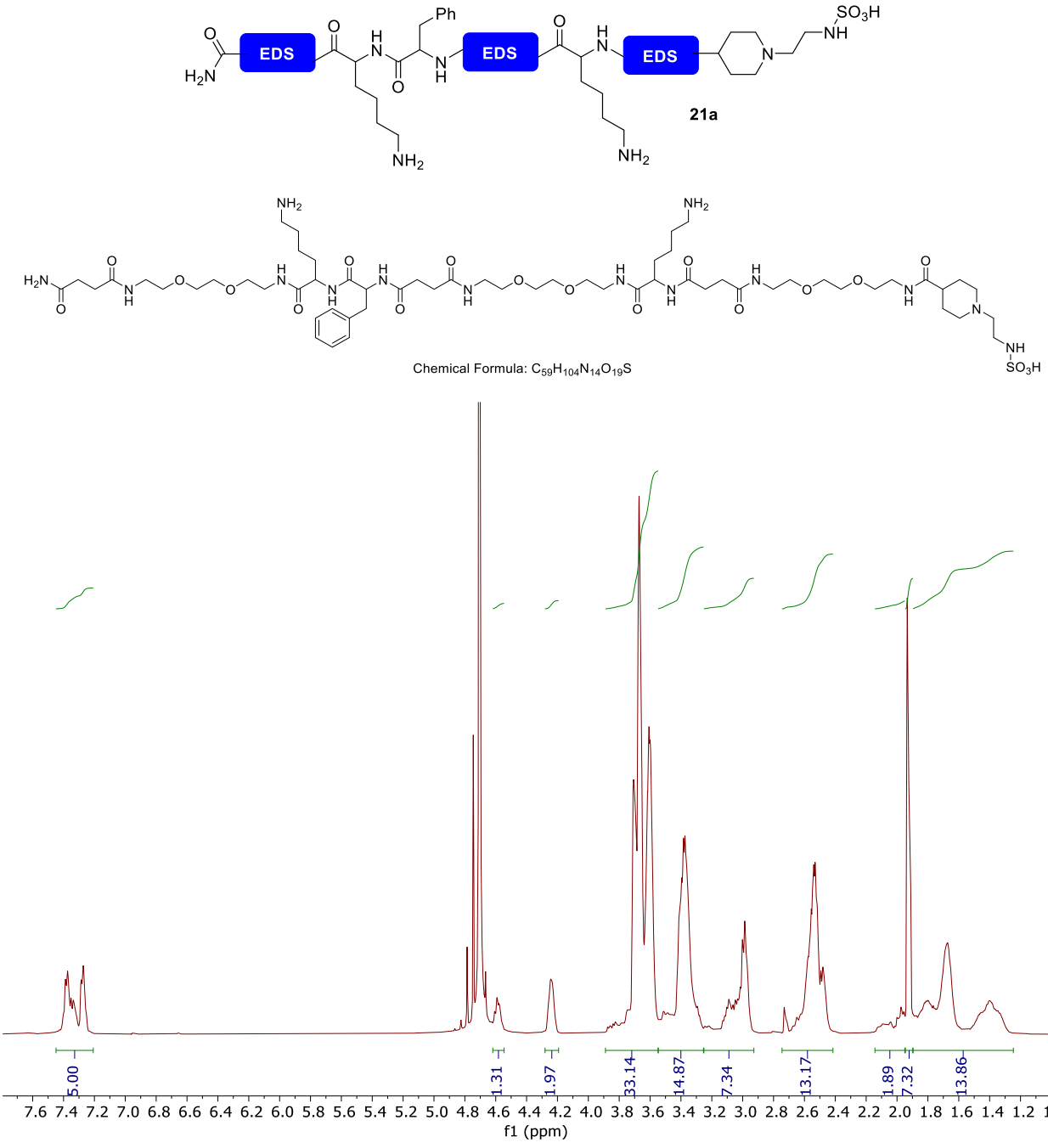

Expected proton count excluding amide and exchangeable protons: **92** **Integrated protons**: **92.56**

Acetate integration: 7.32 = 3 eq.

Figure S36: ^{1}H NMR of **21a** dissolved in D_2O and the integration analysis indicating the proton count (excluding amide and exchangeable protons) and the indicated acetate equivalents

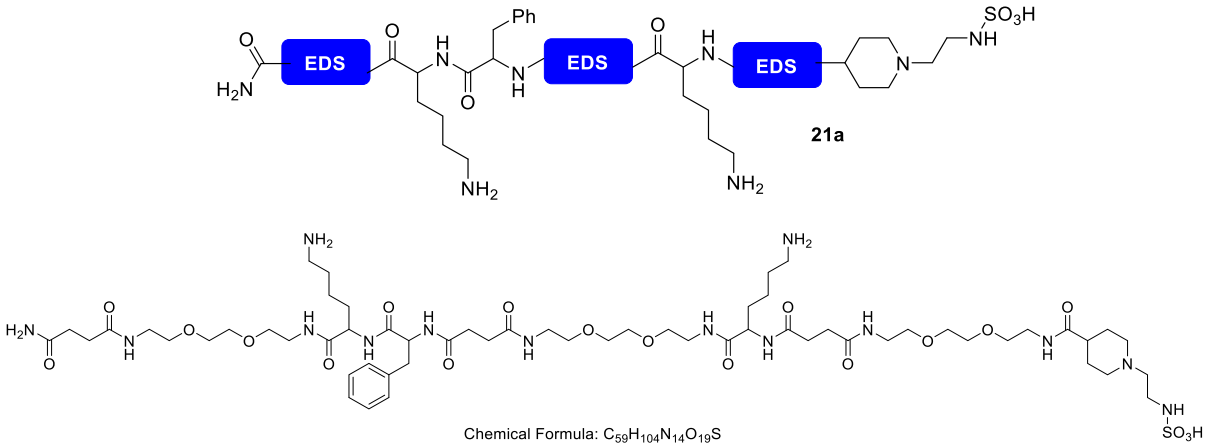

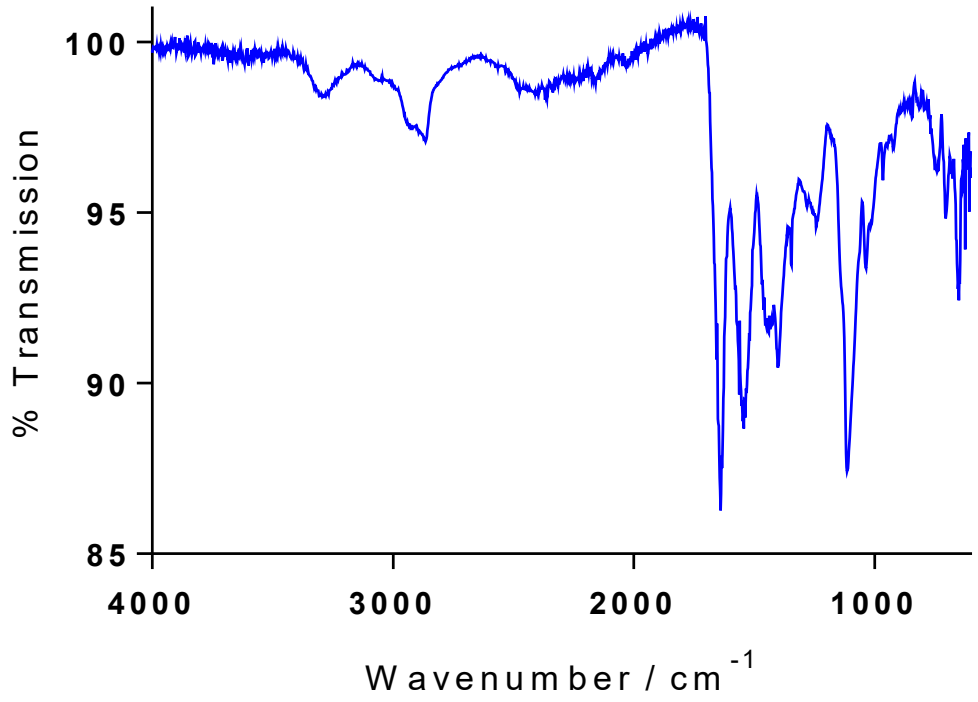

Key peaks: 3265.4 (N-H/O-H str.), 2864.2 (C-H sp^3 str.), 1631.7 (C=O amide), 1541.1 (N-H amide bend), 1400.3 (S=O str.), 1112.9 (C-N/C-O) cm^{-1}

Figure S37: FT-IR spectrum of **21a**

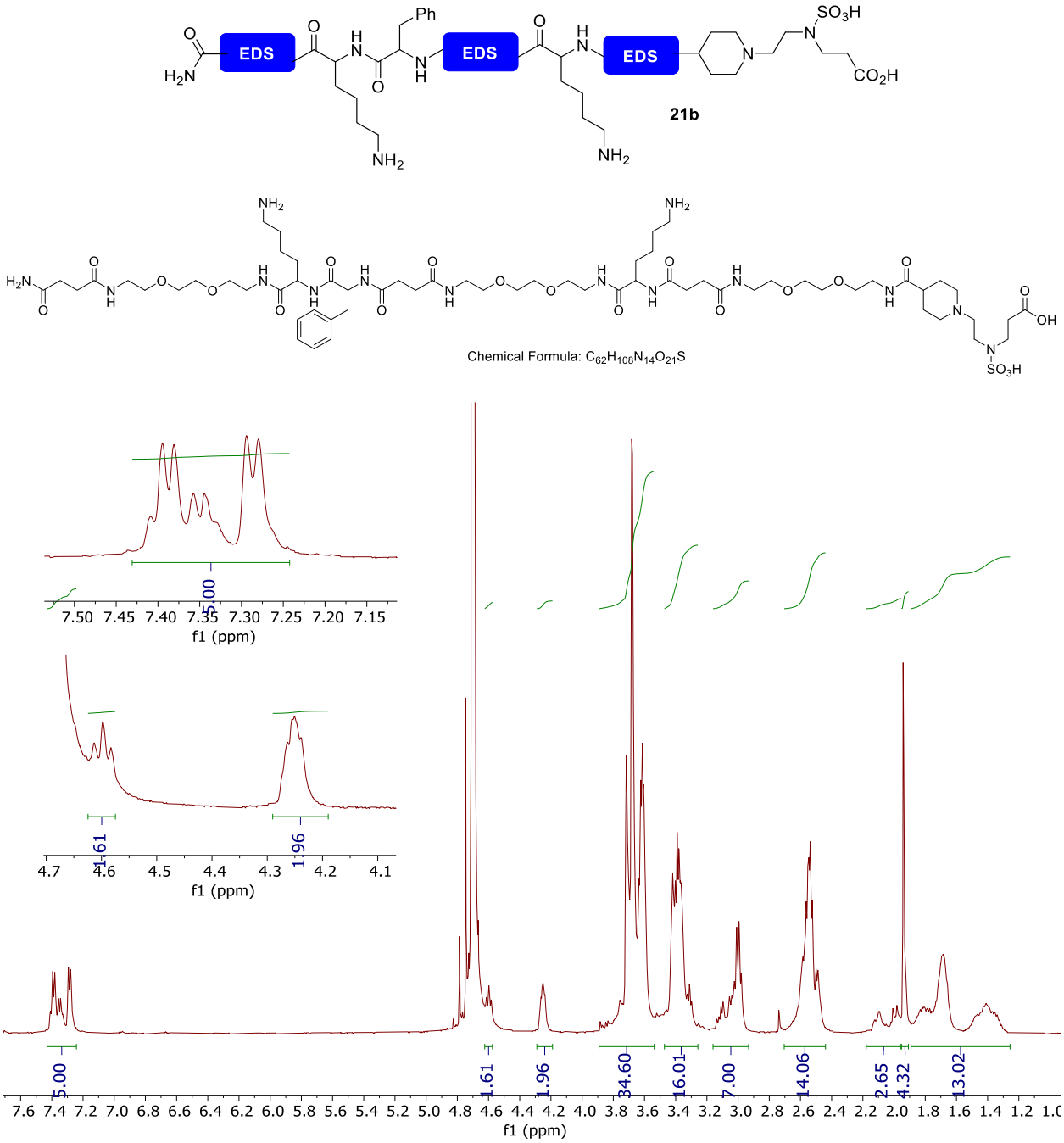

Expected proton count excluding amide and exchangeable protons: **95** **Integrated protons**: **95.91**

Acetate integration: 4.32 = 1 eq.

Figure S38: ^{1}H NMR of **21b** dissolved in D_2O and the integration analysis indicating the proton count (excluding amide and exchangeable protons) and the indicated acetate equivalents

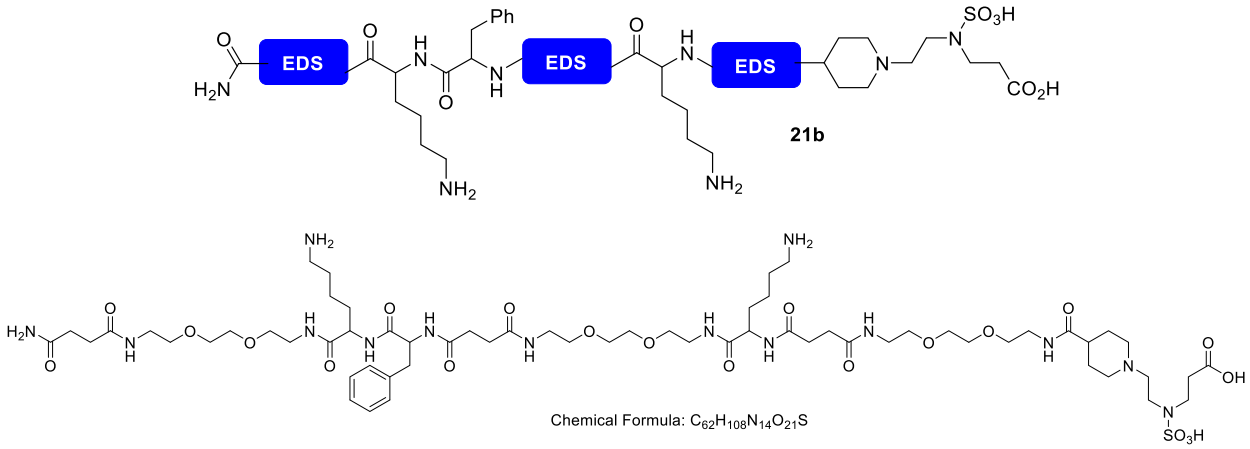

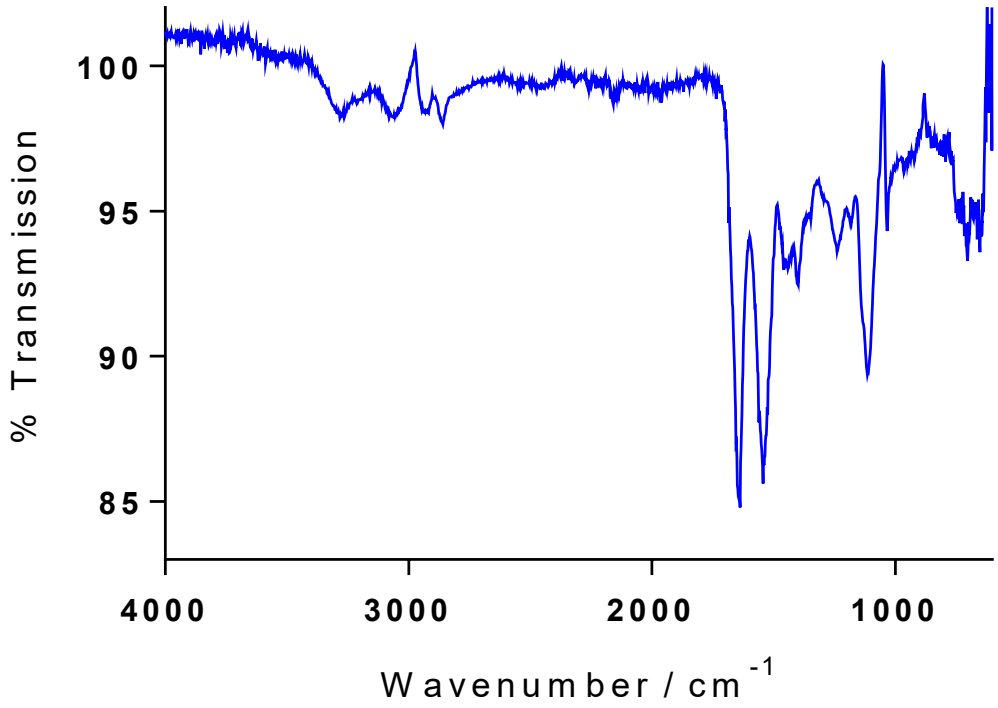

Key peaks: 3271.2 (N-H/O-H str.), 2939 (C-H sp^3 str.), 1635 (C=O amide), 1537 (N-H amide bend), 1452 (methylene str.), 1400 (S=O str.), 1109 (C-N/C-O) cm^{-1}

Figure S39: FT-IR spectrum of **21b**

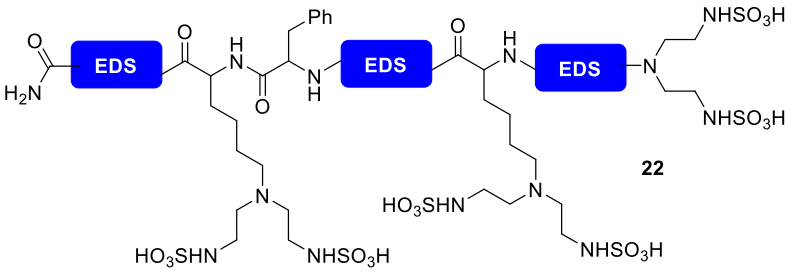

22-"Diethyl"
$[M+3H]^{3+}$ = 427.56
$[M+2H+Na]^{3+}$ = 435.9
$[M+2H]^{2+}$ = 640.8

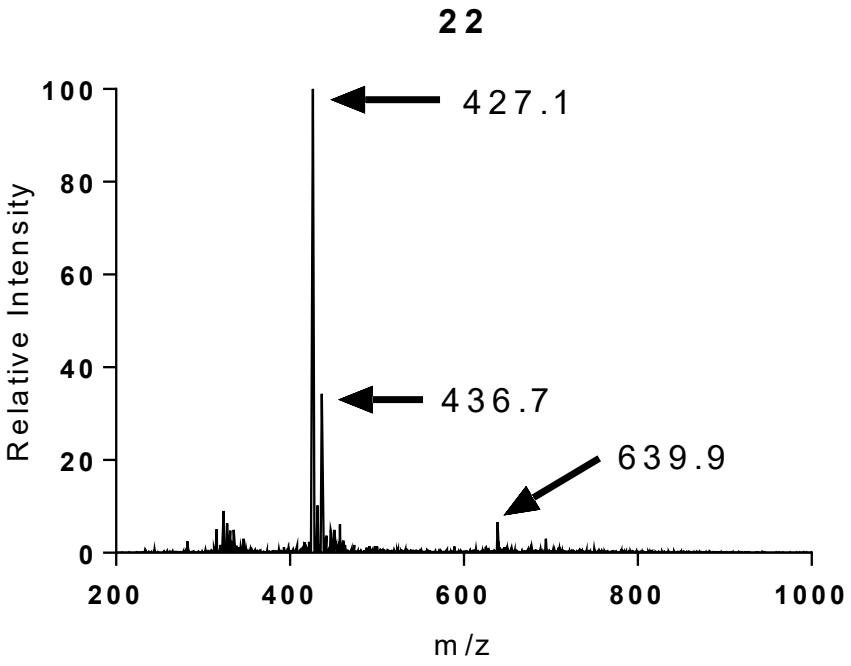

Figure S40: ESI-MS (positive mode) for oligomers **22** with mass peaks identified

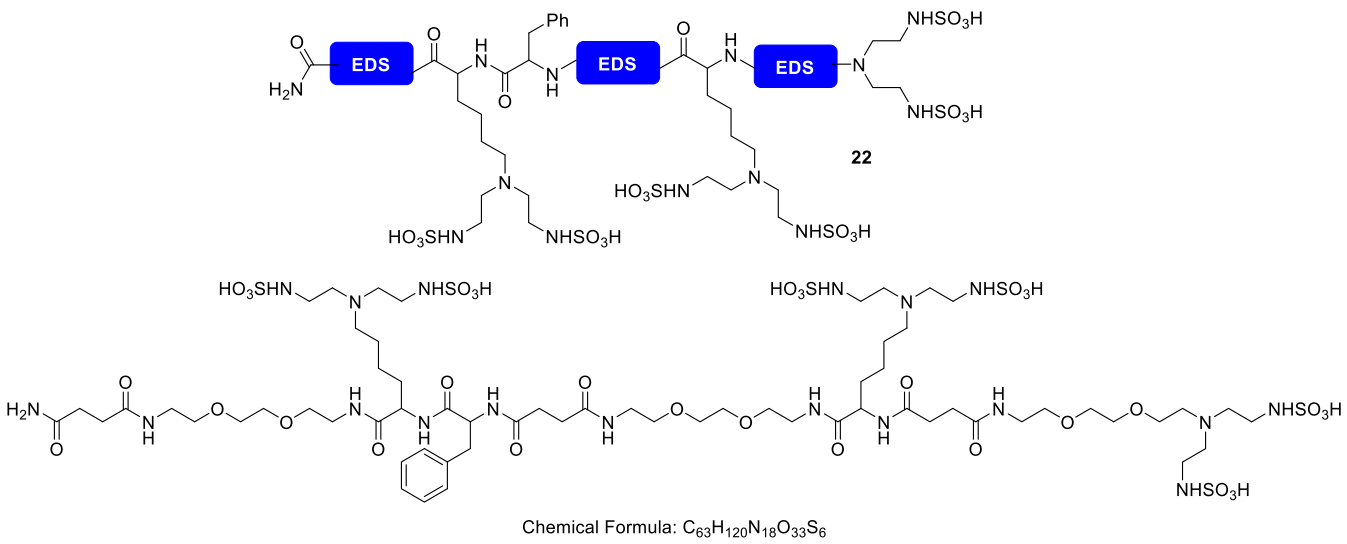

Chemical Formula: $C_{63}H_{120}N_{18}O_{33}S_6$

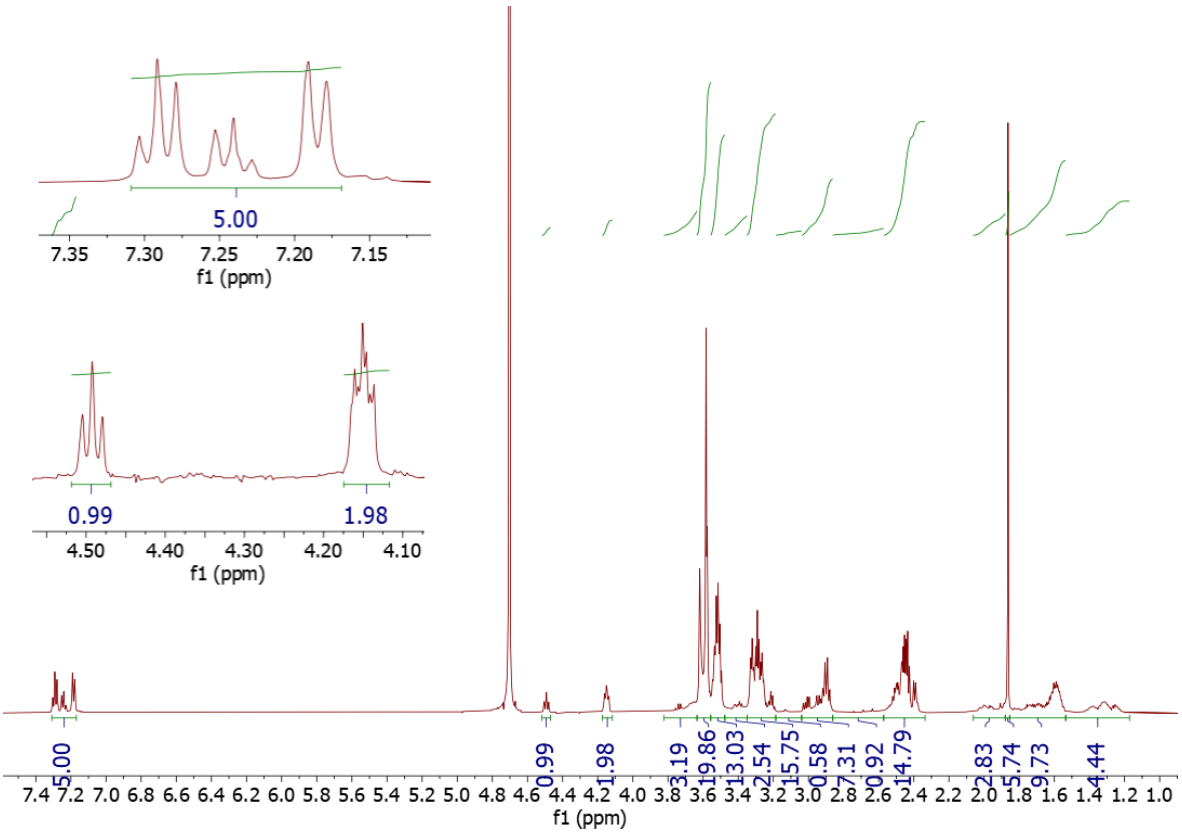

Expected proton count excluding amide and exchangeable protons: **104** **Integrated protons**: **102.95**

Acetate integration: 5.74 = 2 eq.

Figure S41: ^{1}H NMR of **22** dissolved in D_2O and the integration analysis indicating the proton count (excluding amide and exchangeable protons) and the indicated acetate equivalents

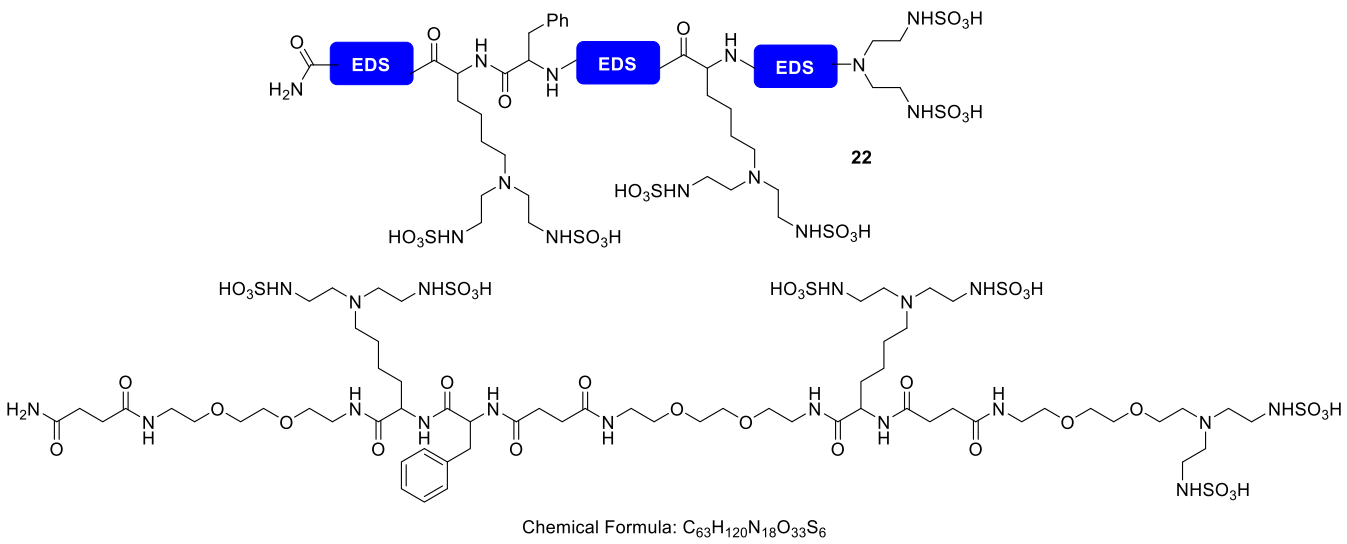

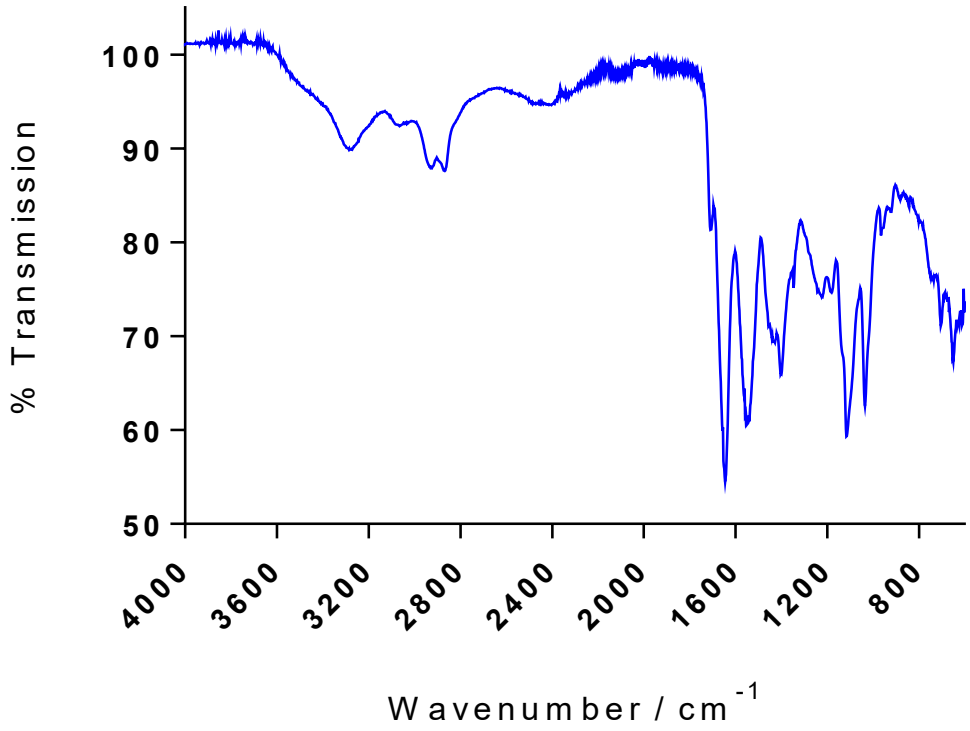

Key peaks: 3277 (N-H/O-H str.), 2868 (C-H sp^3 str.), 1643 (C=O amide), 1548 (N-H amide bend), 1427 (methylene str.), 1398 (S=O str.), 1114 (C-N/C-O) cm^{-1}

Figure S42: FT-IR spectrum of **22**

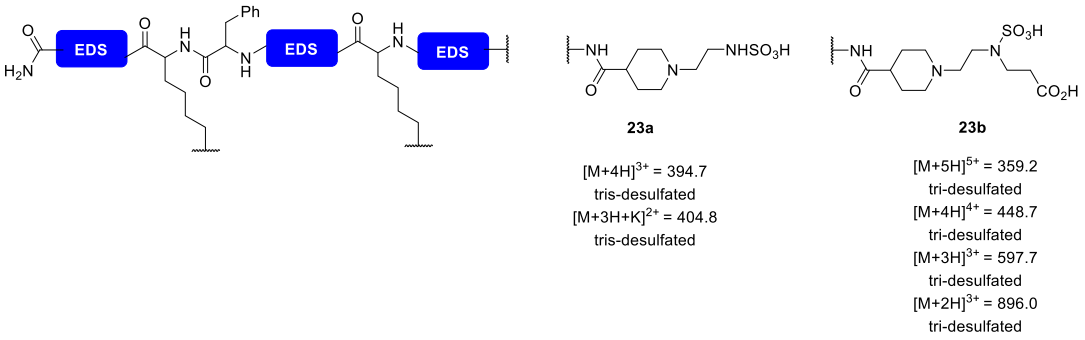

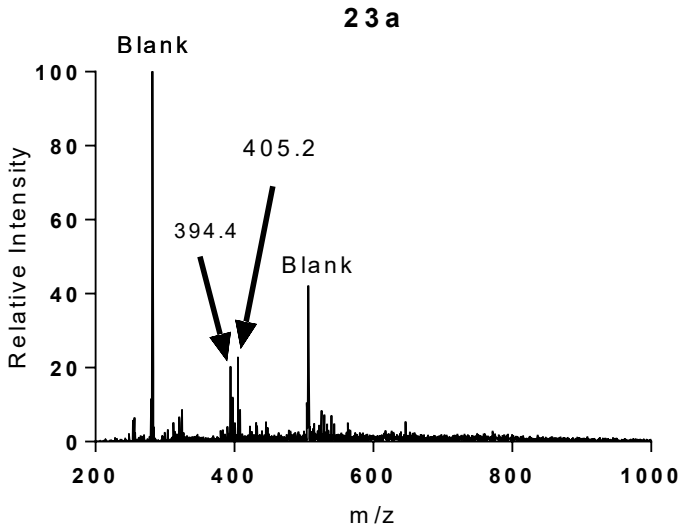

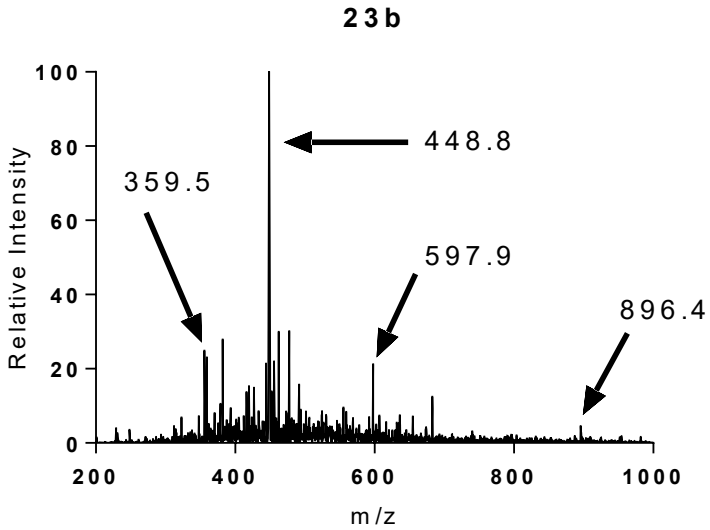

Figure S43: ESI-MS (positive mode) for oligomers **23a-b** with mass peaks identified

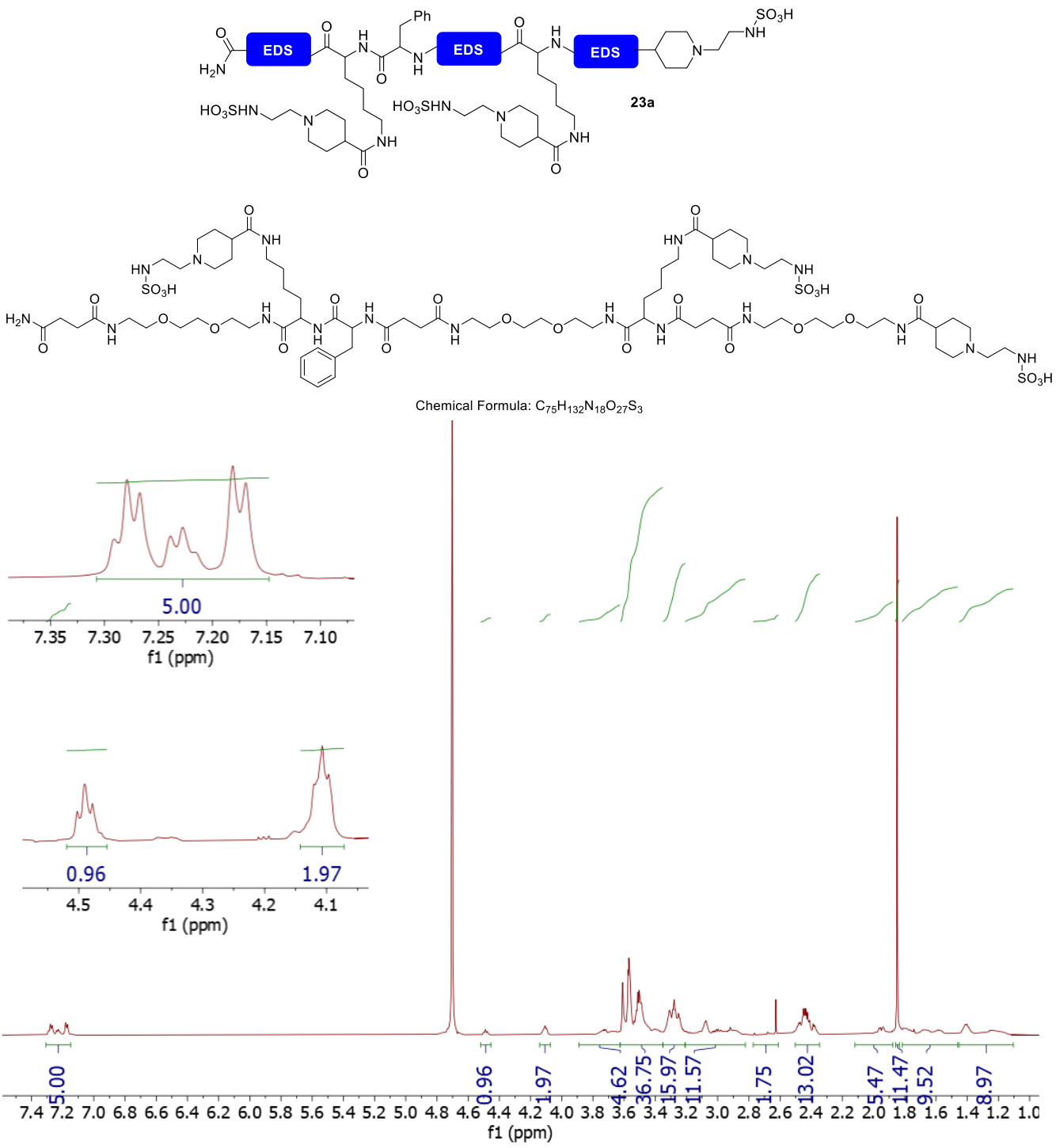

Expected proton count excluding amide and exchangeable protons: **116** **Integrated protons: 115.75**

Acetate integration: 11.47 = 4 eq.

Figure S44: ^{1}H NMR of **23a** dissolved in D_2O and the integration analysis indicating the proton count (excluding amide and exchangeable protons) and the indicated acetate equivalents

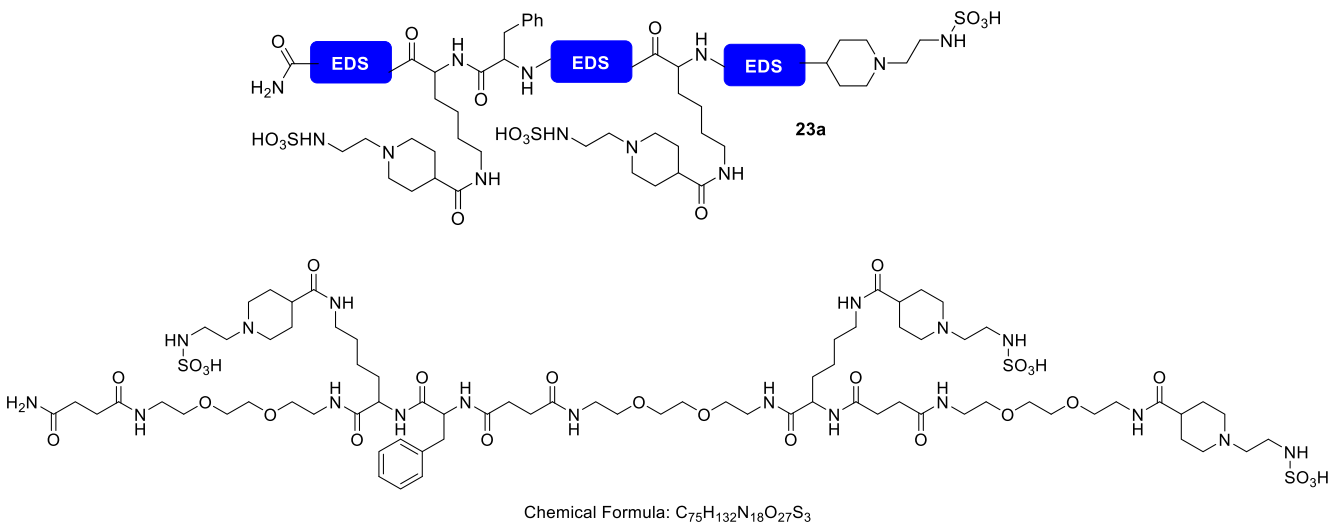

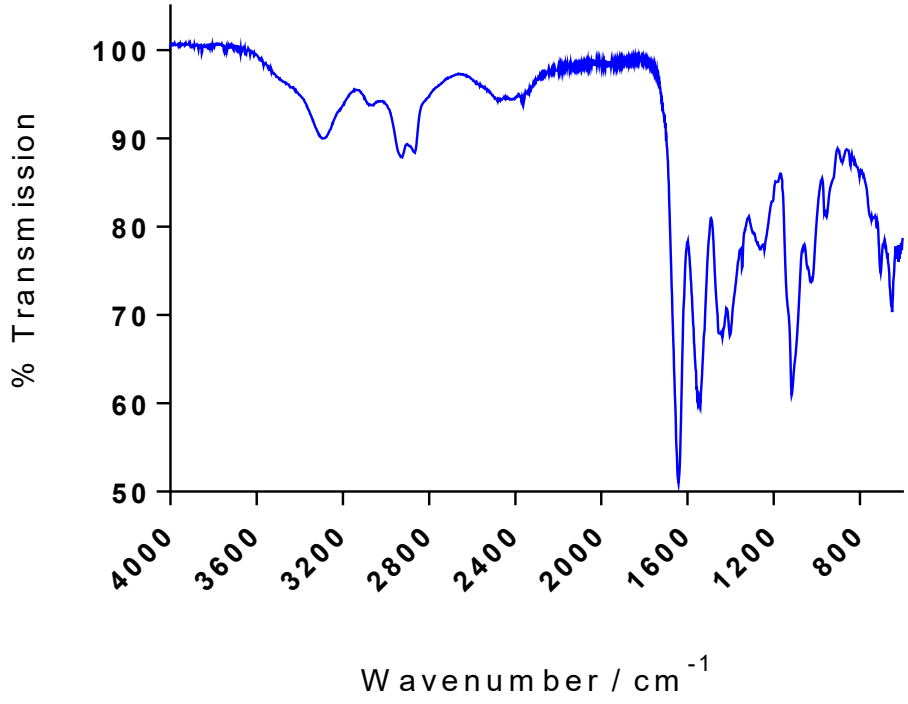

Key peaks: 3288 (N-H/O-H str.), 2864 (C-H sp^3 str.), 1639 (C=O amide), 1541 (N-H amide bend), 1435 (methylene str.), 1402 (S=O str.), 1114 and 1018(C-N/C-O) cm^{-1}

Figure S45: FT-IR spectrum of **23a**

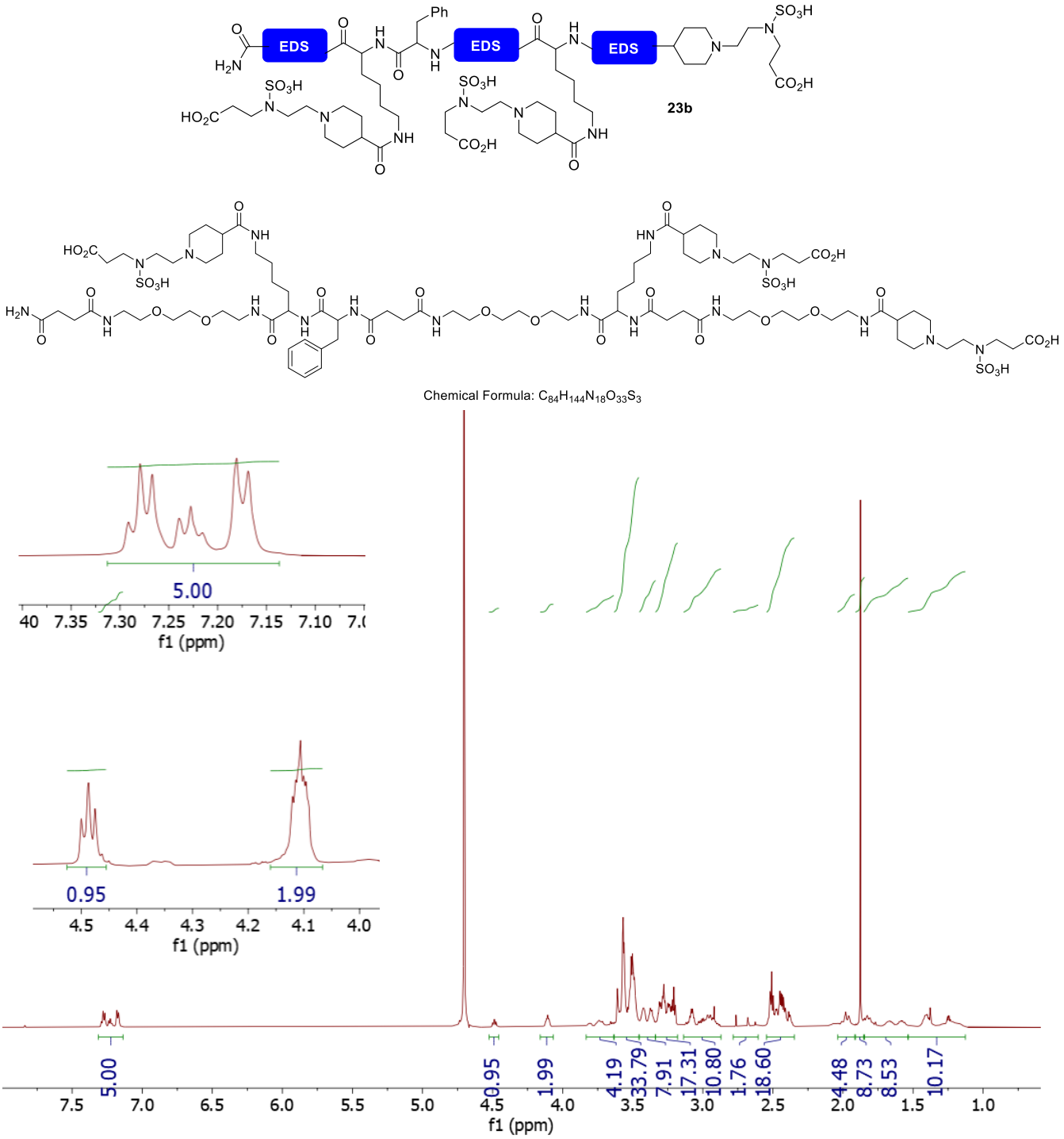

Expected proton count excluding amide/exchangeable protons: **125** **Integrated protons**: **125.54**

Acetate integration: 5.01 = 2 eq.

Figure S46: ^{1}H NMR of **23b** dissolved in D_2O and the integration analysis indicating the proton count (excluding amide and exchangeable protons) and the indicated acetate equivalents

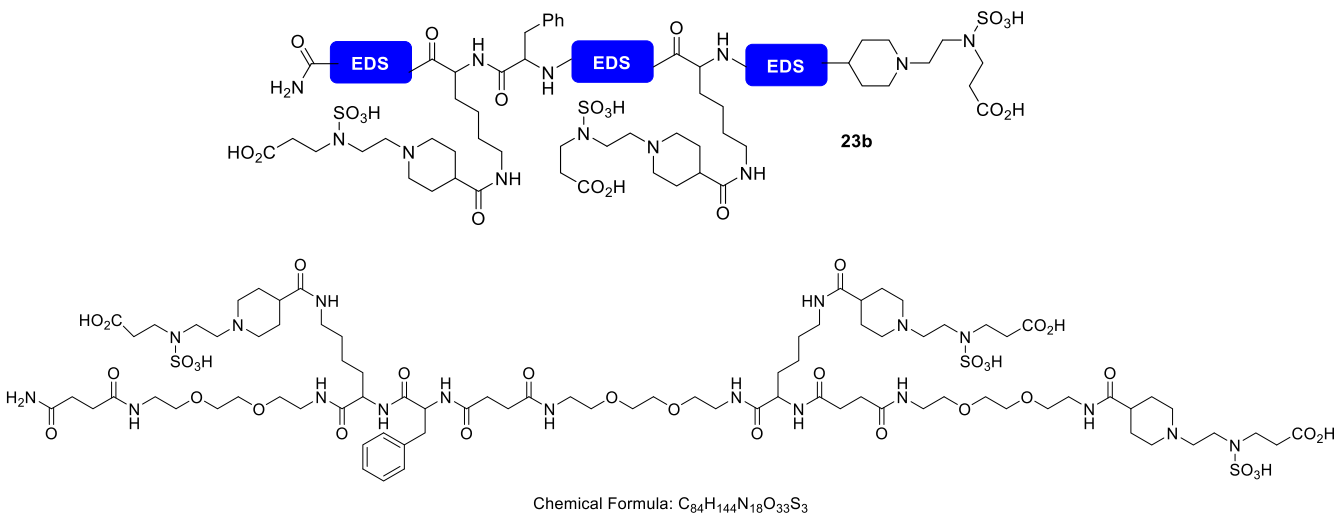

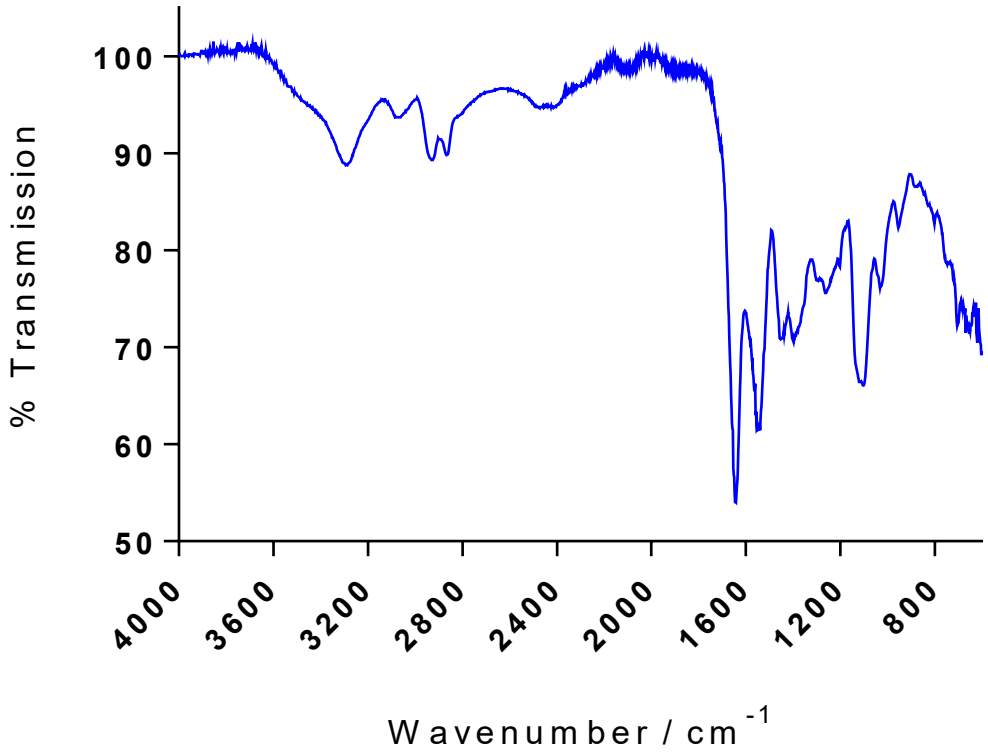

Key peaks: 3288 (N-H/O-H str.), 2929 (C-H sp^3 str.), 1639 (C=O amide), 1544 (N-H amide bend), 1446 (methylene str.), 1392 (S=O str.), 1099 (C-N/C-O) cm^{-1}

Figure S47: FT-IR spectrum of **23b**

Table S4: Elemental analysis of various *N*-sulfated oligmeric probes (results are reported as the average and the associated standard deviation)

Sample	% C	% H	% N	% S
13c (Theoretical)	42.36	7.02	11.11	5.65
13c[a]	46.36	7.93	11.24	2.22
20a (Theoretical)	48.66	7.42	14.44	4.72
20a	48.14 ± 0.20	7.59 ± 0.01	11.54 ± 0.10	2.08 ± 0.29
20b (Theoretical)	51.12	7.57	12.27	2.01
20b	50.55 ± 0.19	6.48 ± 2.03	11.65 ± 0.08	0.93 ± 0.00
21a (Theoretical)	52.66	7.73	14.57	2.38
21a	51.9 ± 0.07	8.01 ± 0.01	12.03 ± 0.04	1.31 ± 0.05
21b (Theoretical)	52.53	7.68	13.83	2.26
21b[a]	50.54	7.60	11.93	3.10
22 (Theoretical)	40.82	6.55	12.42	9.47
22	48.27 ± 0.16	6.48 ± 2.14	12.33 ± 0.03	2.74 ± 0.3
23a (Theoretical)	48.78	7.28	12.64	4.82
23a	51.74 ± 0.04	8.26 ± 0.00	11.91 ± 0.00	0.40 ± 0.08
23b (Theoretical)	48.90	7.11	11.41	4.35
23b	50.71 ± 0.36	8.15 ± 0.05	11.30 ± 0.21	1.415 ± 0.86

a: Only a single sample recorded

Table S5: Recovered yields of oligomers following resin cleavage and anion exchange. Oligomer molecular weights calculated with 3 acetate anion equivalents.

Oligomer	Molecular Weight / gmol^{-1}	Scale / mmol	Recovered mass / mg	Recovered mmol	% Yield
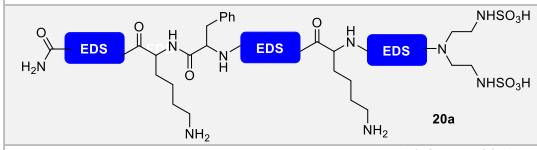 20a	1536.80	0.05	30.15	0.019	38
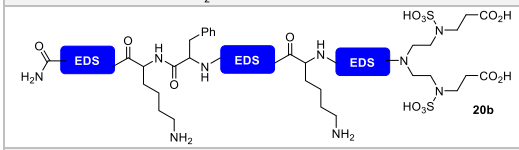 20b	1680.84	0.05	26.64	0.016	32
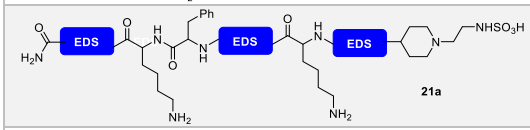 21a	1524.87	0.025	18.66	0.012	48
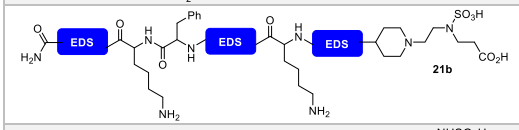 21b	1596.90	0.025	10.83	0.0067	27
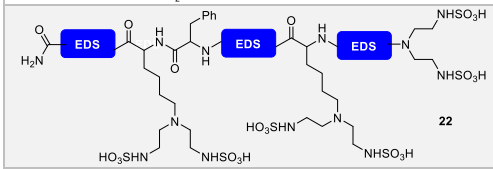 22	2031.21	0.05	36.87	0.018	36
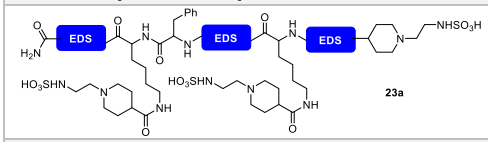 23a	1995.29	0.05	39.76	0.019	38
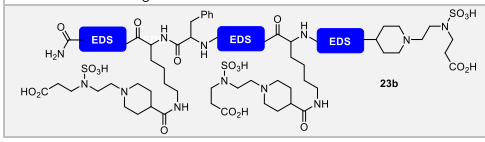 23b	2211.68	0.05	40.91	0.018	36

Appendix

Additional analytical and characterization data of cyclic sulfamidate starting materials, oligomers and controls.

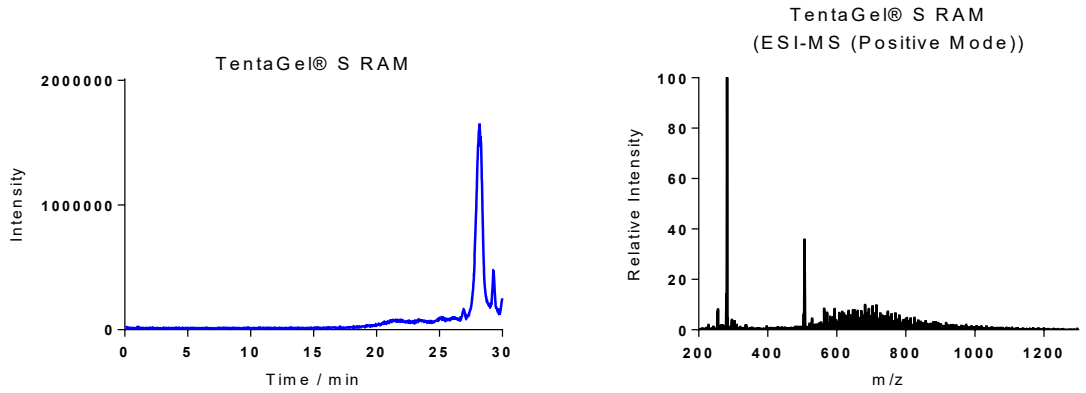

Figure S48: (Left) RP-HPLC trace, and (right) Positive mode ESI-MS of cleavage product exclusively from TentaGel® S RAM following acidic cleavage

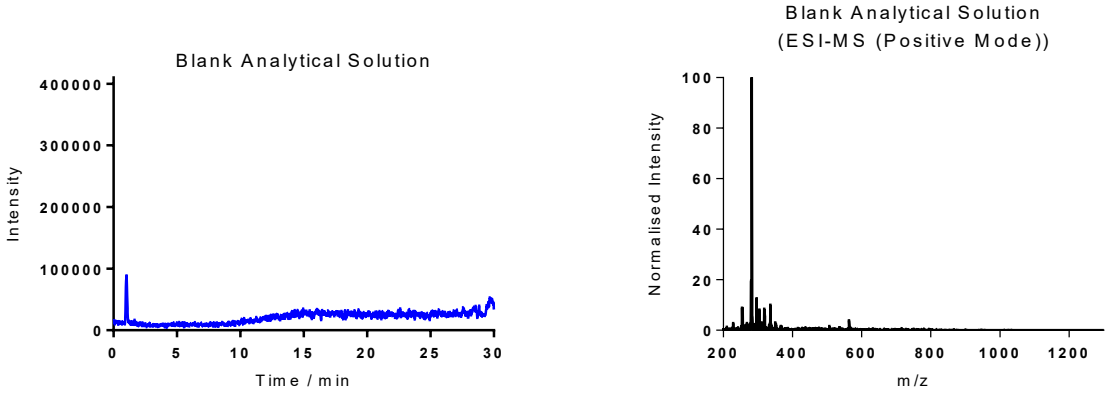

Figure S49: (Left) RP-HPLC trace, (Right) Positive mode ESI-MS of the blank analytical solution (MeCN:H_2O, 9:1, v:v) used for RP-HPLC-MS probes

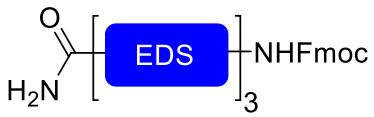

Fmoc-protected **6**

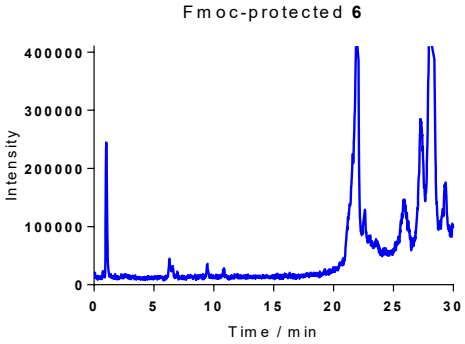

Fmoc-protected **6**
$[M+2H]^{2+}$, $[M+Na+H]^{2+}$, $[M+K+H]^{2+}$
calculated: 465.7, 476.7, 484.7
found: 465.8, 476.5, 484.5

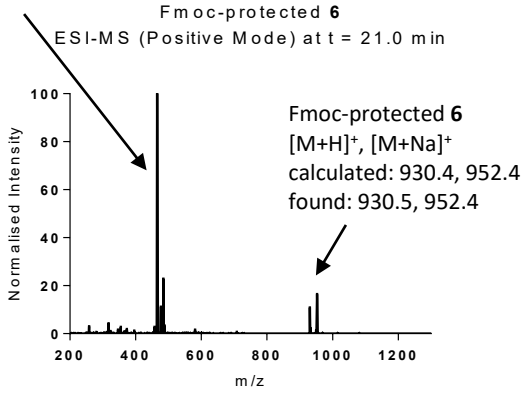

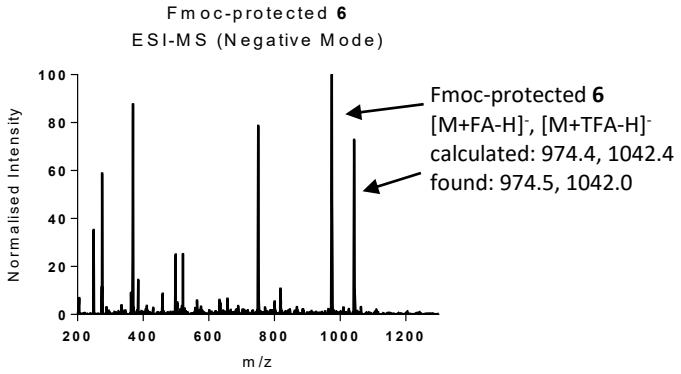

Figure S50: (Top) RP-HPLC trace, (Bottom Left) ESI-MS (Positive mode) at t = 21.0 min, and (Bottom Right) ESI-MS (Negative mode) of Fmoc-protected **6** directly cleaved from solid support

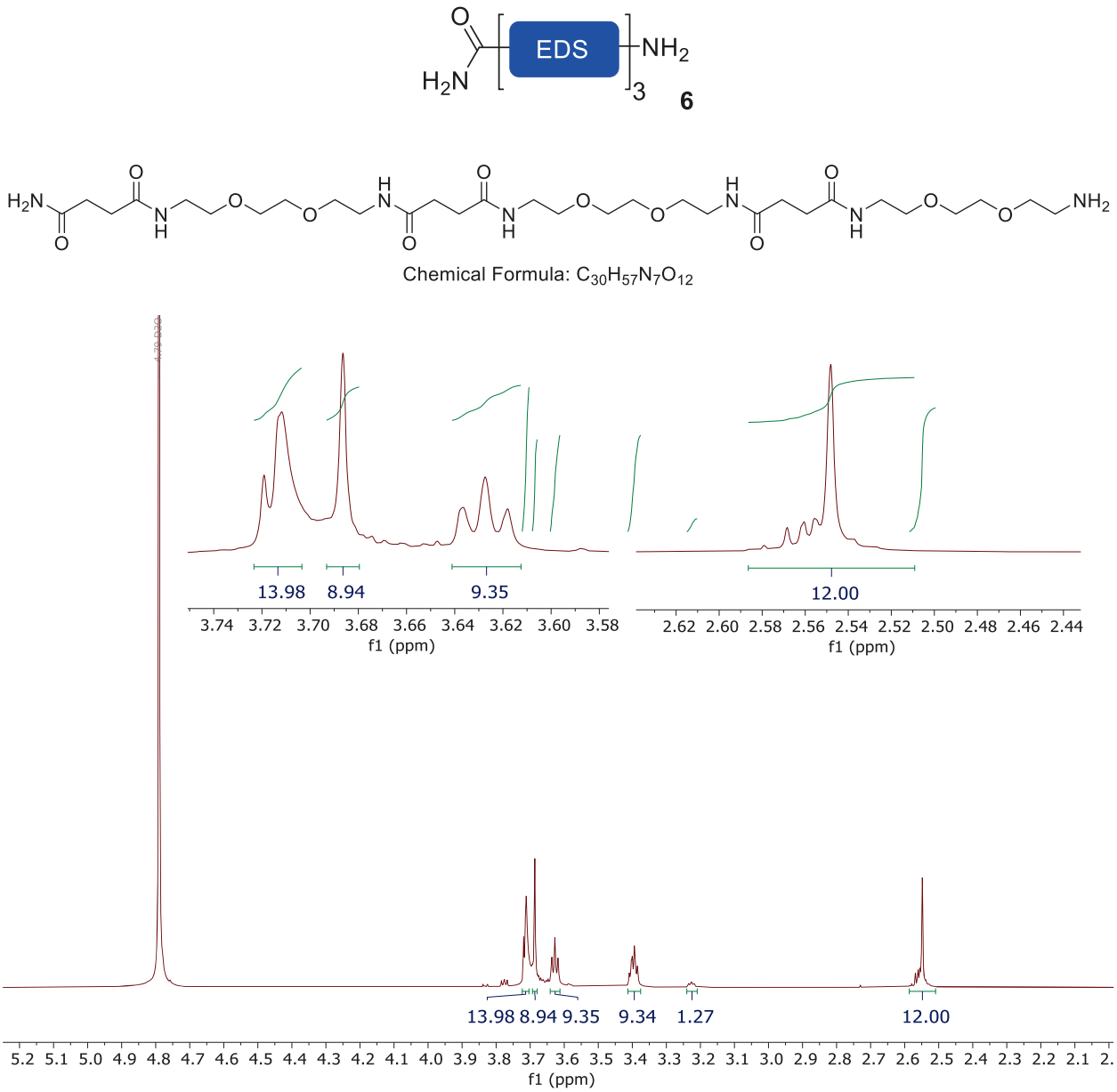

Expected proton count excluding amide protons: **52** **Integrated protons**: **54.87**

Figure S51: ^{1}H NMR of **6** dissolved in D_2O and the integration analysis indicating the proton count (excluding amide protons) and the indicated acetate equivalents

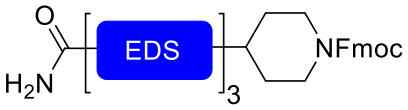

Fmoc-protected **11**

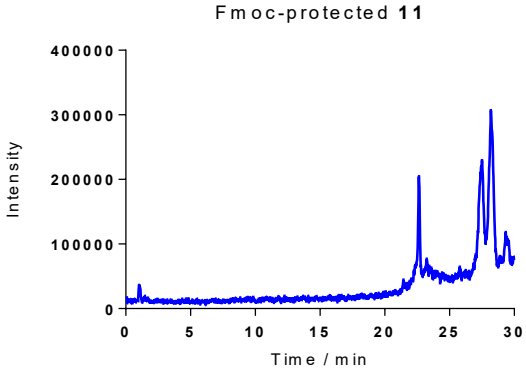

Fmoc-protected **11**
$[M+2H]^{2+}$, $[M+Na+H]^{2+}$, $[M+K+H]^{2+}$
calculated: 521.2, 532.2, 540.2
found: 521.3, 532.3, 540.4

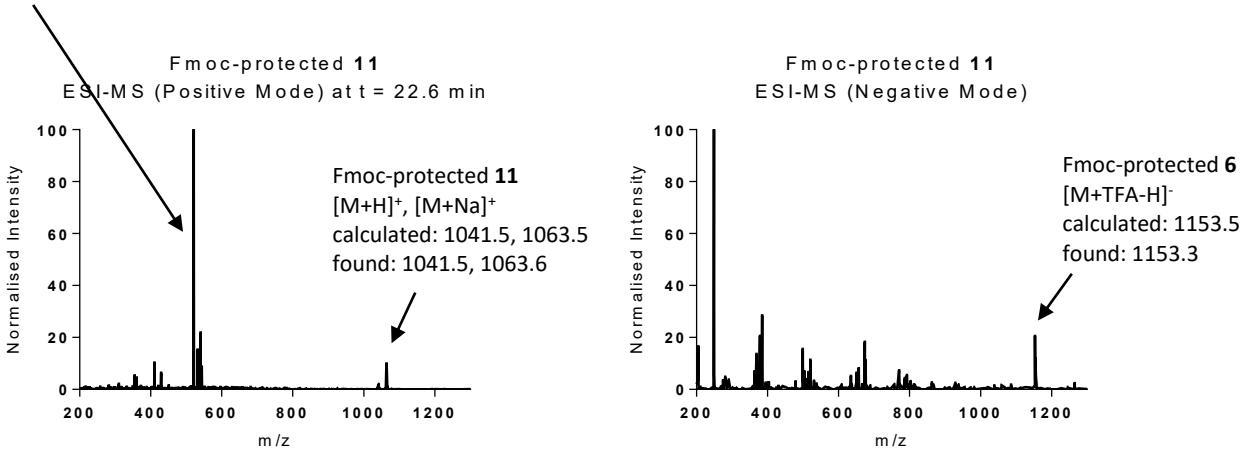

Figure S52: (Top) RP-HPLC trace, (Bottom Left) ESI-MS (Positive mode) at t = 22.6 min, and (Bottom Right) ESI-MS (Negative mode) of Fmoc-protected **11** directly cleaved from solid support

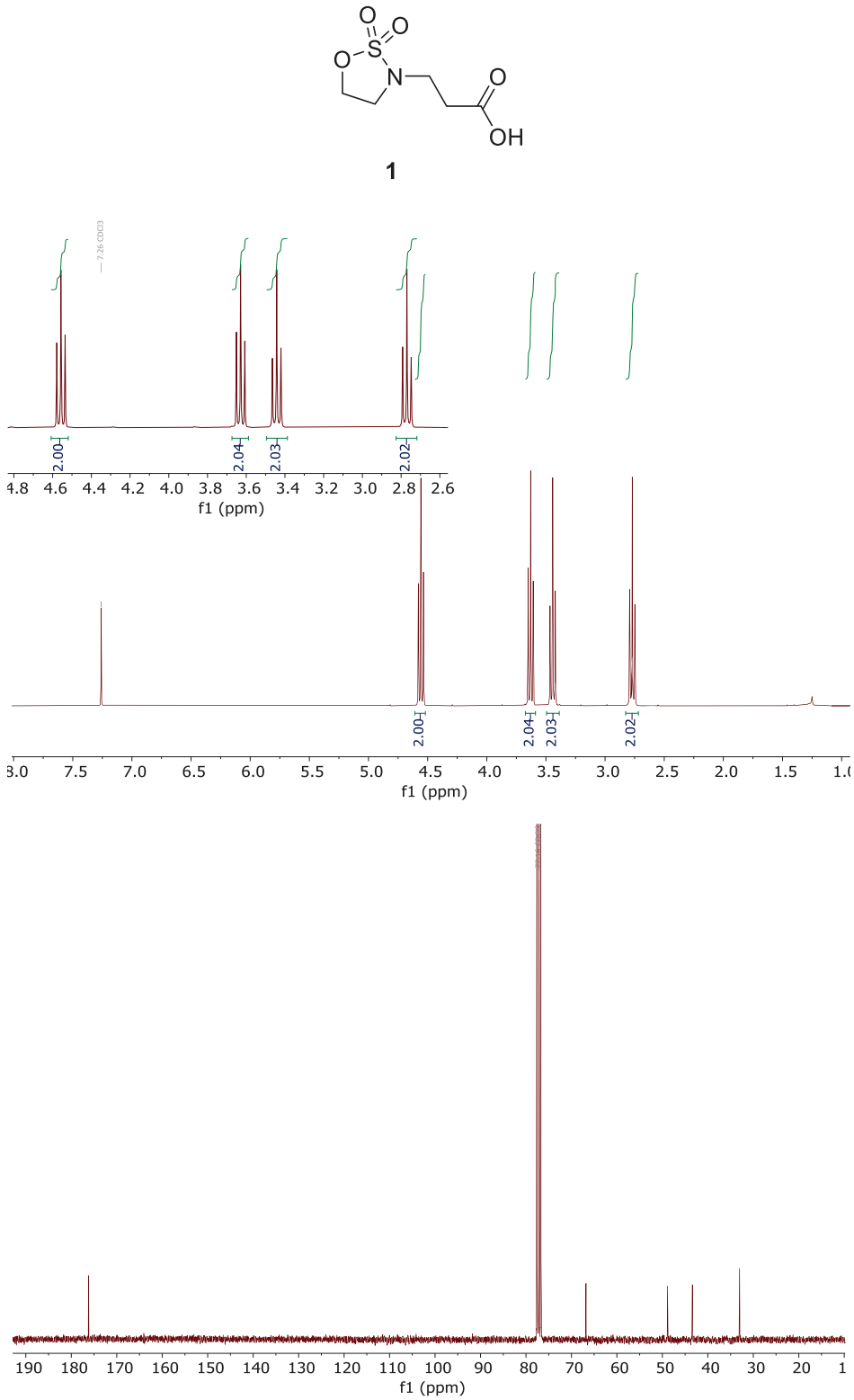

Figure S51: (Top) ^{1}H NMR and (Bottom) ^{13}C NMR of **1** dissolved in $CDCl_3$

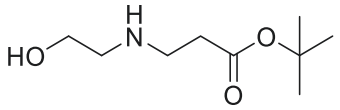
HO
H
N
O
O

4

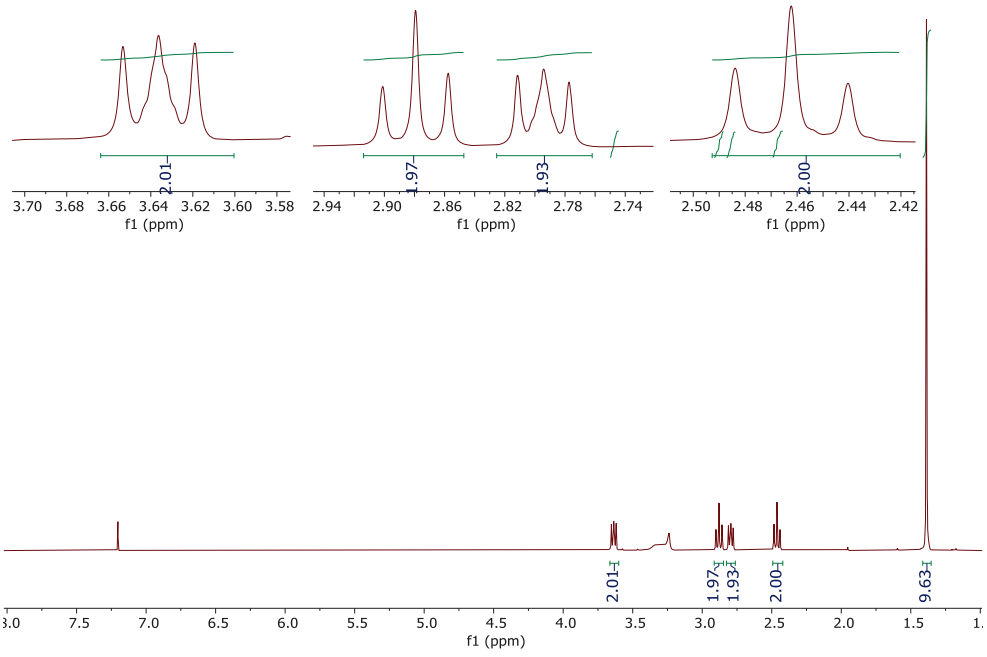
2.01
1.97
1.93
2.00
f1 (ppm)
2.01
1.97
1.93
2.00
9.63
f1 (ppm)

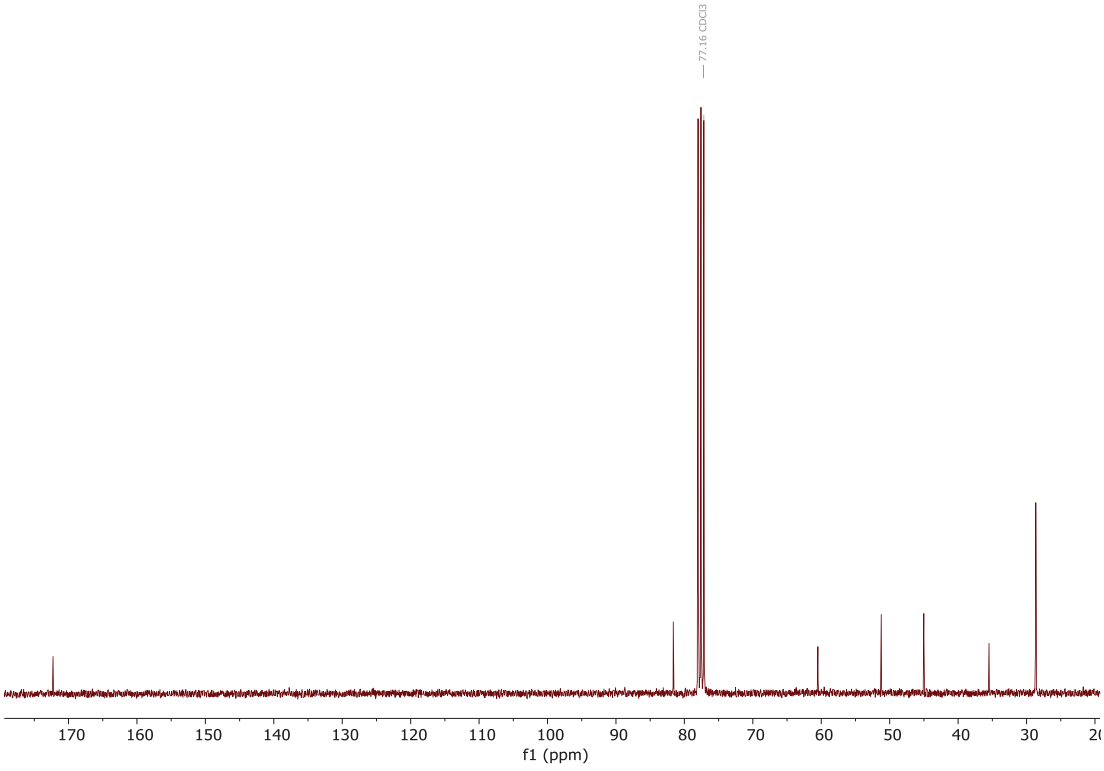
77.16 CDCl3
f1 (ppm)

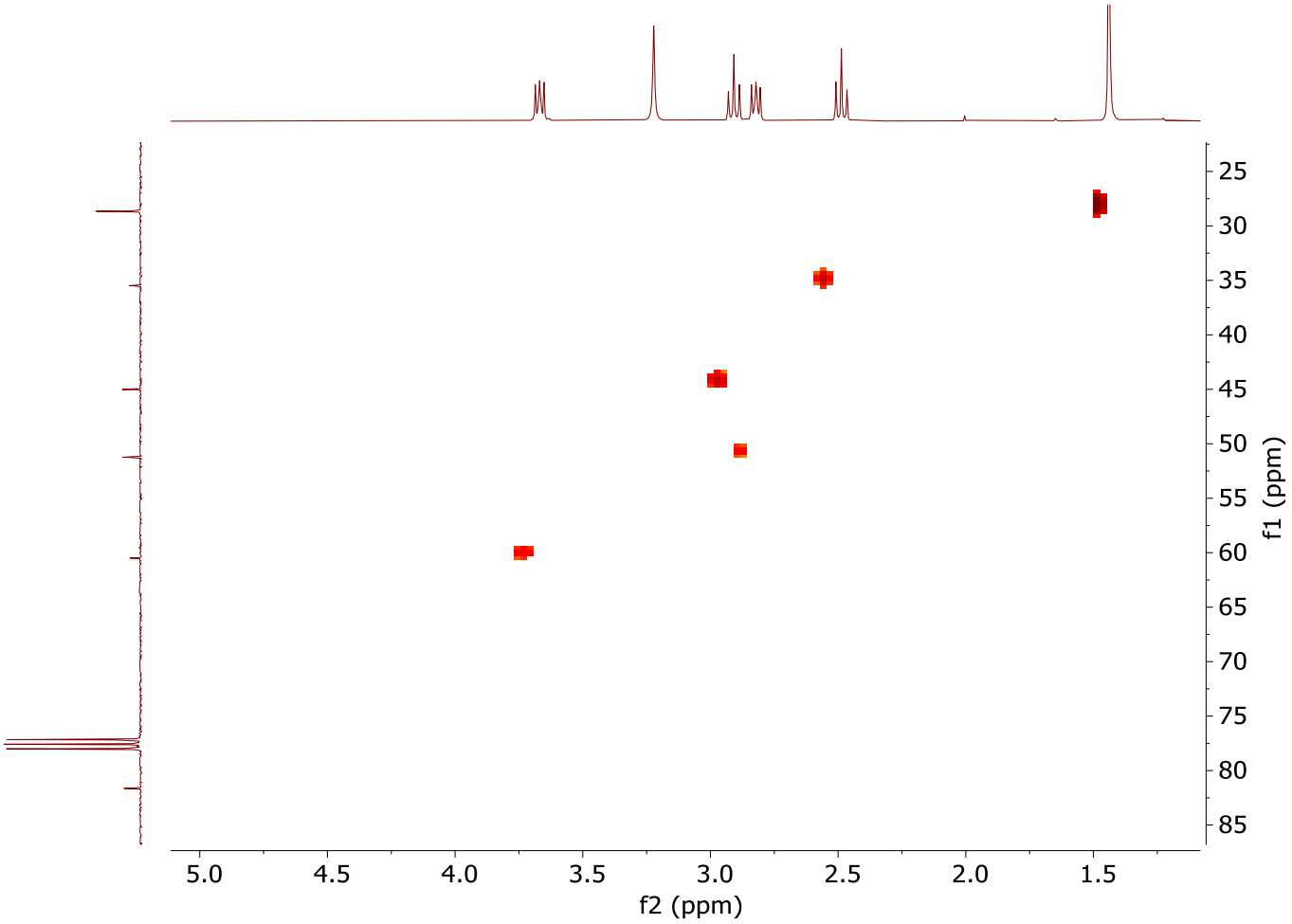

Figure S52: (Top) ^{1}H NMR, (Middle) ^{13}C NMR and (Bottom) ^{1}H-^{13}C HSQC NMR of **4** dissolved in $CDCl_3$

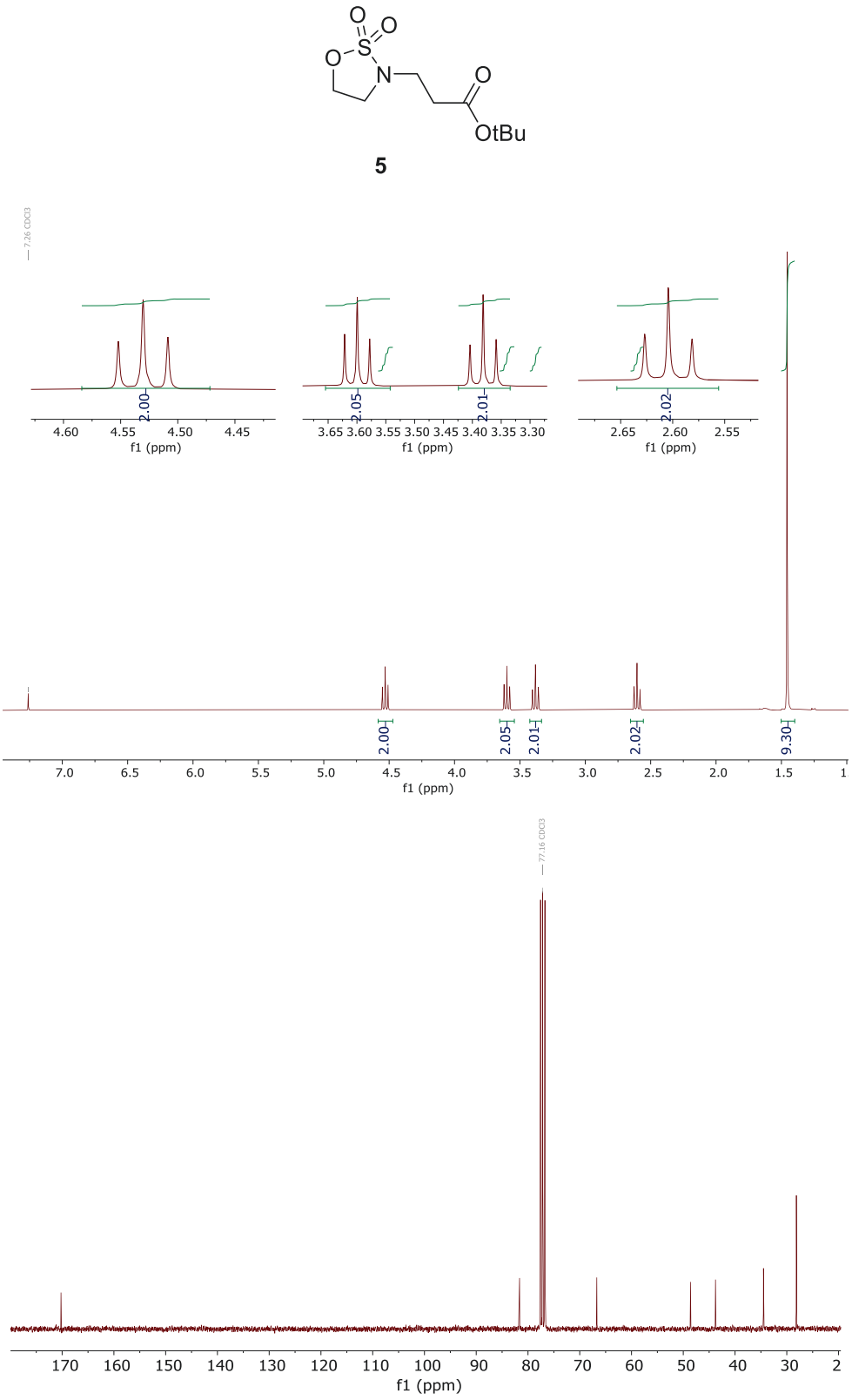

Figure S53: (Top) ^{1}H NMR and (Bottom) ^{13}C NMR of **5** dissolved in $CDCl_3$

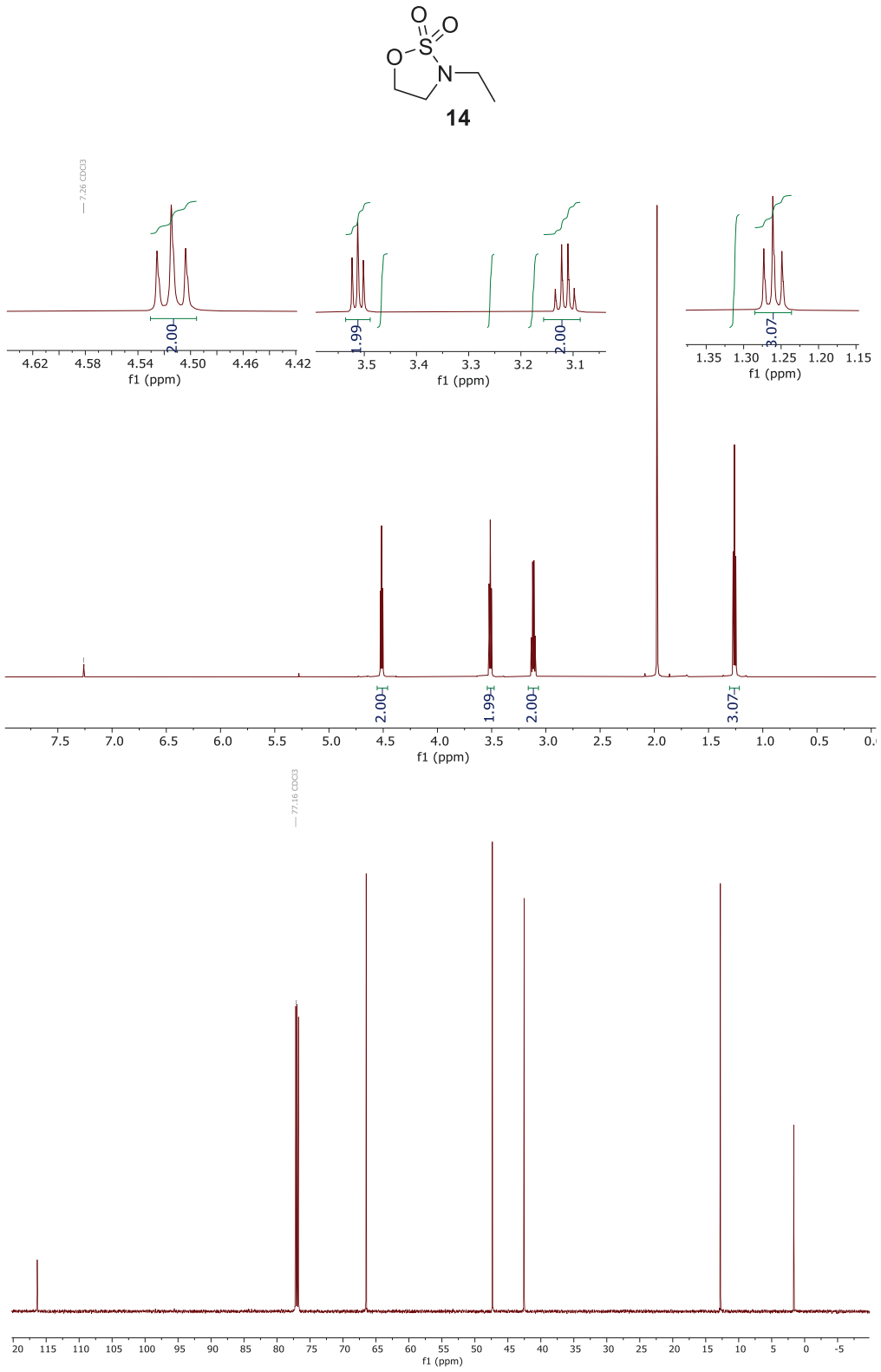

Figure S54: (Top) ^{1}H NMR and (Bottom) ^{13}C NMR of **14** dissolved in $CDCl_3$

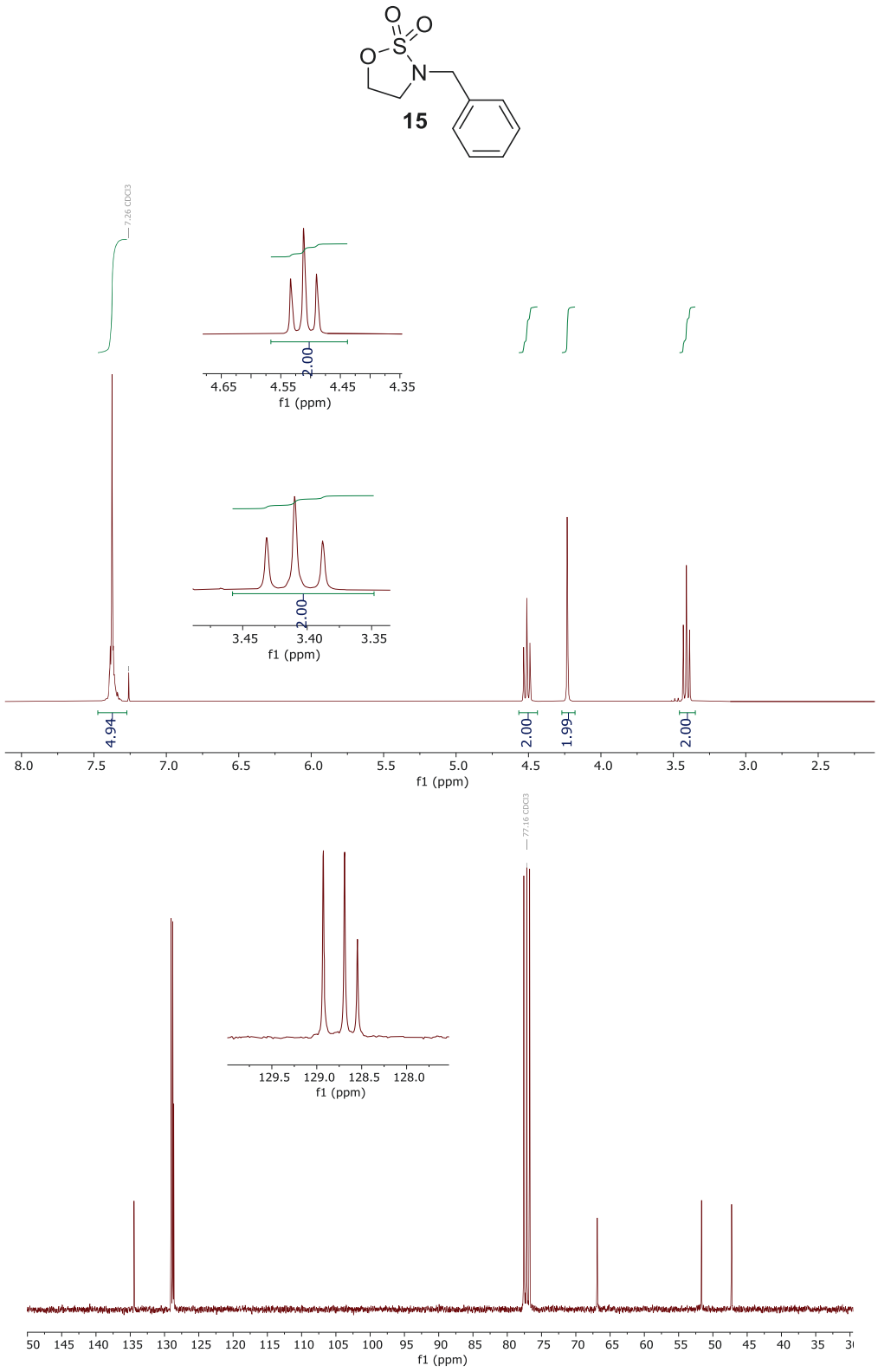

Figure S54: (Top) ^{1}H NMR and (Bottom) ^{13}C NMR of **15** dissolved in $CDCl_3$

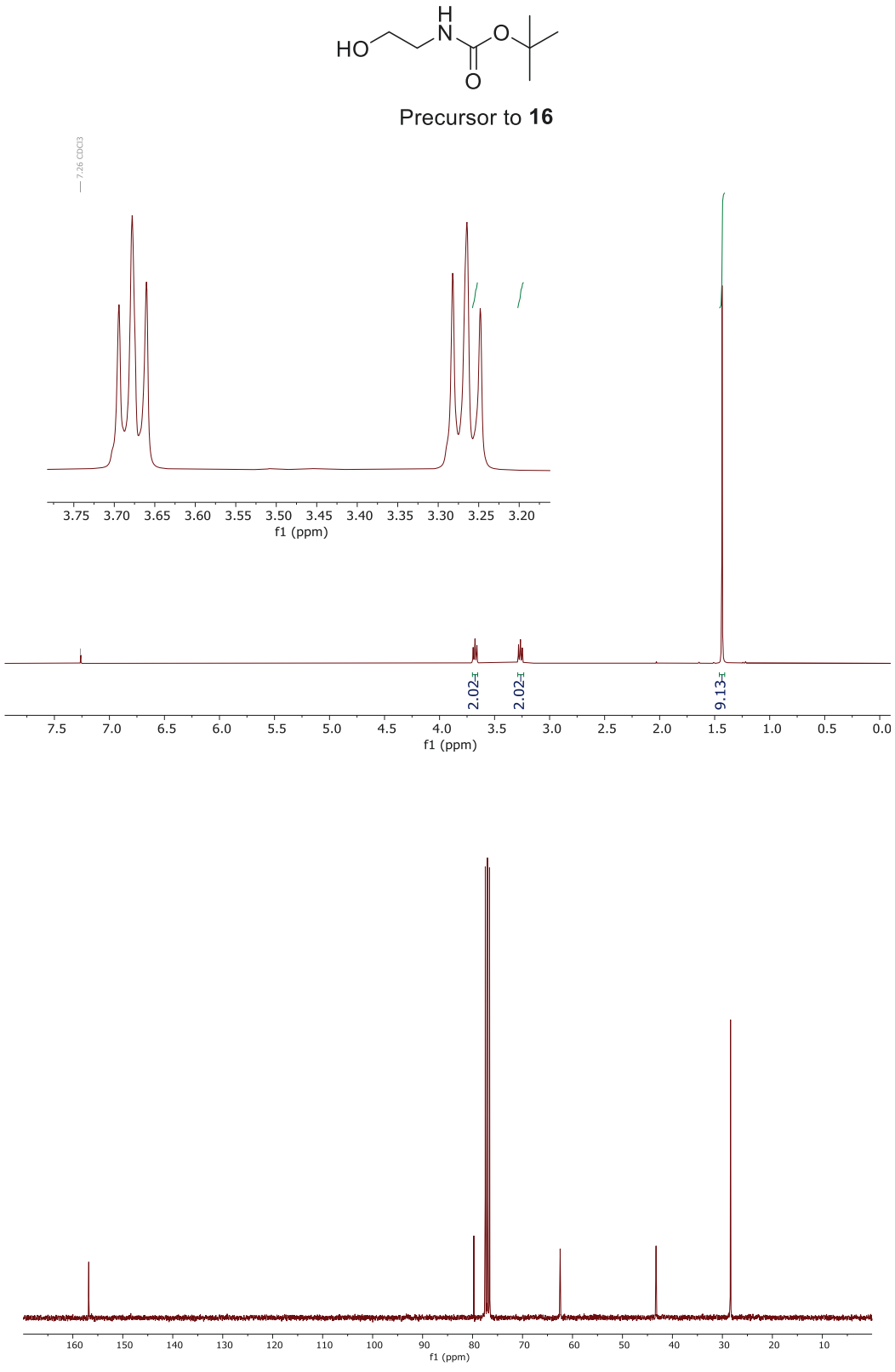

Figure S55: (Top) ^{1}H NMR and (Bottom) ^{13}C NMR of **16** precursor dissolved in $CDCl_3$

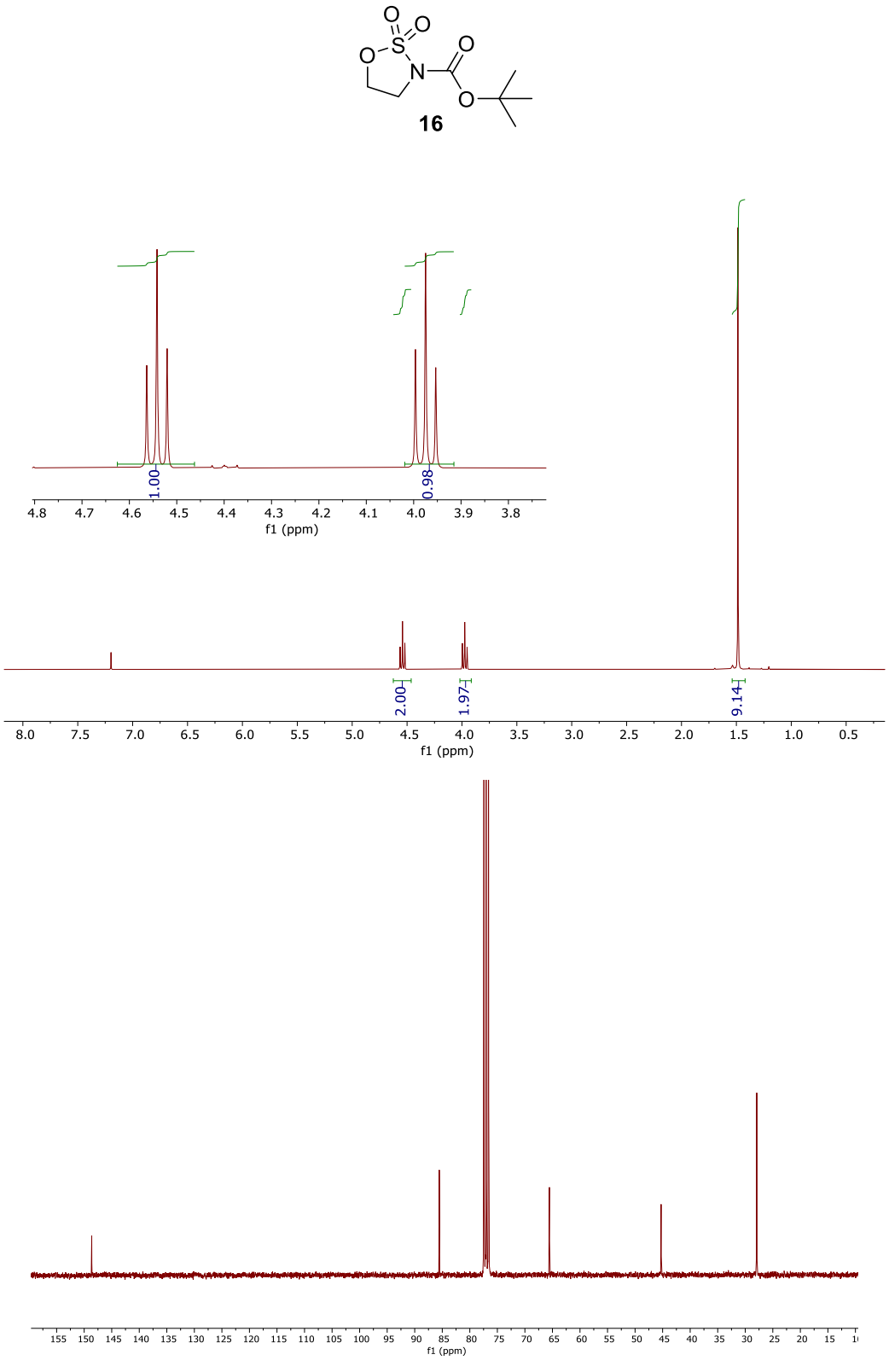

Figure S56: (Top) ^{1}H NMR and (Bottom) ^{13}C NMR of **16** dissolved in $CDCl_3$

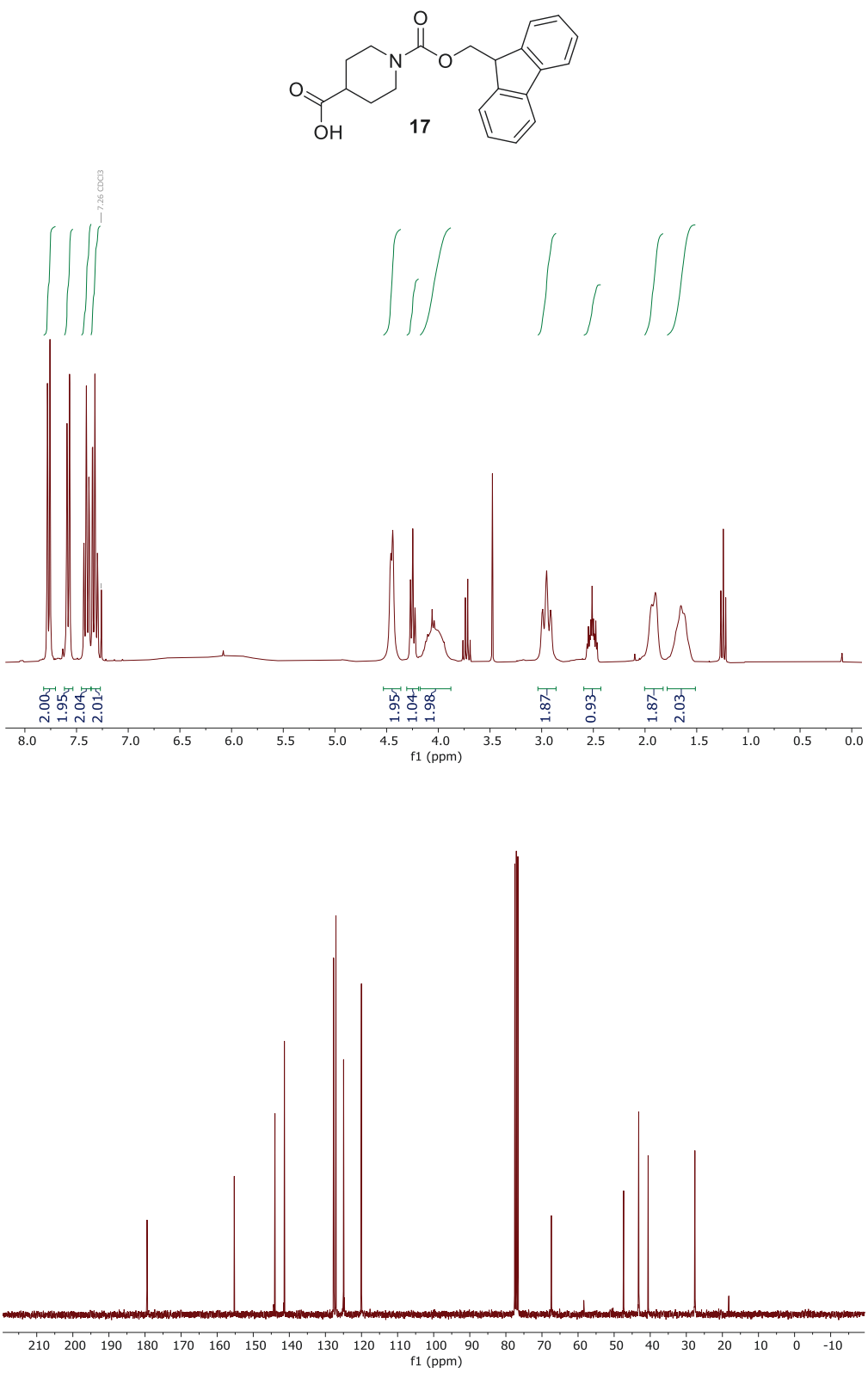

Figure S56: (Top) ^{1}H NMR and (Bottom) ^{13}C NMR of **17** dissolved in $CDCl_3$

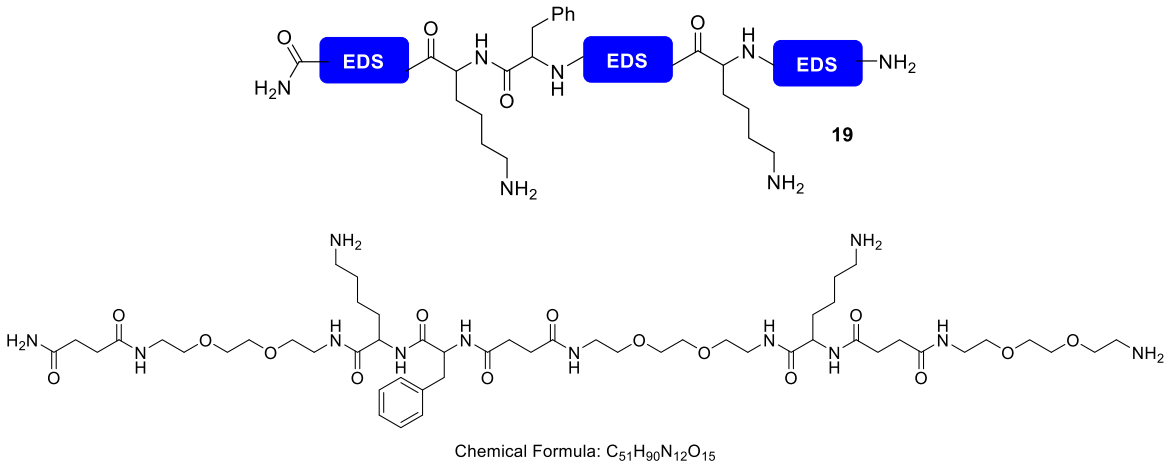

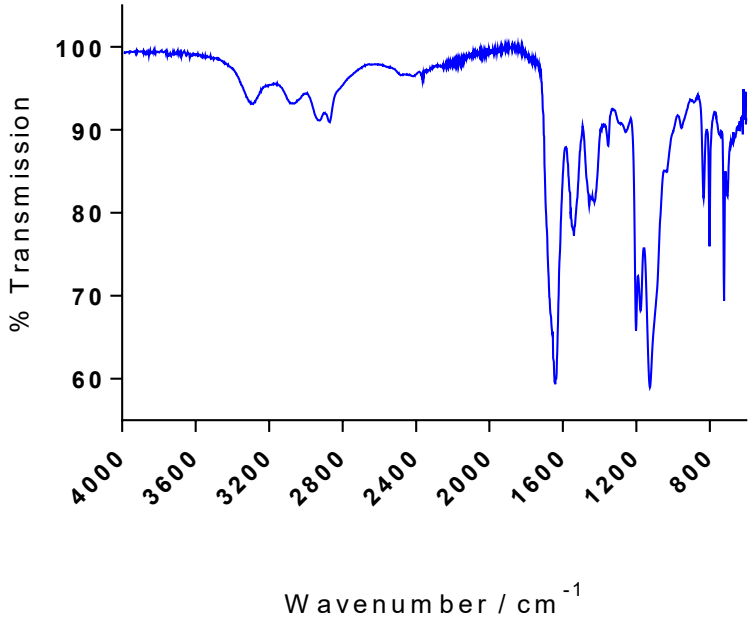

Key peaks: 3284 (N-H/O-H str.), 3064 (C-H sp^2 str.), 2922 (C-H sp^3 str.), 1633 (C=O amide), 1537 (N-H amide bend), 1454 (methylene str.), 1199 and 1124 (C-N/C-O) cm^{-1}

Figure S57: FT-IR spectrum of fully deprotected **19**

References

[1] B. O. Keller, J. Sui, A. B. Young, R. M. Whittal, *Analytica Chimica Acta* **2008**, *627*, 71-81.

[2] D. Ponader, F. Wojcik, F. Beceren-Braun, J. Dernedde, L. Hartmann, *Biomacromolecules* **2012**, *13*, 1845-1852.

[3] C. A. Olsen, M. Witt, J. W. Jaroszewski, H. Franzyk, *The Journal of Organic Chemistry* **2004**, *69*, 6149-6152.

[4] S. Rambharose, R. S. Kalhapure, M. Jadhav, T. Govender, *New Journal of Chemistry* **2018**, *42*, 2232-2242.

[5] H. Moon, Y. Jung, Y. Kim, B. W. Kim, J. G. Choi, N. H. Kim, M. S. Oh, S. Park, B. M. Kim, D. Kim, *Organic Letters* **2019**, *21*, 3891-3894.

[6] T. A. Moss, B. Alonso, D. R. Fenwick, D. J. Dixon, *Angewandte Chemie International Edition* **2010**, *49*, 568-571.

3.2 Cyclic carbonates as protection group free building blocks in solid phase synthesis of sequence-defined macromolecules

Steinfort, R., Hill, S. A., Capar, Ö., Hartmann, L., **"Cyclic carbonates as protection group free building blocks in solid phase synthesis of sequence-defined macromolecules"** *paper draft*, **2023**

Contribution:

Robert Steinfort: Synthesis of all structures and their analysis. Optimization of the coupling conditions. Collaborative writing of the first paper draft. Collaborative writing of the manuscript.

ARTICLE

Cyclic carbonates as protection group free building blocks in solid phase synthesis of sequence-defined macromolecules

Received 00th January 20xx,
Accepted 00th January 20xx

DOI: 10.1039/x0xx00000x

Robert Steinfort,[a] Stephen Hill, [a] Özgür Capar, [a] Laura Hartmann [a,b] *

Cyclic carbonates, as building blocks not yet used in solid-phase synthesis, are produced from epoxides and carbon dioxide and have been successfully used for sequence-defined oligohydroxyurethanes construction. The usual protective group strategies can be dispensed because the reaction with an Diamine is an AA + BB system. They thus follow a submonomeric solid-phase strategy. The addition of a cyclocarbonate to the solid phase was investigated and the optimisation in terms of reaction time, temperature, stoichiometric proportions, solvents, number of coupling steps and the advantages of capping are discribed. Subsequently, the biscyclocarbonate was ring-opened with a diamine. The ring opening of the cyclocarbonates produces an urethane group with an adjacent hydroxy group. The formation and reduction of by-products such as dimers and the advantages of spacing the urethane units further away from each other are also discussed. The cyclocarbonate building block could be successfully incorporated repeatedly into an oligomer.

1. Introduction

Solid phase synthesis, first introduced by Merrifield in 1963, has become an established method for producing sequence-defined macromolecules (SDMs) in recent years.[1–7] The method is based on the step-wise assembly of building blocks on a solid support or so-called resin where in each step a different building block can be chosen, giving in the end the desired primary sequence. The solid support itself enables the use of high excess of building blocks and repetitive couplings to ensure ideally quantitative addition of each building block as the removal of the excess reagents is simply achieved by a filtration/washing step with the product remaining bound to the resin. In peptide synthesis, such stepwise assembly also requires the use of selective protecting groups, most commonly known are the tert-butyloxycarbonyl (Boc) and the fluorenylmethoxycarbonyl (Fmoc) group as orthogonal protecting groups for the primary amine of the amino acid.[8,9] Without the protecting group, amide bond formation could also occur in solution or multiple times with the same amino acid, thus resulting in the loss of the sequence definition. Besides peptides and other biopolymers such as oligonucleotides[10] and oligosaccharides,[11,12] in recent years, the synthesis of synthetic SDMs has gained increasing attention.[1–3,5,6] SDMs have been shown to have great potential in different applications for example, in drug delivery, data storage, or showed antibacterial effects.[4,13]
Since synthetic SDMs are not limited by the natural building blocks, a large variety of different tailor-made building blocks and chemistry for their coupling on solid support has been developed. One differentiation of these strategies is based on the use of building blocks that require protecting groups or building blocks that can be coupled without protecting groups, which can also be classified as a so-called submonomer approach.[14] From a polymer chemist's point-of-view, a typical protecting group strategy introduces one repeating unit per coupling while in the submonomer, protecting group free approach, two coupling steps are required to give one repeating unit. Nevertheless, working without a protecting group typically is a more atom efficient approach and potentially allows for an easier upscaling of the synthesis. In this context, especially cyclic building blocks for SDM synthesis have gained increasing attention over the last couple of years.[15] The products can yield bi- or multifunctionalities, ring opening can be initiated using a range of nucleophiles, usually no catalysts or activating agents are required, and the reaction proceeds with high stereo- and or regioselectivity.[15] Well received examples are thiolactone building blocks introduced by the du Prez lab [ref],[16] epoxid building blocks by Johnson et al.,[17] and maleimides by Zhang et al.[18] Recently, we have introduced the use of cyclic sulfamidates to obtain N-sulfated SDMs as a new class of sequence-defined polyelectrolytes.[19] Here we now explore another class of cyclic building blocks for their use in SDM synthesis: the cyclic carbonates.

Cyclic carbonates (CCs) have attracted attention as they can be generated from the simple combination of epoxides, CO_2, and a catalyst and can be used as green alternative in the synthesis of polyurethanes replacing isocyanate monomers.[20] CCs are typically 5 or 6-membered ring carbonate esters and are characterised by a carbonyl group flanked by two alkoxy groups. CC reactivity normally proceeds via ring-opening, typically proceeding via amine nucleophilic attack at the endocyclic carbonyl. After ring-opening a new urethane linkage is generated and a hydroxyl revealed. Since the ring

[a] Institute of Organic Chemistry and Macromolecular Chemistry, Heinrich Heine University Düsseldorf, Universitätsstraße 1, 40225 Düsseldorf, Germany
[b] Institute for Macromolecular Chemistry, University of Freiburg, Stefan-Meier-Str. 31, 79104 Freiburg I. Br., Germany.

opening is not regioselective, two different products can be formed. The two urethanes that result from this ring opening show different chemical environments and form either primary or secondary hydroxy groups. Whether the primary or secondary hydroxyurethane is formed partially depends on the substituents of the cyclocarbonate group, however, in many cases both, the primary and the secondary hydroxyurethane are formed.[21]

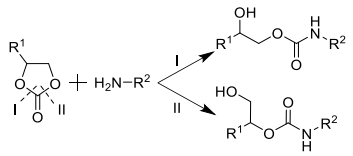

Figure 1: Reaction scheme of the formation of the primary or secondary hydroxyurethane.[21]

The carbonate functionality has previously been applied in solid-phase synthesis as linker,[22] solvent,[23] and for the generation of peptides.[24] Organic carbonate synthesis on solid-phase has also been reported.[25] However, to the best of our knowledge, no reports have yet explored the reactivity of cyclic carbonates on solid support and the iterative coupling of CC based building blocks for SDM construction. Based on our previous studies with biscyclocarbonates (BCCs) in the synthesis of polyhydroxyurethanes for fast curing applications,[26] here we explore BCCs in a submonomer approach together with aliphatic diamines to enable sequence-defined oligohydroxyurethanes (Figure 2).

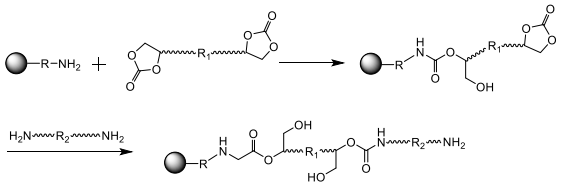

Figure 2: Solid-phase coupling of a BCC building block and subsequent reaction with a diamine to derive one repeating unit of a sequence-defined oligohydroxyurethane.

2. Methods and Experimental Section

Materials:

All solvents and reagents were used for the reactions without any purification. Acetic anhydride was purchased from VWR chemicals, Dimethylformamide (DMF), Fmoc-L-Phenylalanine and N,N-Diisopropylethylamine (DIPEA) were purchased from Carl Roth, Triethylamine (TEA) was purchased from Fisher Scientific, Lithium bromide (LiBr) was purchased from Alfa Aesar, 1,8-diazabicyclo[5.4.0]undec-7-ene (DBU) was purchased from Fluorochem, TentaGel® S RAM was purchased from Rapp Polymere, Triisopropylsilane (TIPS), hexamethylenediamine (HMD), 1,5,7-triazabicyclo[4.4.0]dec-5-ene (TBD), Lithiumtrifluormethansulfonat (LiOTf), benzotriazol-1-yloxytripyrrolidinophosphonium hexafluorophosphate (PyBOP), N-Methyl-2-pyrrolidone (NMP), Diethyl ether, Methanol, 1,4-butanediol diglycidyl ether, and Dichloromethane (DCM) were purchased from Sigma Aldrich, Trifluoroacetic acid (TFA) was purchased from Acros Organics, tetrabutylammonium iodide (TBAI) was purchased from Carbolution Chemicals GmbH, Acetonitrile was purchased from ChemSolute, Fmoc-Glycine was purchased from BLD Pharmatech GmbH, Boc-glycine was purchased from JK Chemicals.

NMR-Spectroscopy:

^{1}H-NMR and ^{13}C-NMR spectra were measured at room temperature on Bruker Avance III 300 (for 300 MHz) or Bruker Avance III 600 (for 600 MHz). The chemical shifts in δ in parts per million (ppm) are reported relative to the solvent peaks.

Reverse Phase – High Performance Liquid Chromatography – Mass Spectrometry (RP-HPLC-MS):

An Agilent 1260 Infinity instrument with an adjusted wavelength of 214 nm and a 6120 Quadrupole LC/MS with an electrospray ionization source was used for HPLC and MS analysis. In the m/z range of 200 to 2000, all measurements were carried out in either positive or negative ionization mode. The following mobile phases were used in the analysis: 95/5 (H2O/MeCN) (mobile phase A) and 5/95 (H2O/MeCN) (mobile phase B), both with 0.1% formic acid, in a poroshell 120 ECC18 3.0x50 mm, 2 m reverse phase (RP) from Agilent.

High resolution ESI (HR-ESI):

On UHR-QTOF maXis 4G, HR-ESI spectra were measured (Bruker Daltonics).

Freeze Dryer:

Cleaved Oligomers got freeze dried (lyophilized) by the Alpha 1-4 LD instrument from the Martin Christ Freeze Dryers GmbH. Temperatures for the measurements are -42 °C and a pressure of 0.1 mbar is maintained while lyophilizing.

Synthetic procedures:

The synthesis of the EDS building block has been reported by Ponader et al.[12] The synthesis of the BCC building was conducted as previously reported by Capar et al.[26] ^{1}H-NMR spectra for these building blocks see SI, Figure 15 and Figure 17. ^{13}C-NMR spectra for these building blocks see SI, Figure 19 and Figure 20.

Resin swelling and Fmoc deprotection:

TentaGel® S RAM is used for all reactions described with a loading of 0.24 mmol/g) which is filled into BD syringe reactors with an inlet frit. 10 mL Synringes were used for batch sizes of 0.5 mmol. Before coupling the building blocks the resin was swollen for 30 min in DCM. The Fmoc protecting group was cleaved by a 25 vol.-% piperidine in DMF solution. Therefore, the syringe was drawn up with 10 mL of the solution and shaken 2 times for 20 min. The resin was subsequently washed 15 times with DMF.

Solid phase synthesis: (oligomeric precursor):

The following procedure refers to the coupling of Glycine-fmoc,

Glycine-boc, EDS and Phenylalanine based on the protocol reported by Ponader et al.[12]

After the swelling and the Fmoc deprotection the resin was washed with DMF 10 times. For the coupling an excess of 5 equivalents of building block and PyBOP was used. DIPEA was used in a 10 equivalents excess. One-fourth fmoc glycine and three-fourths boc glycine were used for amine loading reduction. All components were dissolved in DMF and shaken for 5 min prior to adding it to the resin. The activated solution was raised onto the resin and shaken for 2 h. After the reaction the resin is washed with 15 times DMF and 5 times DCM. The preparations were carried out with 0.5 mmol batch sizes which were subsequently divided into 5 syringes (0.1 mmol) for BCC coupling. All reactions were performed in a syringe with frit on a shaking plate at room temperature.

Coupling of BCC and HMD:

For the coupling of the BCC building block and the HMD, the resin (the oligomeric precursor) was transferred from the plastic syringe to a glass syringe. The LiOTf/TBD catalyst system and the building block dissolved in NMP were then added. The syringe was then sealed with a septum and nitrogen was flowed through the reaction solution. The syringe was kept in a water bath which was adjusted to the appropriate temperature. Temperatures and reaction times can be found in the corresponding tables (see Tables 1-4). After the reaction, the syringe was washed 15 times with NMP and 5 times with DCM.

Capping of the hydroxyl groups:

The syringe was filled with acetic anhydride and shaken for 2 hours at room temperature. Then it was washed with DMF 15 times.

Macro cleavage:

For cleaving the oligomers of the TentaGel® S RAM a cleavage solution of TFA:TIPS:DCM (95:2.5:2.5) was drawn up into the syringe. The solution was shaken for 60 min at room temperature and after that precipitated into iced diethyl ether (45 mL). The solution was centrifuged for 5 min and the supernatant was then decanted. The white precipitate was counter current dried for 1 h in nitrogen. The white precipitate was then dissolved in MilliQ water and lyophilized.

3. Results and Discussion

Based on our previous study[26] on using BCCs in classical polymer chemistry, 1,4-butanediol diglycidyl ether was transcarbonylated using tetrabutylammonium iodide (TBAI) as catalyst giving the BCC building block in a high yield of 96 % and high purity (94 % as determined by ^{1}H-NMR, see SI Figure 15). High purity is of special importance for use of building block in solid phase synthesis as potential side products e.g., the monocyclocarbonate could also react during the coupling but lead to an error or deletion in the monomer sequence. The main factor hampering the high purity of the BCC is indeed not the transcarbonylation but the purity of the starting material, the diglycidyl ether. Most diglycidyl ethers are sold at technical grade and purification by one-step vacuum distillation was not efficient.[26] Therefore, 1,4-butanediol diglycidyl ether with a purity of >95 % was used for this work to ensure high purity of the resulting BCC.

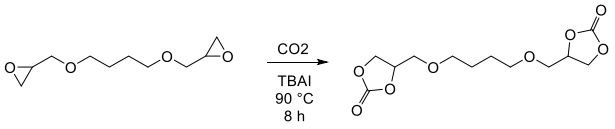

Figure 3: Monomer Synthesis of the BCC building block.

As diamine building block, commercially available hexamethylenediamine (HMD) was chosen based on its good solubility in common solid phase solvents such as dimethylformamide (DMF) and N-methyl-2-pyrrolidone (NMP) and its previous successful use in the synthesis of methacrylamide-dimethylacrylamide oligomers by solid phase protocols.[27]

TentaGel® S RAM was used as the solid-phase resin, as it has been widely used for the synthesis of sequence-defined oligomers.[19,28] Here, protected amino groups form the functional end groups of the resin surface, are linked by a rink amide linker.[8,29]

The oligomeric precursor used for the coupling experiments consists of EDS, a hydrophilic building block which is used in the Hartmann group in solid phase synthesis,[12] and Phenylalanine in the sequence EDS-Phe-EDS. EDS was used to be able to assign the molecular mass in the mass spectrum more precisely and also to increase the distance to the solid phase resin. Phenylalanine was used to enable the conversion analysis by UV-Vis spectroscopy (for the analytics of the oligomeric precursor see SI, Figure 1).

In a very simple first attempt, 5 equivalents (eq.) BCC per amine group was added to the resin for 10 min – a typical protocol e.g., for the addition of an amino acid in solid phase peptide synthesis.[8] Not surprisingly, no coupling was observed via LC-MS data as it has been described typically elevated temperatures are required to induce ring opening and thus conjugation of the BCC.[30] In a second series, therefore the reaction temperature was gradually increased from rt to 37°C to 50°C and reaction times were increased to 60 min. Higher temperatures (>60°C) are not possible because the oligomers would detach from the polystyrene based resins.[31] Also under these reaction conditions, no coupling of the BCC was observed (see SI for table with all reaction conditions). It is also known that the use of different catalysts can promote the CC ring opening already at lower temperatures. Therefore, next, a series of catalysts was tested in promoting BCC coupling working either at rt or at 50°C and increasing the reaction times to 60, 120 and 180 min, respectively (see SI for table with all reaction conditions). The use of triethylamine (TEA), lithium bromide (LiBr) with 1,8-diazabicyclo[5.4.0]undec-7-ene (DBU) and the 1,5,7-triazabicyclo[4.4.0]dec-5-ene (TBD) with LiBr did not result in any BCC coupling. Also the addition of methanol, known to increase the reactivity of the carbonyl carbon by forming hydrogen bonds with the oxygen atom of the carbonate,[21] did

not give any product formation.However, with the catalyst system LiOTf and TBD, previously used by Lombardo et al. for the amylolysis of cyclic carbonates in solution,[32] in DMF coupling 5 eq. BCC for 60 min at rt showed the first successful attachment with 28% conversion as determined by RP-HPLC-MS.

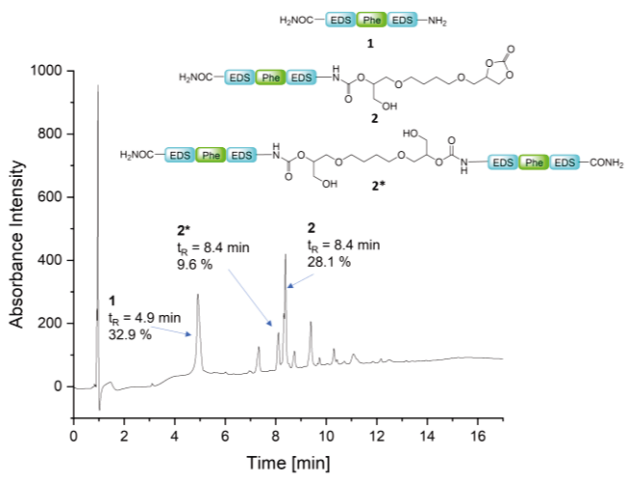

Figure 4: RP-HPLC chromatogram (Gradient 5-95 vol% - MeCN in H_2O (0.1 vol.-% formic acid, run time 17 min) of the oligomer **2**.

By changing the reaction parameters (see Table 1), an increase in conversion up to 45% was achieved (see SI, Figure 5).

Table 1: Coupling of BCC building block to the solid phase using EDS-phenylalanine-EDS (**1**) as the oligomeric precursor in the solvent NMP with LIOTF/TBD as the catalyst system.

Time [min]	Temperature [°C]	BCC [Eq.]	LiOTf/TBD [Eq.]	Product Conversion [%] *
60	RT	5	10	28
120	RT	10	20	33
60	50	5	10	27
90	50	10	20	32
90	50	50	50	45

** Product conversions were determined by integrating an RP-HPLC chromatogram (gradient of 5 to 95% by volume acetonitrile in water containing 0.1% by volume formic acid, run time 17 min).*

However, for solid phase coupling standards usually requiring conversion >90%, this was still unsatisfying. Closer evaluation of the LC-MS data of the products after release from the solid support revealed one of the reasons for such low conversion: Due to the two carbonate functionalities of the BCC building block, both carbonate groups can react on the solid support with two neighboring amine groups leading to the formation of a dimer as can be identified from the ESI-MS data (Figure 6). These dimers will not be able to be extended in following coupling steps and thus dimer formation needs to be avoided. One option is to use higher access of BCC building blocks. However, it is very likely that dimer formation occurs in a two-step process: the BCC attaches with one end to the resin and the proximity of the second carbonyl to remaining amines on the resin promotes the dimer formation as shown in Figure 5.

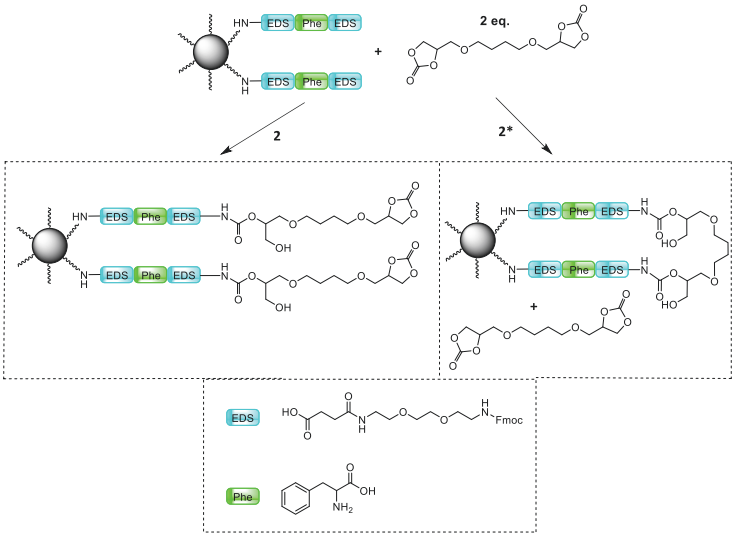

Figure 5: Structure of the dimer by-product and binding to the solid phase resin.

Figure 6 shows the ESI-MS spectrum of the dimer by-product.

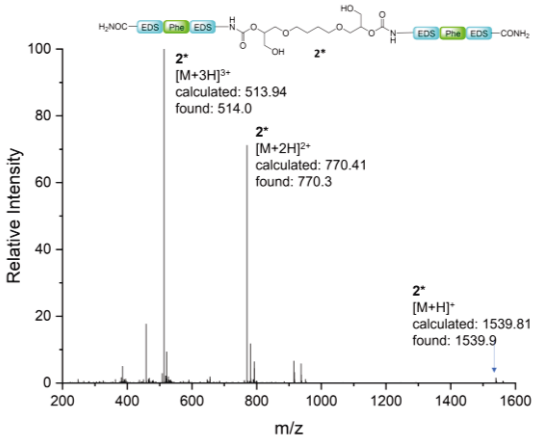

Figure 6: HPLC-ESI-MS of **2*** at t = 7.56 min (gradient of 5 to 95 vol% acetonitrile in water containing 0.1 vol% formic acid, run time 17 min).

Therefore, to reduce dimer formation, the overall loading of the resin (number of primary amine groups) was reduced by using a mixture of Fmoc- and Boc-protected glycine in an extension of the oligomeric precursor (see SI for details). By selective deprotecting only the Fmoc-protected amine groups, an overall reduction in reactive groups for BCC coupling is achieved. Indeed, dimer formation was drastically reduced from about 40 % to less than 10 % (see SI, Figures 7 and 9).

Table 2: Coupling of BCC building block to the solid phase using glycine-EDS-phenylalanine-EDS (**3**) as the oligomeric precursor, with the reduced number of primary amine groups due to the mixture of Fmoc- and Boc-protected glycine. The reactions were performed in the solvent NMP and in a plastic syringe.

Time [min]	Temperature [°C]	BCC [Eq.]	LiOTf/TBD [Eq.]	Product conversion [%] *
60	RT	10	20	59
120	RT	10	20	56
90	40	5	10	44
60	RT	5	10	24
60	RT	20	40	41
60	60	5	10	57
60	60	20	40	66
180	60	20	40	72
180	60	40	80	64
180	60	20	40	73
180	60	20	40	73
180	60	20	40	75
180	60	20	40	82**
180	60	20	40	84**

** Product conversions were determined by integrating an RP-HPLC chromatogram (gradient of 5 to 95% by volume acetonitrile in water containing 0.1% by volume formic acid, run time 17 min).*
*** Reactions were performed in a glass syringe*

In addition to the dimer formation, we also observed a number of side products that we could not identify. So far, solid phase reactions were performed in plastic syringes equipped with a filter that are commonly used for non-automated solid phase protocols as they are cheap, easy to handle and allow straightforward in parallel synthesis e.g., by placing several syringes on a shaker at the same time. However, these syringes were designed for solid phase peptide synthesis that typically is performed at room temperature. We hypothesized that our extended reaction at elevated temperature using also unconditional solvent such as methanol and NMP may have caused leakage e.g., of plasticizers, into our reaction and thus product mixture. In order to avoid this, we changed the reaction set-up to glass syringes. Indeed, further optimization of BCC coupling in glass syringes enabled an increase in conversion of up to 84 %. Together with 12 % dimer formation, this gives a total conversion of 96 % which is now in a range generally suitable for reactions on solid support.[33]

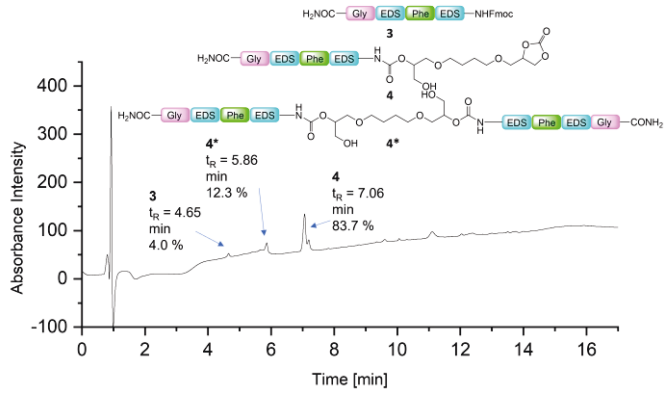

Figure 7: RP-HPLC chromatogram (Gradient 5-95 vol% - MeCN in H_2O (0.1 vol.-% formic acid, run time 17 min) of the oligomer **4**.

In principle, increased reaction times and reaction temperature lead to an increase in product formation while increase in BCC excess beyond 40 eq. and increase in catalyst beyond 40 eq. did not yield a further increase (see Table 2). Different solvents were tested but highest product conversions were observed in NMP. The optimized conditions for solid phase coupling of BCC building block to primary amines comprise of 40 equivalents of BCC and TBD/LiOTf, NMP as solvent, reaction temperature of 60 °C, 3 h reaction time, and repeating the coupling twice (double coupling).

2.3 Chain extension by first diamine coupling

After successful introduction of the first BCC building block, chain extension by HMD was investigated. Reaction of one the primary amine groups of the diamine should ring open the free cyclocarbonate ring at the chain end of the resin-bound oligomer (see Figure 8).

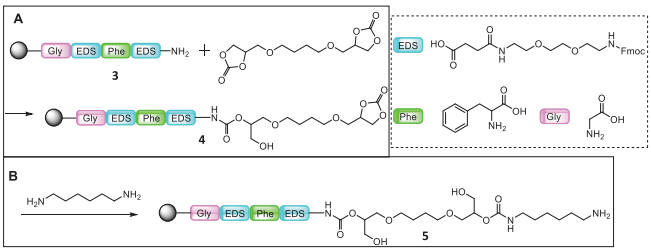

Figure 8: A. Coupling of the BCC building block to the oligomeric precursor **3**.
B. Coupling of the oligomer **4** with HMD.

Different reaction conditions were tested including different equivalents of HMD, catalyst (LiOTF/TBD) and reaction temperature as shown in Table 3. Highest product formation was observed via 20 eq. of HDM and LiOTf/TBD, 60 min reaction time, 60 °C reaction temperature and repeating the coupling twice (double coupling). LC-MS analysis shows no starting material indicating all oligomers with a BCC endgroup were fully extended by one HDM molecule (see SI, Figure 9). However, based on the side products from the previous BCC coupling, e.g., the dimer formation, the overall product conversion is only at 89 % for the optimized reaction condition.

Table 3: Diamine coupling to the oligomer Gly-EDS-Phe-EDS-BCC (**4**) in the solvent NMP in a glass syringe.

Time [min]	Temperature [°C]	HMD [Eq.]	LiOTf/TBD [Eq.]	Product conversion [%] *
60	RT	10	10	56
60	RT	20	20	71
60	60	20	20	87
60	60	20	20	83
60	60	20	20	89

** Product conversions were determined by integrating an RP-HPLC chromatogram (gradient of 5 to 95% by volume acetonitrile in water containing 0.1% by volume formic acid, run time 17 min).*

2.4 Further chain extension beyond the first BCC/diamine repeating unit

Subsequently, a second BCC building block can be used to elongate the chain further, reacting now with the terminal primary amine as introduced in the previous step by the HDM building block. However, when using the previously optimized reaction conditions for the first BCC coupling, product conversion of only 45 % in comparison to the previous 89 % was achieved. Therefore, different attempts to improve coupling efficiency were investigated.

First, we changed the solvent from NMP to methanol as this should increase the activation of the carbonyl carbon and should therefore favour the ring opening of the cyclocarbonate.[21] However, no product conversion was observed.

Another reason for the reduced coupling efficiency could be a potential aggregation. For example in solid phase peptide synthesis, for sequences that have a strong tendency to aggregate, this can prohibit the efficient chain extension and thus synthesis of longer chains.[34] Potentially, the hydroxy groups formed during ring opening can form intermolecular hydrogen bonds and promote such chain-chain aggregation. In addition, the urethane units formed during ring opening can interact with each other and therefore lead to aggregation of the chains as well.[35,36] Therefore, the addition of chaotropic salts was explored to reduce the interaction of the oligomer chains,[37] but no product conversion was detected either.

The idea for the next experiments was that by increasing the distance between the BCC building blocks, one could have less steric hindrance for the nucleophilic attack of the amine on the BCC building block.[1,38] Yen at al. have shown in their work that a high density of urethane groups in the chains can lead to increased interactions between the chains and also within the chains.[36] So, to increase the distance between the BCC block and the next BCC block (and so the formed urethane groups), the spacing building block EDS was implemented.

To investigate whether the effect improves when the distance is increased even further, experiments were performed with two EDS blocks incorporated. One (sample B) or two EDS (samples A, C, D) building blocks were coupled using standard Fmoc peptide coupling conditions. The EDS coupling was complete as shown by the LC-MS analysis. The oligomer **5** with the free amine group of HMD was completely converted (see SI, Figure 11). Next another BCC building block was coupled to the oligomer according to the above optimized conditions and then reacted again with HMD. Finally, another EDS building block was coupled to the oligomer to improve precipitation in diethyl ether after cleavage from the resin (macro cleavage).

In the first experiment, where two EDS building blocks were introduced after the first HMD building block, the mass of the target structure could be detected in the LC-MS, but many by-products had formed so that it was not possible to state how high the product conversion was (see sample A).

In order to reduce the formation of by-products and to reduce the interactions between the chains and to block possible side reactions that the free hydroxy groups could undertake, capping steps were included in the next experiments.

After every BCC coupling step, the hydroxy groups were reacted with acetic anhydride thereby acetylating the hydroxy group and blocking the ability to form hydrogen bonds. This allowed the first successful addition of a further BCC building block to the oligomer (see Table 4). One possible explanation for this is that the hydroxy groups formed during ring opening participate in the reaction. Many by-products from sample A were no longer detected after capping was performed.

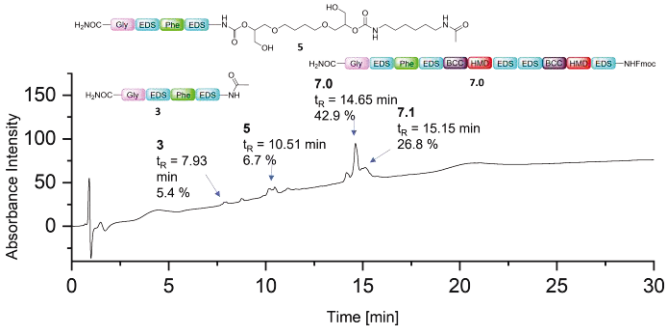

Figure 10: RP-HPLC chromatogram (Gradient 5-95 vol% - MeCN in H_2O (0.1 vol.-% formic acid, run time 30 min) of **7**.

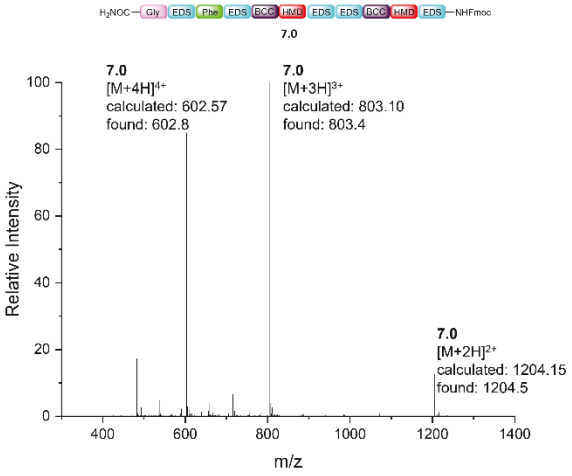

Figure 11: HPLC-ESI-MS of **7.0** at t = 15.15 min (gradient of 5 to 95 vol% acetonitrile in water containing 0.1 vol% formic acid, run time 30 min).

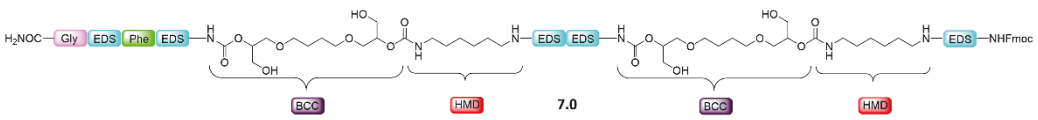

Figure 9: Structure of the oligomer **7.0**.

Comparing sample B with one EDS building block with sample D with two EDS building blocks, it can be concluded that the product conversion with the two EDS building blocks is significantly higher (38 % vs 64 %). This is due to the fact that the urethane groups of the BCC building blocks are further apart from each other and therefore there are fewer interactions between the chains. When analysing the data, it was observed that the product is present in different degrees of acetylation (see SI Figure 14). This is related to the conditions of cleavage from the resin. Here, 95 % TFA is used for the cleavage, which can lead to a loss of the acetyl groups. In further experiments in this area, other temporary protective groups could therefore be used instead of the acetyl groups, which would then be deprotected from the resin before cleaving the oligomer of the resin.

The results of these experiments are shown in Table 4. The target structure (see Figure 9) in which the cyclocarbonate building block was incorporated twice was identified with 64 % with the optimised conditions. For further analytics of the oligomer **7.0** see SI.

Table 4: Synthesis of the oligomer Gly-EDS-Phe-EDS-BCC-HMD-EDS-EDS-BCC-HMD-EDS (**7.0**) in the solvent NMP in a glass syringe.

SAMPLE	TIME [MIN]	TEMPERATURE [°C]	BCC [EQ.]	LIOTF/TBD [EQ.]	PRODUCT CONVERSION [%] *
A	180	55	20	10	-
B (ONLY ONE EDS)	180	55	20	40	38
C	180	55	20	5	60
D	180	55	20	10	64

** Product conversions were determined by integrating an RP-HPLC chromatogram (gradient of 5 to 95% by volume acetonitrile in water containing 0.1% by volume formic acid, run time 30 min).*

Comparing samples C and D, where capping was performed after each BCC and EDS coupling step, it can be noted that higher equivalents of the catalytic system do not result in higher product conversion.

3. Conclusions

In this paper we report the first use of bicyclocarbonate building blocks in a stepwise assembly on solid support. Following a submonomer approach, the combination of biscyclocarbonate and diamine building blocks gives access to sequence-defined oligohydroxyurethanes. We demonstrate that this approach is also readily compatible with other solid phase approaches such as the solid phase polymer synthesis using dimer building blocks and solid phase peptide synthesis using Fmoc-protected amino acids. In the future, further chain extension to achieve higher molecular weights and longer sequences as well as the use of different biscyclocarbonates and diamines will be explored. Furthermore, hydroxy groups introduced upon ring opening of the cyclocarbonate units will be employed for side chain modification e.g., by glycosylation to obtain sequence-defined glycooligourethanes as multivalent glycan mimetics. It can be expected that based on their different inter- and intramolecular hydrogen bond formation such oligourethane backbones will impact the presentation and bining of the side chain glycans in a different way than e.g., previously employed oligoamide chains.

Conflicts of interest

There are no conflicts to declare.

Acknowledgements

Notes and references

[1] S. A. Hill, C. Gerke, L. Hartmann, *Chemistry, an Asian journal* **2018**, *13*, 3611.

[2] B. Genabeek, B. A. G. Lamers, C. J. Hawker, E. W. Meijer, W. R. Gutekunst, B. V. K. J. Schmidt, *Journal of Polymer Science* **2021**, *59*, 373.

[3] R. Aksakal, C. Mertens, M. Soete, N. Badi, F. Du Prez, *Advanced Science* **2021**, *8*, 2004038.

[4] P. Nanjan, M. Porel, *Polym. Chem.* **2019**, *10*, 5406.

[5] M. A. R. Meier, C. Barner-Kowollik, *Advanced Materials* **2019**, *31*, e1806027.

[6] J.-F. Lutz, *Macromolecular rapid communications* **2017**, *38*.

[7] R. B. Merrifield, *Journal of the American Chemical Society* **1963**, *85*, 2149.

[8] M. Amblard, J.-A. Fehrentz, J. Martinez, G. Subra, *MB* **2006**, *33*, 239.

[9] a) R. Behrendt, P. White, J. Offer, *Journal of peptide science : an official publication of the European Peptide Society* **2016**, *22*, 4; b) M. Royo, J. Alsina, E. Giralt, U. Slomcyznska, F. Albericio, *J. Chem. Soc., Perkin Trans. 1* **1995**, 1095.

[10] a) O. Kostov, R. Liboska, O. Páv, P. Novák, I. Rosenberg, *Molecules (Basel, Switzerland)* **2019**, *24*; b) C. Thorpe, S. Epple, B. Woods, A. H. El-Sagheer, T. Brown, *Organic & biomolecular chemistry* **2019**, *17*, 5341; c) D. Vlaho, M. J. Damha, *Current protocols in nucleic acid chemistry* **2018**, *73*, e53.

[11] a) V. Ladmiral, E. Melia, D. M. Haddleton, *ChChT* **2004**, *40*, 431; b) P. B. Konietzny, J. Freytag, M. I. Feldhof, J. C. Müller, D. Ohl, T. Stehle, L. Hartmann, *Biomacromolecules* **2022**, *23*, 5273.

[12] D. Ponader, F. Wojcik, F. Beceren-Braun, J. Dernedde, L. Hartmann, *Biomacromolecules* **2012**, *13*, 1845.

[13] a) A. Al Ouahabi, L. Charles, J.-F. Lutz, *Journal of the American Chemical Society* **2015**, *137*, 5629; b) T. T. Trinh, L. Oswald, D. Chan-Seng, J.-F. Lutz, *Macromol. Rapid Commun.* **2014**, *35*, 141; c) T. Schröder, K. Schmitz, N. Niemeier, T. S. Balaban, H. F. Krug, U. Schepers, S. Bräse,

Bioconjugate Chem. **2007**, *18*, 342; d) M. Soete, C. Mertens, R. Aksakal, N. Badi, F. Du Prez, *ACS Macro Lett.* **2021**, *10*, 616; e) S. Martens, A. Landuyt, P. Espeel, B. Devreese, P. Dawyndt, F. Du Prez, *Nat Commun* **2018**, *9*; f) J.-F. Lutz, *Macromolecules* **2015**, *48*, 4759; g) C. Laure, D. Karamessini, O. Milenkovic, L. Charles, J.-F. Lutz, *Angew. Chem. Int. Ed.* **2016**, *55*, 10722; h) G. H. van Domeselaar, G. S. Kwon, L. C. Andrew, D. S. Wishart, *Colloids and Surfaces B: Biointerfaces* **2003**, *30*, 323; i) S. Mosca, J. Keller, N. Azzouz, S. Wagner, A. Titz, P. H. Seeberger, G. Brezesinski, L. Hartmann, *Biomacromolecules* **2014**, *15*, 1687; j) L. Fischer, R. C. Steffens, T. J. Paul, L. Hartmann, *Polym. Chem.* **2020**, *11*, 6091.

[14] a) S. C. Solleder, R. V. Schneider, K. S. Wetzel, A. C. Boukis, M. A. R. Meier, *Macromolecular rapid communications* **2017**, *38*; b) R. N. Zuckermann, J. M. Kerr, S. B. H. Kent, W. H. Moos, *Journal of the American Chemical Society* **1992**, *114*, 10646.

[15] S. A. Hill, R. Steinfort, L. Hartmann, *Polym. Chem.* **2021**, *12*, 4439.

[16] a) P. Espeel, L. L. G. Carrette, K. Bury, S. Capenberghs, J. C. Martins, F. E. Du Prez, A. Madder, *Angewandte Chemie (International ed. in English)* **2013**, *52*, 13261; b) P. Espeel, F. Goethals, M. M. Stamenović, L. Petton, F. E. Du Prez, *Polym. Chem.* **2012**, *3*, 1007; c) P. Espeel, F. E. Du Prez, *Eur. Polym. J.* **2015**, 247; d) P. Espeel, F. Goethals, F. E. Du Prez, *Journal of the American Chemical Society* **2011**, *133*, 1678; e) K. Bruycker, C. Mertens, F. E. Prez, *J. Polym. Sci. A Polym. Chem.* **2019**, *57*, 322.

[17] a) J. C. Barnes, D. J. C. Ehrlich, A. X. Gao, F. A. Leibfarth, Y. Jiang, E. Zhou, T. F. Jamison, J. A. Johnson, *Nature Chem* **2015**, *7*, 810; b) Y. Jiang, M. R. Golder, H. V.-T. Nguyen, Y. Wang, M. Zhong, J. C. Barnes, D. J. C. Ehrlich, J. A. Johnson, *Journal of the American Chemical Society* **2016**, *138*, 9369; c) M. R. Golder, Y. Jiang, P. E. Teichen, H. V.-T. Nguyen, W. Wang, N. Milos, S. A. Freedman, A. P. Willard, J. A. Johnson, *Journal of the American Chemical Society* **2018**, *140*, 1596.

[18] a) Z. Huang, Q. Shi, J. Guo, F. Meng, Y. Zhang, Y. Lu, Z. Qian, X. Li, N. Zhou, Z. Zhang et al., *Nature communications* **2019**, *10*, 1918; b) Z. Huang, J. Zhao, Z. Wang, F. Meng, K. Ding, X. Pan, N. Zhou, X. Li, Z. Zhang, X. Zhu, *Angewandte Chemie (International ed. in English)* **2017**, *56*, 13612; c) Q. Shi, Y. Zhang, Z. Huang, N. Zhou, Z. Zhang, X. Zhu, *Polym J* **2020**, *52*, 21.

[19] S. A. Hill, R. Steinfort, S. Mücke, J. Reifenberger, T. Sengpiel, L. Hartmann, *Macromolecular rapid communications* **2021**, *42*, e2100193.

[20] a) H. Blattmann, M. Fleischer, M. Bähr, R. Mülhaupt, *Macromolecular rapid communications* **2014**, *35*, 1238; b) M. Fleischer, H. Blattmann, R. Mülhaupt, *Green Chem* **2013**, *15*, 934; c) O. Figovsky, L. Shapovalov, A. Leykin, *ChChT* **2016**, *10*, 553; d) S. Weyand, H. Blattmann, V. Schimpf, R. Mülhaupt, R. Schwaiger, *Mater. Res. Express* **2016**, *3*, 75019; e) V. Besse, F. Camara, C. Voirin, R. Auvergne, S. Caillol, B. Boutevin, *Polym. Chem.* **2013**, *4*, 4545; f) H. Asemani, F. Zareanshahraki, V. Mannari, *J. Appl. Polym. Sci.* **2019**, *136*, 47266.

[21] M. A. Levina, V. G. Krasheninnikov, M. V. Zabalov, R. P. Tiger, *Polym. Sci. Ser. B* **2014**, *56*, 139.

[22] a) B. A. Dressman, L. A. Spangle, S. W. Kaldor, *Tetrahedron Letters* **1996**, *37*, 937; b) C. Y. Ho, M. J. Kukla, *Tetrahedron Letters* **1997**, *38*, 2799.

[23] S. Lawrenson, *PhD Thesis*, University of York, **2018**.

[24] E. Falb, T. Yechezkel, Y. Salitra, C. Gilon, *The journal of peptide research : official journal of the American Peptide Society* **1999**, *53*, 507.

[25] R. N. Salvatore, V. L. Flanders, D. Ha, K. W. Jung, *Org. Lett.* **2000**, *2*, 2797.

[26] Ö. Capar, M. Tabatabai, J. E. Klee, M. Worm, L. Hartmann, H. Ritter, *Polym. Chem.* **2020**, *11*, 6964.

[27] F. Ercole, M. FitzGerald, S. Perera, N. Ede, P. Riley, R. Campbell, *J. Appl. Polym. Sci.* **2003**, *89*, 3371.

[28] a) J. A. W. Kruijtzer, L. J. F. Hofmeyer, W. Heerma, C. Versluis, R. M. J. Liskamp, *Chem. Eur. J.* **1998**, *4*, 1570; b) T. Freichel, D. Laaf, M. Hoffmann, P. B. Konietzny, V. Heine, R. Wawrzinek, C. Rademacher, N. L. Snyder, L. Elling, L. Hartmann, *RSC Adv* **2019**, *9*, 23484; c) I. Coin, R. Dölling, E. Krause, M. Bienert, M. Beyermann, C. D. Sferdean, L. A. Carpino, *The Journal of organic chemistry* **2006**, *71*, 6171.

[29] R. Quarrell, T. D. W. Claridge, G. W. Weaver, G. Lowe, *Mol Divers* **1996**, *1*, 223.

[30] a) A. Steblyanko, W. Choi, F. Sanda, T. Endo, *J. Polym. Sci. A Polym. Chem.* **2000**, *38*, 2375; b) L. Maisonneuve, A. S. More, S. Foltran, C. Alfos, F. Robert, Y. Landais, T. Tassaing, E. Grau, H. Cramail, *RSC Adv* **2014**, *4*, 25795; c) M. Helou, J.-F. Carpentier, S. M. Guillaume, *Green Chem* **2011**, *13*, 266; d) C. Beattie, M. North, P. Villuendas, *Molecules (Basel, Switzerland)* **2011**, *16*, 3420; e) H. Tomita, F. Sanda, T. Endo, *J. Polym. Sci. A Polym. Chem.* **2001**, *39*, 162; f) B. Ochiai, S. Inoue, T. Endo, *J. Polym. Sci. A Polym. Chem.* **2005**, *43*, 6282; g) L. Annunziata, A. K. Diallo, S. Fouquay, G. Michaud, F. Simon, J.-M. Brusson, J.-F. Carpentier, S. M. Guillaume, *Green Chem* **2014**, *16*, 1947.

[31] F. Albericio, J. Tulla-Puche in *The power of functional resins in organic synthesis* (Ed.: J. Tulla-Puche), Wiley, Hoboken, N.J., **2009**, pp. 1–14.

[32] V. M. Lombardo, E. A. Dhulst, E. K. Leitsch, N. Wilmot, W. H. Heath, A. P. Gies, M. D. Miller, J. M. Torkelson, K. A. Scheidt, *Eur. J. Org. Chem.* **2015**, *2015*, 2791.

[33] F. Mende, M. Beisswenger, O. Seitz, *Journal of the American Chemical Society* **2010**, *132*, 11110.

[34] a) D. S. King, C. G. Fields, G. B. Fields, *International journal of peptide and protein research* **1990**, *36*, 255; b) M. Schnölzer, P. Alewood, A. Jones, D. Alewood, S. B. Kent, *International journal of peptide and protein research* **1992**, *40*, 180; c) S. L. Pedersen, A. P. Tofteng, L. Malik, K. J. Jensen, *Chemical Society reviews* **2012**, *41*, 1826.

[35] M. C. Delpech, F. M. Coutinho, *Polymer Testing* **2000**, *19*, 939.

[36] F.-S. Yen, L.-L. Lin, J.-L. Hong, *Macromolecules* **1999**, *32*, 3068.
[37] a) B. Merrifield, *Methods in enzymology* **1997**, *289*, 3; b) K. C. Pugh, E. J. York, J. M. Stewart, *International journal of peptide and protein research* **1992**, *40*, 208.
[38] D. Chan-Seng, J.-F. Lutz in *ACS symposium series*, *Vol. 1170* (Ed.: J.-F. Lutz), American Chemical Soc, Washington, DC, **2014**, pp. 103–116.

Supporting Information

Cyclic carbonates as protection group free building blocks in solid phase synthesis of sequence-defined macromolecules

Robert Steinfort,[a] Stephen Hill, [a] Özgür Capar, [a] Laura Hartmann [a,b] *

[a] Institute of Organic Chemistry and Macromolecular Chemistry, Heinrich Heine University Düsseldorf, Universitätsstraße 1, 40225 Düsseldorf, Germany
[b] Institute for Macromolecular Chemistry, University of Freiburg, Stefan-Meier-Str. 31, 79104 Freiburg I. Br., Germany.

E-mail: laura.hartmann@hhu.de

Table of Contents

General Experimental

Chemicals

All solvents and reagents were used for the reactions without any purification. Acetic anhydride was purchased from VWR chemicals, dimethylformamide (DMF), Fmoc-L-phenylalanine and *N,N*-diisopropylethylamine (DIPEA) were purchased from Carl Roth, triethylamine (TEA) was purchased from Fisher Scientific, lithium bromide (LiBr) was purchased from Alfa Aesar, 1,8-diazabicyclo[5.4.0]undec-7-ene (DBU) was purchased from Fluorochem, TentaGel® S RAM was purchased from Rapp Polymere, triisopropylsilane (TIPS), hexamethylenediamine (HMD), 1,5,7-triazabicyclo[4.4.0]dec-5-ene (TBD), lithiumtrifluormethansulfonat (LiOTf), benzotriazol-1-yloxytripyrrolidinophosphonium hexafluorophosphate (PyBOP), *N*-methyl-2-pyrrolidone (NMP), diethyl ether, methanol, 1,4-butanediol diglycidyl ether, and dichloromethane (DCM) were purchased from Sigma Aldrich, trifluoroacetic acid (TFA) was purchased from Acros Organics, tetrabutylammonium iodide (TBAI) was purchased from Carbolution Chemicals GmbH, acetonitrile was purchased from ChemSolute, Fmoc-glycine was purchased from BLD Pharmatech GmbH, Boc-glycine was purchased from JK Chemicals.

Methods

NMR-Spectroscopy

^{1}H-NMR and ^{13}C-NMR spectra were measured at room temperature on Bruker Avance III 300 (for 300 MHz) or Bruker Avance III 600 (for 600 MHz). The chemical shifts in δ in parts per million (ppm) are reported relative to the solvent peaks.

Reverse Phase – High Performance Liquid Chromatography – Mass Spectrometry (RP-HPLC-MS)

An Agilent 1260 Infinity instrument with an adjusted wavelength of 214 nm and a 6120 Quadrupole LC/MS with an electrospray ionization source was used for HPLC and MS analysis. In the m/z range of 200 to 2000, all measurements were carried out in either positive or negative ionization mode. The following mobile phases were used in the analysis: 95/5 (H_2O/MeCN, *v/v*) (mobile phase A) and 5/95 (H_2O/MeCN, *v/v*) (mobile phase B), both with 0.1 vol.-% formic acid, in a poroshell 120 ECC18 3.0x50 mm, 2 m reverse phase (RP) from Agilent.

High resolution ESI (HR-ESI)

On UHR-QTOF maXis 4G, HR-ESI spectra were measured (Bruker Daltonics).

Freeze Dryer

Cleaved Oligomers got freeze dried (lyophilized) by the Alpha 1-4 LD instrument from the Martin Christ Freeze Dryers GmbH. Temperatures for the measurements are -42 °C and a pressure of 0.1 mbar is maintained while lyophilizing.

General Synthetic Protocols

Synthetic procedures

The synthesis of the EDS building block has been reported by Ponader et al.[1] ^{1}H-NMR spectra is in the Appendix Figure 17 and ^{13}C-NMR spectra in the Appendix Figure 20. The synthesis of the BCC building was conducted as previously reported by Capar et al.[2] ^{1}H-NMR spectra is in the Appendix Figure 15 and ^{13}C-NMR spectra in the Appendix Figure 19.

Resin swelling and Fmoc deprotection

TentaGel® S RAM is used for all reactions described with a loading of 0.24 mmol/g which is filled into BD syringe reactors with an inlet frit. 10 mL Syringes were used for batch sizes of 0.5 mmol. Before coupling the building blocks the resin was swollen for 30 min in DCM. The Fmoc protecting group was cleaved by a 25 vol.-% piperidine in DMF solution. Therefore, the syringe was drawn up with 10 mL of the solution and shaken 2 times for 20 min. The resin was subsequently washed 15 times with DMF.

Solid phase synthesis

The following procedure refers to the coupling of Glycine-fmoc, Glycine-boc, EDS and Phenylalanine based on the protocol reported by Ponader et al.[1]

After the swelling and the Fmoc deprotection the resin was washed with 10 mL DMF ten times. For the coupling an excess of 5 equivalents of building block and PyBOP was used. DIPEA was used in a 10 equivalents excess. One-fourth fmoc glycine and three-fourths boc glycine were used for amine loading reduction. All components were dissolved in DMF and shaken for 5 min prior to adding it to the resin. The activated solution was raised onto the resin and shaken for 2 h. After the reaction the resin is washed with 15 times DMF and 5 times DCM. The preparations were carried out with 0.5 mmol batch sizes which were subsequently divided into 5 syringes (0.1 mmol) for BCC coupling. All reactions were performed in a syringe with frit on a shaking plate at room temperature.

Coupling of BCC and HMD

For the coupling of the BCC building block and the HMD, the resin (the oligomeric precursor) was transferred from the plastic syringe to a glass syringe. The LiOTf/TBD catalyst system and the building block dissolved in NMP were then added. The syringe was then sealed with a septum and nitrogen was flowed through the reaction solution. The syringe was kept in a water bath which was adjusted to the appropriate temperature. Temperatures and reaction times can be found in the corresponding tables (see Tables 1-4). After the reaction, the syringe was washed 15 times with NMP and 5 times with DCM.

Capping of the hydroxyl groups

The syringe was filled with acetic anhydride and shaken for 2 hours at room temperature. Then it was washed with DMF 15 times.

Macro cleavage

For cleaving the oligomers of the TentaGel® S RAM a cleavage solution of TFA:TIPS:DCM (95:2.5:2.5 vol.-%) was drawn up into the syringe. The solution was shaken for 60 min at room temperature and after that precipitated into iced diethyl ether (45 mL). The solution was centrifuged for 5 min and the supernatant was then decanted. The white precipitate was counter current dried for 1 h in nitrogen. The white precipitate was then dissolved in MilliQ water and lyophilized.

Synthesis

Synthesis of the building blocks

4,4'-((butane-1,4-diylbis(oxy))bis(methylene))bis(1,3-dioxolan-2-one)

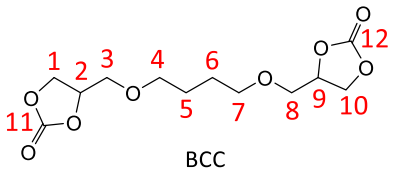

BCC

The BCC building block was synthesized in a modified approach from Capar et al.[2]: 10 mL 1,4-butanediglycidyl ether (202.25 g/mol, 11 g, 54 mmol) was cooled and stirred for 30 minutes in a flask using an ice bath. 502 mg Tetrabutylammonium iodide (TBAI) (2.5 mol-%, 1.35 mmol) was added to the solution in small portions. The flask was closed with a septum. Dry ice was added to a second flask. The two flasks were connected to each other via a tube and an additional cannula was inserted into the flask with the solution as a gas equalizer. The CO_2 was bubbled through the solution for 1 h at room temperature. Subsequently, the solution was heated to 90 °C for 8 h. And then stirred for 16 h at room temperature. The product was obtained as a white solid (15.22 g, 52.46 mmol, 96 %) and analysed by ^{1}H and ^{13}C-NMR spectroscopy. The TBAI was not removed from the solution because, according to the literature, this promotes the aminolysis of cyclic carbonates.[3] For the NMR spectra see Appendix, Figures 9 and 12.

^{1}H-NMR (600 MHz, DMSO-d6): δ [ppm] = 4.91 (m, 2H, **2**, **9**); 4.52 (t, J = 8.37 Hz, 2H, **1**, **10**); 4.25 (dd, J = 8.2, 5.9 Hz, 2H, **1**, **10**); 3.60 (dd, ^{2}J = 11.42 Hz, ^{3}J = 2.69 Hz, 2H, **3**-*cis*, **8**-*cis*, ^{2}J = 11.42 Hz, ^{3}J = 4.06 Hz, 2H, **3**-*trans*, **8**-*trans*); 3.50 – 3.41 (m, 4H, **4**, **7**); 1.54 (m, 4H, **5**, **6**).

^{13}C-NMR (600 MHz, DMSO-d6): δ [ppm] = 155.0 (11, 12), 75.6 (2, 9), 70.6 (3, 8), 69.5 (1, 10), 66.1 (4, 7), 25.6 (5, 6).

ESI-MS (m/z): calculated M_{exact} = 290.10; found $[M+H^{+}]$ = 291.0 and $[M+Na^{+}]$ = 308.2

Figures, Schemes and Tables

Table 1: Coupling of BCC building block to the solid phase using EDS-phenylalanine-EDS as the oligomeric precursor in the solvent DMF.

Reaction Time [min]	Reaction Temperature [°C]	BCC [Eq.]	Catalyst	Product conversion [%] *
10	RT	5	-	-
25	37	5	-	-
60	37	5	-	-
60	50	5	-	-
60	RT	5	TEA	-
180	50	5	TEA	-
180	50	5	LiBr, DBU	-
180	50	5	LiBr, DBU, MeOH	-
60	50	5	TBD, LiBr	-
120	50	5	TBD, LiBr	-

** Product conversions were determined by integrating an RP-HPLC chromatogram (gradient of 5 to 95% by volume acetonitrile in water containing 0.1% by volume formic acid, run time 17 min).*

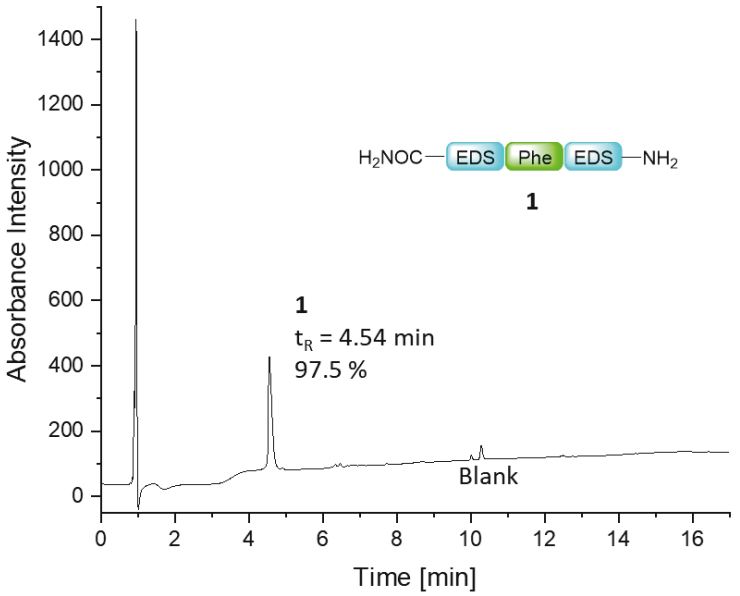

*Figure 1: RP-HPLC chromatogram (Gradient 5-95 vol.-% - MeCN in H_2O (0.1 vol.-% formic acid, run time 17 min) of the oligomer **1**.*

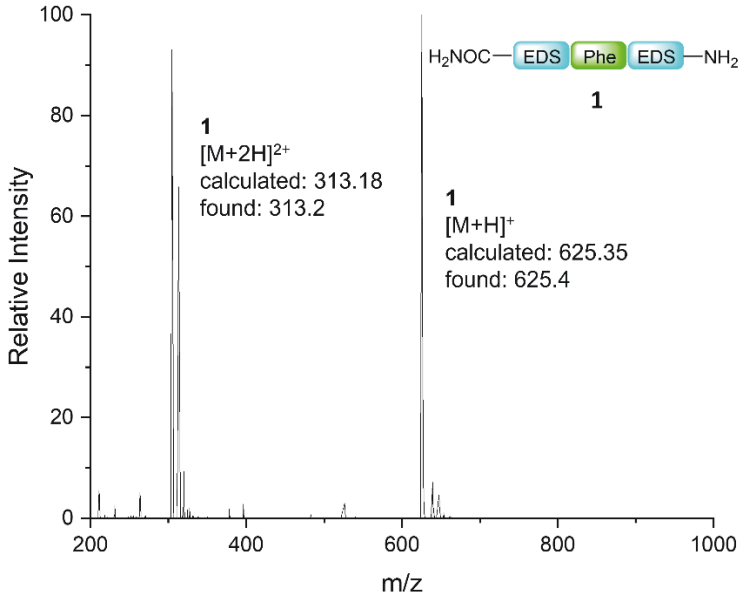

*Figure 2: HPLC-ESI-MS of **1** at t = 4.54 min (gradient of 5 to 95 vol.-% acetonitrile in water containing 0.1 vol.-% formic acid, run time 17 min).*

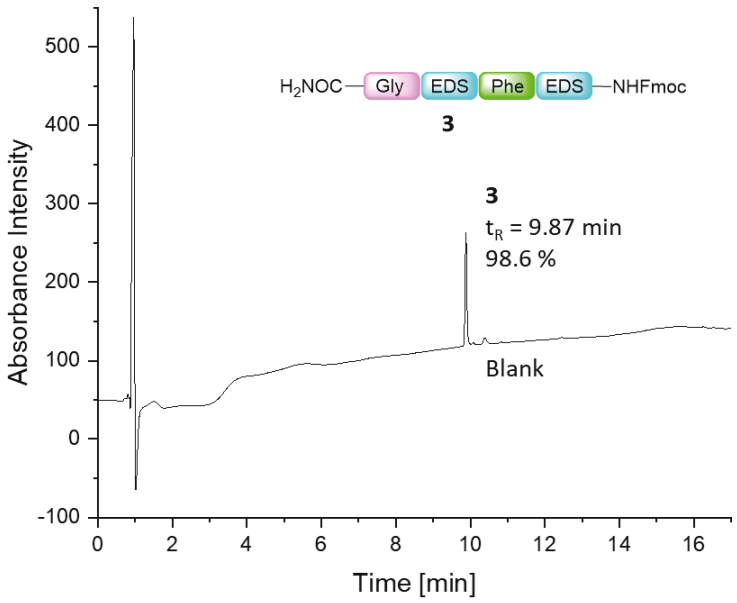

*Figure 3: RP-HPLC chromatogram (Gradient 5-95 vol.-% - MeCN in H_2O (0.1 vol.-% formic acid, run time 17 min) of the oligomer **3**.*

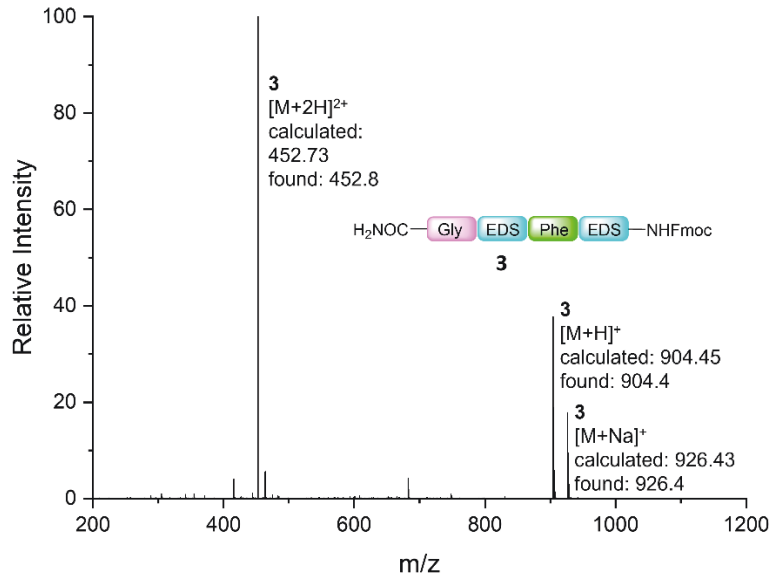

*Figure 4: HPLC-ESI-MS of **3** at t = 9.87 min (gradient of 5 to 95 vol.-% acetonitrile in water containing 0.1 vol.-% formic acid, run time 17 min).*

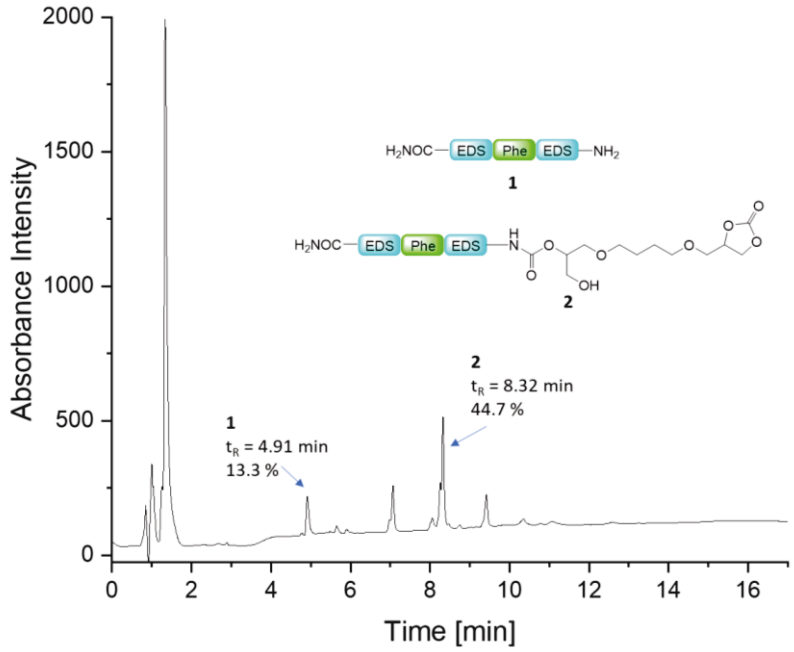

*Figure 5: RP-HPLC chromatogram (Gradient 5-95 vol.-% - MeCN in H_2O (0.1 vol.-% formic acid, run time 17 min) of the oligomer **2** without optimization.*

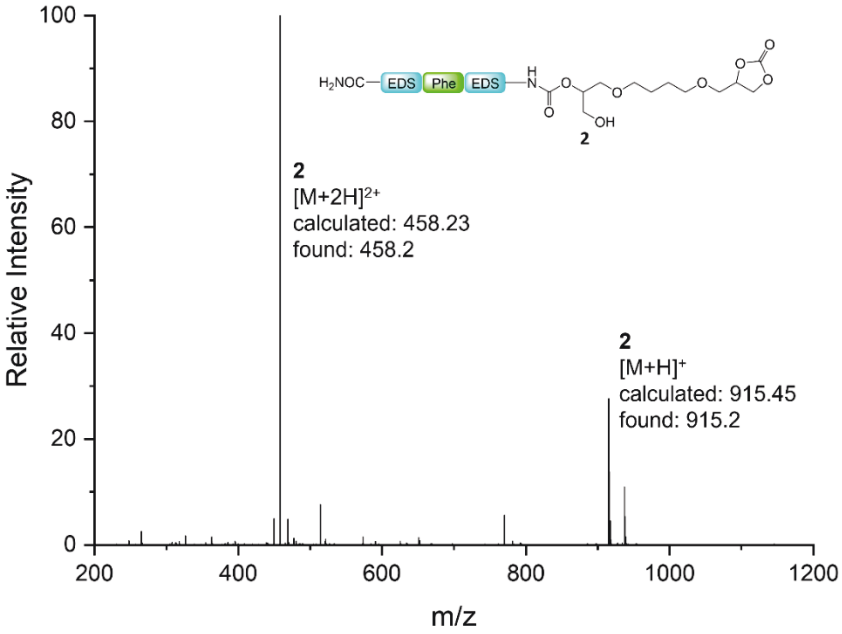

*Figure 6: HPLC-ESI-MS of **2** at t = 8.32 min (gradient of 5 to 95 vol.-% acetonitrile in water containing 0.1 vol.-% formic acid, run time 17 min).*

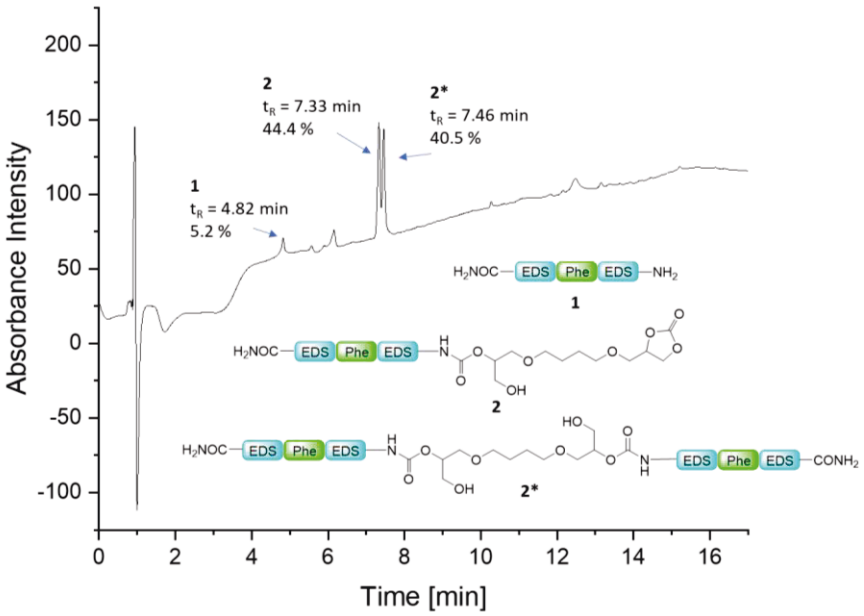

*Figure 7: RP-HPLC chromatogram (Gradient 5-95 vol.-% - MeCN in H_2O (0.1 vol.-% formic acid, run time 17 min) of the oligomer **2**.*

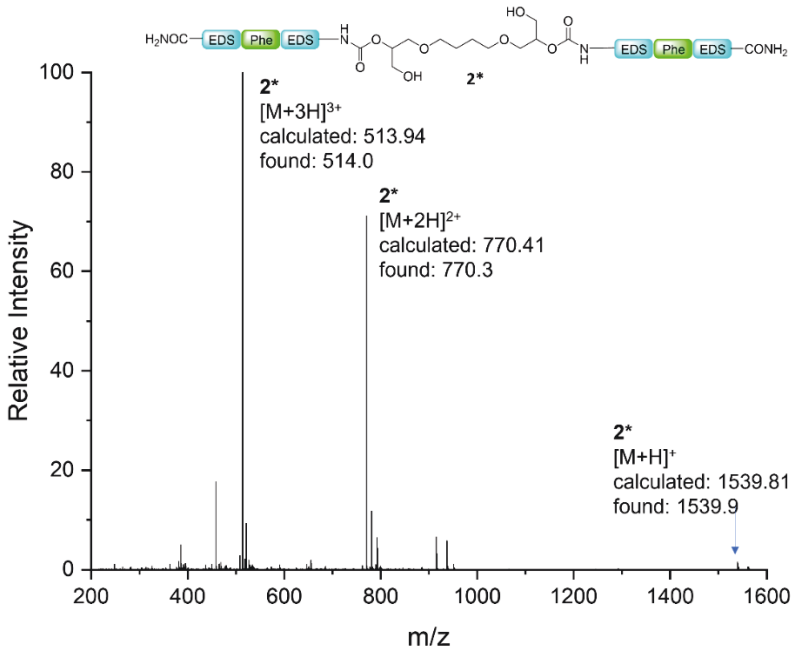

*Figure 8: HPLC-ESI-MS of **2*** at t = 7.56 min (gradient of 5 to 95 vol.-% acetonitrile in water containing 0.1 vol.-% formic acid, run time 17 min).*

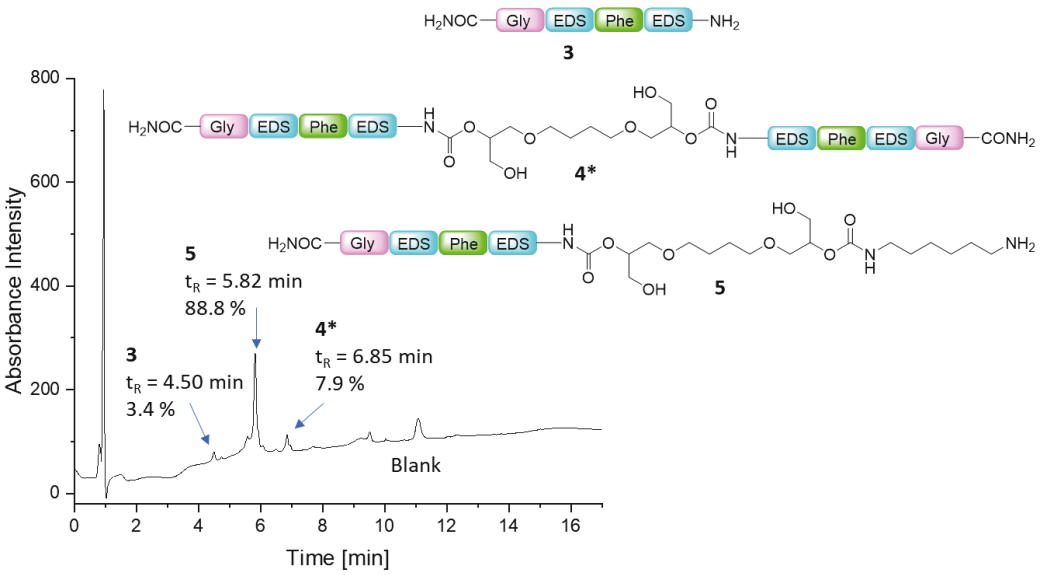

Figure 9: RP-HPLC chromatogram (Gradient 5-95 vol.-% - MeCN in H_2O (0.1 vol.-% formic acid, run time 17 min) of the oligomer 2.

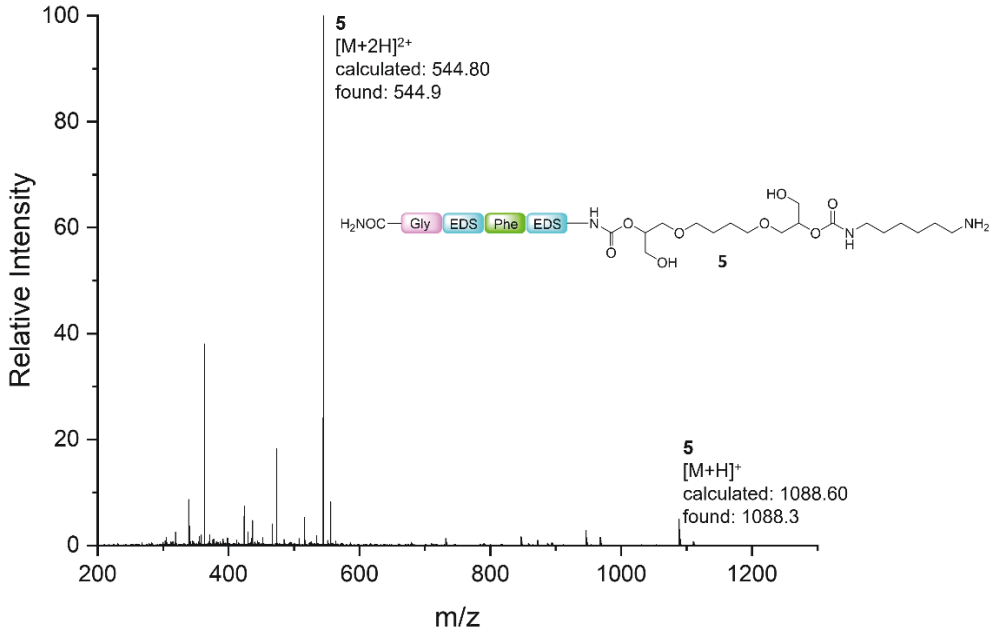

*Figure 10: HPLC-ESI-MS of **5** at t = 5.82 min (gradient of 5 to 95 vol.-% acetonitrile in water containing 0.1 vol.-% formic acid, run time 17 min).*

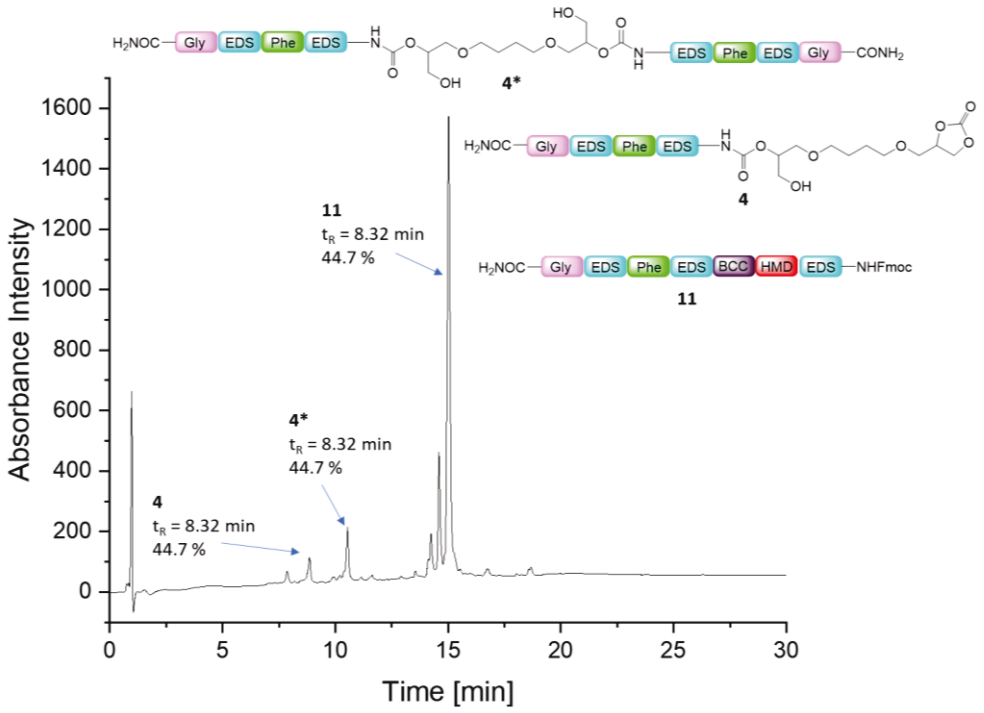

*Figure 11: RP-HPLC chromatogram (Gradient 5-95 vol.-% - MeCN in H_2O (0.1 vol.-% formic acid, run time 30 min) of the oligomer **11**.*

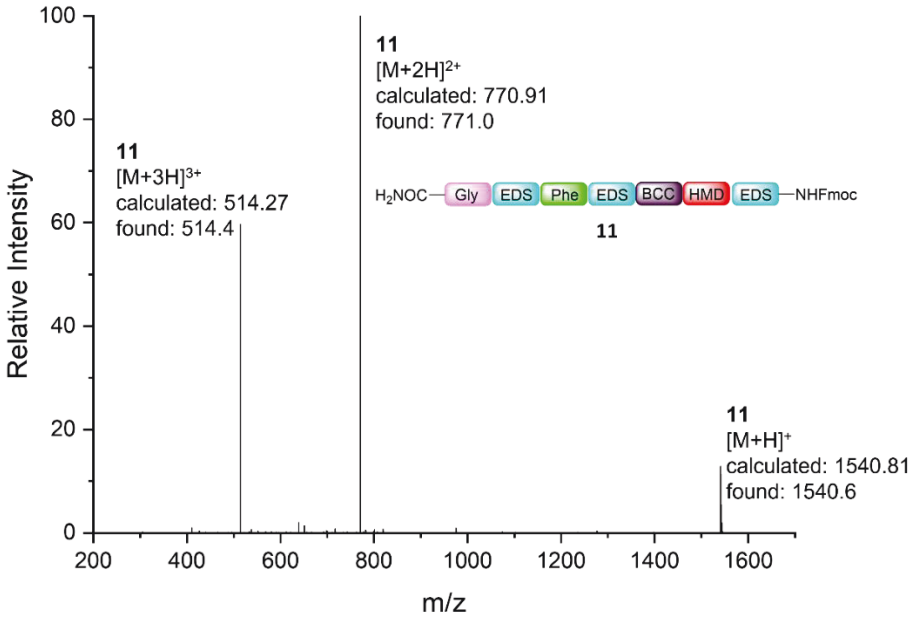

*Figure 12: HPLC-ESI-MS of **11** at t = 8.32 min (gradient of 5 to 95 vol.-% acetonitrile in water containing 0.1 vol.-% formic acid, run time 30 min).*

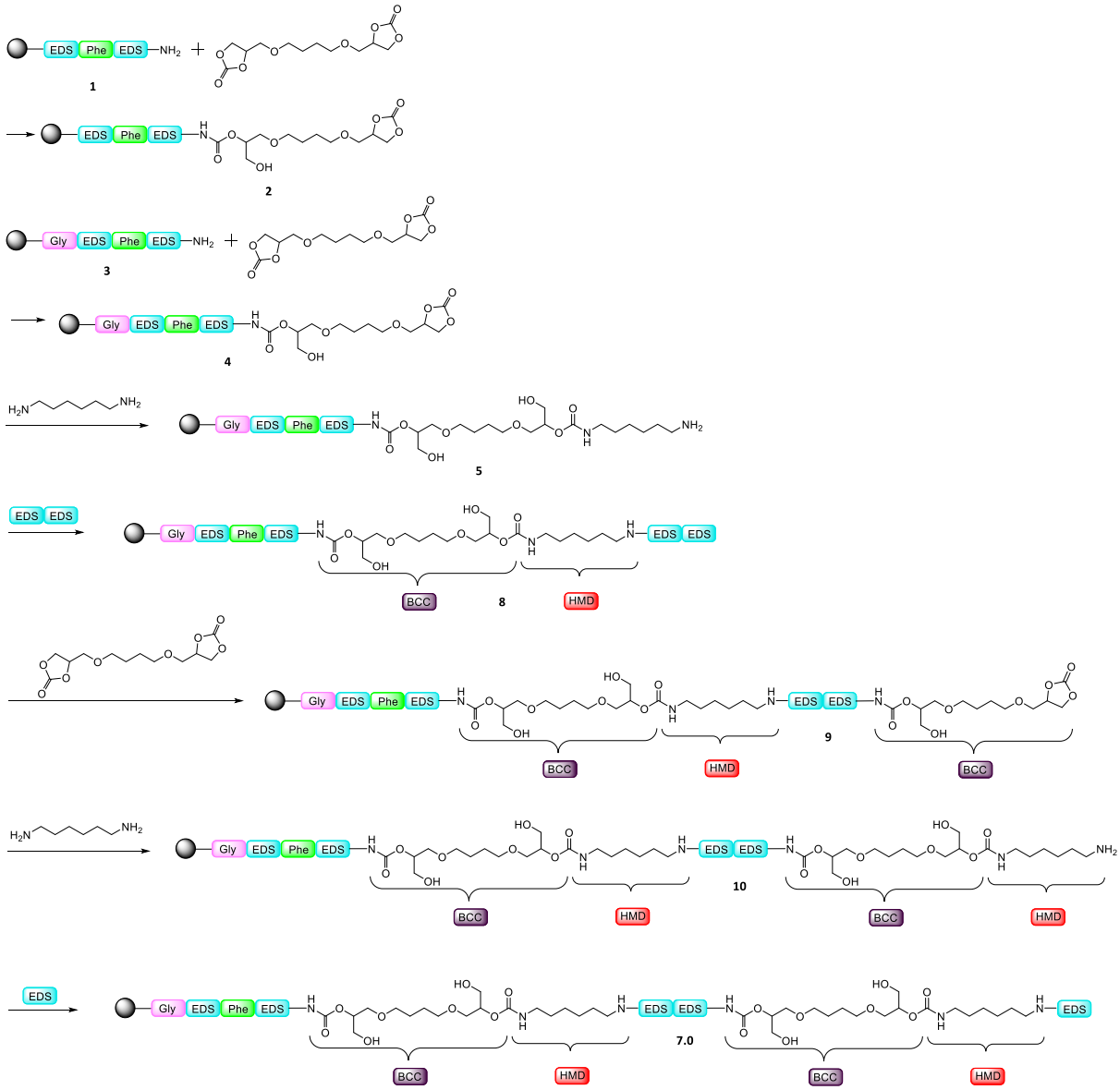

Figure 13: Synthesis route for the repeated coupling of BCC building blocks to the solid phase.

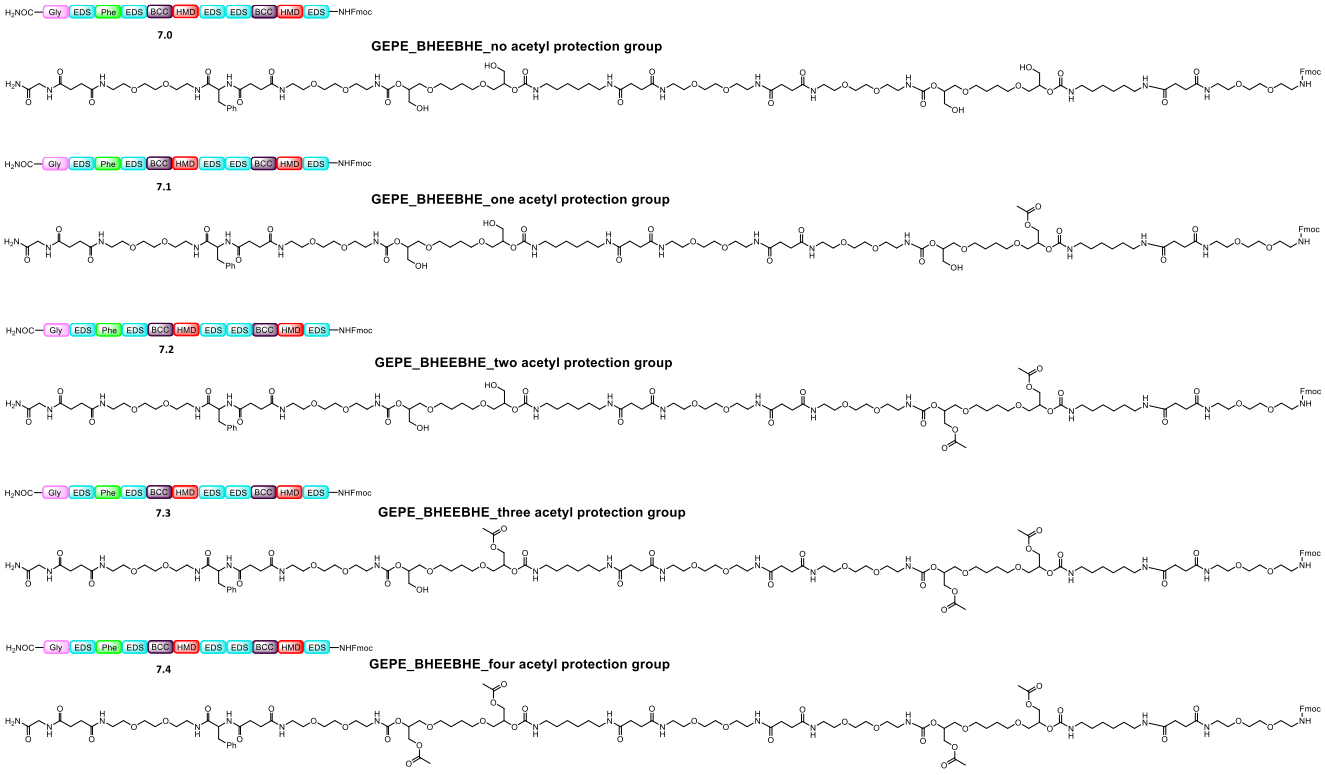

*Figure 14: Degrees of acetylation for the oligomer **7.***

Appendix

^{1}H-NMR

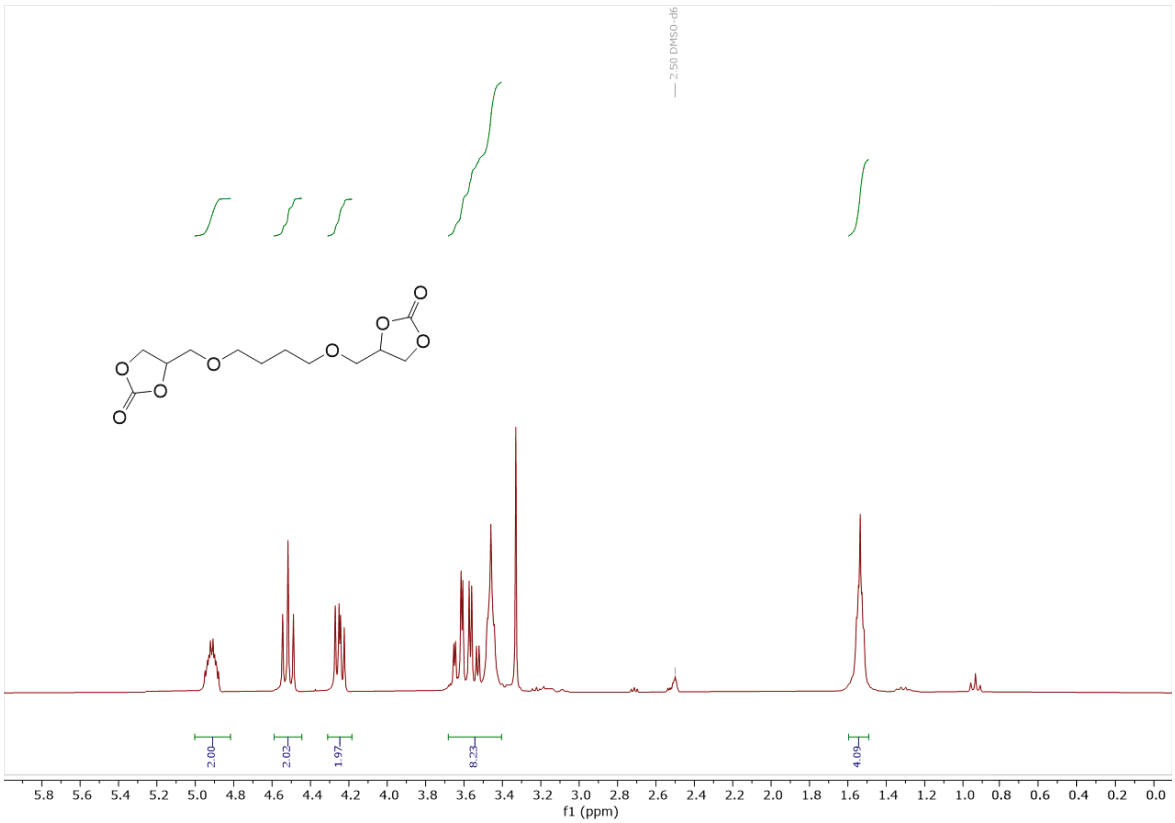

Figure 15: 300 MHz ^{1}H NMR of BCC building block in DMSO-d_6 and the integration analysis indicating the proton count.

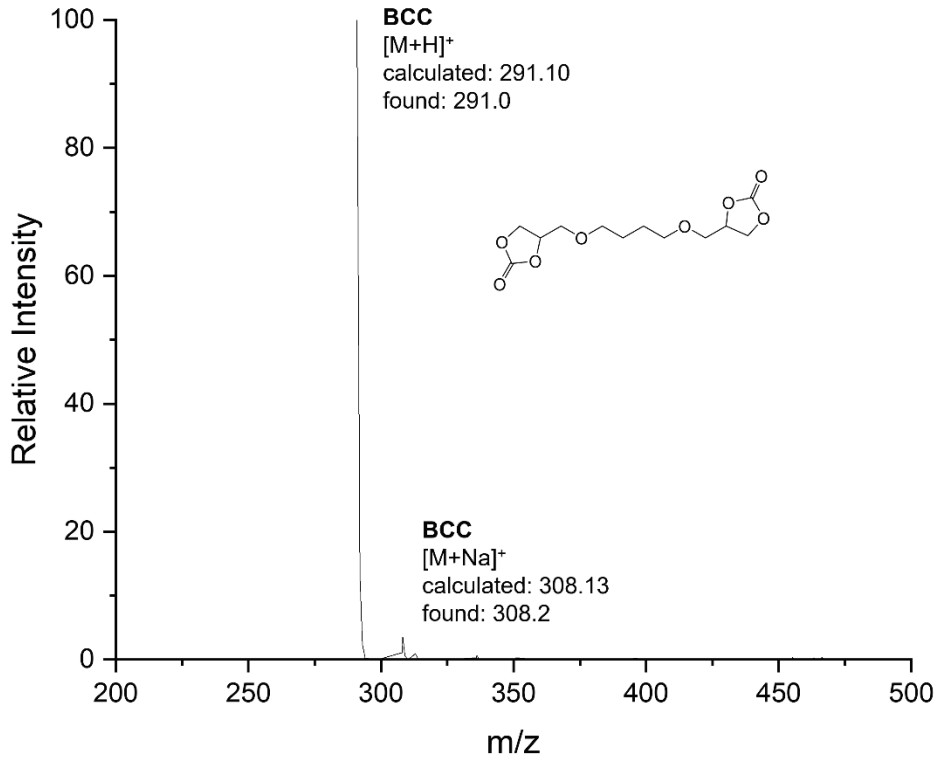

Figure 16: ESI-MS of BCC.

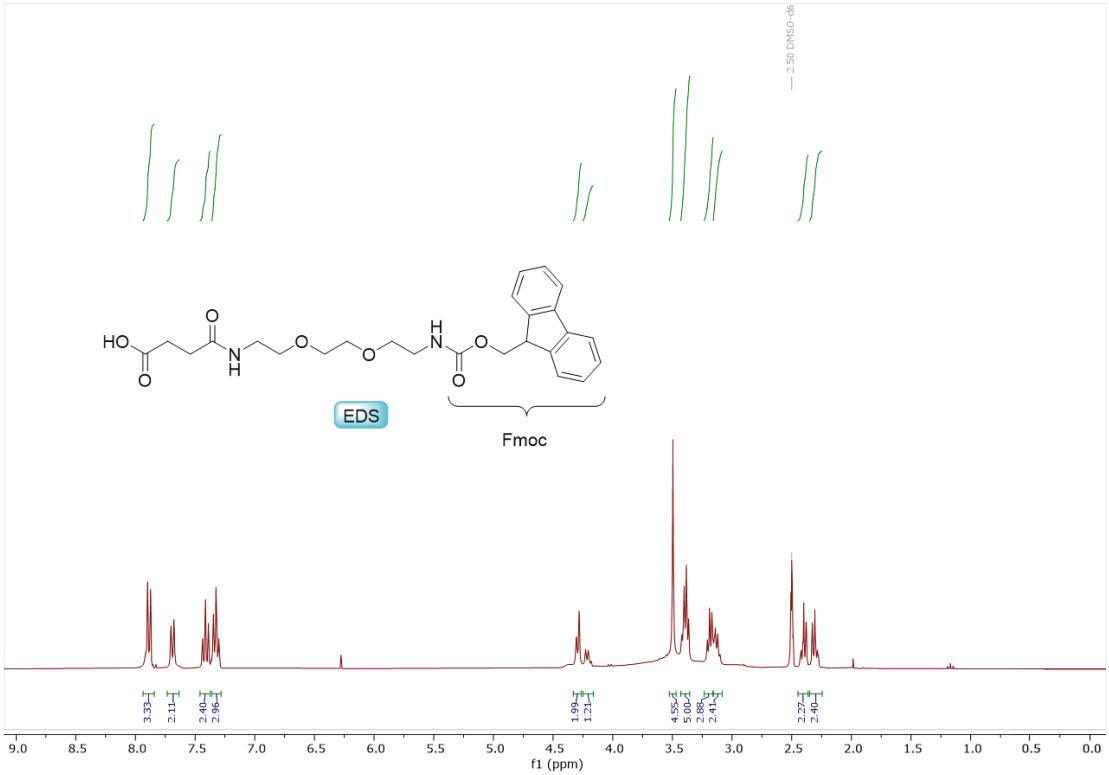

Figure 17: 300 MHz ^{1}H NMR of EDS in DMSO-d_6 and the integration analysis indicating the proton count.

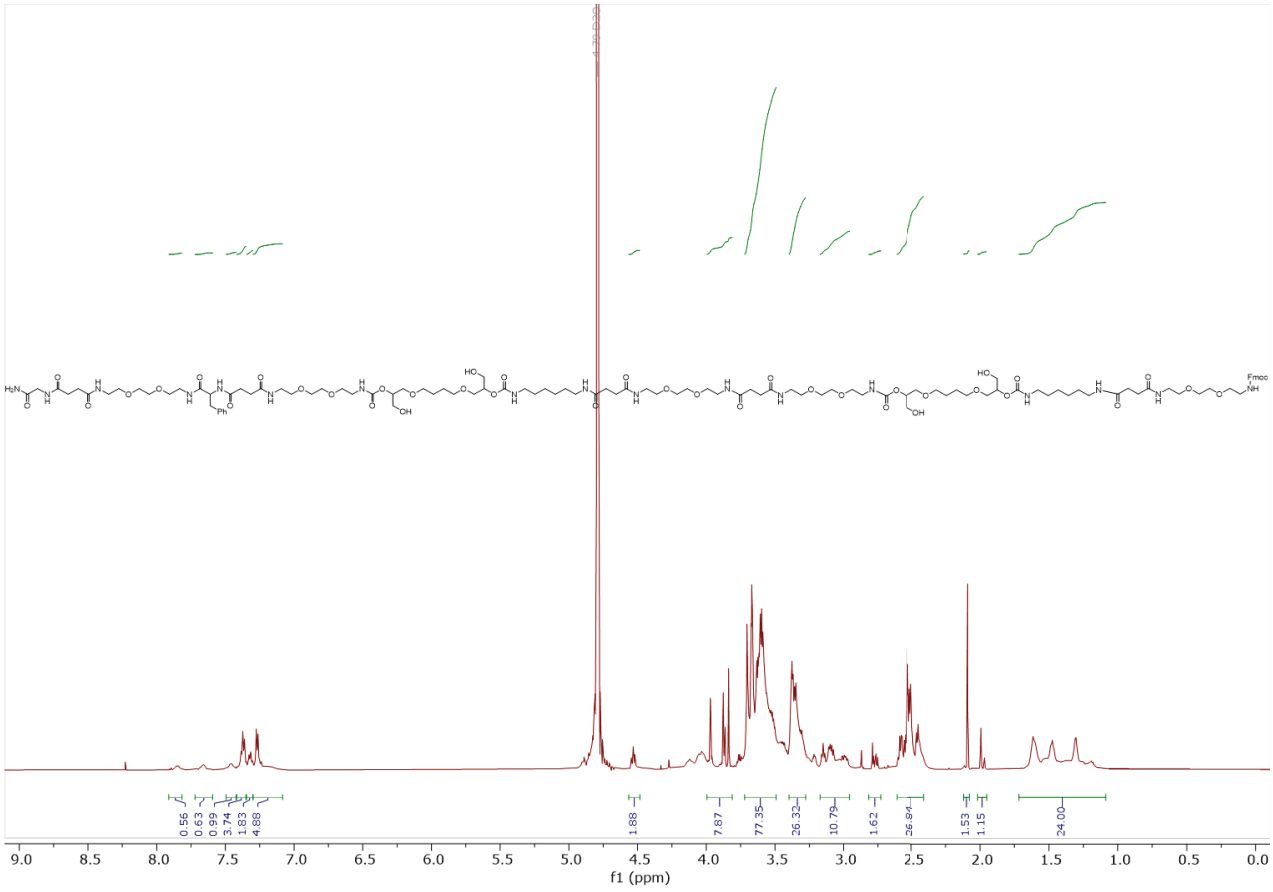

*Figure 18: 600 MHz ^{1}H NMR of the oligomer **7.0** in D_2O and the integration analysis indicating the proton count.*

^{13}C-NMR

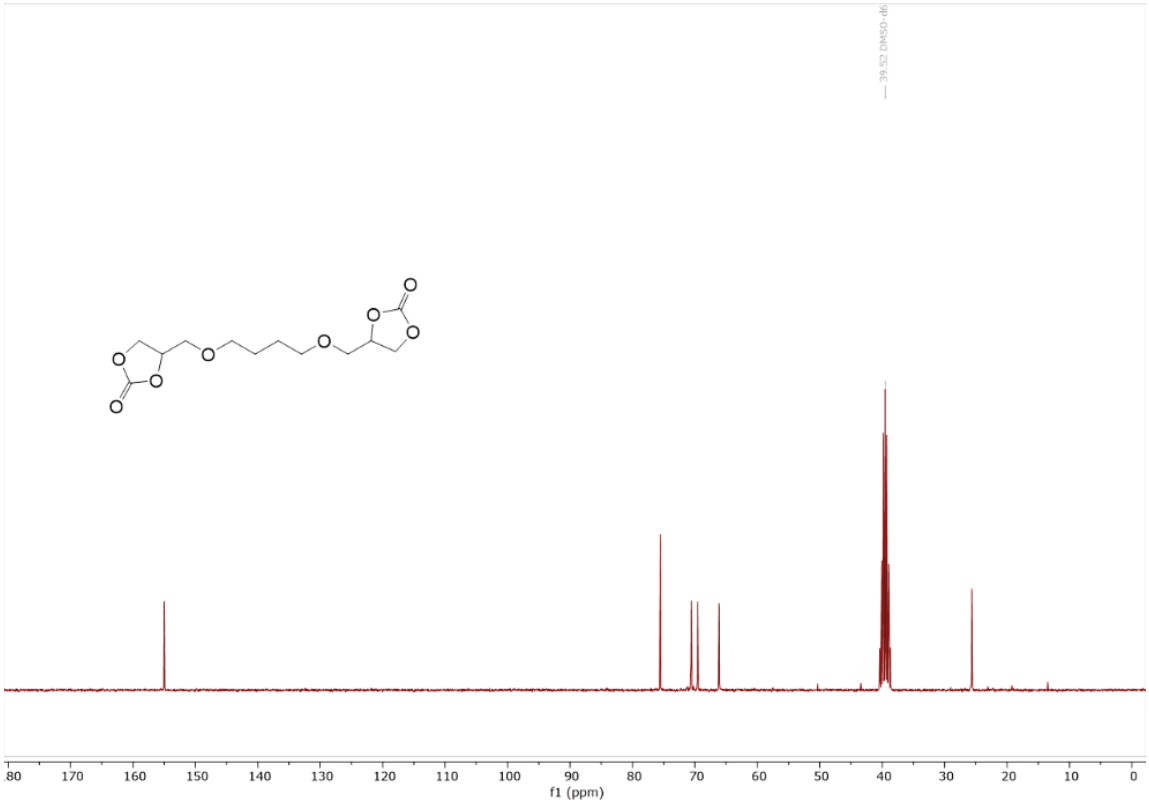

Figure 19: 75 MHz ^{13}C NMR of BCC building block in DMSO-d_6.

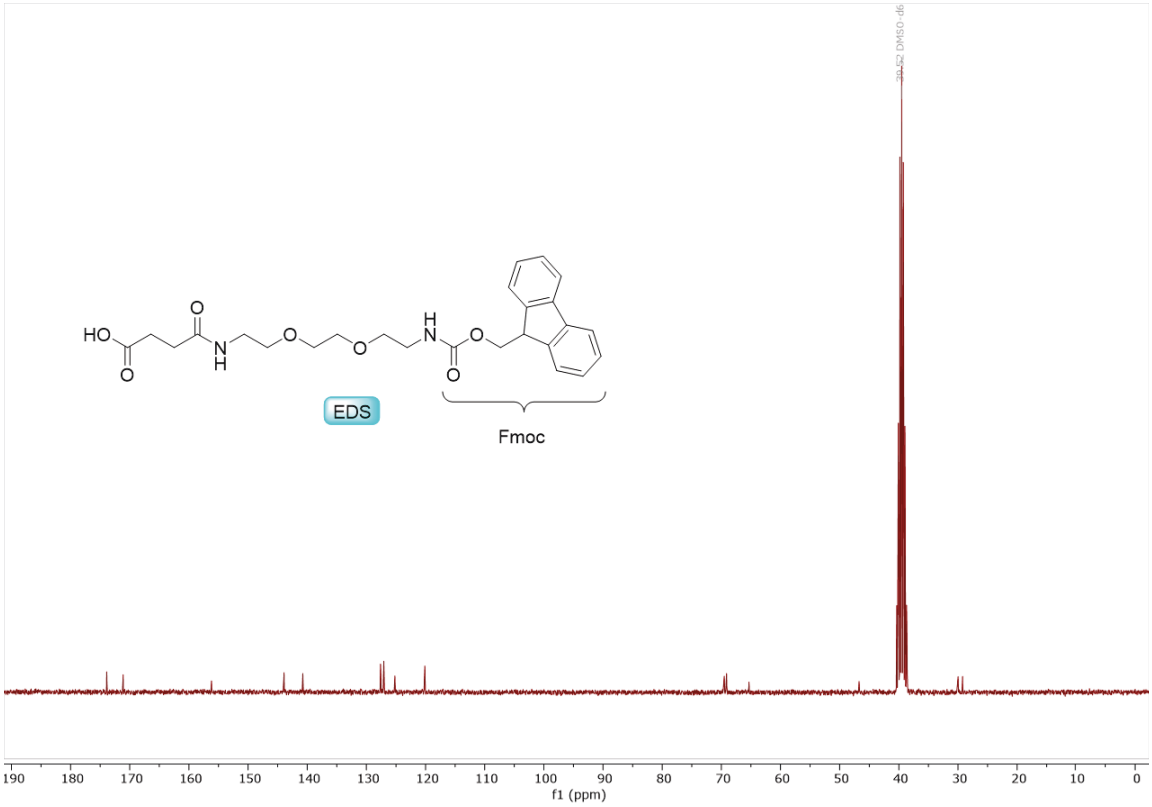

Figure 20: 75 MHz ^{13}C NMR of EDS in DMSO-d_6.

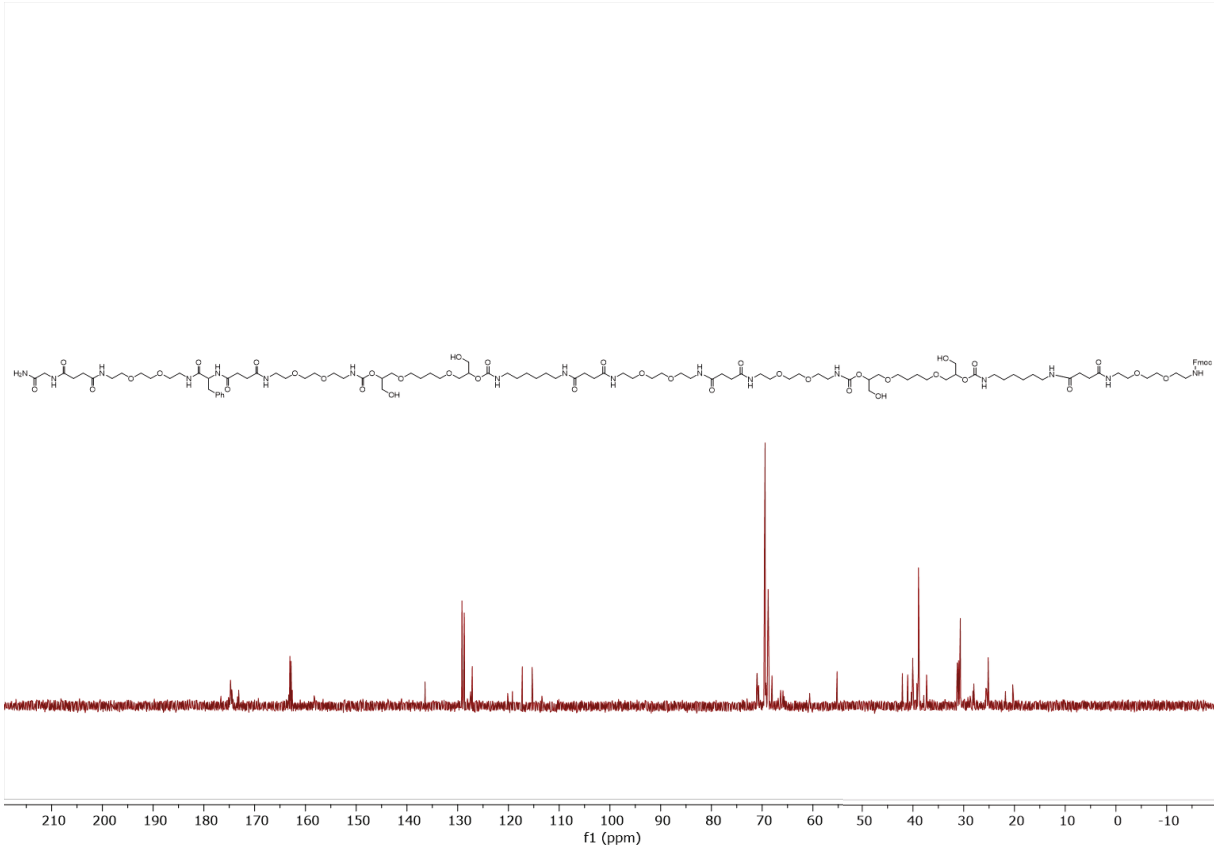

*Figure 21: 75 MHz ^{13}C NMR of the oligomer **7.0** in D_2O.*

HR-ESI

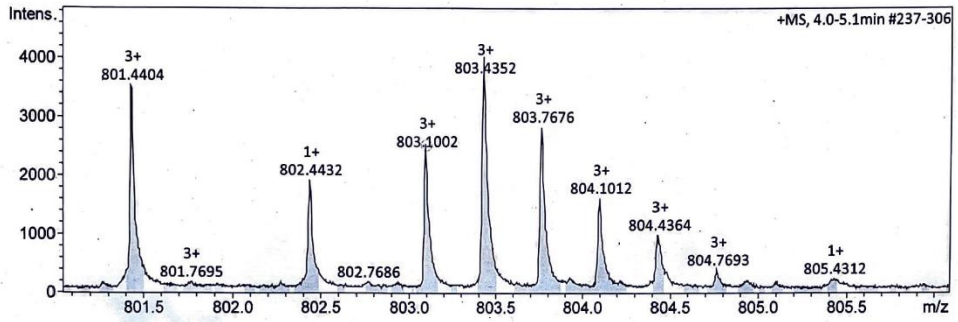

Meas. m/z	#	Ion Formula	m/z	err [ppm]	mSigma	# mSigma	Score	rdb	e⁻ Conf	N-Rule
803.1002	1	C113H186N15O41	803.0971	-3.8	75.6	1	18.27	28.5	even	ok
	2	C112H186N17O40	803.1009	0.8	77.7	2	100.00	28.5	even	ok
	3	C110H190N15O43	803.1042	4.9	83.2	3	5.11	23.5	even	ok
	4	C106H190N15O46	803.0991	-1.4	93.7	4	39.59	19.5	even	ok
	5	C105H190N17O45	803.1028	3.3	95.8	5	11.77	19.5	even	ok
	6	C101H190N17O48	803.0978	-3.1	106.9	6	8.01	15.5	even	ok

*Figure 22: HR-ESI of the Oligomer **7.0.***

Literature

[1] D. Ponader, F. Wojcik, F. Beceren-Braun, J. Dernedde, L. Hartmann, *Biomacromolecules* **2012**, *13*, 1845.

[2] Ö. Capar, M. Tabatabai, J. E. Klee, M. Worm, L. Hartmann, H. Ritter, *Polym. Chem.* **2020**, *11*, 6964.

[3] C. D. Diakoumakos, D. L. Kotzev, *Macromolecular Symposia* **2004**.

3.2.1 Exploring glycerol carbonate building blocks

In the previous chapter, it was successfully shown how biscyclocarbonates could be coupled to the solid phase. Since the coupling of the biscyclocarbonate building blocks requires the use of a catalyst system as well as elevated temperatures and long reaction times, possibilities were sought for coupling cyclic carbonate building blocks to the solid phase under milder conditions.[106] Based on the results of the biscyclocarbonates, hetero-bisfunctional building blocks based on the cyclocarbonate motif will be investigated for their use in the solid phase in the following chapter.

In order to be able to use a building block for solid phase synthesis, it should carry a carboxy functionality which can be coupled to the *N*-terminus of an oligomer. It was searched for a building block that had both the cyclocarbonate motif and a carboxy functionality (see Figure 11).

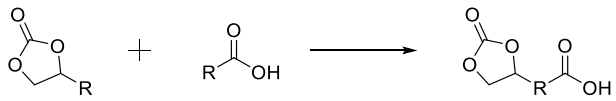

Figure 11: Envisioned solid phase building block carrying both the cyclocarbonate motif and a carboxy functionality.

The cyclocarbonate motif occurs, for example, in glycerol carbonate, which is produced from glycerol and is available in large quantities. Glycerol carbonate is a waste product of biodiesel production, where glycerol is reacted with CO_2 which is shown in Figure 12.[107–109]

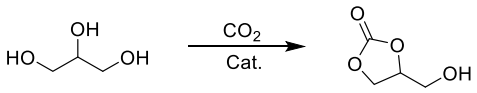

Figure 12: Reaction of glycerol with CO_2 using catalysts to form glycerol carbonate.[107]

In recent years, glycerol carbonate has gained interest as sustainable awareness has increased significantly since the greenhouse gas CO_2 can be used as an educt in its synthesis.[108] Glycerol carbonate carries a hydroxy group on one side and the 5-membered cyclocarbonate ring on the other.[110]

Glycerol as a base for a solid-phase building block is attractive because it is soluble in polar solvents and is non-toxic.[107] In order to make the glycerol carbonate accessible as a building block for solid-phase synthesis, the initial goal was to oxidize the hydroxyl group to a carboxy functionality. The building block can then be added directly to the *N*-terminus of an oligomer

via the carboxy functionality and can subsequently be further built up in the following under the conditions optimized in the previous chapter for the ring opening of the cyclic carbonates.

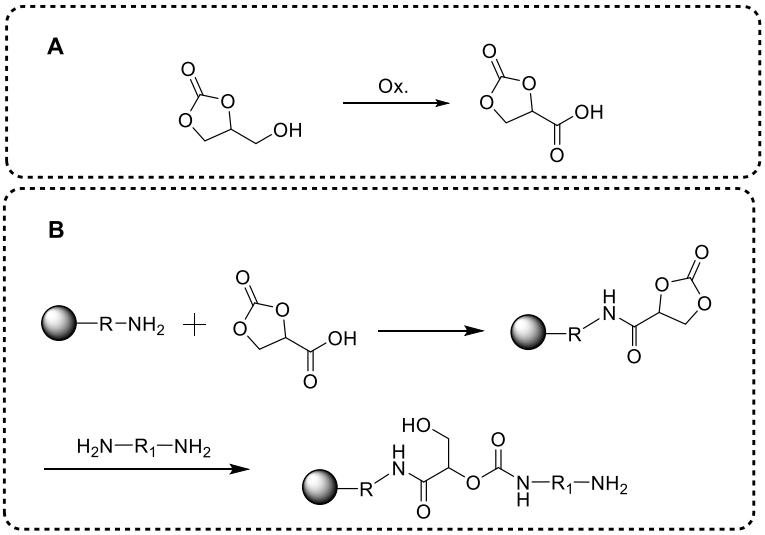

Figure 13: A: Envisioned direct oxidation of glycerol carbonate. B: Envisioned solid phase coupling of the building block with subsequent ring opening.

3.2.1.1 Synthesis of the glycerol carbonate building block(s)

Different synthetic routes were tried for the oxidation of glycerol carbonate. Initially, an attempt was made to oxidize the glycerol carbonate directly at the hydroxy group. Glycerol carbonate was reacted with trichloroisocyanuric acid under basic conditions, as described by Wölfele et al.[111] For this purpose, glycerol carbonate was mixed with sodium bicarbonate, NaBr, H_2O, acetone, (2,2,6,6-Tetramethylpiperidin-1-yl)oxyl (TEMPO) and trichloroisoycanuric acid and cooled to 0 °C in an ice bath. The solution was then stirred for 18 h at RT. Next, the solution was heated for three hours to reflux. The solution was then filtered over silica gel and the remaining liquid was evaporated. The resulting colorless solid was dissolved in ethyl acetate and extracted with aqueous sodium bicarbonate solution. The organic phase was dried and evaporated. Analysis of the structure by ^{1}H NMR and ESI-MS showed no conversion to the oxidized glycerol carbonate.

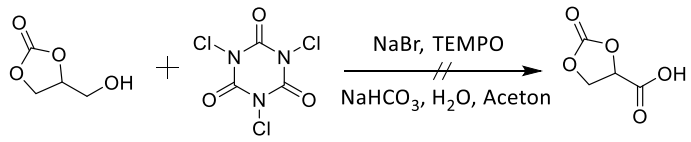

Figure 14: Reaction of glycerol carbonate with trichloroisocyanuric acid.[111]

Since the direct oxidation of the glycerol carbonate was not successful attempts were made to react glycerol carbonate with bromoacetic acid to implement the carboxy functionality in the building block. The reaction was performed following the experiments of Eh.[112] For this purpose, sodium hydride was dissolved in tetrahydrofuran (THF) in a nitrogen countercurrent and then glycerol carbonate was added dropwise over one hour. Bromoacetic acid was then dissolved in THF and added over 30 min. The reaction was heated to reflux at 90 °C for six hours and then stirred at RT for 18 hours. Hydrochloric acid was then added to the solution to quench the reaction. The purification of the product was crucial for its purity. For this purpose, different purification steps were tried out. The best purification method was to extract the solution four times with ethyl acetate and then evaporate the previously dried organic phase. The remaining residue was dissolved in DCM and placed in the freezer for two days.

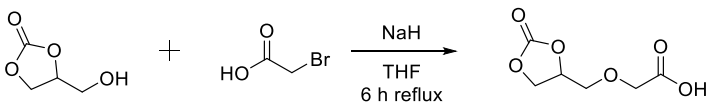

Figure 15: Reaction of glycerol carbonate with bromoacetic acid.[112]

A colorless solid precipitates which was extracted. The Glycerol Carbonate Bromoacetic acid (GCBr) building block was isolated with a yield of 93 %. The compound was analysed and identified via ^{1}H-NMR which is shown in Figure 16, ^{13}C-NMR (see Appendix Figure 74) and HR-ESI-MS (see Appendix Figure 75).

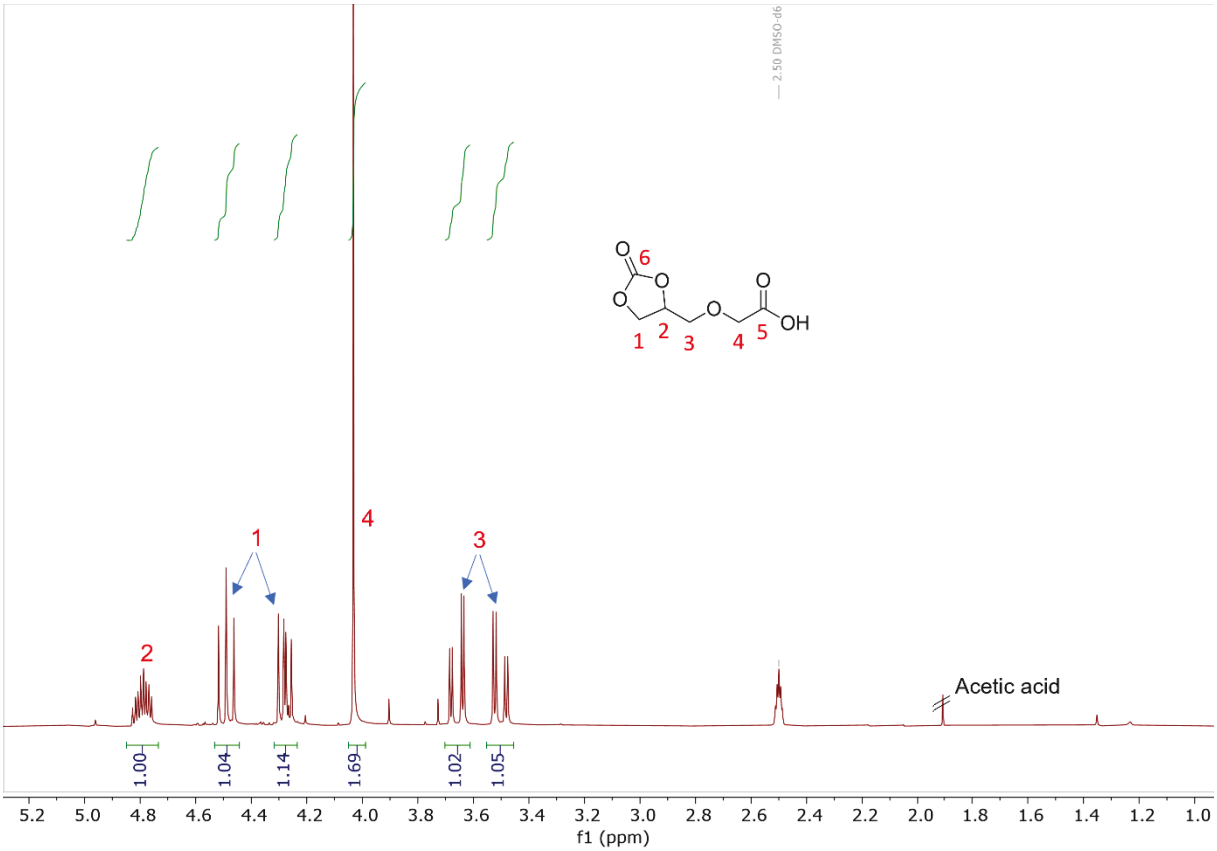

Figure 16: 300 MHz ^{1}H-NMR measured at RT of the GCBr building block in DMSO-d_6 and the integration analysis indicating the proton count. The individual protons are assigned by number.

The multiplet from 4.83 to 4.76 ppm was referenced which was assigned to position 2 with 1 proton. The spectrum shows a total of 7 protons which corresponds to the sum of the protons of the GCBr building block. The triplet at 4.49 ppm and the doublet of doublets at 4.28 ppm could be assigned to position 1 with an integral of 2. The doublet of doublets at 3.66 and 3.50 ppm could be assigned to position 3 with an integral of 2 protons. The remaining singlet with an integral of 2 protons at 4.03 ppm could be assigned to position 4.

3.2.1.2 Solid phase coupling of the glycerol carbonate building block(s)

Attempts were then made to couple the GCBr building block to the solid phase. The oligomer EDS-Phenylalanine-EDS (EPE) was chosen as the oligomeric precursor which had previously been used with the biscyclocarbonates for the coupling of cyclic ring building blocks to the solid phase.[106] EDS was introduced to increase the distance from the solid phase resin and to better assign the mass of the oligomer in the mass spectrum. Phenylalanine was used because the phenyl ring improves the conversion analysis by UV-Vis spectroscopy.[106]

Various coupling conditions were tested, which are shown in Table 1.

Table 1: Different coupling conditions for the coupling of GCBr building block to the solid phase using EDS-phenylalanine-EDS as the oligomeric precursor.

Time	Temperature	Solvent	Coupling reagents	GCBr equivalents	Product conversion [%] *
1 h	RT	DMF	PyBOP/DIPEA	20	71
2 h	RT	DMF	PyBOP/DIPEA	20	74
2 h	RT	NMP	PyBOP/DIPEA	5	41
18 h	RT	DMF	PyBOP/DIPEA	20	85
18 h	RT	DMF	OxymaPure DIC/DIPEA	5	27

** Product conversions were determined by integrating an RP-HPLC chromatogram (gradient of 5 to 95 % by volume acetonitrile in water containing 0.1% by volume formic acid, run time 17 min).*

The highest conversion of 85 % was determined with 20 equivalents of the GCBr building block and the coupling reagents PyBOP and DIPEA in the solvent DMF at RT and a reaction time of 18 hours.

Since the mass 843.4 could be detected in HPLC-ESI-MS analysis as the main product during the coupling of the oligomer EPE with GCBr, it can be assumed that the carboxy functionality did couple to the oligomer as shown in Figure 17.

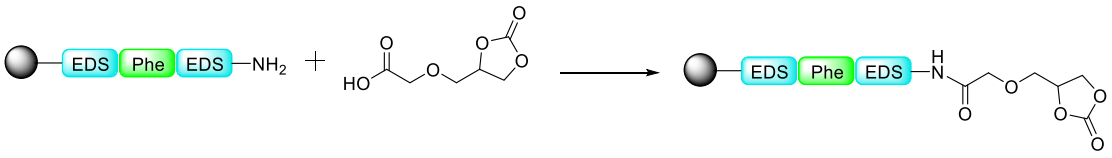

Figure 17: Solid phase coupling of the GCBr building block.

The RP-HPLC chromatogram and the corresponding HPLC-ESI-MS of the experiment with the highest product conversion is shown in Figure 18.

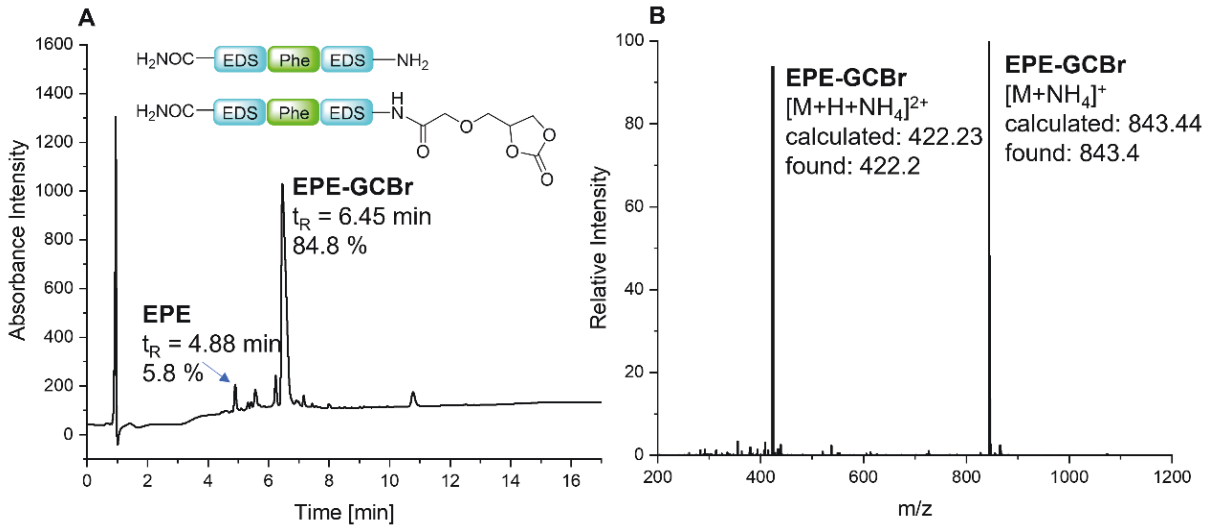

Figure 18: A: RP-HPLC chromatogram (Gradient 5-95 vol.-% - MeCN in H_2O (0.1 vol.-% formic acid, run time 17 min) of the oligomer EPE-GCBr. B: HPLC-ESI-MS of EPE-GCBr at t = 6.45 min (gradient of 5 to 95 vol.-% acetonitrile in water containing 0.1 vol.-% formic acid, run time 17 min).

As can be seen in Figure 18, by-products were formed. Attempts were made to assign them, but no plausible explanations for the by-product formation could be observed. Dimer formation was observed in the biscyclocarbonate experiments.[106] It was tested whether the oligomeric precursor attacks the GCBr building block at both ends. However, this could not be detected via the RP-HPLC chromatogram.

In the case of biscyclocarbonates, the conditions for the ring opening of cyclic carbonates have already been studied extensively.[106] Therefore, in the next step, with the optimized conditions, the terminal cyclic carbonate ring was attempted with hexamethylenediamine and the catalyst system TBD/LiOTf, NMP as solvent at 60 °C reaction temperature for two hours. Although this reaction was carried out repeatedly, no product conversion was observed.

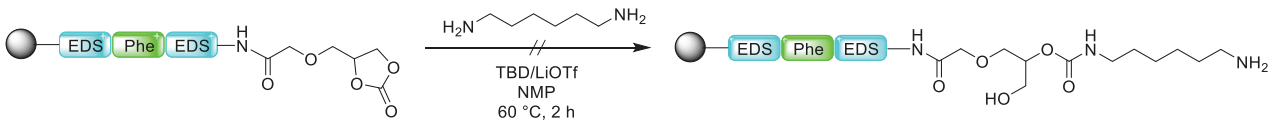

Figure 19: Diamine coupling to the solid phase bound GCBr building block.

Since the experiments with the GCBr building block did not lead to a sequence-defined structure of an oligomer, another way of coupling the glycerol carbonate to the solid phase was explored. In the following attempt to couple the glycerol carbonate building block to the solid phase, glycerol carbonate was reacted with tosyl chloride in a first step.[113] Using triethylamine (TEA) as the base and dry THF as the solvent, the reaction yielded 71 % after

purification. The ^{1}H-NMR and ^{13}C-NMR spectra are shown in Figure 57 and Figure 58 (see chapter 5.3.1).

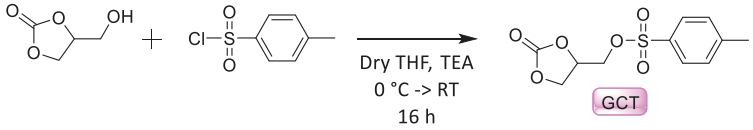

Figure 20: Reaction of glycerol carbonate with tosyl chloride.[113]

The obtained building block Glycerol Carbonate Tosyl chloride (GCT) was then coupled to the solid phase for one hour at RT in the solvent NMP as shown in Figure 21.

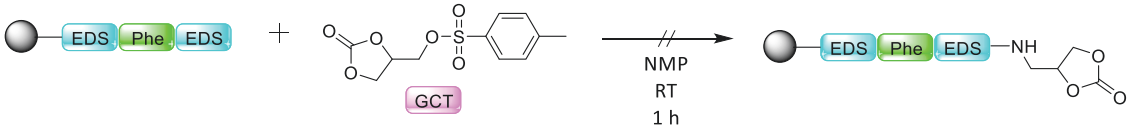

Figure 21: Solid phase coupling from the building block CCT to an EDS-Phe-EDS oligomer.

A single peak was identified in the RP-HPLC spectrum which is shown in Figure 22 with the corresponding HPLC-ESI-MS spectrum. The corresponding mass signal was identified as the oligomer EPE with the Tosyl group attached to the *N*-terminus.

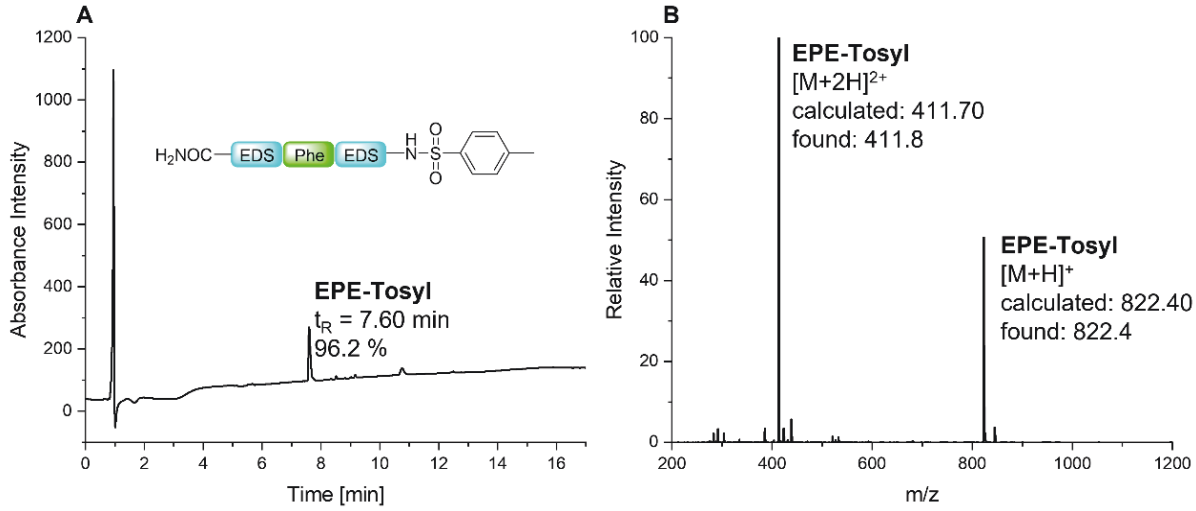

Figure 22: A: RP-HPLC chromatogram (Gradient 5-95 vol.-% - MeCN in H_2O (0.1 vol.-% formic acid, run time 17 min) of EPE-Tosyl. B: HPLC-ESI-MS of EPE-Tosyl at t = 7.60 min (gradient of 5 to 95 vol.-% acetonitrile in water containing 0.1 vol.-% formic acid, run time 17 min).

Apparently, the tosyl group did not leave as the leaving group as planned, but the glycerol carbonate left as the leaving group and the tosyl group coupled to the amine.

Following these results, an attempt was made to replace the GCT building block with an even better leaving group. For this purpose, the building block was first heated with sodium iodide

in acetone under reflux.[114] After purification by column chromatography, the building block Glycerol Carbonate Sodium Iodide (GCI) was isolated with a yield of 83 %. The ^{1}H-NMR and ^{13}C-NMR spectra are shown in Figure 60 and Figure 61 (see chapter 5.3.1).

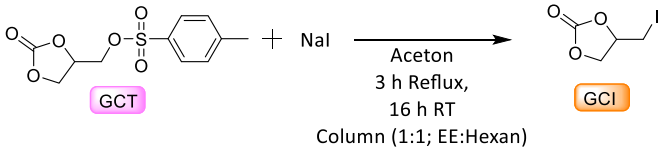

Figure 23: Reaction of the GCT building block with sodium iodide.[114]

The building block was then tested for its applicability as a building block for solid phase synthesis. For these reactions, 1-Fmoc-piperidine-4-carboxylic acid (PCA) was first coupled to the EDS-phenylalanine-EDS oligomer to prevent possible double additions of the building block as observed with the cyclic sulfamidates.[68] The first experiments with the GCI building block were performed in DMF at room temperature for one hour. No product conversion was observed under these conditions.

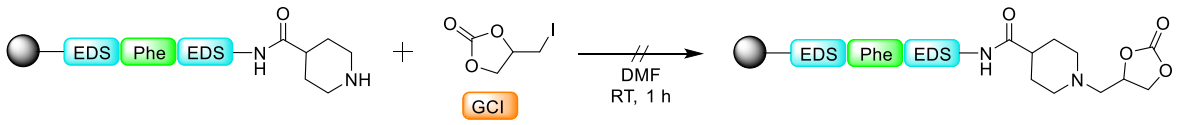

Figure 24: Solid phase coupling of the building block GCI to an EDS-Phe-EDS-PCA oligomer.

Experiments with NMP and DCM as solvents did not lead to any product conversion either. Also, when raising reaction temperatures to 50 °C and prolonging reaction times to five hours no product conversion could be observed.

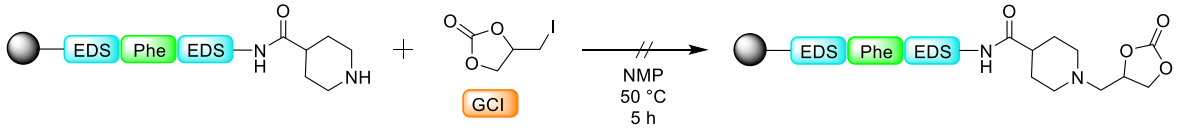

Figure 25: Solid phase coupling of the building block GCI to an EDS-Phe-EDS-PCA oligomer with modified reaction conditions.

The coupling of the building block could only be achieved when potassium carbonate was added as a base for the coupling to promote the iodine to split off as a leaving group. However, with a product conversion of 9.2 %, the result was not in a suitable range, requiring conversions > 90 % for couplings on the solid phase.[115] The RP-HPLC spectrum and the corresponding HPLC-ESI-MS spectrum are shown in the Appendix in Figure 76.

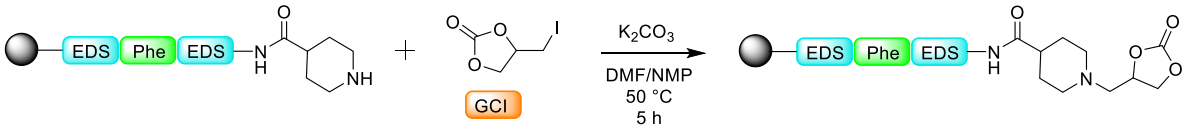

Figure 26: Solid phase coupling of the building block GCI to an EDS-Phe-EDS-PCA oligomer with addition of potassium carbonate.

With the conditions presented here, it was possible to use glycerol carbonate as a building block for solid-phase synthesis, but the conversions were in a range not suitable for solid-phase synthesis. However, cyclic carbonates could still be made accessible as a building block class for solid phase synthesis. Biscyclocarbonate and diamine building blocks could be reacted on the solid phase to oligohydroxyurethanes with higher conversion rates (see chapter 3.2).

3.2.1.3 Conclusion and Outlook

In this chapter, different ways of synthesizing glycerol carbonate-based building blocks and subsequently coupling them to the solid phase were presented. The basic idea was to oxidize the hydroxyl group of the glycerol carbonate to obtain a carboxy functionality that can then be coupled to the solid phase under standard solid phase conditions (PyBOP and DIPEA). Since the direct oxidation attempts were not successful, an attempt was made to first react glycerol carbonate with bromoacetic acid, where the bromide atom was substituted by the alcohol of glycerol carbonate, thus obtaining a terminal carboxy functionality on the building block. The GCBr building block was successfully coupled to the solid phase with a product conversion of 85 %. A ring opening of the cyclic carbonate with hexamethylenediamine, as had already been successfully carried out with the biscyclocarbonates, could not be observed.

Therefore, a further possibility was sought to couple the glycerol carbonate building block to the solid phase. For this purpose, glycerol carbonate was first reacted with tosyl chloride. The building block was synthesized in a yield of 71 %. Subsequently, the cyclic carbonate ring was to be opened by the amine of the oligomeric precursor during solid phase coupling. Instead, the nitrogen atom nucleophilically attacked the sulphur atom of the GCT building block and glycerol carbonate was cleaved off. To create a more attractive leaving group, the GCT building block was reacted with sodium iodide. The resulting GCI building block (83 % yield) was also attempted to couple to the solid phase, but despite optimization attempts, no conversion above 9 % could be achieved.

In order to enable the coupling of a glycerol carbonate-based building blocks to the solid phase, future studies could try to first react glycerol carbonates with a halogen alkane protected with the Fmoc protection group at the nitrogen atom. A possible example of this is shown in Figure 27 with 2-(Fmoc-amino)-ethyl bromide as an example and results in the building block GCEA (Glycerol Carbonate Ethylene Amine). With the results obtained with the biscyclocarbonates, an attempt could be made to couple the cyclic carbonate ring to the solid phase. Subsequently, the Fmoc group could be cleaved off and thus the oligomer could be further built up.

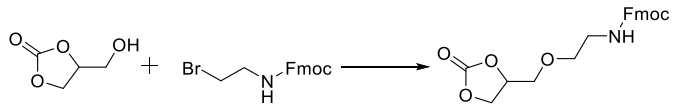

Figure 27: Envisioned reaction of glycerol carbonate with 2-(Fmoc-amino)-ethyl bromide.

The coupling of the building block described above to the solid phase and the further assembly of the oligomer is illustrated in Figure 28.

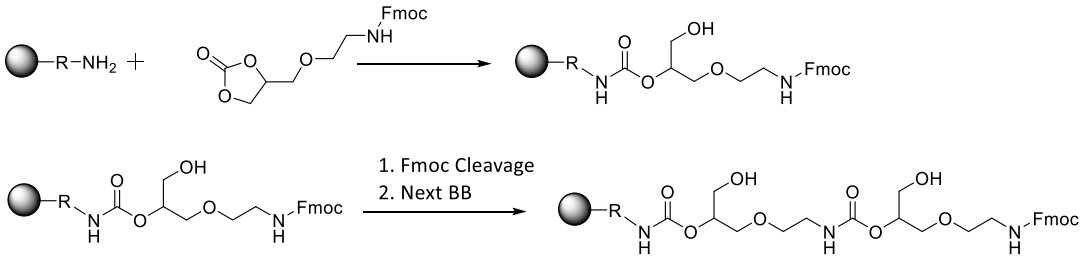

Figure 28: Envisioned coupling of the GCEA building block to the solid phase.

3.3 Exploring cyclic amine building blocks

Cyclic amines are an interesting building block for solid phase synthesis since they form *N*-substituted amide linkages upon ring opening which have different chain interactions in oligomers than the peptides typically formed in solid phase synthesis.[116] In principle, cyclic amines can be used as a ring-shaped building blocks in solid phase synthesis, carrying either a secondary or a tertiary amine. However, this has not been shown before.* The reactivity of the ring opening of cyclic amines depends, among other things, on the ring size, the associated ring tension and the substituent on the nitrogen atom.[117]

In the solid-phase synthesis presented by Merrifield, building blocks are used that have an *N*- and *C*- terminus.[9] When these are coupled to an oligomer, peptides are formed. Hydrogen bonds can form between the oligomer chains located on the solid phase resin, since the nitrogen can act as a proton donor and the oxygen atom as a proton acceptor.[118] As chain length increases, peptides experience greater interchain interactions, which means that the chain ends are not as easily accessible as with small chains, and therefore conversion rates are reduced. Peptides can be found in nature as proteins. More specifically, they are α-peptides because they are substituted in the α-position.[119,120]

Unlike peptides, peptoids have an alkyl chain attached to the nitrogen. Therefore, the nitrogen is no longer able to act as a proton donor and therefore less hydrogen bonds occur between the oligomer chains.[120] The three structures as well as the ability to form interactions between the chains are shown in Figure 29.

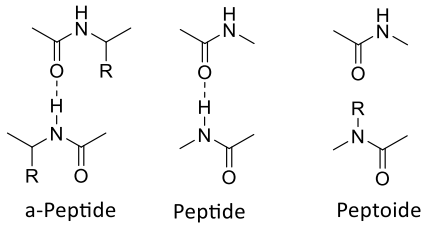

Figure 29: Structures of an α-Peptide, Peptide and a Peptoide.

The different interactions of the chains with each other can also be observed in nature. Peptides tend to form secondary structures due to the intramolecular interactions. The most

* The idea to use cyclic amines in solid phase synthesis was originally proposed by Dr. Stephen Hill and then further developed together with him. All experiments and results presented here were carried out independently.

common secondary structures that can be observed are the α-helix[121] and the ß-sheet[120]. Due to the formations of such secondary structures, peptides often possess conformational rigidity that peptoids do not. The tertiary amines in the peptoids can switch easier between the cis- and trans- forms than the secondary amines in the peptides.[122] The alkyl chains that carry the nitrogen atoms in the peptoids also increase the distance between the chains, further reducing the chain interactions.[123] It follows from these structural properties that the peptoids are more flexible than the peptides.[124]

The reactivity of the ring opening of these building blocks with chloroformates in solution was already explored by different research groups.[125,126] Cho et al.[126] studied the ring opening of cyclic amines of different sizes. Three and four rings (aziridines and azetidines) undergo ring opening when reacted with chloroformates. Rings carrying six or more atoms undergo *N*-dealkylation. Here the cyclic amine ring is not opened, but the previous substituent on the nitrogen is replaced by the ester group of the chloroformate. Five membered rings can undergo both reactions, ring opening and *N*-dealkylation. Which of these two reaction pathways is subverted depends on the *N*-alkyl substituent. The reaction pathways of the different sized cyclic amines are shown in Figure 30.[126]

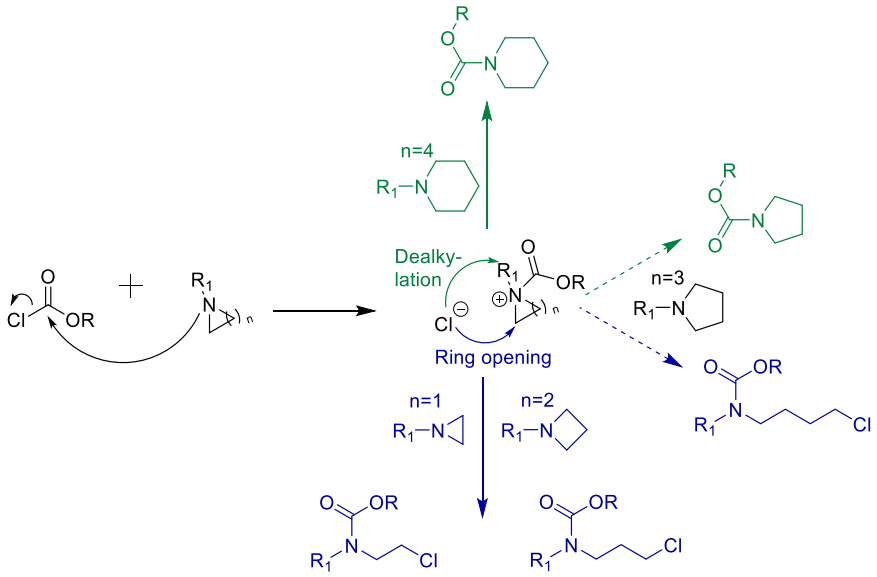

Figure 30: Ring opening or N-dealkylation depending on the size of the cyclic amines ring.[126]

The reason for the different pathways is that the reaction is via an ammonium intermediate with a chloride ion. The substituent on the nitrogen atom therefore has an influence on this transition state. Sterically non-demanding substituents such as a methyl or ethyl radical caused the pyrrolidine rings to pass mainly through the ring opening pathway. Substituents

carrying sterically demanding groups such as a benzyl group resulted in a product mixture in which, however, mainly the *N*-dealkylated product was present.[126] In addition, the influence of the solvent on the reaction was investigated and it was noticed that only acetonitrile had a negative influence on the reaction yield and the other solvents tested had only a minor influence on the yield.[126] In this work, the ring opening of the cyclic amines was to be exploited and substituents at the nitrogen atom were selected which are not sterically demanding to ensure that the cyclic amines are ring-opened and no *N*-dealkylation occurs.

In their experiments, Endo et al. showed that four membered rings undergo faster ring opening than five membered rings.[105] The ring opening experiments was carried out with chloroformates as shown in Figure 31.[125]

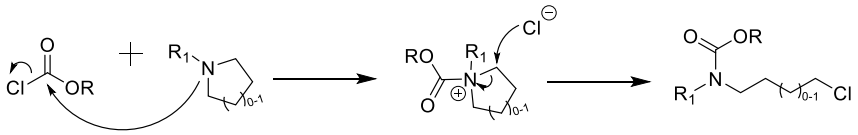

Figure 31: Scheme of the ring opening of a cyclic amine by a chloroformate.[125]

The nitrogen atom of the cyclic amine nucleophilically attacks the carbon atom of the chloroformate. This causes the chloride atom to split off. In the next step, the split off chloride attacks the ring which is then opened. The mechanism is the same for four and five rings.

The work of Cho et al.[126] and Evano et al.[125] have shown that the chloroformates selectively open the ring and no by-products are formed in the process, where the ring is still closed when low sterically demanding alkyl chains were used as nitrogen substituents. Furthermore, the ring opening proceeds under mild reaction conditions, with high yields and without the addition of further additives, which are important criteria for solid phase synthesis.

In this work, different cyclic amine building blocks were synthesized. They were prepared from various compounds of azetidine and pyrrolidine with bromoacetic acid and brompropionic acid. Azetidine is a four- and pyrrolidine a five-membered ring with a nitrogen atom in the heterocycle. The building blocks were coupled to the solid phase with their carboxy functionality and then the cyclic amine rings were ring-opened with different chloroformates and acid chlorides.

3.3.1 Synthesis of the cyclic amine building blocks

In the present work, four building blocks were prepared two based on azetidine and two based on pyrrolidine. The four building blocks are shown in Figure 32.

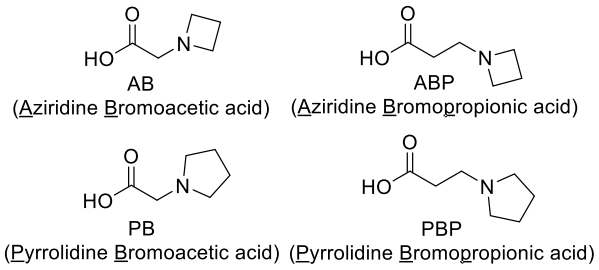

Figure 32: Synthesized cyclic amine building blocks.

The Aziridine Bromoacetic acid (AB) building block is formed by the reaction of bromoacetic acid with azetidine and the base sodium hydroxide in water at 72 hours reaction time.[127] The Aziridine Bromopropionic acid (ABP) building block is prepared in the same way but is reacted with bromopropionic acid instead of bromoacetic acid. Similarly, two building blocks were also prepared with pyrrolidine. The Pyrrolidine Bromoacetic acid (PB) building block is prepared by reacting pyrrolidine with bromoacetic acid and the Pyrrolidine Bromopropionic acid (PBP) building block is prepared correspondingly with bromopropionic acid. The schematic synthesis of the building blocks is shown in Figure 33.

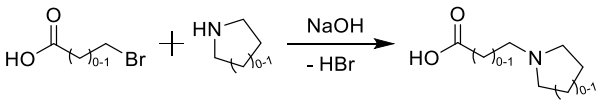

Figure 33: Scheme for the synthesis of cyclic amine building blocks.[127]

A ratio of 1:1 equivalents of bromoacetic acid and pyrrolidine was initially used for the synthesis of the building blocks. NMR evaluation of the building blocks indicated that the bromoacetic acid did not react to full conversion. Since remaining bromoacetic acid would cause amine groups of the oligomer to react with the acid functionality of the bromoacetic acid and thus not be available for sequential assembly, the equivalents were adjusted to a ratio of 1:1.5 bromoacetic acid: pyrrolidine. This ensured that the bromoacetic acid fully reacted. Remaining pyrrolidine residues can be neglected in small amounts, since they are washed out when the syringe is washed and do not undergo side reactions with the oligomer. The ^{1}H NMR spectra of the building blocks are shown in Figure 34 to Figure 37 (for ^{13}C-NMR spectra, see Appendix Figure 70 to Figure 73).

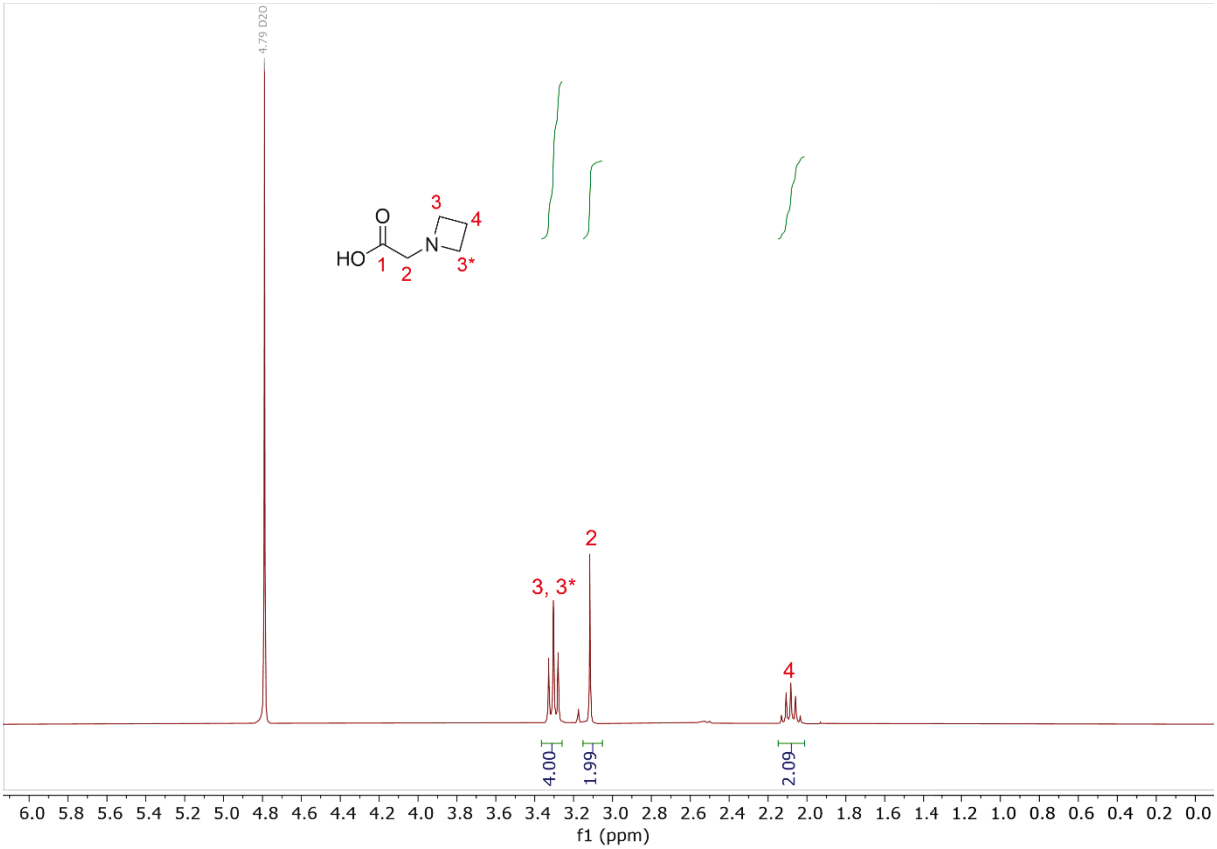

Figure 34: 300 MHz ^{1}H-NMR measured at RT of the AB building block in D_2O and the integration analysis indicating the proton count. The individual protons are assigned by number.[128]

For the AB building block, the triplet at 3.30 ppm was referenced which could be assigned to the chemically equivalent 3 and 3* position with 4 protons in the building block. The peaks of the protons in this and the following spectra are shifted downfield, due to the electron pulling effect of the nitrogen atom. The spectrum has a total of 8 protons which corresponds to the sum of the protons of the AB building block. The singlet at 3.12 ppm was assigned to position 2 with an integral of 2 and the remaining quintet to position 4 with an integral of 2 protons and a shift of 2.08 ppm. The corresponding ^{13}C-NMR spectrum is shown in the Appendix on Figure 70 with the corresponding assignments of the peaks.

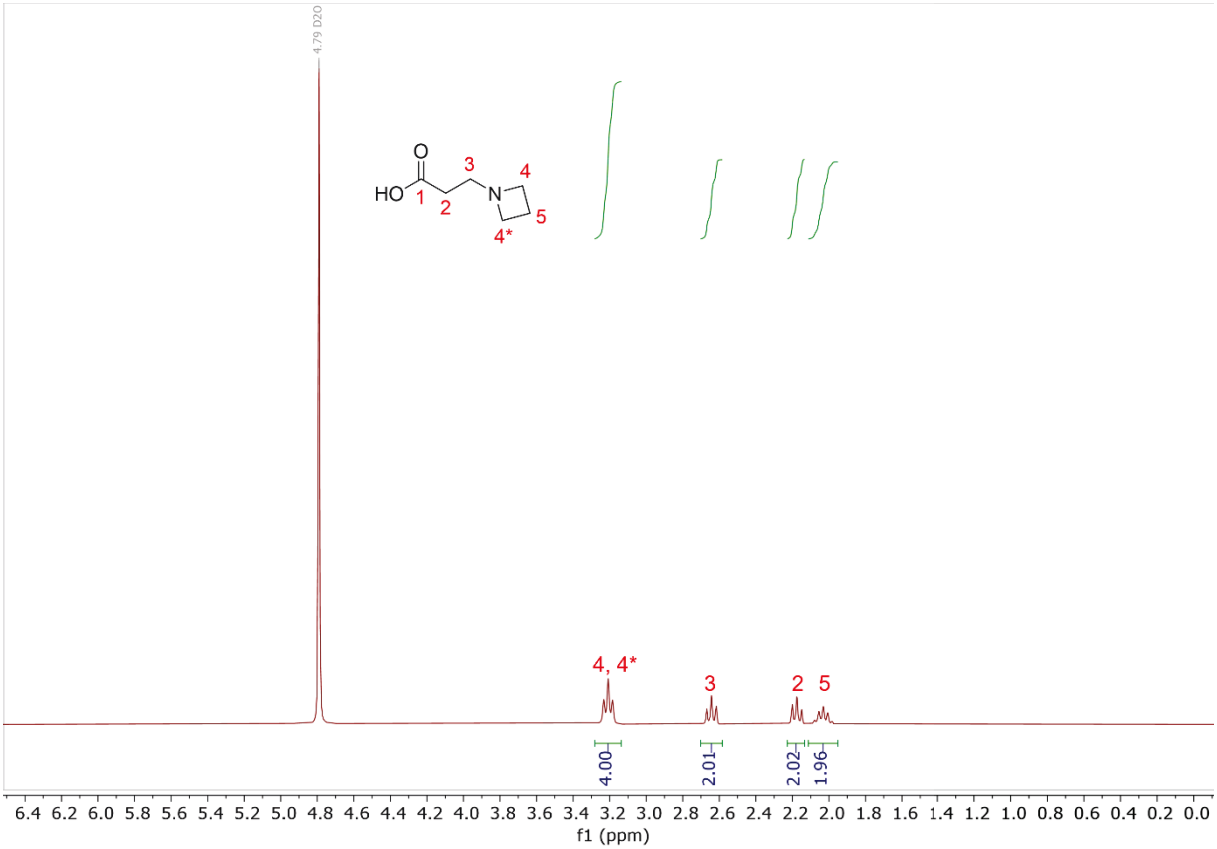

Figure 35: 300 MHz ^{1}H-NMR measured at RT of the ABP building block in D_2O and the integration analysis indicating the proton count. The individual protons are assigned by number.[128]

For the ABP building block, the triplet at 3.21 ppm was referenced which was assigned to the chemically equivalent 4 and 4* position with 4 protons in the building block. The spectrum shows a total of 10 protons which corresponds to the sum of the protons of the ABP building block. The triplet at 2.64 ppm was assigned to position 3 with an integral of 2. The triplet at 2.18 ppm and an integral of 2 protons was assigned to position 2. The remaining quintet with an integral of 2 protons and a shift of 2.03 ppm was assigned to position 5. The corresponding ^{13}C-NMR spectrum is shown in the Appendix on Figure 71 with the corresponding assignments of the peaks.

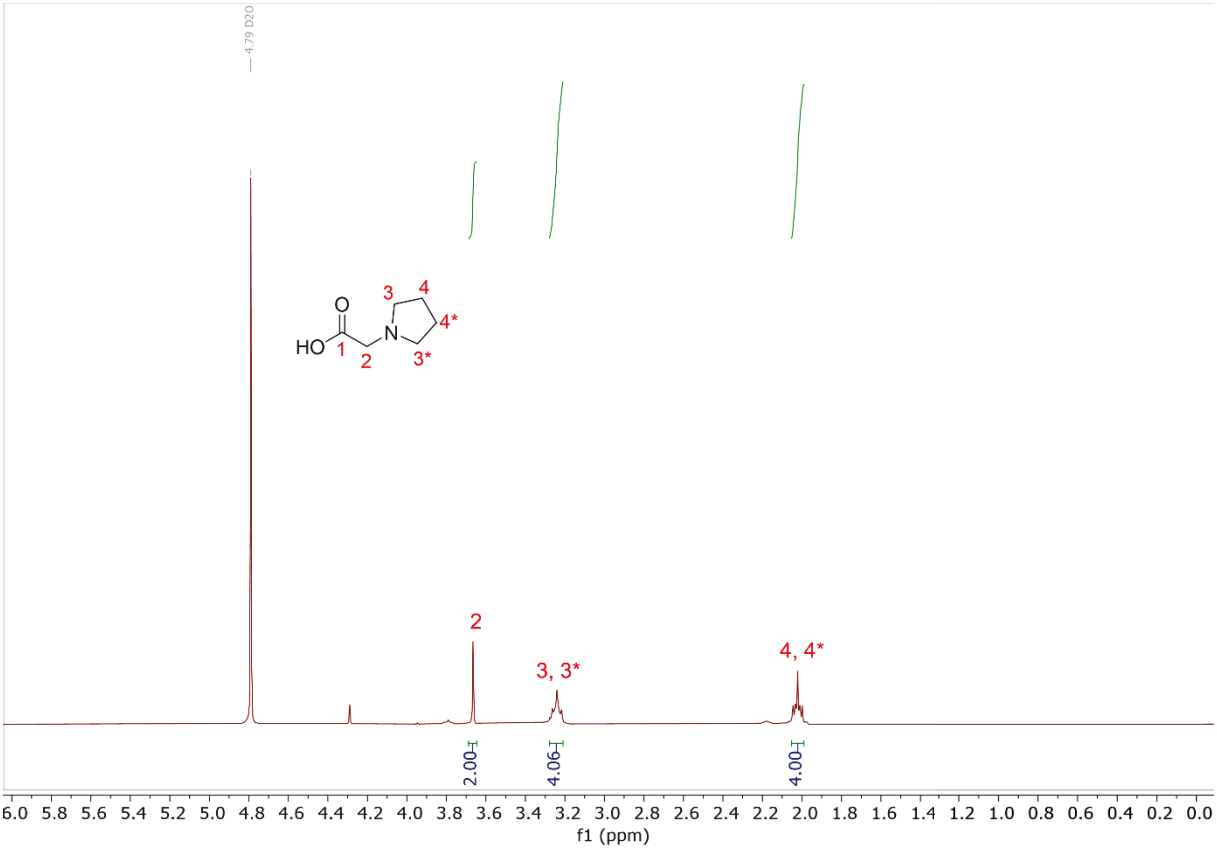

Figure 36: 300 MHz ^{1}H-NMR measured at RT of the PB building block in D_2O and the integration analysis indicating the proton count. The individual protons are assigned by number.

For the PB building block, the singlet at 3.67 ppm was referenced, which was assigned to position 2 with 2 protons. The spectrum has a total of 10 protons which corresponds to the sum of the protons of the PB building block. The multiplet from 3.28 - 3.21 ppm was assigned to the chemically equivalent 3 and 3* position with 4 protons. The remaining multiplet of 2.05 - 1.99 ppm are the 4 protons of the 4 and 4* position. The corresponding ^{13}C-NMR spectrum is shown in the Appendix on Figure 72 with the corresponding assignments of the peaks.

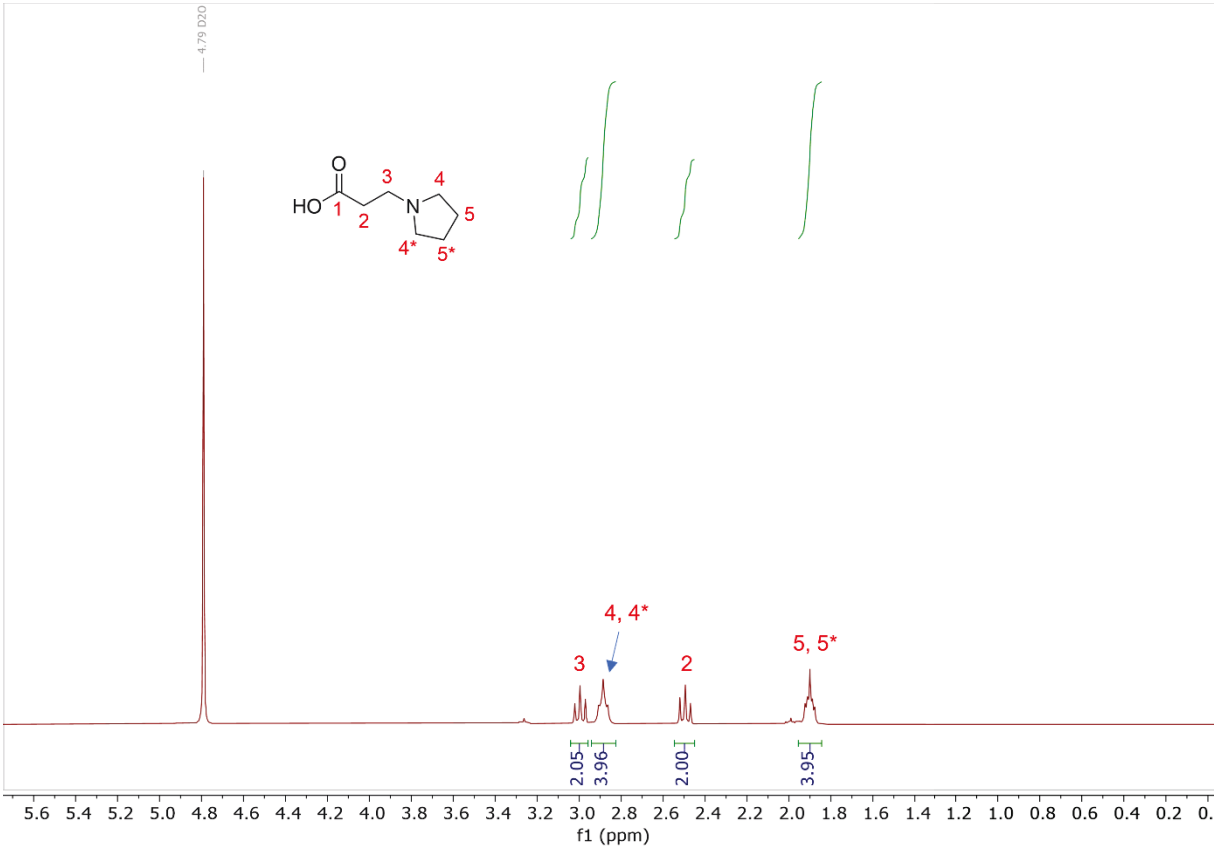

Figure 37: 300 MHz ^{1}H-NMR measured at RT of the PBP building block in D_2O and the integration analysis indicating the proton count. The individual protons are assigned by number.

For the PBP building block, the triplet at 2.49 ppm was referenced, which could be assigned to position 2 with 2 Protons. The spectrum has a total of 12 protons which corresponds to the sum of the protons of the PBP building block. The triplet at 2.99 ppm can be assigned to position 3 with 2 protons. The chemically equivalent position at 4 and 4* with 4 protons could be assigned to the triplet at a shift of 2.88 ppm. The remaining quintet with an integral of 4 protons and a shift of 1.91 ppm was assigned to position 5 and 5*. The corresponding ^{13}C-NMR spectrum is shown in the Appendix on Figure 73 with the corresponding assignments of the peaks.

In conclusion, all building blocks were isolated in high purities. When determining the yields of the four building blocks, it was noted that the yields were above 100 %. This can be explained because during the reaction, a salt with sodium hydroxide is formed. The salt can be used without further workup because the carboxy functionality of the building block is activated in the solid phase synthesis using the coupling reagents PyBOP and DIPEA. Even if salt formation is considered in the yield analysis, the yields are still above 100 %. The reason for this is that the building blocks were not completely dried. The protons of the water cannot

be identified in the NMR spectrum because the sample was measured in deuterium oxide (D_2O) and thus the proton peaks from the water are in the reference peak.

The different building blocks were prepared to verify whether the results of Cho et al.[126] regarding the higher reactivity of the four membered rings (AB, ABP) in comparison to the five membered rings (PB, PBP) can be transferred to solid phase synthesis. The alkane chain of different length was chosen to investigate whether the larger distance between the carboxy functionality and the ring changes the reactivity and coupling efficiency when coupled to the solid phase.

3.3.2 Coupling of the cyclic amine building blocks to the solid phase

The scheme for coupling and ring opening of the cyclic amine building blocks on solid phase is shown in Figure 38.

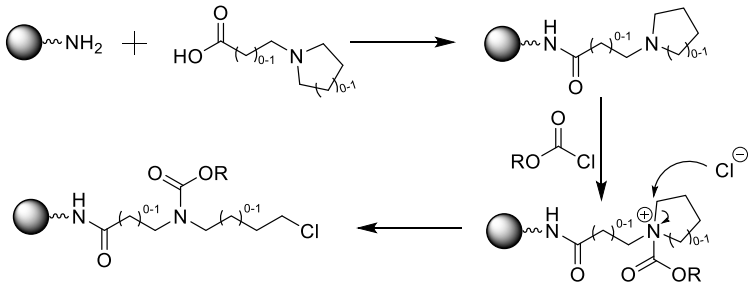

Figure 38: Coupling and ring opening of the cyclic amine building blocks on solid phase.

First, the cyclic amine building block is coupled to the oligomer under standard solid-phase conditions using the coupling reagents PyBOP and DIPEA (see chapter 5.3.2). Then the oligomer is reacted with a chloroformate. Here, the tertiary amine nucleophilically attacks the carbon atom of the chloroformate. This then cleaves off a chloride ion. In the following step, the cleaved chloride ion attacks the carbon atom next to the amine and opens the ring, thus opening the ring and forming a peptoid. The mechanism is the same for four- and five-membered rings.

All four building blocks were coupled to the solid phase, and TentaGel® S RAM resin was chosen as the resin for this purpose, as it has been widely used for the synthesis of sequence-defined oligomers.[13,68,129,130] Here, protected amino groups form the functional end groups of the resin surface, are linked by a rink amide linker.[13,68,129,130]

Oligomer EDS_3 was used as the starting sequence. EDS is a hydrophilic building block that is used in the Hartmann group in solid phase synthesis.[11] EDS was used to extend the distance to the solid phase resin as well as to be able to more precisely assign the molecular mass in the mass spectrum.

When polystyrene resins are used, as is often the case in the Hartmann working group, the solvent DMF is often chosen due to its good swelling properties.[14,68,131] However, the synthesized building blocks do not dissolve in DMF. Therefore, an alternative solvent was sought. For this purpose, solubility tests were carried out with different solvents and different ratios thereof, which are shown in Table 1.

Table 2: Solubility test of cyclic amine building blocks and PyBOP.

	DMF	NMP	Water	Hexane	Methanol	1,4-Dioxane
Cyclic amine building blocks	x	x	✓	x	✓	✓
PyBOP	✓	✓	x	x	x	x

The building blocks as well as PyBOP should be well soluble in the solvent mixture. As shown in the table, a single solvent is not sufficient to dissolve both solids. Therefore, solvent mixtures were sought in order to dissolve both solids. The mixture of 2:1:1 vol.-% DMF:dioxane:water was identified as the most suitable solvent. During the subsequent coupling experiments, it was observed that it was crucial that the building blocks were completely dissolved before being drawn into the syringe. Best results were achieved when PyBOP was pre-dissolved in 1 mL DMF and then mixed with the solvent mixture.

First, an attempt was made to couple the PB building block to the oligomer EDS_3. The coupling of the building block proceeds with high conversions (95 %). Figure 39 shows the HPLC-ESI-MS spectrum recorded for the sample in the RP-HPLC run at t= 0.94 min (see Appendix Figure 81 for the full RP-HPLC spectrum).

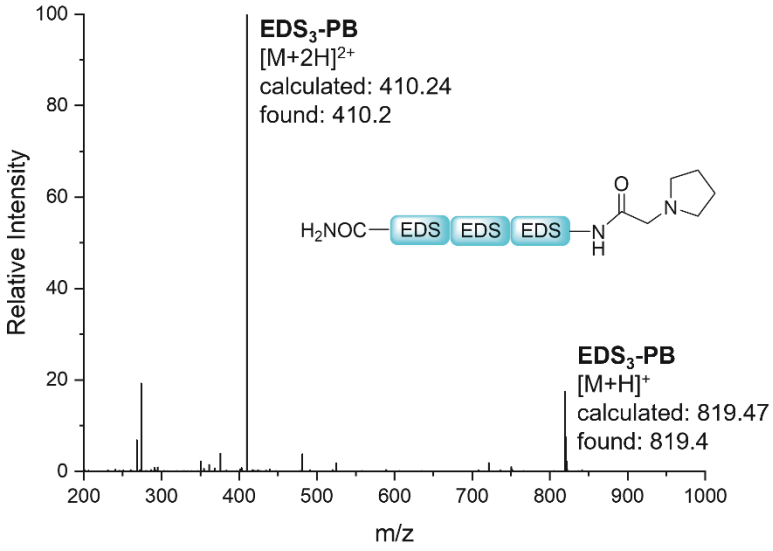

Figure 39: HPLC-ESI-MS of EDS_3-PB at t = 0.94 min (gradient of 5 to 95 vol.-% acetonitrile in water containing 0.1 vol.-% formic acid, run time 17 min) which corresponds to the RP-HPLC spectrum in Figure 81 in the appendix.

After the successful coupling of the PB building block, an attempt was also made to couple the PBP building block to the solid phase. Figure 40 shows the HPLC-ESI-MS spectrum recorded

for the sample in the RP-HPLC run at t= 1.00 min (see Appendix Figure 82 for the full RP-HPLC spectrum).

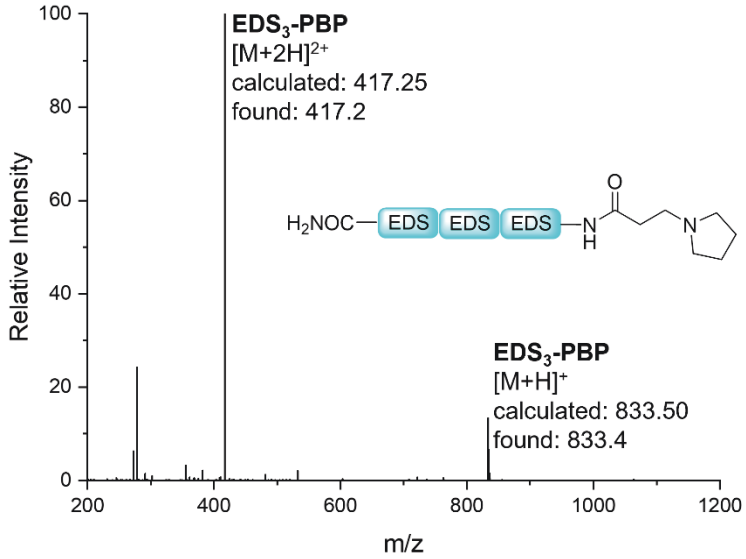

Figure 40: HPLC-ESI-MS of EDS$_3$-PBP at t = 1.00 min (gradient of 5 to 95 vol.-% acetonitrile in water containing 0.1 vol.-% formic acid, run time 30 min) which corresponds to the RP-HPLC spectrum in Figure 82 in the appendix.

As can be seen in Figure 82, the coupling of the PBP building block has also been successful with a product conversion of 93 %.

After the two pyrrolidine building blocks were successfully coupled to the solid phase, the AB and the ABP building blocks were also coupled to the solid phase. This work was carried out by Nathalie Bolten during her bachelor thesis under my supervision.[128] The product conversion for the AB building block was only 17.6 % and that of the ABP building block 6.8 %. The RP-HPLC chromatograms of these experiments are shown in the Appendix in Figure 77 and Figure 79. Since the conversions in these experiments were significantly lower than those of the pyrrolidine building blocks, the PB and PBP building blocks were used in the further experiments.

3.3.3 Ring opening of the cyclic amine building blocks on the solid phase

After coupling the cyclic amines to the solid phase, the terminal cyclic amine ring should be ring opened. Various experiments were carried out for this purpose. Fmoc-Cl, benzyl chloroformate (Cbz-Cl), acetylchlroid, allyloxy carbonyl chloride (Alloc-Cl) and acryloyl chloride were used for ring opening experiments.

The above-mentioned substances can be roughly divided into two groups. Fmoc-Cl, Cbz-Cl and Alloc-Cl are classified as chloroformates in which the chloride atom is bound to an ester. The other group is the acid chlorides, which include acetyl chloride and acryloyl chlorides. The structures of the compounds are shown in Figure 41.

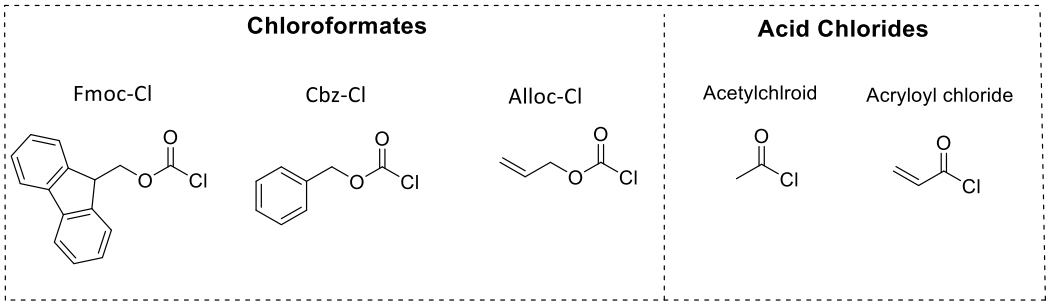

Figure 41: Structures of Chloroformates and Acid Chlorides used for the ring opening experiments.

In the first experiments, the chloroformate Fmoc-Cl was used to open the PB building block ring. The RP-HPLC chromatogram and the corresponding HPLC-ESI-MS of the coupling of Fmoc-Cl to the oligomer EDS_3-PB is shown in Figure 42. No additional coupling reagents were used for this reaction.

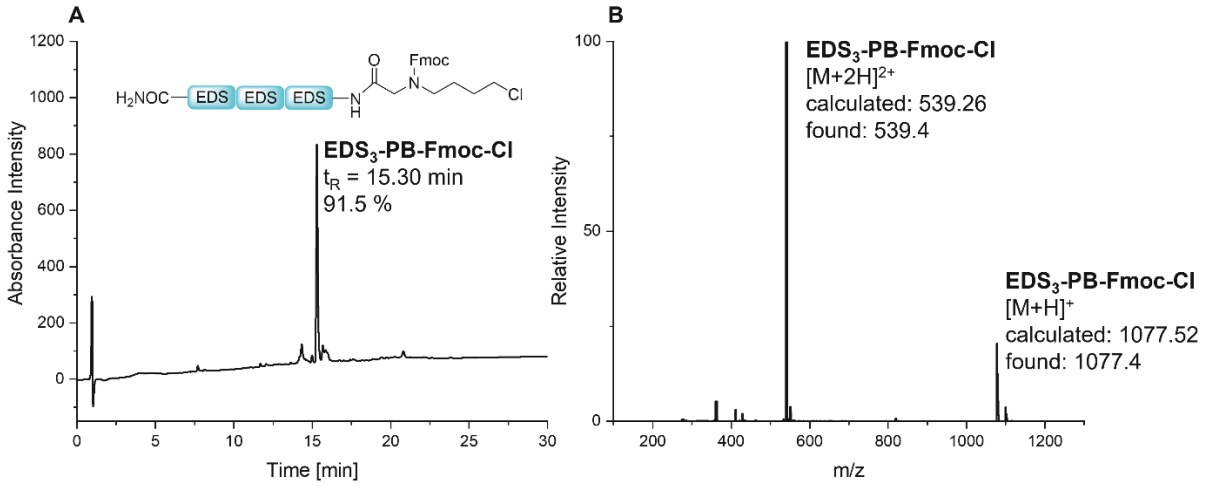

Figure 42: A: RP-HPLC chromatogram (Gradient 5-95 vol.-% - MeCN in H_2O (0.1 vol.-% formic acid, run time 30 min) of EDS_3-PB-Fmoc-Cl. B: HPLC-ESI-MS of EDS_3-PB-Fmoc-Cl at t = 15.30 min (gradient of 5 to 95 vol.-% acetonitrile in water containing 0.1 vol.-% formic acid, run time 30 min).

The ring opening by Fmoc-Cl was successful with a product conversion of 92 %. In this reaction, a double coupling was already carried out to increase the conversion. To further increase the conversion, the reaction time of 2 h could be further increased and a triple coupling could be considered in the future. In the following, the other chloroformates and acid chlorides were investigated for their ability to open the cyclic amine ring.

No product conversion was observed when ring opening was performed with the acid chloride acetyl chloride. Also, when varying the solvent from DMF to DCM or NMP, no product conversion was observed. This is likely because the PB building block was not very soluble in these solvents. No reaction was also observed when adding bases such as DIPEA or TEA. The reason that no product conversion occurs with acetyl chloride is probably because the nucleophilic attack of the amine from the cyclic amine building block on an acetyl chloride is slower than on a chloroformate, since the absence of the oxygen atom next to the carbonyl carbon atom makes it much less polarized than in the chloroformates and therefore a nucleophilic attack is energetically less favoured.

The reactions with allyloxy carbonyl chloride and acryloyl chloride were strongly exothermic. The reactions were carried out in a syringe reactor. After a few seconds, the plunger of the syringe expanded strongly. The explanation for this is the formation of HCl gas during the reaction. After a few minutes, the plunger detached from the syringe and the gas escaped from the syringe. In the first experiments, the plunger was deliberately removed from the syringe to prevent the plunger from falling out. Despite long reaction times, only a product

conversion of 7.1 % was observed via RP-HPLC. The explanation for the low conversion is that the chloride atom is needed for the ring opening of the cyclic amine. However, when the chloride leaves the syringe as a gas, it is no longer available for ring opening and the reaction cannot proceed.

In further experiments, attempts were made to partially vent the gas during the reaction by briefly removing the plunger when too much pressure was applied to the syringe. These experiments showed better product conversions as more chloride atoms were available for the reaction. This increased the conversion to 34 %. The RP-HPLC chromatogram with the corresponding HPLC-ESI-MS for this reaction is shown in Figure 43.

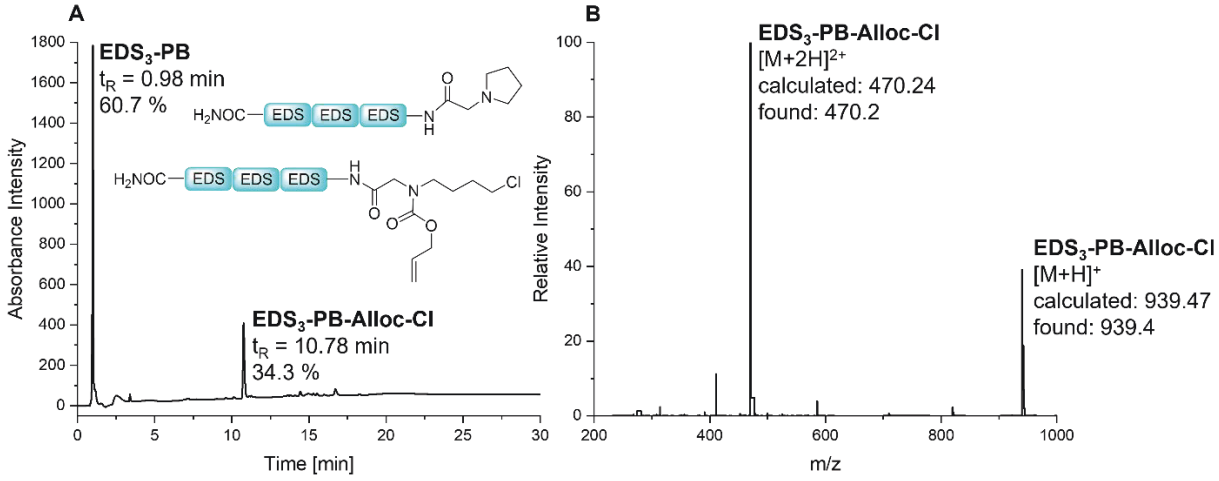

Figure 43: A: RP-HPLC chromatogram (Gradient 5-95 vol.-% - MeCN in H_2O (0.1 vol.-% formic acid, run time 30 min) of EDS_3-PB-Alloc-Cl. B: HPLC-ESI-MS of EDS_3-PB-Alloc-Cl at t = 10.8 min (gradient of 5 to 95 vol.-% acetonitrile in water containing 0.1 vol.-% formic acid, run time 30 min).

However, the conversions with the Alloc-Cl remained behind those with Fmoc-Cl, so they were not included in the further experiments.

3.3.4 Further build-up of the oligomer after ring opening

Highest conversions of 92 % were obtained with the chloroformate Fmoc-Cl. Therefore, this was used in the following experiments. The original idea of the project was, after the successful coupling of the cyclic amine building block and the subsequent ring opening by Fmoc-Cl, to cleave off the protecting group at the nitrogen atom and to couple another building block to the amine, or to substitute in a nucleophilic attack the terminal chloride atom and to further build up the oligomer chain in this direction. The two possibilities are shown in Figure 44.

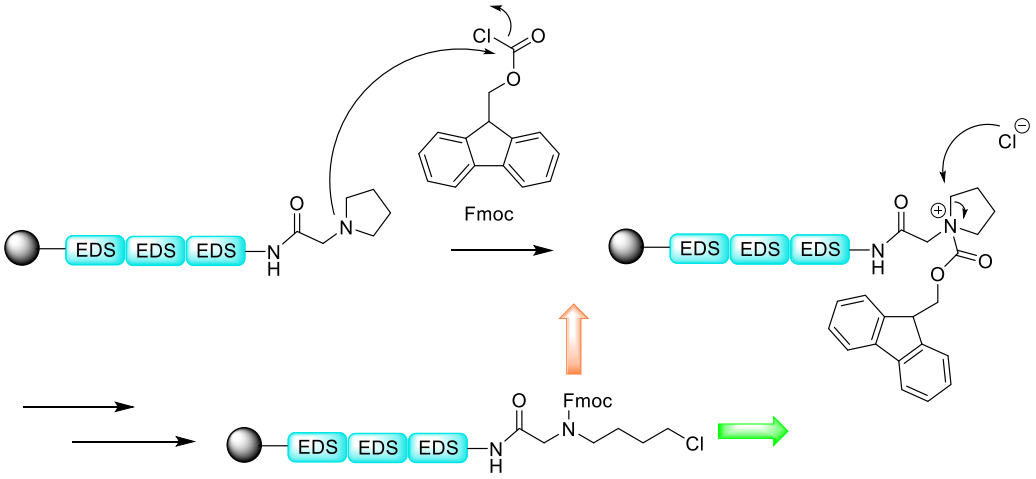

Figure 44: Scheme of the coupling of Fmoc-Cl to the oligomer EDS_3-PB and the subsequent possibilities of further construction of the oligomer.

First, an attempt was made to cleave the Fmoc protecting group with a piperidine in DMF solution (25 vol.-%) (orange arrow). Then, under standard solid phase conditions (PyBOP and DIPEA), an EDS or another PB building block could be coupled to the oligomer as shown in Figure 45.

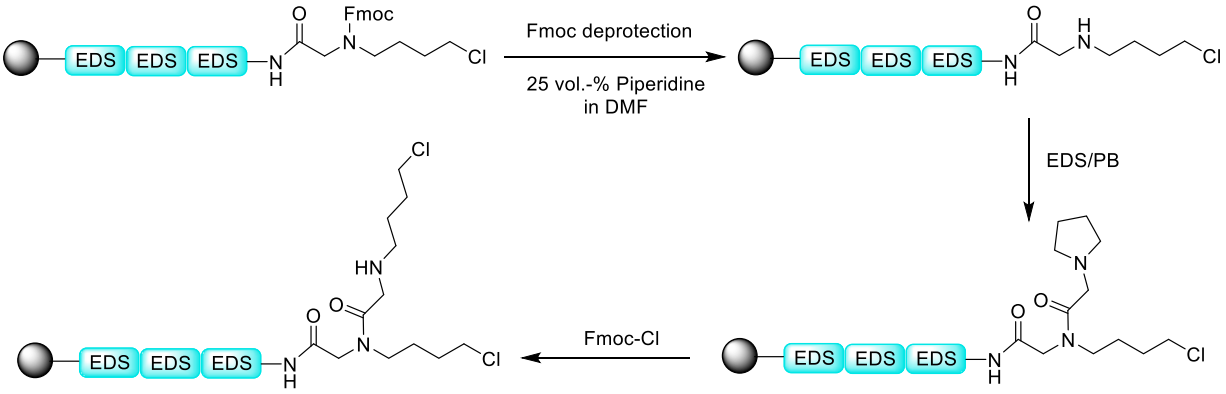

Figure 45: Schema of the envisioned oligomer construction. Fmoc cleavage followed by coupling of an EDS or PB building block and subsequent ring opening using Fmoc-Cl.

The result of this reaction was that only the mass of the oligomer EDS_3-PB was observed in the RP-HPLC spectra. The spectrum in Figure 83 (see Appendix) shows high similarity to the spectrum in Figure 81 (see Appendix), where only the cyclic amine building block had coupled to the solid phase. This can potentially be explained as follows: when the Fmoc protecting group is cleaved off, the now unprotected amine undergoes intramolecular ring closure. Such intramolecular ring closure is shown in Figure 46.

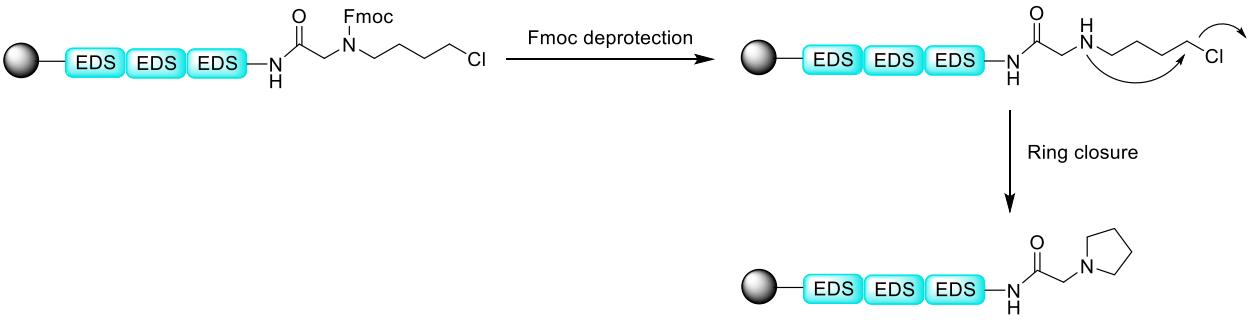

Figure 46: Intramolecular ring closure after Fmoc deprotection.

Figure 47 shows the HPLC-ESI-MS spectrum recorded for the sample in the RP-HPLC run at t = 0.96 min (see Appendix Figure 83 for the full RP-HPLC spectrum).

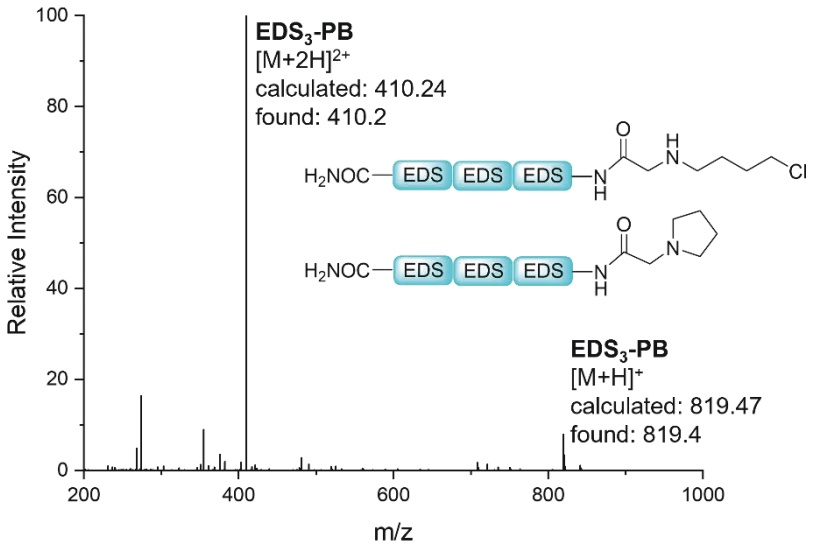

Figure 47: HPLC-ESI-MS of the oligomer EDS_3-PB-Fmoc-Cl after deprotection at t = 0.96 min (gradient of 5 to 95 vol.-% acetonitrile in water containing 0.1 vol.-% formic acid, run time 17 min) which corresponds to the RP-HPLC spectrum in Figure 83 in the appendix.

As can be seen from Figure 47, the desired product was not observed and only the oligomer EDS_3-PB was present after cleavage.

After the attempt to cleave off the Fmoc protecting group and to couple further building blocks to the free amine did not work (orange arrow in Figure 44), the other possibility of further building up the oligomer was taken (green arrow in Figure 44). After the cyclic amine building block was added to the solid phase and ring opened, the chloride was to be substituted. Subsequently, the added chloroformate should be cleaved from the oligomer and another building block should be coupled. The scheme for this reaction is shown in Figure 48.

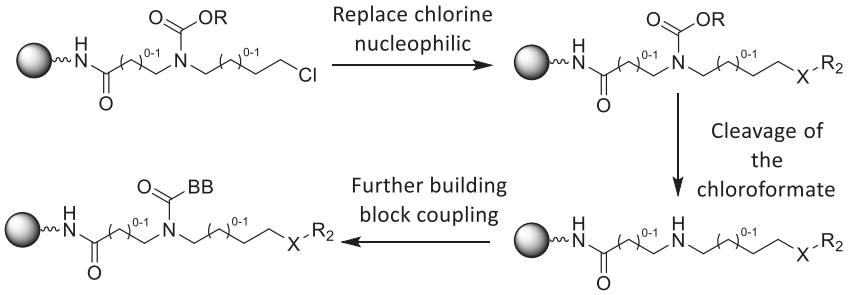

Figure 48: Scheme for nucleophilic chloride substitution with subsequent cleavage of the chloroformate and further building block coupling.

The three substances used for nucleophilic substitution are shown in Figure 49.

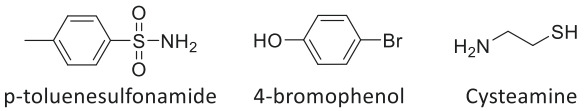

Figure 49: Structures of p-toluenesulfonamide, 4-bromphenol and Cysteamine.

The first experiment for the nucleophilic substitution of the chloride was performed with p-toluenesulfonamide. It has the advantage that it is stable at the basic conditions under which the Fmoc protecting group is cleaved off and therefore no intramolecular ring closure can occur as shown in Figure 46. The reaction with the p-toluenesulfonamide was carried out following the experiments of Deng et al.[132] They had performed the reaction in solution with $FeCl_2$ and K_2CO_3. Here an attempt was made to transfer their results to solid phase synthesis. Under the conditions given, no reaction with the terminal chloride was observed. The reason for that is probably that the reaction from Deng et al. was carried out at 135 °C. However, temperatures higher than 60 °C cannot be used on the solid phase, otherwise the oligomer would detach from the solid support.[133]

Another attempt was to try to etherify the chloride with 4-bromophenol following the experiments of Nishimura et al.[134] Here, the oligomer EDS_3-PB-Fmoc-Cl was reacted with 4-bromophenol and sodium hydride, each in an excess of 2 equivalents. In these attempts, as in the previous attempts to deprotect the Fmoc protecting group, it was assumed that Fmoc-Cl was cleaved off and intramolecular ring closure likely occurred again.

The last attempt to substitute the chloride was to react it with a thiol. Again, most likely an intramolecular ring closure occurred. The free amines of both p-toluenesulfonamide and cysteamine thiol are likely sufficiently basic to deprotect the Fmoc group and thus ring closure occurs as shown in Figure 46.

Since the Fmoc protecting group appears to be unsuitable for further oligomer synthesis, initial experiments were carried out with a different protecting group. The Cbz protecting group was used for this purpose, since it can be cleaved under acidic conditions and should therefore remain stable during the subsequent substitution of the chloride. For these experiments, a different oligomer was used than in the previous experiments. It consists of four building blocks: Glycine, EDS, Phenylalanine and EDS (GEPE). This oligomer was chosen because in the previous attempts the oligomers were often running in the Injection peak of the RP-HPLC chromatogram. The oligomer GEPE which has already been used in experiments with the cyclic carbonates has proven to be advantageous for the analysis of building block oligomer couplings.[106]

Figure 50 shows the HPLC-ESI-MS spectrum recorded for the ring opening of the oligomer GEPE-PB with Cbz-Cl in the RP-HPLC run at t = 14.19 min (see Appendix Figure 84 for the full RP-HPLC spectrum).

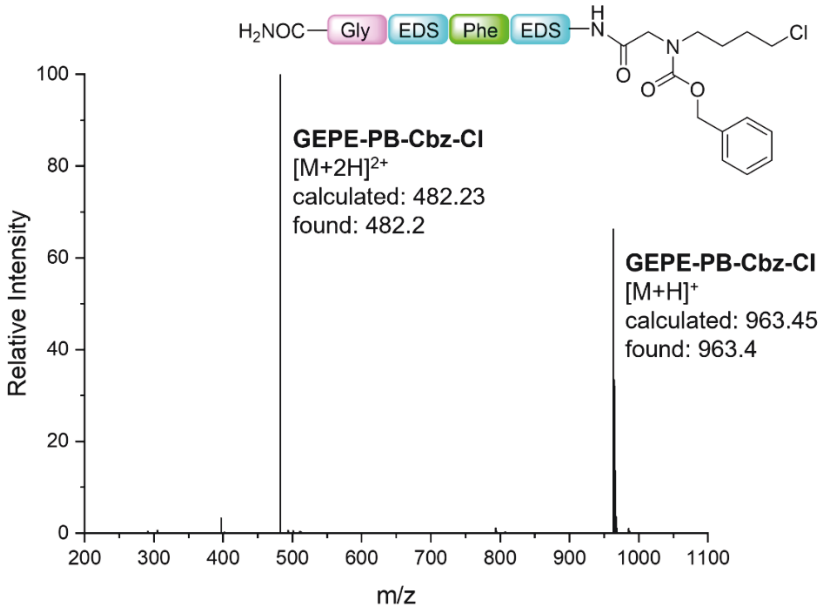

Figure 50: HPLC-ESI-MS of GEPE-PB-Cbz-Cl at t = 14.19 min (gradient of 5 to 95 vol.-% acetonitrile in water containing 0.1 vol.-% formic acid, run time 30 min) which corresponds to the RP-HPLC spectrum in Figure 84 in the appendix.

As can be seen in Figure 84, the product conversion when reacting the oligomer GEPE-PB with Cbz-Cl is only 26 %. This result is already a double coupling with a reaction time of three hours each, which suggests that the ring opening of the cyclic amine with Cbz-Cl is not as efficient as with Fmoc-Cl.

Similar to the experiments with the allyloxy carbonyl chloride and acryloyl chloride, a lot of pressure was generated in the syringe during the reaction with the Cbz-Cl and the syringe had to be ventilated frequently, which leads to a loss of chloride atoms, which reduces the conversion. In future experiments ways to prevent this could be explored. One possibility is to choose a larger syringe, where there is more volume in the syringe and therefore more gas can be produced before the plunger has to be vented. In these experiments, a 10 mL syringe was used. One could therefore use a 25 mL syringe and observe whether this can prevent the stamp from falling out and thus achieve better conversions.

3.3.5 Conclusion and Outlook

In this chapter, it is described how the four cyclic amine building blocks AB, ABP, PB and PBP were synthesized and then successfully coupled to the solid phase. The AB and ABP building block are based on azetidine and the PB and PBP building block are based on pyrrolidine. The ABP and PBP building block have a longer alkyl chain than the AB and PB building block. The PB and PBP building blocks coupled with high conversions (95 % and 94 %) and therefore are well suited for coupling to an oligomer on solid phase. The AB and ABP building blocks had only low coupling conversions and were not used in further experiments.

Subsequently, it was shown how different chloroformates and acid chlorides were used to open the cyclic amine rings on the solid phase. In these experiments it was observed that the three chloroformates Fmoc-Cl, Cbz-Cl and Alloc-Cl are able to open the cyclic amine ring. Fmoc-Cl showed the highest conversion of 92 %. Cbz-Cl and Alloc-Cl were not in a range suitable for solid phase coupling with conversions of 26 and 34 %, respectively. The two acid chlorides acetyl chloride and acryloyl chlorides were not able to open the ring, which can probably be explained by the fact that the carbonyl carbon of the acid chloride is not as attractive for a nucleophilic attack of the nitrogen of the cyclic amine as in the case of the chloroformates.

Subsequently, attempts were made to further build up the oligomer in which the cyclic amine ring was already opened by Fmoc-Cl. For this purpose, the Fmoc protecting group was cleaved off with the aim of coupling further building blocks to the free amine. It is assumed that the free amine undergoes intramolecular ring closure and is therefore no longer available for further oligomer assembly. An attempt was made to substitute the terminal chloride before the protective group was cleaved off. Experiments were carried out with p-toluenesulfonamide, 4-bromophenol and cysteamine. The basic conditions or the free amines of the components were sufficient to unintentionally cleave the protective group, which again led to an intramolecular ring closure.

In summary, the successful coupling of the cyclic amine building blocks and their ring opening on the solid phase has provided a possibility to incorporate peptoids into oligomers on the solid phase. The further assembly of these structures can be the target of future studies. Different approaches can be taken. Either the coupling efficiency of the ring opening can be

improved with the Cbz protecting group and then the terminal chloride can be substituted. Alternatively, another chloroformate can be sought that opens the cyclic amine ring with similarly high conversions as Fmoc-Cl but remains stable under basic conditions (e.g., phenyl chloroformate, isopropyl chloroformate or S-ethyl chlorothiolformate). In addition, a way of etherification of the chloride could be developed that does not proceed under basic conditions and therefore does not remove the Fmoc protecting group, which would allow further building blocks to be coupled to the nitrogen atom.

4. Conclusion and Outlook

In this thesis, different cyclic building block classes were investigated for their use in solid phase synthesis to expand the building block toolbox for the sequence-defined synthesis of oligomers on solid phase. Cyclic building blocks can have the advantage that it is not necessary to use protecting group strategies and that no or different activation reagents are needed for their couplings.[65] For the studies, the different building blocks were conceived and synthesized in sufficient purity and yields. The building blocks were then coupled to the solid phase either directly, exploiting the ring's reactivity, or via another functional group on the building block. For the coupling to the solid phase, parameters such as reaction time, reaction temperature, resin loading, reactant stoichiometry, solvents, catalysts and the number of coupling steps per reaction were investigated.

The first part of this thesis explored cyclic sulfamidates. First, a synthesis was developed and optimized for the building blocks that were subsequently to be used for solid phase synthesis. The cyclic sulfamidate building blocks were coupled to the solid phase via two different strategies. In the latent strategy, the functional group at the other end of the building blocks alkyl chain is coupled to the solid phase and the cyclic sulfamidate ring is the terminal functional group of the oligomer. The latent strategy thus follows an AB + CD pattern, with "AB" being the carboxylic acid – cyclic sulfamidate building block and "CD" being an appropriate bifunctional nucleophile. In addition to the coupling reagents PyBOP and DIPEA used in classical solid phase synthesis, COMU, PyOxim and OxymaPure were also used in the optimization of the coupling efficiency and investigated for possible improvement of the coupling efficiency. Here, following extensive investigations it was discovered that by-products were generated by the coupling reagents. Since the by-products due to the coupling reagents accounted for a high proportion of the conversion, a different approach was used to make the cyclic sulfamidates accessible for solid-phase synthesis. In the active Strategy, the ring of the cyclic sulfamidate was opened by the terminal amine of the growing peptide chain on the solid phase. Since the terminal amine (primary amine) was able to open two cyclic sulfamidate rings, branched growth occurs. The oligomer can be built up in two directions by this approach. To also enable linear growth, the primary amine of the oligomer was first reacted with Fmoc-piperidine carboxylic acid. After cleavage of the Fmoc protecting group, the secondary amine could only ring-open a cyclic sulfamidate building block and thus

the oligomer could only grow in the main chain direction. Different oligomers were prepared that were both branched and linear, or a mixture of both.

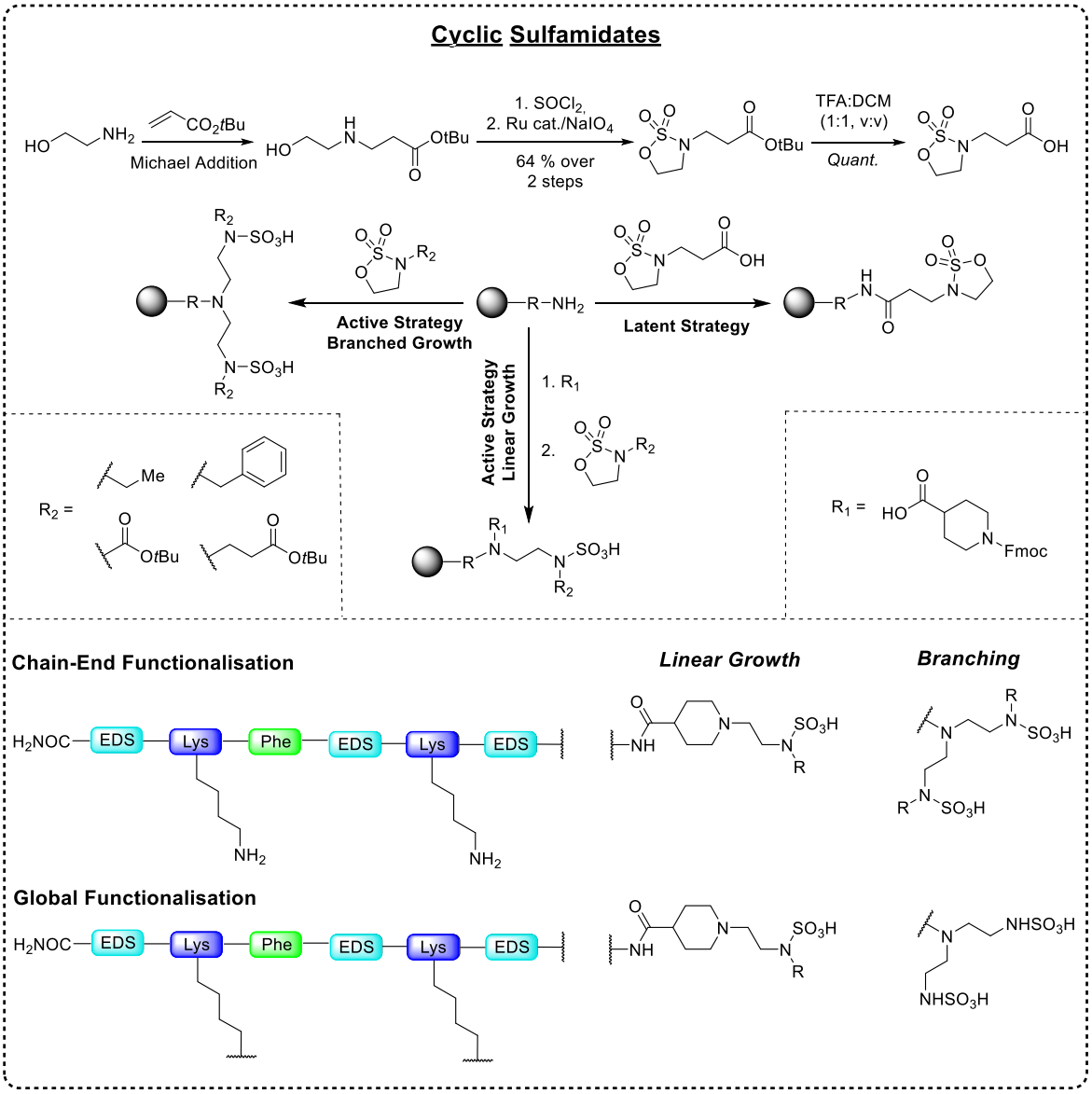

Figure 51: Graphical overview showing the synthesis of the cyclic sulfamidate building blocks and the solid phase coupling by active strategy or by latent strategy. Also, the representation of the linear growth and branching oligomers.

In future work, the oligomers prepared could be further extended by cleaving off the *N*-sulfonate group, afforded after cyclic sulfamidate ring-opening and inserting additional side chains at the revealed secondary amine e.g., leading to asymmetric branched growth. The reaction conditions for such cleavage of the sulfonate group have already been investigated by Dr. Stephen Hill. The cleavage can be carried out using a pyridine:water mixture in the ratio 99:1 vol.-% at 60 °C for one hour. In addition, further cleavage possibilities for the *N*-sulfonate group could be investigated. Another aspect that could be investigated is how far the

structures can be build up until the conversions drop sharply and whether there is a difference between the linear and the branched growth. Furthermore, alternative latent coupling strategies could be investigated, such as click chemistry. Finally, the oligomers based on the cyclic sulfamidates could be investigated for their potential applications, e.g., as oligoanions to prevent viral adhesion.[98]

The second part of this thesis deals with cyclic carbonates. These building blocks are typically five or six membered rings characterized by a carbonyl group flanked by two alkoxy groups. The cyclic carbonates are an interesting class of building blocks because they can be produced in a simple reaction from epoxides and CO_2 in the presence of a catalyst. Cyclic carbonates react with amines to form a urethane linkage, with an appending hydroxy group. Given the CO_2 starting materials, this represents a green alternative to the otherwise common production of urethanes via isocyanates and diols.[99,100,102] Ring opening does not occur regioselectively and both a primary and a secondary hydroxy group can be formed. Which of the two is formed depends on the substituents on the cyclic carbonate.[135] Biscyclocarbonates were reacted with aliphatic diamines in a submonomeric approach to obtain oligohydroxyurethanes. Here, the otherwise common use of protecting group strategies can be dispensed, which is a more atom efficient approach. The cyclic carbonate building block used was butyl biscyclocarbonate, which was modified according to a synthesis protocol established in the Hartmann group.[103] In the first attempts, the building block could not be coupled to an oligomer using standard solid phase coupling conditions. Therefore, parameters such as reaction time, reaction temperature, resin loading, reactant stoichiometry, solvents, catalysts and the number of coupling steps per reaction were investigated for the coupling of the building block. This was the first time that a coupling of the BCC building block to the solid phase was demonstrated, mainly enabled by the use of a catalyst system and the increase in temperature. During these first successful couplings, various by-products were identified, including a dimer in which the biscyclocarbonate ring was ring-opened by two amines of the oligomeric precursor and was thus no longer available for further couplings in a sequence-defined assembly. The proportion of this dimer was reduced from 40 to less than 10 % by further optimization of the coupling conditions. A key factor in this improvement was the modification of the oligomeric precursor in which the loading of the functional groups on the solid phase resin was reduced.

4. Conclusion and Outlook

Different catalyst systems were tested for the reaction, with the system of LiOTf/TBD giving the highest yields. Different solvents were tested as well, and the highest conversion was obtained with the use of NMP. The optimized synthesis conditions for coupling the BCC building block to an oligomer on the solid phase are: 60 °C reaction temperature, NMP as solvent, three hours reaction time, 40 eq. of BCC building block and LiOTf/TBD, and double couplings at each step. The oligomer with the BCC building block coupled to the solid phase was further reacted with hexamethylenediamine in the next step under ring opening of the second cyclic carbonate ring. The coupling conditions were also optimized for this reaction step. The optimized conditions for the couplings of diamine are 20 eq. of hexamethylenediamine and LiOTf/TBD, 60 min reaction time, 60 °C reaction temperature and double couplings at each step.

First attempts to couple another BCC building block after these two building blocks showed a significant decrease in conversion from 89 % to 45 %. One reason for this could be the aggregation of the oligomer chains. Both the hydroxy groups formed during ring opening and the urethane groups can form intermolecular hydrogen bonds that lead to chain-to-chain aggregation and thus hamper further chain elongation. To reduce the interactions between the chains, hydroxy groups were capped with acetic acid anhydride after each EDS and BCC coupling step. In addition, to further distance the urethane groups from each other, two EDS building blocks were incorporated after the first hexamethylenediamine building block. Through these optimization steps, the oligomer Gly-EDS-Phe-EDS-BCC-HMD-EDS-EDS-BCC-HMD-EDS could be produced with a yield of 64 %. This demonstrated that it is possible to insert cyclic carbonates in the solid phase and repeatedly incorporate them into an oligomer. When analysing this structure, it should be noted that due to the cleavage conditions of the oligomer from the solid phase resin (strongly acidic), the acetyl groups are partially deprotected and therefore no homogeneous product peak was obtained in the RP-HPLC spectrum. Therefore, the use of other temporary protecting groups, which could then be cleaved from the resin prior to cleavage of the oligomer, could potentially afford an easier product analysis in the future.

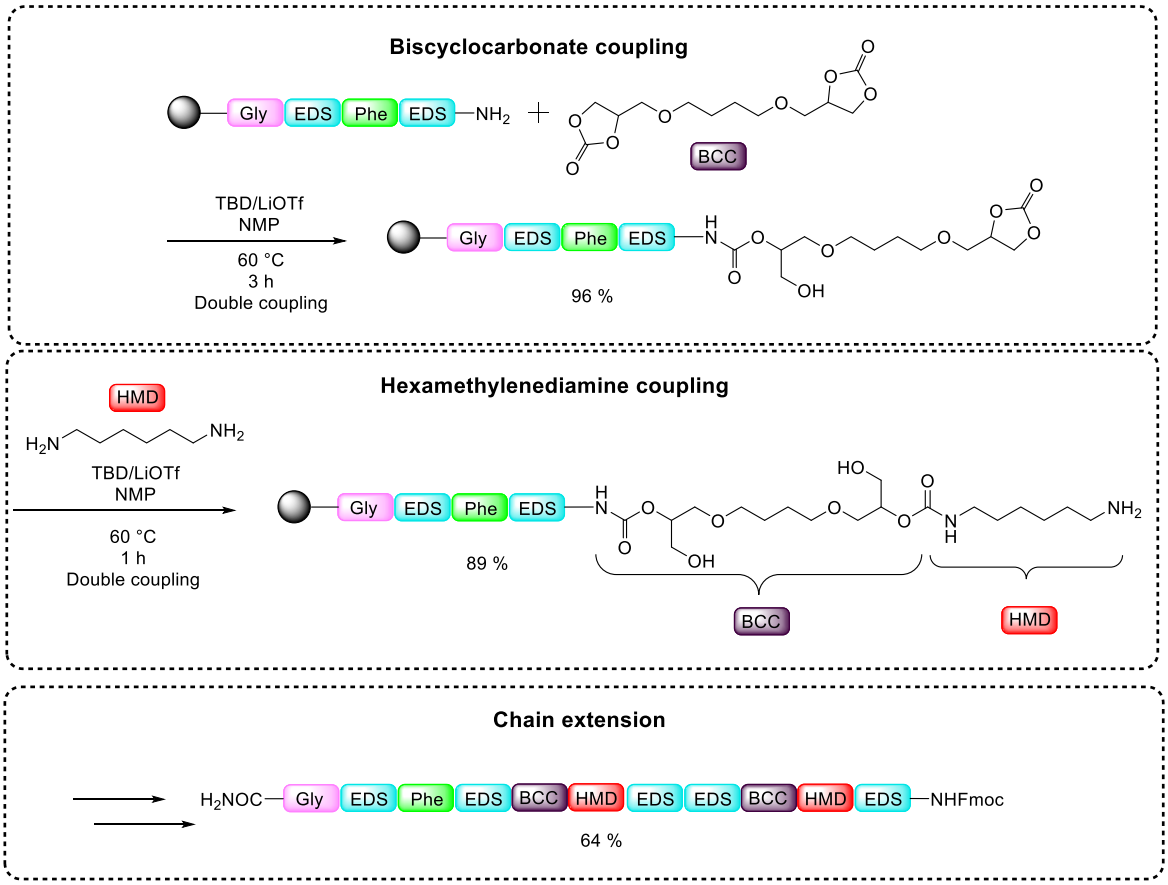

Figure 52: Graphical overview over the coupling of the BCC building block to the solid phase followed by ring opening with hexamethylenediamine. Subsequent extension of the oligomer.

Future studies could also investigate to what extent the different inter- and intramolecular hydrogen bonds in the oligohydroxyurethanes affect the chain conformation e.g., in comparison to oligoamide chains. Furthermore, the hydroxy groups formed during ring opening of the cyclocarbonate building blocks could be used for further modifications of the macromolecules e.g., by glycosylation to obtain multivalent glycan mimetics.

In addition to the biscyclocarbonate building block, various glycerol carbonate-based building blocks were synthesized and attempted to be coupled to the solid phase. The idea was to use glycerol carbonate as a building block for the solid phase and to add a carboxy functionality to couple it to an oligomer by classical solid phase peptide synthesis. Attempts to oxidize glycerol carbonate directly with trichloroisocyanuric acid were not successful. Therefore, glycerol carbonate was reacted with bromoacetic acid where the alcohol of the glycerol carbonate substituted the bromide. The building block (GCBr) was synthesized with a yield of 93 %. The coupling of the GCBr building block to the solid phase was successful. Different reaction conditions were used and the highest product conversion of 85 % was obtained with 20 eq. of

the building block, PyBOP and DIPEA over 18 h reaction time at RT. With the conditions investigated for the ring opening of cyclic carbonate rings for the biscyclocarbonates, the cyclic ring of the GCBr building block could not be opened despite repeated experiments.

Since a further build-up of the oligomer was not possible, it was tried to couple other glycerol carbonate building blocks to the solid phase. Glycerol carbonate was reacted with tosyl chloride. The resulting GCT building block was synthesized with a yield of 71 %. Subsequent coupling experiments to the solid phase showed that the amine of the oligomeric precursor did not attack the sulphur and remove the tosyl group, but that the glycerol carbonate was removed as the leaving group and the amine became tosyl protected i.e., formed a sulphonamide. Therefore, an attempt was made to generate a better leaving group. For this purpose, the GCT building block was reacted with sodium iodide. The resulting GCI building block (83 % yield) was also coupled to the solid phase, but the conversions in these experiments were at a maximum of 9 %, which is not in a suitable range for couplings to the solid phase.

In future studies, other building blocks based on glycerol carbonate could be synthesized and coupled to the solid phase. One possibility is to react glycerol carbonate with a molecule carrying a halogen atom on one side, to which the hydroxy group of the glycerol carbonate could be coupled, and an Fmoc-protected amine on the other side (e.g., 2-(Fmoc-amino)-ethyl bromide). Subsequently, the cyclic carbonate ring could be coupled to the solid phase using the conditions optimized for the biscyclocarbonates, then the Fmoc group could be cleaved off and further building blocks could be added.

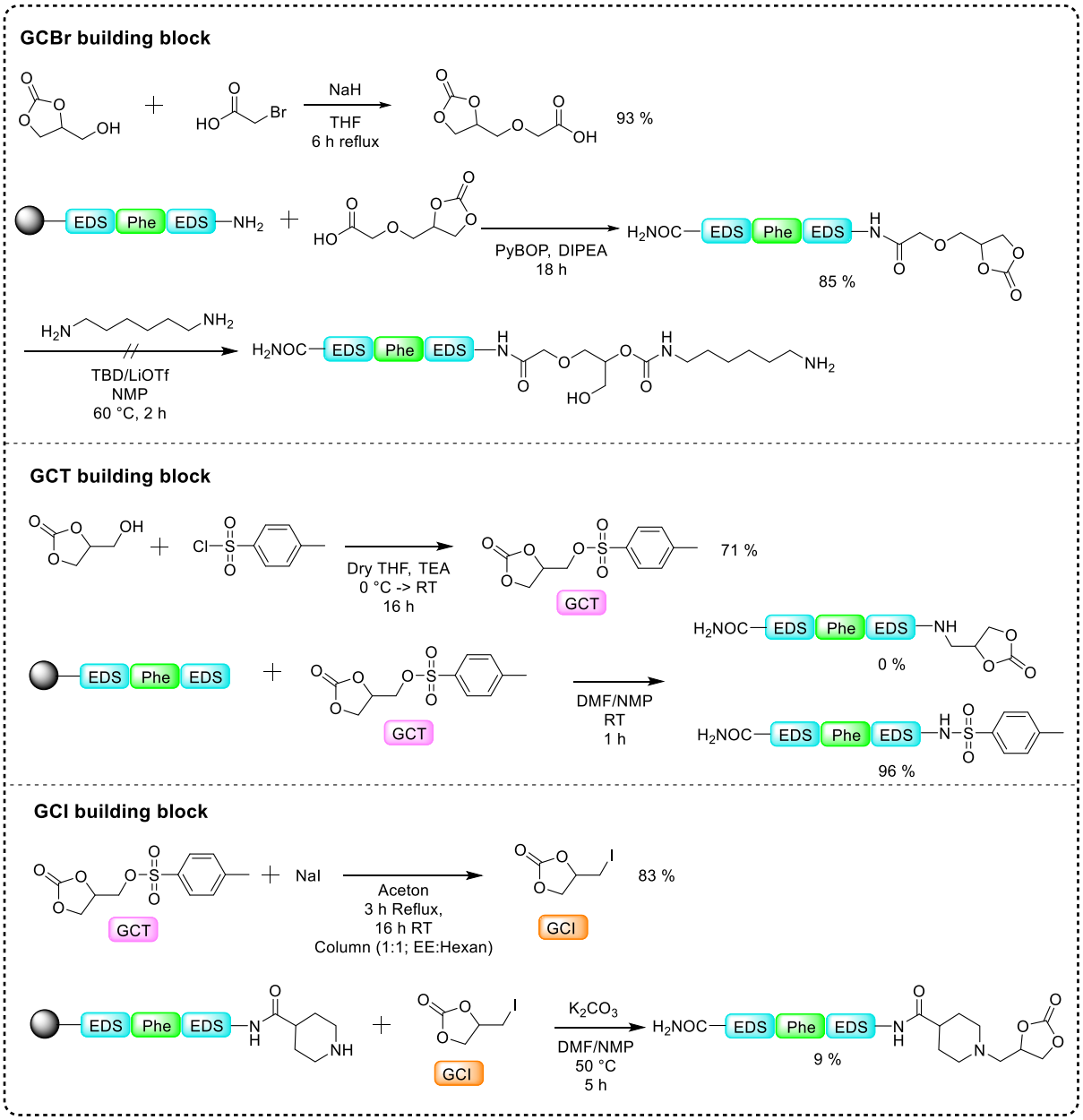

Figure 53: Graphical overview showing the synthesis and coupling of cyclic carbonate building blocks GCBr, GCT and GCI to the solid phase.

The third and final part of this thesis explored cyclic amines as building blocks for solid phase synthesis. Four building blocks were synthesized which differ in ring size and alkyl chain between the ring and the carboxy functionality (AB, ABP, PB, PBP). The AB and ABP building blocks are based on the four-ring azetidine while the PB and PBP building blocks are based on the five-ring pyrrolidine. The AB and PB building block have a shorter alkyl chain than the ABP and PBP building block. After solid phase coupling, these cyclic amine building blocks should lead to *N*-substituted amides in the main chain by ring opening with chloroformates.[125] The building blocks were coupled to the solid phase with the carboxy functionality. In this way, peptoids were produced which differ in their properties from the peptides due to their

different interactions between the chains since they are alkylated at the nitrogen atom and thus cannot form hydrogen bonds. For the coupling of the building blocks to the solid phase, solvent mixtures were tested to completely dissolve all reaction components. The mixture of DMF:dioxane:H_2O 2:1:1 vol.-% was chosen for the solid phase couplings because it was able to dissolve the cyclic amine building blocks as well as PyBOP and DIPEA.

Subsequently, attempts were made to bring the cyclic amines to ring opening by different pathways. The chloroformates Fmoc-Cl, Cbz-Cl and Alloc-Cl and the acid chlorides acetyl chloride and acryloyl chloride were used. With Fmoc-Cl, the best conversions of up to 95 % were achieved. With the chloroformates Cbz-Cl and Alloc-Cl the ring opening of the cyclic amine was achieved but only with conversions of 26 and 34 %, respectively, which were not in a range suitable for solid phase coupling. The ring opening with Cbz-Cl and Alloc-Cl probably had lower conversions because pressure developed during the reaction and the syringe had to be vented during the coupling reaction, otherwise the plunger of the solid phase syringe would fall out. The venting causes the HCl gas produced during the reaction to escape. The chloride is then no longer available for the ring opening, which leads to the reduced conversions. In future studies, attempts could be made to use a larger syringe, which has a larger volume and can therefore contain greater gas formation before the syringe has to be vented. In addition to the chloroformates, attempts were also made to open the rings of the cyclic amine building blocks with acid chlorides. However, no conversion was observed in these reactions, which is due to the fact that the absence of the oxygen atom next to the carbonyl carbon atom, in comparison to the chloroformates, making acid chlorides far less positively polarized than in the chloroformates and therefore less attractive for a nucleophilic attack.

The highest conversions of 92 % were achieved with Fmoc-Cl, so the next step was to try to deprotect the Fmoc protecting group and to couple another cyclic amine building block to the secondary amine. It was assumed that after deprotection of the Fmoc protecting group, the amine attaches to the carbon atom next to the chloride, which is positioned terminal at the end of the alkyl chain after the ring opening, and thus closes the ring intramolecularly, preventing further assembly of the oligomer. To extend the oligomer, an attempt was made not to deprotect the Fmoc group but to substitute the chloride. Attempts were made to substitute the chloride by using 4-bromophenol, p-toluenesulfonamide and cysteamine.

However, all reaction conditions tested resulted in the Fmoc protecting group being deprotected and the ring being closed again due to the basic reaction conditions.

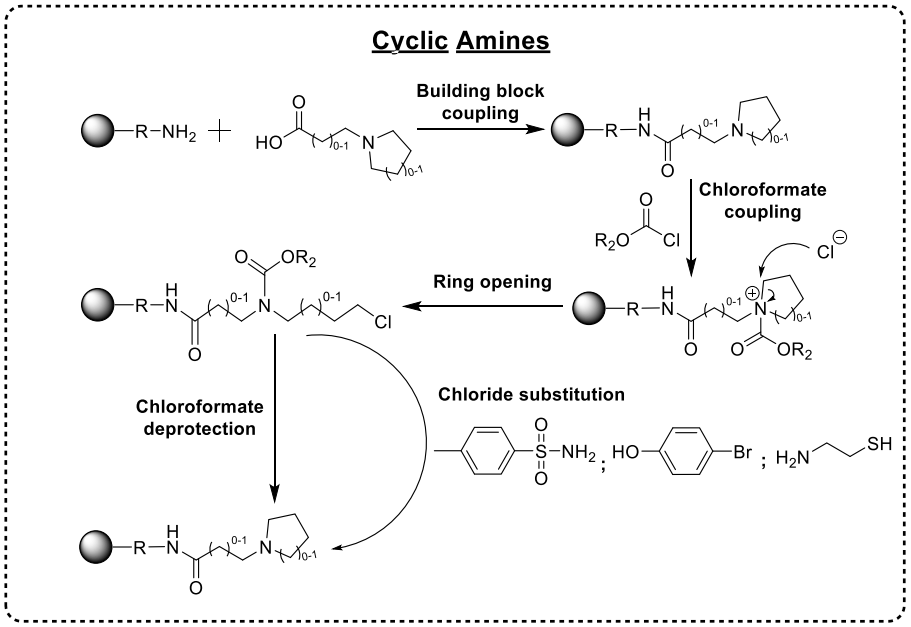

Figure 54: Graphical overview showing the coupling of cyclic amine building blocks to the solid phase and the ring opening by chloroformates. Subsequent chloroformate deprotection or chloride substitution.

In future studies, the coupling efficiency of the Cbz-Cl coupling could be improved and the attempts to substitute the chloride with this protecting group could be repeated, since Cbz should be stable under the basic reaction conditions. In addition, other reactions to substitute the chloride could be explored where basic conditions are not required and therefore the Fmoc protecting group would not be cleaved off. In addition, other chloroformates for ring opening could be tested e.g., phenyl chloroformate, isopropyl chloroformate or S-ethyl chlorothiolformate.

In summary, in this thesis the building block classes of cyclic sulfamidates, carbonates and amines were successfully explored for their use in solid phase synthesis to produce sequence-defined oligomers. New building blocks were developed and synthesized, their coupling to resin and subsequent reactivity was established. Through the cyclic building blocks of this study, different functional groups e.g., sulfate side chains or urethane main chain motifs were introduced into sequence-defined macromolecules and combined with the previously established solid phase polymer synthesis of oligo(amidoamines). Thus, this work extends the toolbox of building blocks accessible for the synthesis of precision macromolecules.

5. Experimental Part

5.1 Materials

All solvents and chemicals used are commercially available unless otherwise described and were used without further purification.

Fmoc-L-Phenylalanine ≥ 98.5 % and *N,N*-Diisopropylethylamine (DIPEA) were purchased from Carl Roth. Triethylamine (TEA) ≥ 99.5 % and 1,4-Dioxan ≥ 99.8 % were purchased from Fisher Scientific. Triisopropylsilane (TIPS), hexamethylenediamine (HMD), benzotriazol-1-yloxytripyrrolidinophosphonium hexafluorophosphate (PyBOP), 4-Bromophenol, p-Toluenesulfonamide, Pyrrolidine, Diethyl ether ≥ 99.8 %, Methanol, Deuterium oxide 99.9 % D, Deuterium Chloroform 99.8 % D and Dichloromethane (DCM) ≥ 99.9 % were purchased from Sigma Aldrich. Silica Gel 60 M, 0,04 - 0,063 mm was purchased from Machery-Nagel. Sodium hydroxide was purchased from VWR BDH Prolabo Chemicals. Trifluoroacetic acid (TFA) 99.5 %, 2-Bromopropionic acid, Bromoacetic acid > 98 %, Piperidine and allyl chloroformate 97 % were purchased from Acros Organics. Fmoc-Glycine, Fmoc-chloride 98 %, Oxyma Pure, 98.57 % and 4-(Hydroxymethyl)-1,3-dioxolan-2-on were purchased from BLD Pharmatech GmbH. Boc-glycine 99 % and p-Toluenesulfonyl chloride 99 % were purchased from JK Chemicals. 3-Bromopropionic acid 97 %, was purchased from thermos scientific. For instrumental chromatographic procedures, acetonitrile from Fisher Scientific was used with a HPLC purity grade. Couplings at the solid phase were used in the solvents, DMF and NMP from the company Biosolve B.V. each with designated suitability for peptide synthesis. Polyethylene syringes with a polyethylene frit and volume sizes of 10 ml or 20 ml from Multisyntech GmbH were used for solid phase synthesis. The syringes were sealed with a B7 septum from Aldrich. TentaGel® S RAM resin with a reported loading density of 0.23 mmol/g was purchased from Rapp Polymers.

5.2 Devices

NMR spectroscopy:

NMR measurements were performed at the Heinrich-Heine-University by PD Dr. Klaus Schaper, Maria Beuer and Mohanad Aian. ^{1}H-NMR and ^{13}C-NMR spectra were measured at room temperature on Bruker Avance III 300 (for 300 MHz) or Bruker Avance III 600 (for 600 MHz) for the ^{1}H-NMR and at 75 MHz and 150 MHz for the ^{13}C-NMR. The spectra were recorded in deuterated solvents. The chemical shifts (δ) are given in parts per million (ppm) and are reported relative to the solvent peaks. The coupling constant J is given in Hz (Hertz). The multiplicities are given by the following abbreviations: s (singlet), d (doublet), t (triplet), q (quartet), pent (pentet), m (multiplet).

Mass Spectrometry

Mass Spectrometry measurements were performed at the Heinrich-Heine-University by Dr. Peter Tommes). The mass spectrometer used for the Electrospray ionization (ESI) mass spectra was the type Ion-Trap-API Finningan LCQ Deca.

Thin layer chromatography:

For thin-layer chromatography, custom-cut precast plates from Macherey-Nagel, "ALUGRAM Xtra SIL G/UV254" with integrated fluorescence indicator were used.

Reversed-phase high-performance liquid chromatography coupled with mass spectroscopy (RP-HPLC-MS)

RP-HPLC-MS spectra were measured using a combination of Agilent 1260 Infinity instruments. In this analyser, a variable wavelength detector is set at 214 nm and coupled to a 6120-quadrupole mass spectrometer and an electron spray ionization (ESI) source. Measurements were performed in positive or negative ionization mode with a 200 to 2000 m/z range. The eluent system used is a water/acetonitrile mixture used in a gradient of 5 vol.-% to 95 vol.-% in 17 or 30 min and with 0.1 vol.-% formic acid. The separation column used is an MZ-AquaPerfekt C18 from MZ-Analysentechnik (length: 50 mm; inner diameter: 3.0 mm; particle size: 3 µm). The flow rate was 0.4 ml/min and the temperature set to 25 °C. OpenLab ChemStation software for LC/MS was used to analyse MS and UV spectra from the firm Agilent Technologies.

Freeze Dryer

The oligomers obtained after macro cleavage were freed from solvent residues (lyophilization). The Alpha 1-4 LD plus instrument from Martin Christ Freeze Dryers GmbH was used. To dry the oligomers, the instrument was set to a temperature of -54 °C and a pressure of 0.1 mbar and those settings are maintained throughout the process.

Water treatment system

Milli-Q water was obtained via a Barnstead MicroPure water treatment system from Thermo Scientific, which had an electrical conductivity of 18.20 MΩ·cm at room temperature.

High resolution ESI (HR-ESI):

On an UHR-QTOF maXis 4G instrument, HR-ESI spectra were measured (Bruker Daltonics). Measurements were performed by Dr. Peter Tommes.

5.3 Synthesis

5.3.1 Synthesis of the building blocks

Synthesis of 2-((2-oxo-1,3-dioxolan-4-yl)methoxy)acetic acid (GCBr)

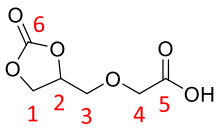

Figure 55: Structure of the GCBr building block.

The synthesis of the GCBr building block was performed using a modified approach of Eh et al.[112] Sodium hydride (1.2 g, 30 mmol, 60 % dispersion in mineral oil) was dissolved in 40 mL THF in a nitrogen countercurrent and then glycerol carbonate (4.43 g, 3.14 mL, 37.5 mmol), dissolved in 20 mL THF, was added dropwise over one hour. Bromoacetic acid (3.47 g, 25.0 mmol) was then dissolved in 20 mL THF and added dropwise over 30 min. The reaction was heated to reflux at 90 °C for six hours and then stirred at RT for 18 hours. 40 mL Hydrochloric acid (6.6 mL 12 M HCl and 33.4 mL H_2O) were then added to the solution to quench the reaction. Next the solution was extracted four times with 150 mL ethyl acetate. The organic phase was dried over magnesium sulfate. The solvent was removed under vacuum. The remaining residue was dissolved in 250 mL DCM and placed in the freezer for two days. The colorless solid was extracted with a yield of 4.09 g (23.3 mmol, 93 %) and analysed by ^{1}H-NMR (see Figure 16), ^{13}C-NMR (see Figure 74) and HR-ESI (see Figure 75).

^{1}H-NMR (300 MHz, DMSO-d_6): δ (ppm) = 4.86 – 4.73 (m, 1H, **2**); 4.49 (t, J = 8.3 Hz, 1H, **1**), 4.28 (dd, J = 8.1, 5.8 Hz, 1H, **1**), 4.03 (s, 2H, **4**), 3.66 (dd, J = 12.6, 2.8 Hz, 1H, **3**), 3.50 (dd, J = 12.6, 3.4 Hz, 1H, **3**) (Figure 16).

^{13}C-NMR (75 MHz, DMSO-d_6): δ (ppm) = 168.54 (**5**), 155.19 (**6**), 77.04 (**2**), 65.89 (**1**), 60.61 (**3**), 28.05 (**4**) (Figure 74).

HR-ESI-MS: m/z calculated for $C_6H_8NaO_6$: 199.02; found: 199.02 [M+Na]. (Figure 75)

Synthesis of (2-oxo-1,3-dioxolan-4-yl)methyl 4-methylbenzenesulfonate (GCT)

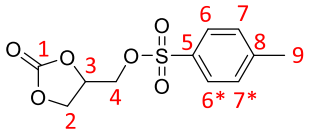

Figure 56: Structure of the GCT building block.

The synthesis of the GCT building block was performed using a modified approach of Poulsen et al.[113] Tosyl chloride (4.56 g, 23.9 mmol) was dissolved in 10 mL THF and cooled to 0 °C with an ice bath. Triethylamine (4.2 mL, 30 mmol) was added dropwise over half an hour. Next glycerol carbonate (2.36 g, 20.0 mmol) is dissolved in 10 mL THF and added to the solution. The reaction was stirred for 16 hours. 100 mL ethyl acetate were added, and the solution was washed with water (4 x 100 mL), once with 20 mL 0.2M HCl and finally once with 20 mL sodium bicarbonate. The organic phase was dried over magnesium sulfate and the solvent was removed under vacuum. The crude product was recrystallized three times from ethyl acetat:hexane to yield colorless crystals (3.87 g, 14.2 mmol, 71 %). The ^{1}H-NMR of the GCT building block is shown in Figure 57 and the ^{13}C-NMR in Figure 58.

^{1}H-NMR (600 MHz, CD_3CN): δ (ppm) = 7.83 – 7.78 (m, 2H, **7,7***); 7.49 – 7.44 (m, 2H, **6,6***); 4.94 – 4.87 (m, 1H, **3**); 4.49 (t, J = 8.8 Hz, 1H, **2**); 4.27 (dd, J = 11.7, 2.5 Hz, 1H, **4**); 4.22 – 4.14 (m, 2H, **2,4**); 2.45 (s, 3H, **9**) (Figure 57).

^{13}C-NMR (150 MHz, CD_3CN): δ (ppm) = 155.56 (**1**), 146.98 (**8**), 133.04 (**5**), 131.20 (**6,6***) 128.90 (**7,7***), 74.63 (**3**), 69.92 (**4**), 66.54 (**2**), 21.68 (**9**) (Figure 58).

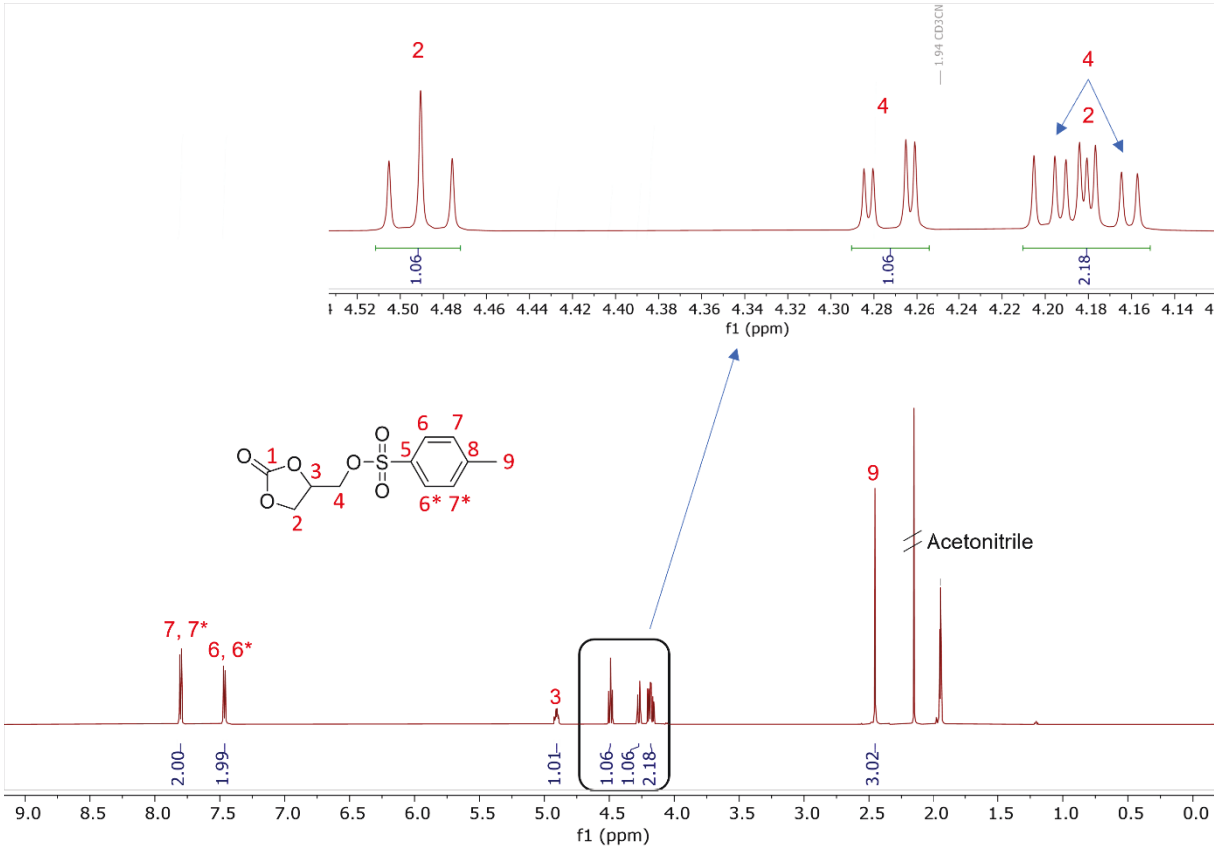

Figure 57: 600 MHz ^{1}H-NMR of the GCT building block in CD_3CN and the integration analysis indicating the proton count. The individual protons are assigned by number.

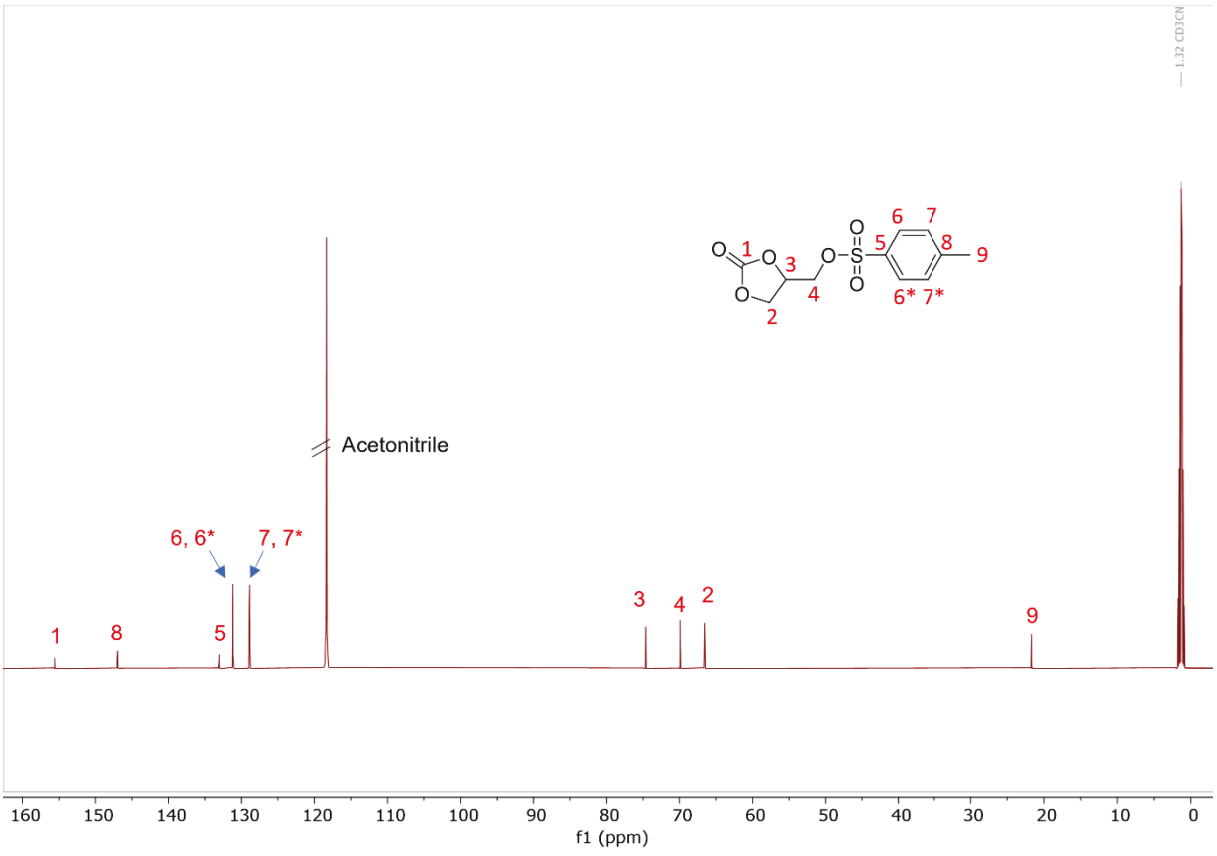

Figure 58: 150 MHz ^{13}C-NMR of the GCT building block in CD_3CN and the integration analysis indicating the proton count.

Synthesis of 4-(iodomethyl)-1,3-dioxolan-2-one (GCI)

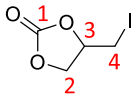

Figure 59: Structure of the GCI building block.

The synthesis of the GCT building block was performed using a modified approach of Tatibouët et al.[114] (2-oxo-1,3-dioxolan-4-yl)methyl 4-methylbenzenesulfonate (1.00 g, 3.67 mmol) was dissolved in 8 mL acetone. 1.10 g (7.35 mmol) sodium iodide were added. The solution was heated under reflux for three hours. Next 20 mL ethyl acetate and 20 mL water were added. The organic layer was washed three times with 20 mL water and after those two times with 20 mL brine. The organic phase was dried over magnesium sulfate and the solvent was removed under vacuum. 694 mg (3.05 mmol, 83 %) of 4-(iodomethyl)-1,3-dioxolan-2-one (GCI) could be isolated after purification by column chromatography (eluent hexane:ethyl acetate 1:1). The GCI building block was analysed via ^{1}H-NMR (shown in the Figure 60) and ^{13}C-NMR (shown in the Figure 61).

^{1}H-NMR (300 MHz, $CDCl_3$): δ (ppm) = 4.89 – 4.74 (m, 1H, **3**); 4.59 (dd, 1H, **2**); 4.22 (dd, J = 8.9, 6.3 Hz, 1H, **2**), 3.42 (dd, 1H, **4**); 3.32 (dd, J = 10.5, 8.3 Hz, 1H, **4**) (Figure 60).

^{13}C-NMR (75 MHz, $CDCl_3$): δ (ppm) = 154.22 (**1**), 74.83 (**3**), 69.90 (**2**), 3.82 (**4**) (Figure 61).

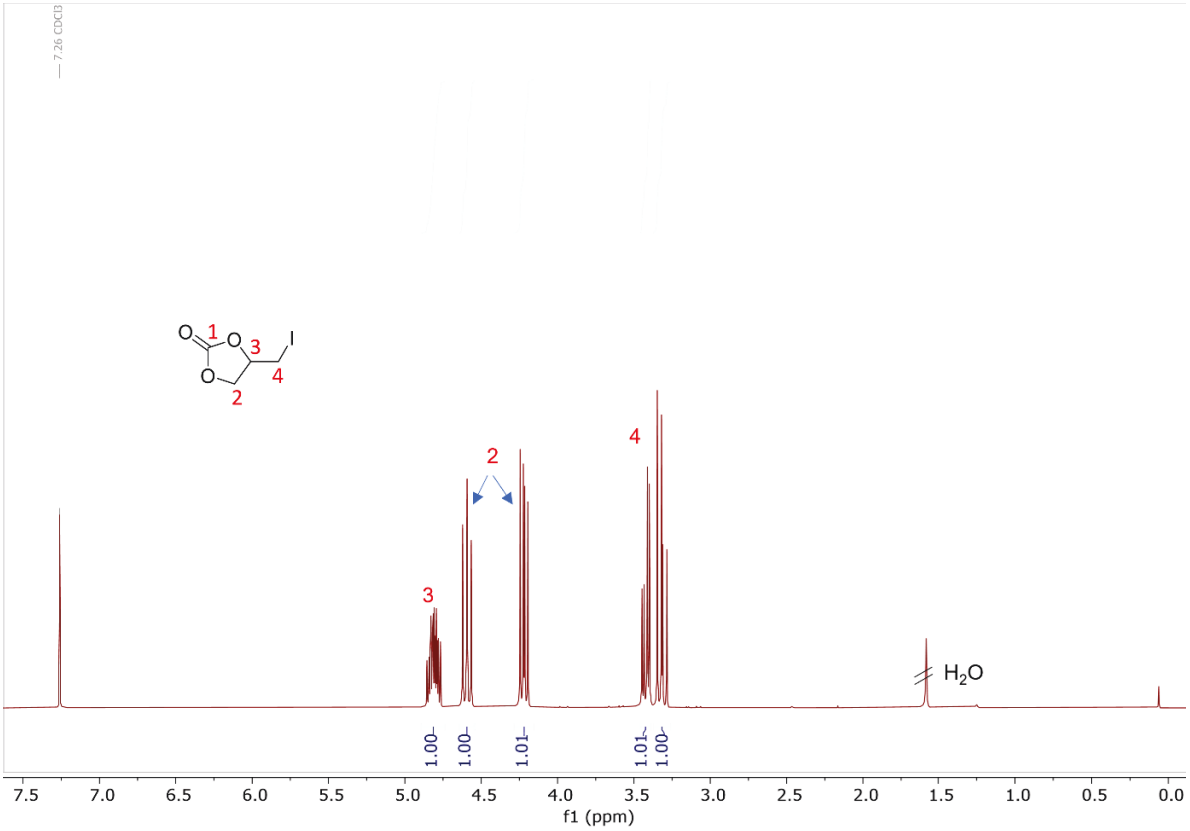

Figure 60: 300 MHz ^{1}H-NMR of the GCI building block in $CDCl_3$ and the integration analysis indicating the proton count. The individual protons are assigned by number.

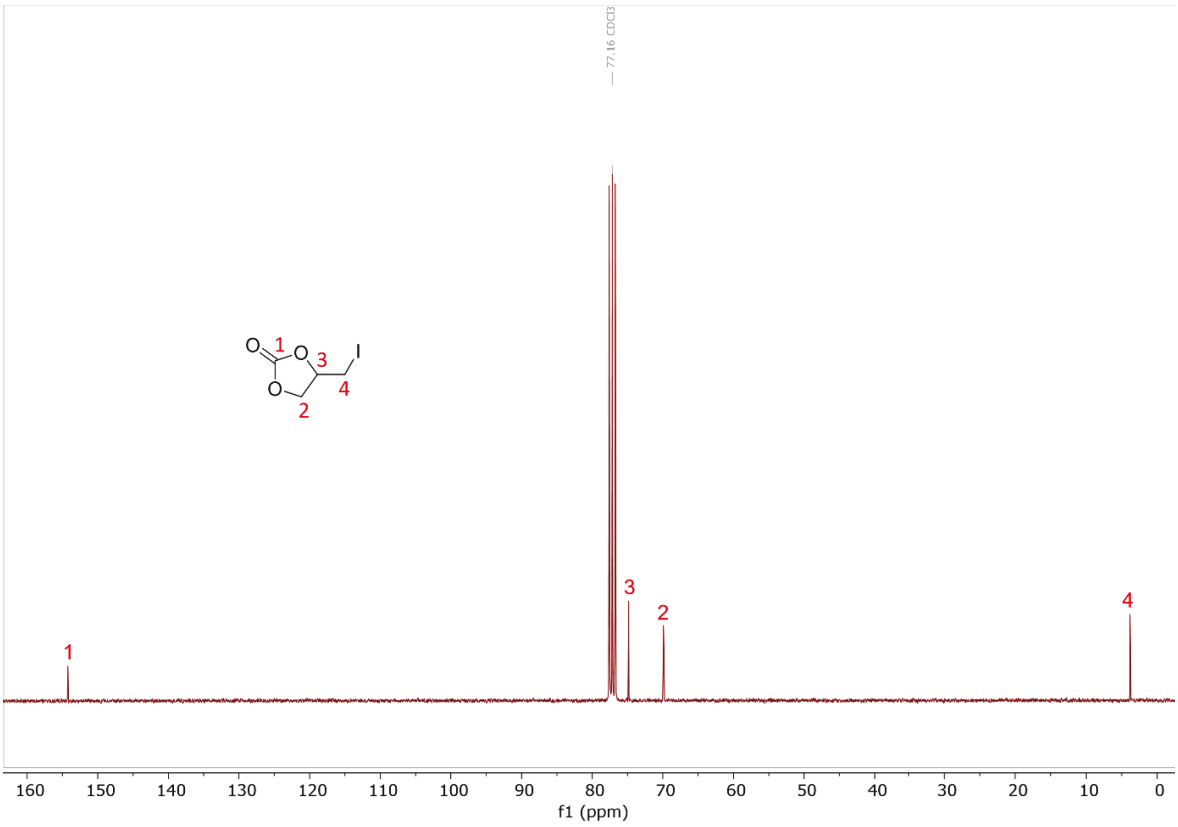

Figure 61: 75 MHz ^{13}C-NMR of the GCI building block in $CDCl_3$ and the integration analysis indicating the proton count.

Synthesis of the AB building block (2-(azetidin-1-yl)acetic acid)

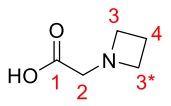

Figure 62: Structure of the AB building block.

The synthesis of the AB building block was performed using a modified approach of Sieg et al.[127] and was performed by Nathalie Bolten during her bachelor thesis under my supervision.[128]

Bromoacetic acid (407 mg, 2.92 mmol) was dissolved in 4 mL of distilled water and 2.5 mL of a 3.3 M sodium hydroxide solution. The 3.3 M NaOH solution was synthesized by dissolving 1.65 g NaOH in 12.5 mL distilled water. The reaction solution was cooled to 0 °C by an ice bath. Next 250 mg (4.25 mmol) azetidine were added dropwise. The solution was stirred for 72 h while warming to room temperature. After the reaction, the residual solvent was removed under vacuum using a rotary evaporator. 1.19 g (8.61 mmol, 295 %) (2-(azetidin-1-yl)acetic acid) were obtained as a colorless solid. The yield is > 100 % since water and azetidine residues are still present in the product. The AB building block was analysed via ^{1}H-NMR (shown in the Figure 34) and ^{13}C-NMR (shown in the Figure 70).

^{1}H-NMR (600 MHz, D_2O): δ (ppm) = 3.30 (t, 4H, ^{3}J = 7.24 Hz, **3,3***); 3.12 (s, 2H, **2**); 2.06 (quin, 4H, ^{3}J = 7.26 Hz, **4**) (Figure 34).

^{13}C-NMR (75 MHz, D_2O): δ (ppm) = 178.44 (**1**), 62.02 (**2**), 54.58 (**3, 3***), 17.41 (**4**) (Figure 70)

Synthesis of the ABP building block (3-(azetidin-1-yl)propanoic acid).

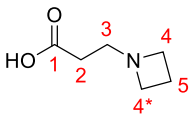

Figure 63: Structure of the ABP building block.

The synthesis of the ABP building block was synthesized analogously to the synthesis of the AB building block, except that bromopropionic acid was used instead of bromoacetic acid. The synthesis of the ABP building block was performed using a modified approach of Sieg et al.[127] and was performed by Nathalie Bolten during her bachelor thesis under my supervision.[128]

Bromopropionic acid (447 mg, 2.92 mmol) was dissolved in 4 mL of distilled water and 2.5 mL of a 3.3 M sodium hydroxide solution. The 3.3 M NaOH solution was synthesized by dissolving 1.65 g NaOH in 12.5 mL distilled water. The reaction solution was cooled to 0 °C by an ice bath. Next 250 mg (4.25 mmol) azetidine were added dropwise. The solution was stirred for 72 h while warming to room temperature. After the reaction, the residual solvent was removed under vacuum using a rotary evaporator. 989 mg (6.54 mmol, 224 %) (3-(azetidin-1-yl)propanoic acid) were obtained as a colorless solid. The yield is > 100 % since water and azetidine residues are still present in the product. The ABP building block was analysed via ^{1}H-NMR (shown in the Figure 35) and ^{13}C-NMR (shown in the Figure 71).

^{1}H-NMR (300 MHz, D_2O): δ (ppm) = 3.21 (t, 4H, ^{3}J = 7.06 Hz, **4, 4***); 2.64 (t, 2H, ^{3}J = 7.96 Hz, **3**); 2.18 (t, 2H, ^{3}J = 7.92 Hz, **2**); 2.03 (quin, 2H, ^{3}J = 7.08 Hz, **5**) (Figure 35).

^{13}C-NMR (75 MHz, D_2O): δ (ppm) = 181.39 (**1**), 55.11 (**3**), 54.95 (**4, 4***), 35.42 (**2**), 16.93 (**5**) (Figure 71)

Synthesis of the PB building block (2-(pyrrolidin-1-yl)acetic acid).

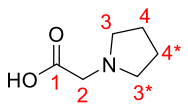

Figure 64: Structure of the PB building block.

The synthesis of the PB building block was performed using a modified approach of Sieg et al.[127]

Bromoacetic acid (2.72 g, 19.6 mmol) was dissolved in 15 mL of distilled water and 9 mL of a 3.3 M sodium hydroxide solution. The 3.3 M NaOH solution was synthesized by dissolving 1.65 g NaOH in 12.5 mL distilled water. The reaction solution was cooled to 0 °C by an ice bath. Next 1.96 mL (1.67 g, 23.53 mmol) pyrrolidine were added dropwise. The solution was stirred for 72 h while warming to room temperature. After the reaction, the residual solvent was removed under vacuum using a rotary evaporator. 3.85 g (29.8 mmol, 152 %) (2-(pyrrolidin-1-yl)acetic acid) were obtained as a colorless solid. The yield is > 100 % since water and pyrrolidine residues are still present in the product. The PB building block was analysed via ^{1}H-NMR (shown in the Figure 36) and ^{13}C-NMR (shown in the Figure 72).

^{1}H-NMR (300 MHz, D_2O): δ (ppm) = 3.67 (s, 2H, **2**); 3.28-3.21 (m, 4H, **3, 3***); 2.05-1.99 (m, 4H, **4, 4***) (Figure 36)

^{13}C-NMR (75 MHz, D_2O):[128] δ (ppm) = 174.60 (**1**), 58.36 (**2**), 54.12 (**3, 3***), 22.95 (**4, 4***) (Figure 72)

Synthesis of the PBP building block (3-(pyrrolidin-1-yl)propanoic acid)

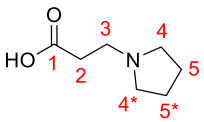

Figure 65: Structure of the PBP building block.

The synthesis of the PBP building block was synthesized analogously to the synthesis of the PB building block, except that bromopropionic acid was used here instead of bromoacetic acid. The synthesis of the PBP building block was performed using a modified approach of Sieg et al.[127]

Bromopropionic acid (3.00 g, 19.6 mmol) was dissolved in 15 mL of distilled water and 9 mL of a 3.3 M sodium hydroxide solution. The 3.3 M NaOH solution was synthesized by dissolving 1.65 g NaOH in 12.5 mL distilled water. The reaction solution was cooled to 0 °C by an ice bath. Next 1.96 mL (1.67 g, 23.53 mmol) pyrrolidine were added dropwise. The solution was stirred for 72 h while warming to room temperature. After the reaction, the residual solvent was removed under vacuum using a rotary evaporator. 5.14 g (35.9 mmol, 183 %) (3-(pyrrolidin-1-yl)propanoic acid) were obtained as a colorless solid. The yield is > 100 % since water and pyrrolidine residues are still present in the product. The PBP building block was analysed via ^{1}H-NMR (shown in the Figure 37) and ^{13}C-NMR (shown in the Figure 73).

^{1}H-NMR (300 MHz, D_2O): δ (ppm) = 2.99 (t, 2H, ^{3}J = 7.42 Hz, **3**); 2.88 (t, 4H, **4, 4***); 2.49 (t, 2H, ^{3}J = 7.49 Hz, **2**); 1.91 (quin, 4H, 7.04 Hz, **5, 5***) (Figure 37).

^{13}C-NMR (75 MHz, D_2O):[128] δ (ppm) = 179.47 (**1**), 53.67 (**4, 4***), 52.11 (**3**), 34.75 (**2**), 22.89 (**5, 5***) (Figure 73).

5.3.2 Solid phase protocol

Pre-swelling of resin

At the beginning of the solid phase synthesis, TentaGel® S RAM resin from RAPP Polymere, with a loading density of 0.23 mmol/g was shaken (swelled) with 15 mL of DCM for about 30 min. Afterwards, the resin was washed with fifteen times 10 ml DMF. Before the first coupling, the Fmoc protecting group is cleaved from the resin (see Fmoc deprotection for details).

Fmoc deprotection

To remove the Fmoc protecting group, 10 ml of a piperidine solution (25 vol.-% in DMF) was added to the resin and shaken for 20 min at room temperature. The resin was then washed five times with 10 ml of DMF each time. The washing steps were repeated, with only 15 min of shaking the second time. Finally, the resin was washed fifteen times with 10 ml DMF each time followed by 5 times washing with DCM.

General coupling of the oligomeric precursor building blocks.

After cleavage of the terminal Fmoc protecting group, the building blocks were coupled, requiring Fmoc cleavage again after each individual added building block. To couple the building blocks, 5.0 eq. each of the building block and 5.0 eq. PyBOP were combined with 5 ml DMF and 20 eq. DIPEA. The mixture was shaken with the resin for one hour. Finally, the mixture was washed ten times with DMF and five times with DCM. The preparations were carried out with 0.5 mmol batch sizes which were subsequently divided into 5 syringes (0.1 mmol) for coupling experiments. All reactions were performed in a syringe with frit on a shaking plate at room temperature.

Cleavage of the oligomer from the resin (micro cleavage).

To cleave the oligomer from the resin, a spatula tip of the resin was placed in an Eppendorf tube. To this end, 10 drops of a solution of TFA, DCM and TIPS (95/2.5/2.5 vol.-%) was added. The mixture was shaken for 30 min. Then, the solution was dropped into 10 ml of cold diethyl ether using a pipette. This was followed by waiting for 5 min and then centrifugation for 5 min. Next, the supernatant was decanted off. The remaining residue was dried in a nitrogen countercurrent for 20 min.

To measure the samples by RP-HPLC-MS, the residue was resuspended in 0.7 ml of an acetonitrile/H_2O mixture (1:1 vol.-%). The solution was then transferred through a filter into a sample vial and subsequently measured by RP-HPLC-MS.

Cleavage of the oligomer from the resin (macro cleavage).

The oligomers on the TentaGel® S RAM resin were cleaved with 20 mL of a solution of TFA:TIPS:DCM (95:2.5:2.5 vol.-%) which was drawn up into the syringe. The syringe with the solution was shaken at room temperature for 60 min. After that the solution was precipitated into iced diethyl ether (45 mL). After half an hour in the fridge the solution was centrifuged for 4 min and the supernatant was decanted. The colorless precipitate was dried against a nitrogen flow for one hour. The colorless precipitate was then lyophilized after being dissolved in MilliQ water. For RP-HPLC-MS analysis 1 mg of the oligomer was dissolved in 1 mL of an acetonitrile/H_2O mixture (1:1 vol.-%). After that the solution was transferred through a filter into a sample vial and then measured by RP-HPLC-MS.

5.3.3 Synthesis of the oligomeric precursors

The following procedure refers to the synthesis of the oligomeric precursors. Oligomeric precursors EDS_3, EPE, GEPE and EKPEKE got synthesized based on the protocol reported by Ponader et al.[11]

The general synthesis for the oligomeric precursors is described in chapter 5.3.2. In the following, the analytics of these oligomers are shown.

The RP-HPLC chromatogram for EDS_3 is shown in Figure 66 and the corresponding HPLC-ESI-MS in Figure 67.

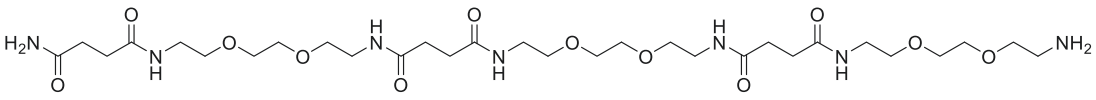

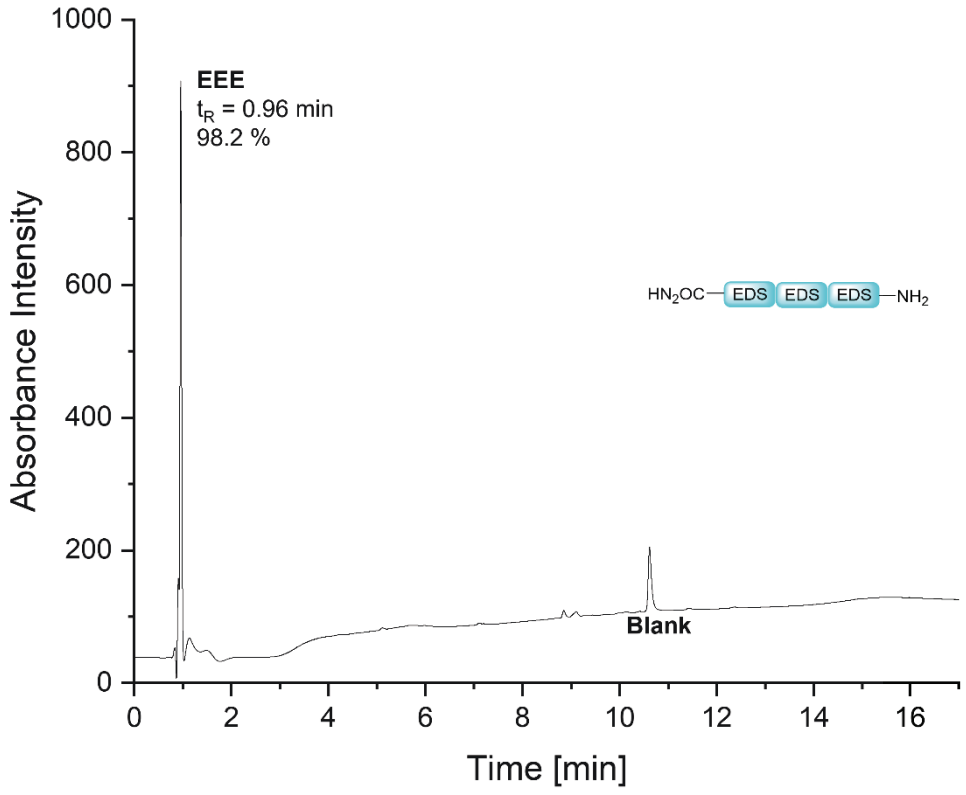

Figure 66 RP-HPLC chromatogram (Gradient 5-95 vol.-% - MeCN in H_2O (0.1 vol.-% formic acid, run time 17 min) of EDS_3.

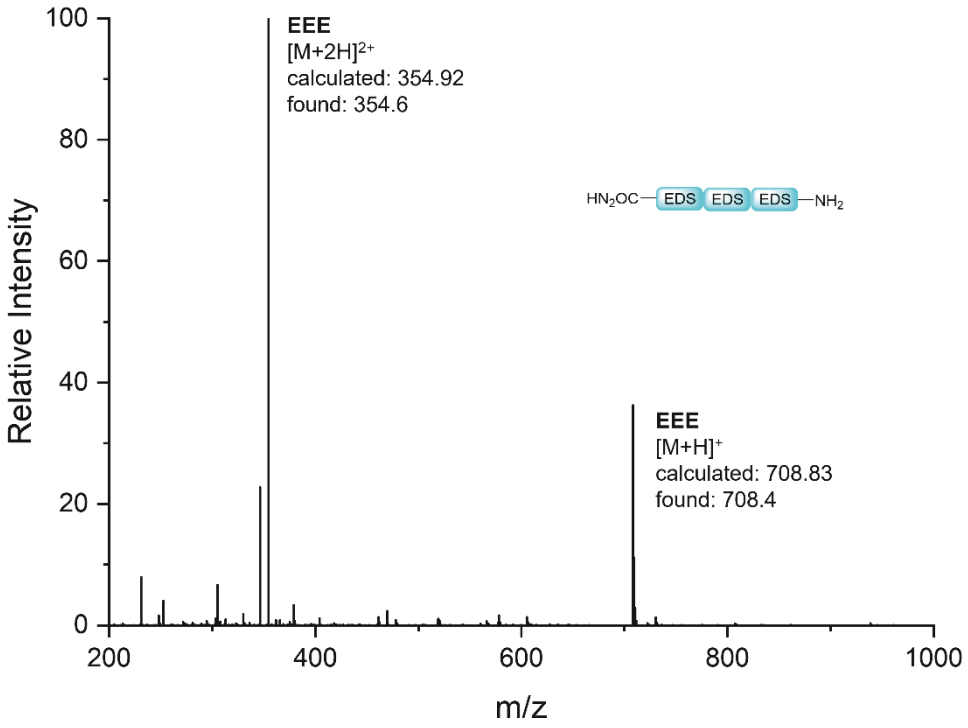

Figure 67: HPLC-ESI-MS of EDS_3 at t = 0.96 min (gradient of 5 to 95 vol.-% acetonitrile in water containing 0.1 vol.-% formic acid, run time 17 min).

The RP-HPLC chromatogram for EPE is shown in Figure 68 and the corresponding HPLC-ESI-MS in Figure 69.

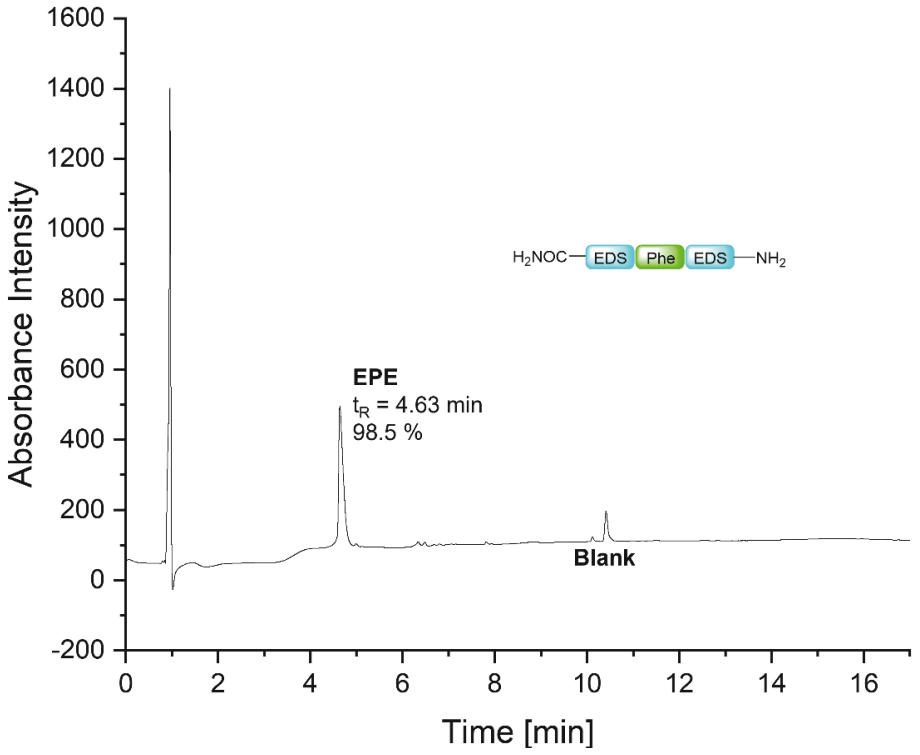

Figure 68: RP-HPLC chromatogram (Gradient 5-95 vol.-% - MeCN in H_2O (0.1 vol.-% formic acid, run time 17 min) of EPE.

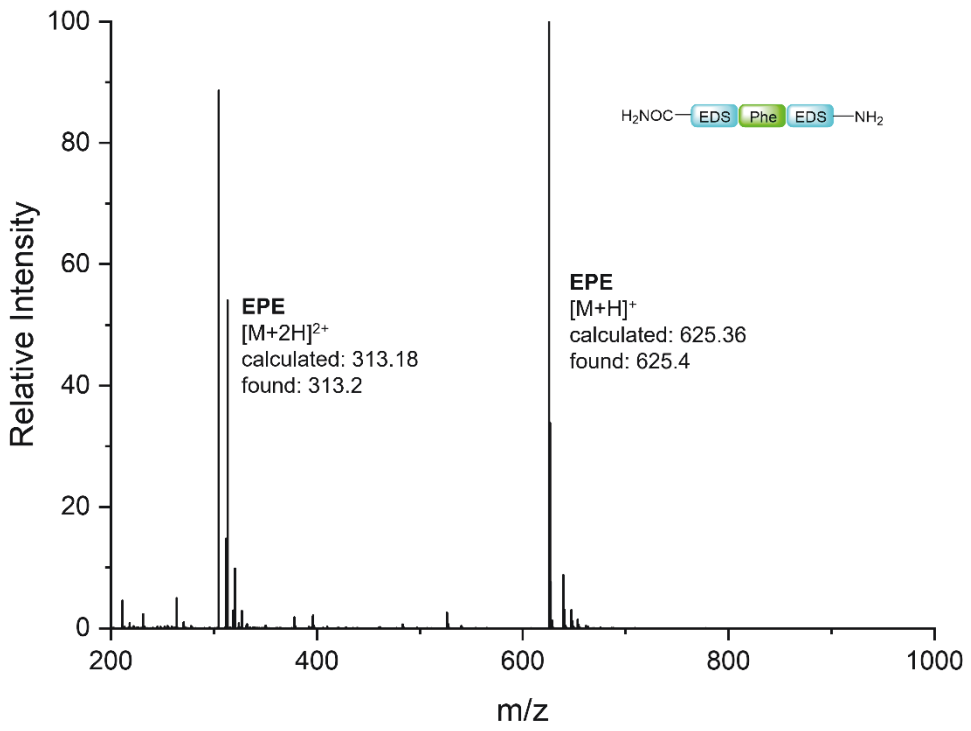

Figure 69: HPLC-ESI-MS of EPE at t = 4.63 min (gradient of 5 to 95 vol.-% acetonitrile in water containing 0.1 vol.-% formic acid, run time 17 min).

The RP-HPLC chromatogram for GEPE and the corresponding HPLC-ESI-MS are in the SI of the cyclic carbonate paper (see Figure 3).[106]

The RP-HPLC chromatogram for EKPEKE and the corresponding HPLC-ESI-MS are in the SI of the cyclic sulfamidate paper (see Figure 28).[68]

5.3.4 Solid phase synthesis

Cyclic carbonate building blocks

Coupling of the GCBr building block to the oligomeric precursor EPE

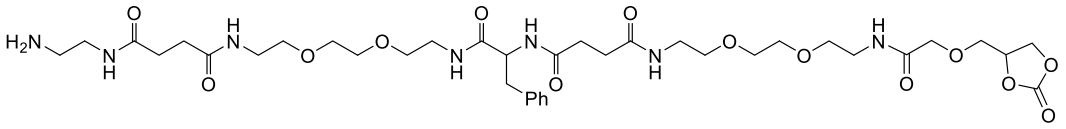

The oligomeric precursor EDS-phenylalanine-EDS was coupled to the solid phase on a 0.5 mmol scale using a solid phase protocol as described in Chapter 5.3.2. The batch was then divided among five syringe reactors (0.1 mmol each). The RP-HPLC spectrum of the oligomeric precursor is shown in Figure 68. For the synthesis of the oligomer EPE-GCBr, 352.2 mg (2.00 mmol, 20 eq.) of the GCBr building block dissolved in 3 mL DMF were added to one of the syringe reactors (0.1 mmol). 1.04 g of PyBOP (2.00 mmol, 20 eq.) dissolved in 3 mL DMF and 0.35 mL DIPEA (2.00 mmol, 20 eq.) mixed with 1 mL of DMF were added. The reaction solution in the syringe was shaken for 18 h at RT. The syringe was then washed 15 times with DMF followed by washing five times with DCM. The reaction conditions of the further experiments with the GCBr building block are shown in Table 1 (see chapter 3.2.1.2).

The reaction success was observed by macro cleavages (see section 5.3.2).

ESI-MS (m/z) for $C_{37}H_{59}N_7O_{14}$ (exact mass: 825.41): $[M+NH_4]^+$ calculated: 843.44, found: 843.4; $[M+H+NH_4]^{2+}$ calculated: 422.23, found: 422.2. (See Figure 18)

RP-HPLC (Gradient 5-95 vol.-% - MeCN in H_2O containing 0.1 vol.-% formic acid, run time 17 min): t_R= 6.45 min. Determined purity 84.8 %. (See Figure 18)

Coupling of the GCT building block to the oligomeric precursor EPE

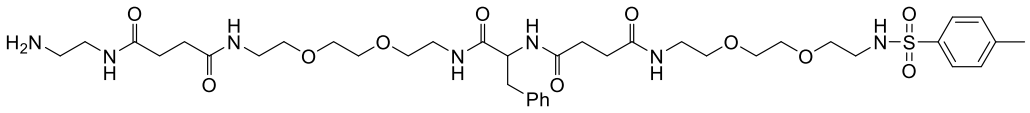

The oligomeric precursor EDS-phenylalanine-EDS was coupled to the solid phase on a 0.5 mmol scale using a solid phase protocol as described in Chapter 5.3.2. The batch was then divided among five syringe reactors (0.1 mmol each). The RP-HPLC spectrum of the oligomeric precursor is shown in Figure 68. For the synthesis of the oligomer EPE-GCT, 680.7 mg (2.5 mmol, 25 eq.) of the GCT building block dissolved in 3 mL NMP were added to one of the syringe reactors (0.1 mmol). 0.35 mL of DIPEA (2.00 mmol, 20 eq.) mixed with 1 mL of NMP were added. The reaction solution in the syringe was shaken for 1 h at RT. The syringe was then washed 15 times with followed by washing five times with DCM.

The reaction success was observed by macro cleavages (see section 5.3.2).

ESI-MS (m/z) for $C_{38}H_{59}N_7O_{11}S$ (exact mass: 821.40): $[M+H]^+$ calculated: 822.40, found: 822.4; $[M+2H]^{2+}$ calculated: 411.70 , found: 411.8. (See Figure 22)

RP-HPLC (Gradient 5-95 vol.-% - MeCN in H_2O containing 0.1 vol.-% formic acid, run time 17 min): t_R= 7.60 min. Determined purity 96.2 %. (See Figure 22)

Coupling of the GCI building block to the oligomeric precursor EPE-PCA

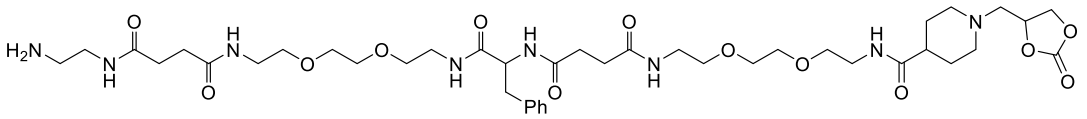

The oligomeric precursor EDS-phenylalanine-EDS was coupled to the solid phase on a 0.5 mmol scale using a solid phase protocol as described in Chapter 5.3.2. The batch was then divided among five syringe reactors (0.1 mmol each). The RP-HPLC spectrum of the oligomeric precursor is shown in Figure 68. For the synthesis of the oligomer EPE-PCA-GCI, 351.4 mg (1.00 mmol, 10 eq.) of 1-Fmoc-piperidine-4-carboxylic acid were dissolved in DMF and 1.04 g of PyBOP (2.00 mmol, 20 eq.) dissolved in 3 mL DMF and 0.35 mL DIPEA (2.00 mmol, 20 eq.) were added to one of the syringe reactors (0.1 mmol). The reaction solution in the syringe was shaken for 3 h at RT. Then the syringe was washed with DMF ten times, and the coupling was performed again with the same conditions. Subsequently, the syringe was washed 15 times with DMF followed by washing five times with DCM. After that 114.0 mg (0.5 mmol, 5 eq.) of the GCI building block dissolved in 3 mL NMP were added with 138.2 mg (1.0 mmol, 10 eq.) of potassium carbonate dissolved in 4 mL NMP. The reaction solution was transferred to a glass reactor which was placed in a water bath and heated to 50 °C. The solution was bubbled through with nitrogen for five hours. Next the solution was transferred to a syringe. The syringe was then washed 15 times with DMF followed by washing five times with DCM.

The reaction success was observed by macro cleavages (see section 5.3.2).

ESI-MS (m/z) for $C_{55}H_{94}N_{12}O_{18}$ (exact mass: 878.47): $[M+H]^+$ calculated: 879.4, found: 879.47; $[M+2H]^{2+}$ calculated: 440.24, found: 440.2. (See Figure 76)

RP-HPLC (Gradient 5-95 vol.-% - MeCN in H_2O containing 0.1 vol.-% formic acid, run time 17 min): t_R= 4.61 min. Determined purity 9.2 %. (See Figure 76)

N-Heterocyclic building blocks

Coupling of the AB building block to the oligomeric precursor EDS_3

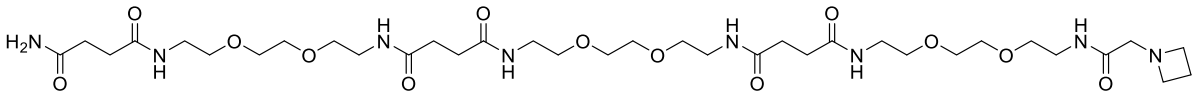

The oligomeric precursor EDS-EDS-EDS was coupled to the solid phase on a 0.5 mmol scale as described in section 5.3.2 using a solid phase protocol. The batch was then divided among ten syringe reactors (0.05 mmol each). The RP-HPLC spectrum of the oligomeric precursor is shown in Figure 66. For the synthesis of the oligomer EDS_3-AB, 137.3 mg (1.0 mmol, 20 eq.) of the AB building block were added to one of the syringe reactors (0.05 mmol) which were previously dissolved in 3 mL of a DMF:dioxane:water solution (2:1:1 vol.-%). 130.1 mg of PyBOP (0.25 mmol, 5 eq.) dissolved in 3 mL of DMF:dioxane:water solution (2:1:1 vol.-%) and 0.17 mL DIPEA (1.0 mmol, 20 eq.) mixed with 1 mL of DMF:dioxane:water solution (2:1:1 vol.-%) were added. The reaction solution in the syringe was shaken for 3 h at RT. Then the syringe was washed with DMF ten times, and the coupling was performed again with the same conditions. Subsequently, the syringe was washed 15 times with DMF followed by washing five times with DCM.

The reaction success was observed by macro cleavages (see section 5.3.2).

ESI-MS (m/z) for $C_{35}H_{64}N_8O_{13}$ (exact mass: 804.46): $[M+H]^+$ calculated: 805.47, found: 805.4; $[M+2H]^{2+}$ calculated: 403.24 , found: 403.3. (See Figure 78)

RP-HPLC (Gradient 5-95 vol.-% - MeCN in H_2O containing 0.1 vol.-% formic acid, run time 17 min): t_R= 4.65 min. Determined purity 17.6 %. (See Figure 77)

Coupling of the ABP building block to the oligomeric precursor EDS_3

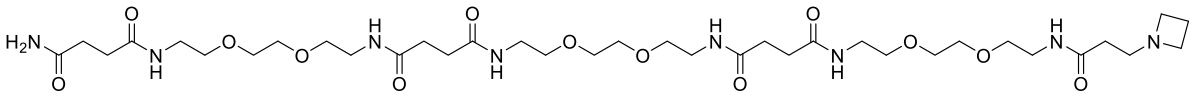

The oligomeric precursor EDS-EDS-EDS was coupled to the solid phase on a 0.5 mmol scale as described in section 5.3.2 using a solid phase protocol. The batch was then divided among five syringe reactors (0.05 mmol each). The RP-HPLC spectrum of the oligomeric precursor is shown in Figure 66. For the synthesis of the oligomer EDS_3-ABP, 151.3 mg (1.0 mmol, 20 eq.) of the ABP building block were added to one of the syringe reactors (0.05 mmol) which were previously dissolved in 3 mL of a DMF:dioxane:water solution (2:1:1 vol.-%). To this, 130.1 mg of PyBOP (0.25 mmol, 5 eq.) dissolved in 3 mL of DMF:dioxane:water solution (2:1:1 vol.-%) and 0.17 mL DIPEA (1.0 mmol, 20 eq.) mixed with 1 mL of DMF:dioxane:water solution (2:1:1 vol.-%) were added. The reaction solution in the syringe was shaken for 3 h at RT. Then the syringe was washed with DMF ten times, and the coupling was performed again with the same conditions. Subsequently, the syringe was washed 15 times with DMF followed by washing five times with DCM.

The reaction success was observed by macro cleavages (see section 5.3.2).

ESI-MS (m/z) for $C_{36}H_{66}N_8O_{13}$ (exact mass: 818.47): $[M+H]^+$ calculated: 819.47, found: 819.4; $[M+2H]^{2+}$ calculated: 410.24 , found: 410.2. (See Figure 80)

RP-HPLC (Gradient 5-95 vol.-% - MeCN in H_2O containing 0.1 vol.-% formic acid, run time 17 min): t_R= 4.85 min. Determined purity 6.8 %. (See Figure 79)

Coupling of the PB building block to the oligomeric precursor EDS_3

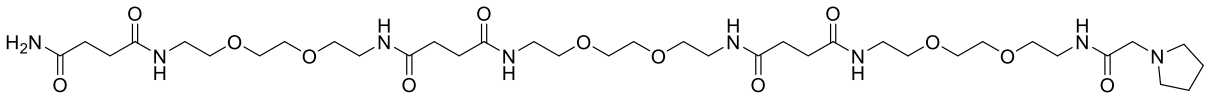

The oligomeric precursor EDS-EDS-EDS was coupled to the solid phase on a 0.5 mmol scale as described in section 5.3.2 using a solid phase protocol. The batch was then divided among ten syringe reactors (0.05 mmol each). The RP-HPLC spectrum of the oligomeric precursor is shown in Figure 66. For the synthesis of the oligomer EDS_3-PB, 129.2 mg (1.00 mmol, 20 eq.) of the PB building block were added to one of the syringe reactors (0.05 mmol) which were previously dissolved in 3 mL of a DMF:dioxane:water solution (2:1:1 vol.-%). 130.1 mg of PyBOP (0.25 mmol, 5 eq.) dissolved in 3 mL of DMF:dioxane:water solution (2:1:1 vol.-%) and 0.17 mL of DIPEA (1.0 mmol, 20 eq.) mixed with 1 mL of DMF:dioxane:water solution (2:1:1 vol.-%) were added. The reaction solution in the syringe was shaken for 3 h at RT. Then the syringe was washed with DMF ten times, and the coupling was performed again with the same conditions. Subsequently, the syringe was washed 15 times with DMF followed by washing five times with DCM.

The reaction success was observed by macro cleavages (see section 5.3.2).

ESI-MS (m/z) for $C_{36}H_{66}N_8O_{13}$ (exact mass: 818.47): $[M+H]^+$ calculated: 819.47, found: 819.4; $[M+2H]^{2+}$ calculated: 410.24 , found: 410.2. (See Figure 39)

RP-HPLC (Gradient 5-95 vol.-% - MeCN in H_2O containing 0.1 vol.-% formic acid, run time 17 min): t_R= 0.94 min. Determined purity 95.1 %. (See Figure 81)

Coupling of the PBP building block to the oligomeric precursor EDS_3

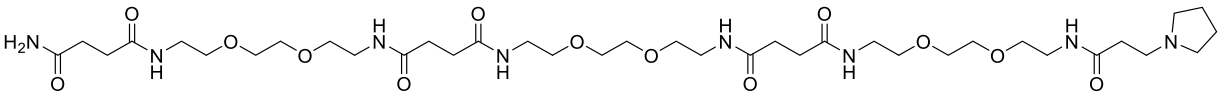

The oligomeric precursor EDS-EDS-EDS was coupled to the solid phase on a 0.5 mmol scale as described in section 5.3.2 using a solid phase protocol. The batch was then divided among five syringe reactors (0.05 mmol each). The RP-HPLC spectrum of the oligomeric precursor is shown in Figure 66. For the synthesis of the oligomer EDS_3-PBP, 143.2 mg (1.00 mmol, 20 eq.) of the PBP building block were added to one of the syringe reactors (0.05 mmol) which were previously dissolved in 3 mL of a DMF:dioxane:water solution (2:1:1 vol.-%). 130.1 mg of PyBOP (0.25 mmol, 5 eq.) dissolved in 3 mL of DMF:dioxane:water solution (2:1:1 vol.-%) and 0.17 mL of DIPEA (1.0 mmol, 20 eq.) mixed with 1 mL of DMF:dioxane:water solution (2:1:1 vol.-%) were added. The reaction solution in the syringe was shaken for 3 h at RT. Then the syringe was washed with DMF ten times, and the coupling was performed again with the same conditions. Subsequently, the syringe was washed 15 times with DMF followed by washing five times with DCM.

The reaction success was observed by macro cleavages (see section 5.3.2).

ESI-MS (m/z) for $C_{37}H_{68}N_8O_{13}$ (exact mass: 832.49): $[M+H]^+$ calculated: 833.50, found: 833.4; $[M+2H]^{2+}$ calculated: 417.25 , found: 417.2. (See Figure 40)

RP-HPLC (Gradient 5-95 vol.-% - MeCN in H_2O containing 0.1 vol.-% formic acid, run time 30 min): t_R= 1.00 min. Determined purity 93.6 %. (See Figure 82)

Coupling of the oligomer EDS_3-PB with Fmoc-Cl

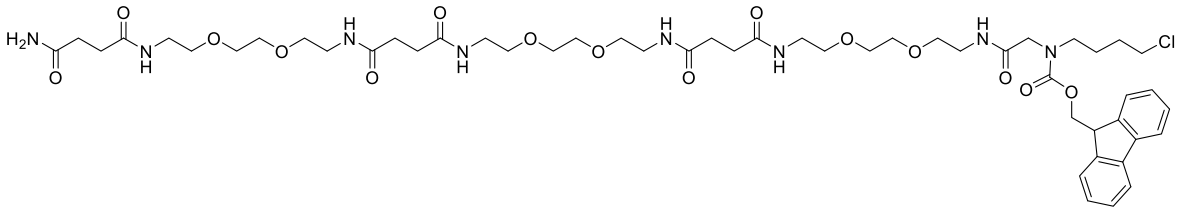

The oligomer EDS_3-PB was synthesised as described above. For the synthesis of the oligomer EDS_3-PB-Fmoc-Cl, 258.7 mg (1.00 mmol, 20 eq.) Fmoc-Cl were dissolved in 5 mL DMF and were added to the syringe with the EDS_3-PB oligomer (0.05 mmol). The reaction solution in the syringe was shaken for 2 h at RT. Coupling was performed again with the same conditions. The syringe was then washed 15 times with DMF followed by washing five times with DCM.

The reaction success was observed by macro cleavages (see section 5.3.2).

ESI-MS (m/z) for $C_{51}H_{77}ClN_8O_{15}$ (exact mass: 1076.52): $[M+H]^+$ calculated: 1077.52, found: 539.4; $[M+2H]^{2+}$ calculated: 539.26, found: 539.4. (See Figure 42)

RP-HPLC (Gradient 5-95 vol.-% - MeCN in H_2O containing 0.1 vol.-% formic acid, run time 30 min): t_R= 15.30 min. Determined purity 91.5 %. (See Figure 42)

Coupling of the oligomer GEPE-PB with Cbz-Cl

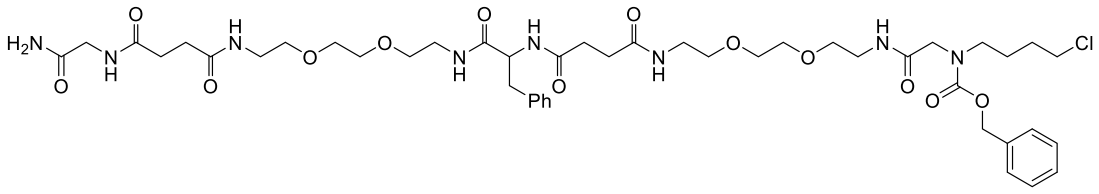

The oligomer GEPE-PB was synthesised as described above. For the synthesis of the oligomer GEPE-PB-Cbz-Cl, 170.6 mg (0.14 mL, 1.00 mmol, 20 eq.) Cbz-Cl were mixed with 5 mL DMF and were added to the syringe with the GEPE-PB oligomer (0.05 mmol). The reaction solution in the syringe was shaken for 2 h at RT. During the reaction, the syringe plunger was pulled out several times to ventilate the syringe. Coupling was performed again with the same conditions. The syringe was then washed 15 times with DMF followed by washing five times with DCM.

The reaction success was observed by macro cleavages (see section 5.3.2).

ESI-MS (m/z) for $C_{45}H_{67}ClN_8O_{13}$ (exact mass: 962.45): $[M+H]^+$ calculated: 963.45, found: 963.4; $[M+2H]^{2+}$ calculated: 482.23, found: 482.2. (See Figure 50)

RP-HPLC (Gradient 5-95 vol.-% - MeCN in H_2O containing 0.1 vol.-% formic acid, run time 30 min): t_R= 14.19 min. Determined purity 25.7 %. (See Figure 84)

Coupling of the oligomer EDS_3-PB with allyl chloroformate

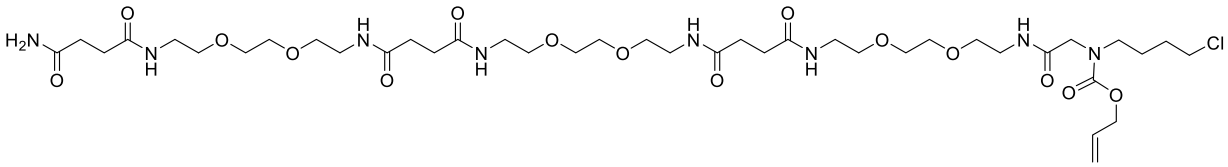

The oligomer EDS_3-PB was synthesised as described above. For the synthesis of the oligomer EDS_3-PB-Alloc-Cl, 120.5 mg (0.11 mL, 1.00 mmol, 20 eq.) Alloc-Cl were mixed with 5 mL DMF and were added to the syringe with the EDS_3-PB oligomer (0.05 mmol). The reaction solution in the syringe was shaken for 2 h at RT. During the reaction, the syringe plunger was pulled out several times to ventilate the syringe. Coupling was performed again with the same conditions. The syringe was then washed 15 times with DMF followed by washing five times with DCM.

The reaction success was observed by macro cleavages (see section 5.3.2).

ESI-MS (m/z) for $C_{40}H_{71}ClN_8O_{15}$ (exact mass: 938.47): $[M+H]^+$ calculated: 939.48, found: 939.4; $[M+2H]^{2+}$ calculated: 470.24, found: 470.2. (See Figure 43)

RP-HPLC (Gradient 5-95 vol.-% - MeCN in H_2O containing 0.1 vol.-% formic acid, run time 30 min): t_R= 10.78 min. Determined purity 34.3 %. (See Figure 43)

6. List of References

[1] S. C. Solleder, R. V. Schneider, K. S. Wetzel, A. C. Boukis, M. A. R. Meier, *Macromolecular rapid communications* **2017**, *38*.

[2] S. Martens, A. Landuyt, P. Espeel, B. Devreese, P. Dawyndt, F. Du Prez, *Nat Commun* **2018**, *9*.

[3] a) J. S. Mattick, *BioEssays: news and reviews in molecular, cellular and developmental biology* **2003**, *25*, 930; b) C. Bustamante, W. Cheng, Y. X. Mejia, Y. X. Meija, *Cell* **2011**, *144*, 480.

[4] S. A. Hill, C. Gerke, L. Hartmann, *Chemistry, an Asian journal* **2018**, *13*, 3611.

[5] a) J.-F. Lutz, M. Ouchi, D. R. Liu, M. Sawamoto, *Science (New York, N.Y.)* **2013**, *341*, 1238149; b) J.-F. Lutz, J.-M. Lehn, E. W. Meijer, K. Matyjaszewski, *Nat Rev Mater* **2016**, *1*, 2836.

[6] J.-F. Lutz (Ed.) *ACS symposium series*, *Vol. 1170*, American Chemical Soc, Washington, DC, **2014**.

[7] C. Gerke, M. F. Ebbesen, D. Jansen, S. Boden, T. Freichel, L. Hartmann, *Biomacromolecules* **2017**, *18*, 787.

[8] a) M. A. R. Meier, C. Barner-Kowollik, *Advanced Materials* **2019**, *31*, e1806027; b) P. Nanjan, M. Porel, *Polym. Chem.* **2019**, *10*, 5406; c) R. Aksakal, C. Mertens, M. Soete, N. Badi, F. Du Prez, *Advanced Science* **2021**, *8*, 2004038.

[9] R. B. Merrifield, *Journal of the American Chemical Society* **1963**, *85*, 2149.

[10] a) O. Kostov, R. Liboska, O. Páv, P. Novák, I. Rosenberg, *Molecules (Basel, Switzerland)* **2019**, *24*; b) C. Thorpe, S. Epple, B. Woods, A. H. El-Sagheer, T. Brown, *Organic & biomolecular chemistry* **2019**, *17*, 5341; c) D. Vlaho, M. J. Damha, *Current protocols in nucleic acid chemistry* **2018**, *73*, e53.

[11] D. Ponader, F. Wojcik, F. Beceren-Braun, J. Dernedde, L. Hartmann, *Biomacromolecules* **2012**, *13*, 1845.

[12] L. Hartmann, E. Krause, M. Antonietti, H. G. Börner, *Biomacromolecules* **2006**, *7*, 1239.

[13] T. Freichel, D. Laaf, M. Hoffmann, P. B. Konietzny, V. Heine, R. Wawrzinek, C. Rademacher, N. L. Snyder, L. Elling, L. Hartmann, *RSC Adv* **2019**, *9*, 23484.

[14] M. Hoffmann, N. L. Snyder, L. Hartmann, *Biomacromolecules* **2022**, *23*, 4004.

[15] a) G. S. Cremosnik, A. Hofer, H. J. Jessen, *Angewandte Chemie (International ed. in English)* **2014**, *53*, 286; b) P. H. Seeberger, *Chemical Society reviews* **2008**, *37*, 19; c) K. Naresh, F. Schumacher, H. S. Hahm, P. H. Seeberger, *Chemical communications (Cambridge, England)* **2017**, *53*, 9085; d) E. L. Elliott, C. R. Ray, S. Kraft, J. R. Atkins, J. S. Moore, *The Journal of organic chemistry* **2006**, *71*, 5282; e) S. Maechling, J. Good, S. D. Lindell, *Journal of combinatorial chemistry* **2010**, *12*, 818; f) J. Li, A. S. Grillo, M. D. Burke, *Accounts of chemical research* **2015**, *48*, 2297.

[16] M. Amblard, J.-A. Fehrentz, J. Martinez, G. Subra, *MB* **2006**, *33*, 239.

[17] F. Shamout, L. Fischer, N. L. Snyder, L. Hartmann, *Macromolecular rapid communications* **2020**, *41*, e1900473.

[18] J. W. Labadie, *Current Opinion in Chemical Biology* **1998**, *2*, 346.

[19] S. Mosca, F. Wojcik, L. Hartmann, *Macromolecular rapid communications* **2011**, *32*, 197.

[20] R. Quarrell, T. D. W. Claridge, G. W. Weaver, G. Lowe, *Mol Divers* **1996**, *1*, 223.

[21] D. Orain, J. Ellard, M. Bradley, *Journal of combinatorial chemistry* **2002**, *4*, 1.

[22] R. B. Merrifield, *Angew. Chem. Int. Ed. Engl.* **1985**, *24*, 799.

[23] *Standard Fmoc protocols*, **1997**.

[24] a) T. S. Burkoth, E. Beausoleil, S. Kaur, D. Tang, F. E. Cohen, R. N. Zuckermann, *Chemistry & Biology* **2002**, *9*, 647; b) D. Orain, J. Ellard, M. Bradley, *Journal of combinatorial chemistry* **2002**, *4*, 1.

[25] I. Clark-Lewis, L. E. Hood, S. B. Kent, *Proceedings of the National Academy of Sciences of the United States of America* **1988**, *85*, 7897.

[26] S. W. Pedersen, C. J. Armishaw, K. Strømgaard, *Methods in molecular biology (Clifton, N.J.)* **2013**, *1047*, 65.

[27] K. B. Jadhav, K. J. Woolcock, M. Muttenthaler, *Methods in molecular biology (Clifton, N.J.)* **2020**, *2103*, 41.

[28] S. Carganico, A. M. Papini in *Amino acids, peptides and proteins in organic chemistry* (Ed.: A. B. Hughes), Wiley-VCH, Weinheim, **2009-**, pp. 313–348.

[29] R. Behrendt, P. White, J. Offer, *Journal of peptide science: an official publication of the European Peptide Society* **2016**, *22*, 4.

[30] P. Gomez-Martinez, M. Dessolin, F. Guibé, F. Albericio, *J. Chem. Soc., Perkin Trans. 1* **1999**, 2871.

[31] F. Guibé, *Tetrahedron* **1998**, *54*, 2967.

[32] a) R. L. Prestidge, D. R. Harding, W. S. Hancock, *The Journal of organic chemistry* **1976**, *41*, 2579; b) J. P. Tam, W. F. Heath, R. B. Merrifield, *J. Am. Chem. Soc.* **1986**, *108*, 5242.

[33] R. J. Spears, C. McMahon, V. Chudasama, *Chemical Society reviews* **2021**, *50*, 11098.

[34] *The Synthesis of Oxytocin1*, **1954**.

[35] U. Ragnarsson, *Journal of peptide science: an official publication of the European Peptide Society* **2007**, *13*, 431.

[36] C. A. Montalbetti, V. Falque, *Tetrahedron* **2005**, *61*, 10827.

[37] D. S. Bose, A. V. Narsaiah, *Synthesis* **2001**, *2001*, 373.

[38] T. I. Al-Warhi, H. M. Al-Hazimi, A. El-Faham, *Journal of Saudi Chemical Society* **2012**, *16*, 97.

[39] L. Christensen, R. Fitzpatrick, B. Gildea, K. H. Petersen, H. F. Hansen, T. Koch, M. Egholm, O. Buchardt, P. E. Nielsen, J. Coull et al., *Journal of peptide science: an official publication of the European Peptide Society* **1995**, *1*, 175.

[40] C. U. Hjørringgaard, A. Brust, P. F. Alewood, *Journal of Peptide Science* **2012**, *18*, 199.

[41] F. Albeiicio, R. Chinchilla, D. J. Dodsworth, C. Nájera, *Organic Preparations and Procedures International* **2001**, *33*, 203.

[42] S. Roy, M. Caruthers, *Molecules (Basel, Switzerland)* **2013**, *18*, 14268.

[43] a) D. M. M. Jaradat, *Amino acids* **2018**, *50*, 39; b) E. Valeur, M. Bradley, *Chemical Society reviews* **2009**, *38*, 606.

[44] a) A. A. Joseph, A. Pardo-Vargas, P. H. Seeberger, *Journal of the American Chemical Society* **2020**, *142*, 8561; b) A. Pardo-Vargas, M. Delbianco, P. H. Seeberger, *Current opinion in chemical biology* **2018**, *46*, 48.

[45] F. Wojcik, A. G. O'Brien, S. Götze, P. H. Seeberger, L. Hartmann, *Chem. Eur. J.* **2013**, *19*, 3090.

[46] a) S. Boden, K. G. Wagner, M. Karg, L. Hartmann, *Polymers* **2017**, *9*; b) T. Freichel, V. Heine, D. Laaf, E. E. Mackintosh, S. Sarafova, L. Elling, N. L. Snyder, L. Hartmann, *Macromolecular bioscience* **2020**, *20*, e2000163; c) S. Igde, S. Röblitz, A. Müller, K. Kolbe, S. Boden, C. Fessele, T. K. Lindhorst, M. Weber, L. Hartmann, *Macromolecular bioscience* **2017**, *17*.

[47] M. Baier, M. Giesler, L. Hartmann, *Chem. Eur. J.* **2018**, *24*, 1619.

[48] T. Freichel, S. Eierhoff, N. L. Snyder, L. Hartmann, *The Journal of organic chemistry* **2017**, *82*, 9400.

[49] D. Ponader, S. Igde, M. Wehle, K. Märker, M. Santer, D. Bléger, L. Hartmann, *Beilstein journal of organic chemistry* **2014**, *10*, 1603.

[50] D. Ponader, Freie Universität Berlin, *Synthesis of Sequence-defined Glycooligomers for Studying Multivalent Interactions,* **2014**.

[51] B. Merrifield, *Methods in enzymology* **1997**, *289*, 3.

[52] R. N. Zuckermann, J. M. Kerr, S. B. H. Kent, W. H. Moos, *Journal of the American Chemical Society* **1992**, *114*, 10646.

[53] a) S. Volpi, A. Rozzi, N. Rivi, M. Neri, W. Knoll, R. Corradini, *Org. Lett.* **2021**, *23*, 902; b) D. Sabatino, C. Proulx, S. Klocek, C. B. Bourguet, D. Boeglin, H. Ong, W. D. Lubell, *Org. Lett.* **2009**, *11*, 3650.

[54] T. S. Burkoth, A. T. Fafarman, D. H. Charych, M. D. Connolly, R. N. Zuckermann, *Journal of the American Chemical Society* **2003**, *125*, 8841.

[55] R. N. Zuckermann, E. J. Martin, D. C. Spellmeyer, G. B. Stauber, K. R. Shoemaker, J. M. Kerr, G. M. Figliozzi, D. A. Goff, M. A. Siani, R. J. Simon, *Journal of medicinal chemistry* **1994**, *37*, 2678.

[56] J. E. Murphy, T. Uno, J. D. Hamer, F. E. Cohen, V. Dwarki, R. N. Zuckermann, *Proceedings of the National Academy of Sciences of the United States of America* **1998**, *95*, 1517.

[57] P. A. Wender, D. J. Mitchell, K. Pattabiraman, E. T. Pelkey, L. Steinman, J. B. Rothbard, *Proceedings of the National Academy of Sciences of the United States of America* **2000**, *97*, 13003.

[58] K. Kirshenbaum, A. E. Barron, R. A. Goldsmith, P. Armand, E. K. Bradley, K. T. Truong, K. A. Dill, F. E. Cohen, R. N. Zuckermann, *Proceedings of the National Academy of Sciences of the United States of America* **1998**, *95*, 4303.

[59] T. Horn, B.-C. Lee, K. A. Dill, R. N. Zuckermann, *Bioconjugate chemistry* **2004**, *15*, 428.

[60] T. T. Trinh, L. Oswald, D. Chan-Seng, J.-F. Lutz, *Macromol. Rapid Commun.* **2014**, *35*, 141.

[61] G. Fiers, D. Chouikhi, L. Oswald, A. Al Ouahabi, D. Chan-Seng, L. Charles, J.-F. Lutz, *Chem. Eur. J.* **2016**, *22*, 17945.

[62] U. S. Gunay, B. E. Petit, D. Karamessini, A. Al Ouahabi, J.-A. Amalian, C. Chendo, M. Bouquey, D. Gigmes, L. Charles, J.-F. Lutz, *Chem* **2016**, *1*, 114.

[63] L. Hartmann, H. G. Börner, *Advanced Materials* **2009**, *21*, 3425.

[64] T. T. Trinh, C. Laure, J.-F. Lutz, *Macromol. Chem. Phys.* **2015**, *216*, 1498.

[65] S. A. Hill, R. Steinfort, L. Hartmann, *Polym. Chem.* **2021**, *12*, 4439.

[66] R. A. Sheldon, *Chemical Society reviews* **2012**, *41*, 1437.

[67] B. Merrifield, *Science (New York, N.Y.)* **1986**, *232*, 341.

[68] S. A. Hill, R. Steinfort, S. Mücke, J. Reifenberger, T. Sengpiel, L. Hartmann, *Macromolecular rapid communications* **2021**, *42*, e2100193.

[69] D. van Lysebetten, S. Felissati, E. Antonatou, L. L. G. Carrette, P. Espeel, E. Focquet, F. E. Du Prez, A. Madder, *Chembiochem: a European journal of chemical biology* **2018**, *19*, 641.

[70] C. Mertens, R. Aksakal, N. Badi, F. E. Du Prez, *Polym. Chem.* **2021**, *12*, 4193.

[71] P. Espeel, F. Goethals, F. E. Du Prez, *Journal of the American Chemical Society* **2011**, *133*, 1678.

[72] P. Espeel, L. L. G. Carrette, K. Bury, S. Capenberghs, J. C. Martins, F. E. Du Prez, A. Madder, *Angewandte Chemie (International ed. in English)* **2013**, *52*, 13261.

[73] S. C. Solleder, S. Martens, P. Espeel, F. Du Prez, M. A. R. Meier, *Chem. Eur. J.* **2017**, *23*, 13906.

[74] H.-P. Buchstaller, *Journal of combinatorial chemistry* **2003**, *5*, 789.

[75] C. Le Hetet, M. David, F. Carreaux, B. Carboni, A. Sauleau, *Tetrahedron Letters* **1997**, *38*, 5153.

[76] a) D. J. Hall, H. M. van den Berghe, A. P. Dove, *Polym. Int.* **2011**, *60*, 1149; b) E. Dolci, V. Froidevaux, C. Joly-Duhamel, R. Auvergne, B. Boutevin, S. Caillol, *Polymer Reviews* **2016**, *56*, 512.

[77] A. D. Baldwin, K. L. Kiick, *Polym. Chem.* **2013**, *4*, 133.

[78] Q. Shi, Y. Zhang, Z. Huang, N. Zhou, Z. Zhang, X. Zhu, *Polym J* **2020**, *52*, 21.

[79] Z. Huang, J. Zhao, Z. Wang, F. Meng, K. Ding, X. Pan, N. Zhou, X. Li, Z. Zhang, X. Zhu, *Angew. Chem. Int. Ed. Engl.* **2017**, *56*, 13612.

[80] Z. Huang, Q. Shi, J. Guo, F. Meng, Y. Zhang, Y. Lu, Z. Qian, X. Li, N. Zhou, Z. Zhang et al., *Nat Commun* **2019**, *10*, 1918.

[81] Bruce C. Hamper, Daniel R. Dukesherer, Michael S. South, *Tetrahedron Letters*, *1996*, 3671.

[82] A. Nefzi, J. M. Ostresh, J.-P. Meyer, R. A. Houghten, *Tetrahedron Letters* **1997**, *38*, 931.

[83] A. Nefzi, M. A. Giulianotti, R. A. Houghten, *Journal of combinatorial chemistry* **2001**, *3*, 68.

[84] K. J. Lee, H.-S. Lim, *Org. Lett.* **2014**, *16*, 5710.

[85] I. Atodiresei, I. Schiffers, C. Bolm, *Chem. Rev.* **2007**, *107*, 5683.

[86] N. Salewska, M. J. Milewska, *J. Heterocyclic Chem.* **2014**, *51*, 999.

[87] L. Hartmann, S. Häfele, R. Peschka-Süss, M. Antonietti, H. G. Börner, *Chem. Eur. J.* **2008**, *14*, 2025.

[88] A. Sharma, A. El-Faham, B. G. de La Torre, F. Albericio, *Front. Chem.* **2018**, *6*, 516.

[89] D. Scharn, L. Germeroth, J. Schneider-Mergener, H. Wenschuh, *The Journal of organic chemistry* **2001**, *66*, 507.

[90] E. A. Arvanitis, N. Chadha, R. S. Pottorf, M. R. Player, *Journal of combinatorial chemistry* **2004**, *6*, 414.

[91] J. W. Grate, K.-F. Mo, M. D. Daily, *Angew. Chem.* **2016**, *128*, 3993.

[92] S.-H. Ahn, J. W. Grate, *The journal of physical chemistry. B* **2019**, *123*, 9364.

[93] W. Konrad, F. R. Bloesser, K. S. Wetzel, A. C. Boukis, M. A. R. Meier, C. Barner-Kowollik, *Chem. Eur. J.* **2018**, *24*, 3413.

[94] W. Yang, Q. Yin, C.-L. Chen, *Chem. Mater.* **2021**, *33*, 3047.

[95] a) P. Espeel, F. E. Du Prez, *Eur. Polym. J.* **2015**, 247; b) P. Espeel, F. Goethals, M. M. Stamenović, L. Petton, F. E. Du Prez, *Polym. Chem.* **2012**, *3*, 1007.

[96] a) Z. Huang, J. Zhao, Z. Wang, F. Meng, K. Ding, X. Pan, N. Zhou, X. Li, Z. Zhang, X. Zhu, *Angewandte Chemie (International ed. in English)* **2017**, *56*, 13612; b) Z. Huang, Q. Shi, J. Guo, F. Meng, Y. Zhang, Y. Lu, Z. Qian, X. Li, N. Zhou, Z. Zhang et al., *Nature communications* **2019**, *10*, 1918; c) Q. Shi, Y. Zhang, Z. Huang, N. Zhou, Z. Zhang, X. Zhu, *Polym J* **2020**, *52*, 21.

[97] a) J. C. Barnes, D. J. C. Ehrlich, A. X. Gao, F. A. Leibfarth, Y. Jiang, E. Zhou, T. F. Jamison, J. A. Johnson, *Nature Chem* **2015**, *7*, 810; b) Y. Jiang, M. R. Golder, H. V.-T. Nguyen, Y. Wang, M. Zhong, J. C. Barnes, D. J. C. Ehrlich, J. A. Johnson, *Journal of the American Chemical Society* **2016**, *138*, 9369; c) M. R. Golder, Y. Jiang, P. E. Teichen, H. V.-T. Nguyen, W. Wang, N. Milos, S. A. Freedman, A. P. Willard, J. A. Johnson, *Journal of the American Chemical Society* **2018**, *140*, 1596.

[98] L. Soria-Martinez, S. Bauer, M. Giesler, S. Schelhaas, J. Materlik, K. Janus, P. Pierzyna, M. Becker, N. L. Snyder, L. Hartmann et al., *Journal of the American Chemical Society* **2020**, *142*, 5252.

[99] H. Blattmann, M. Fleischer, M. Bähr, R. Mülhaupt, *Macromolecular rapid communications* **2014**, *35*, 1238.

[100] S. Weyand, H. Blattmann, V. Schimpf, R. Mülhaupt, R. Schwaiger, *Mater. Res. Express* **2016**, *3*, 75019.

[101] a) O. Figovsky, L. Shapovalov, A. Leykin, *ChChT* **2016**, *10*, 553; b) V. Besse, F. Camara, C. Voirin, R. Auvergne, S. Caillol, B. Boutevin, *Polym. Chem.* **2013**, *4*, 4545; c) H. Asemani, F. Zareanshahraki, V. Mannari, *J. Appl. Polym. Sci.* **2019**, *136*, 47266.

[102] M. Fleischer, H. Blattmann, R. Mülhaupt, *Green Chem* **2013**, *15*, 934.

[103] Ö. Capar, M. Tabatabai, J. E. Klee, M. Worm, L. Hartmann, H. Ritter, *Polym. Chem.* **2020**, *11*, 6964.

[104] a) N. Qvit, S. J. S. Rubin, T. J. Urban, D. Mochly-Rosen, E. R. Gross, *Drug discovery today* **2017**, *22*, 454; b) S. Koutsopoulos (Ed.) *Woodhead publishing series in biomaterials*, Woodhead Publishing, Duxford, **2018**; c) J. Sun, Z. Li in *Woodhead publishing series in biomaterials* (Ed.: S. Koutsopoulos), Woodhead Publishing, Duxford, **2018**, pp. 183–213; d) B. Zhang, M. Li, M. Lin, X. Yang, J. Sun, *Biomaterials science* **2020**, *8*, 6969; e) A. R. Statz, R. J. Meagher, A. E. Barron, P. B. Messersmith, *Journal of the American Chemical Society* **2005**, *127*, 7972; f) L. Zhu, J. M. Simpson, X. Xu, H. He, D. Zhang, L. Yin, *ACS applied materials & interfaces* **2017**, *9*, 23476.

[105] H. Tomita, F. Sanda, T. Endo, *J. Polym. Sci. A Polym. Chem.* **2001**, *39*, 162.

[106] Steinfort, R., Hill, S., Capar, Ö., Hartmann, L., *Paperdraft*, Heinrich-Heine-Universität, Düsseldorf, **2023**.

[107] S. van Mileghem, W. M. de Borggraeve, I. R. Baxendale, *Chem. Eng. Technol.* **2018**, *41*, 2014.

[108] M. O. Sonnati, S. Amigoni, E. P. Taffin de Givenchy, T. Darmanin, O. Choulet, F. Guittard, *Green Chem* **2013**, *15*, 283.

[109] J. Liu, Y. Li, H. Liu, D. He, *Biomass and Bioenergy* **2018**, *118*, 74.

[110] S. Sahani, S. N. Upadhyay, Y. C. Sharma, *Ind. Eng. Chem. Res.* **2021**, *60*, 67.

[111] Heimo Wölfle, Burkhard Walther, Sophie Putzien, WO2014118268A1.

[112] M. Eh, *Synthesis* **2003**, *2003*, 365.

[113] Alan Gene Olivero, Jonathan Martin Cassel, James Robert Poulsen, **1993**.

[114] J. Rousseau, C. Rousseau, B. Lynikaite˙, A. Šačkus, C. de Leon, P. Rollin, A. Tatibouët, *Tetrahedron* **2009**, *65*, 8571.

[115] F. Mende, M. Beisswenger, O. Seitz, *Journal of the American Chemical Society* **2010**, *132*, 11110.

[116] E. J. Goethals, B. Dervaux in *Polymer science*. *A comprehensive reference; 10 volume-set* (Eds.: K. Matyjaszewski, M. Möller), Elsevier Science, Amsterdam [u.a.], **2012**, pp. 309–330.

[117] Y. Kim, J. Heo, D. Kim, S. Chang, S. Seo, *Nat Commun* **2020**, *11*, 4761.

[118] J. S. Smith, J. M. Scholtz, *Biochemistry* **1998**, *37*, 33.

[119] a) F. Loffler, Y.-C. Cheng, T. Fortsch, E. Dorsam, R. Bischoff, F. Breitling, A. Nesterov-Muller, *Biotechnol. Biopolym*, *2011*; b) J. F. Im Klotz, *Hydrogen bonds between model peptide groups in solution*, Journal of the American Chemical Society, **1962**.

[120] S.-Y. Sheu, D.-Y. Yang, H. L. Selzle, E. W. Schlag, *Proceedings of the National Academy of Sciences of the United States of America* **2003**, *100*, 12683.

[121] K. M. Eckes, K. Baek, L. J. Suggs, *ACS omega* **2018**, *3*, 1635.

[122] L. Vitagliano, R. Berisio, A. Mastrangelo, L. Mazzarella, A. Zagari, *Protein science: a publication of the Protein Society* **2001**, *10*, 2627.

[123] R. N. Zuckermann, *Biopolymers* **2011**, *96*, 545.

[124] S. A. Fowler, H. E. Blackwell, *Organic & biomolecular chemistry* **2009**, *7*, 1508.

[125] M. Vargas-Sanchez, S. Lakhdar, F. Couty, G. Evano, *Organic letters* **2006**, *8*, 5501.

[126] C. Yu, M. A. Shoaib, N. Iqbal, J. S. Kim, H.-J. Ha, E. J. Cho, *The Journal of organic chemistry* **2017**, *82*, 6615.

[127] M. Y. H. Lai, M. A. Brimble, D. J. Callis, P. W. R. Harris, M. S. Levi, F. Sieg, *Bioorganic & medicinal chemistry* **2005**, *13*, 533.

[128] Nathalie Bolten, *Bachelorarbeit*, Heinrich-Heine-Universität, Düsseldorf, **2022**.

[129] J. A. W. Kruijtzer, L. J. F. Hofmeyer, W. Heerma, C. Versluis, R. M. J. Liskamp, *Chem. Eur. J.* **1998**, *4*, 1570.

[130] I. Coin, R. Dölling, E. Krause, M. Bienert, M. Beyermann, C. D. Sferdean, L. A. Carpino, *The Journal of organic chemistry* **2006**, *71*, 6171.

[131] L. Fischer, A. K. Strzelczyk, N. Wedler, C. Kropf, S. Schmidt, L. Hartmann, *Chemical science* **2020**, *11*, 9919.

[132] a) H. D. Pickford, J. Nugent, B. Owen, J. J. Mousseau, R. C. Smith, E. A. Anderson, *Journal of the American Chemical Society* **2021**, *143*, 9729; b) X. Cui, F. Shi, Y. Zhang, Y. Deng, *Tetrahedron Letters* **2010**, *51*, 2048.

[133] F. Albericio, J. Tulla-Puche in *The power of functional resins in organic synthesis* (Ed.: J. Tulla-Puche), Wiley, Hoboken, N.J., **2009**, pp. 1–14.

[134] J. Nishimura, S. Inokuma, K. Kimura, T. Funaki, *HETEROCYCLES* **2001**, *54*, 123.

[135] M. A. Levina, V. G. Krasheninnikov, M. V. Zabalov, R. P. Tiger, *Polym. Sci. Ser. B* **2014**, *56*, 139.

7. Acknowledgements

First of all, I would like to thank my supervisor Prof. Dr. Laura Hartmann for giving me the opportunity to do my PhD thesis in her research group. During my work I always had the opportunity to contact her with questions, problems, or successes and to receive valuable ideas and suggestions from her. I am very grateful to her for the trusting relationship and her motivating manner. She stood behind me in the good and the bad times and I am very happy to have made the decision to do my PhD thesis in her working group.

I would also like to thank Prof. Dr. Thomas J. J. Müller for agreeing to be my co-supervisor and mentor during this dissertation.

Also, I would like to express my sincere gratitude to Dr. Monir Tabatabai. Not only was she always approachable and able to help with problems, but she also created a climate in which I felt very comfortable through her caring manner. Thank you for always being a contact person for both professional and personal issues.

I would also like to thank Michaela Kitza and Stephanie Scheelen for all the organizational work they did and for always helping when there was a problem.

Thanks also go to PD Dr. Klaus Schaper, Maria Beuer and Mohanad Aian for measuring my NMR spectra. Furthermore, I thank Dr. Peter Tommes for the HR-MS and MALDI-TOF-MS measurements.

A big thank you also goes to the students I supervised during this work, Sandra Mücke, Josefine Reifenberger, Nathalie Bolten and Jolana Both. You all contributed to the success of this work, and I thank you for the good and trustful cooperation.

I would also like to especially thank Dr. Stephen Hill with whom I worked in different parts of this thesis. I was able to learn a lot from him and at the same time had lots of funny and interesting chats.

In general, I would like to thank the entire working group for the friendly and positive atmosphere that made it possible to work without any problems. Over the years I have been able to work with many of them and learn a lot from them. “Sozialraum-Partys”, laser ball

sessions, game nights, Christmas and summer parties we were able to have a lot of fun together even outside of the work context!

A very special thank you to my lab partners Dr. Stephen Hill, Alisa Kayser, Lennart Hofer, Nicole Hugo and Theresa Seiler. Thank you for the trustful cooperation, your tips, the many professional discussions, and the things I could learn from you. Last but not least, the many occasions when we chatted and laughed together. I would also like to thank Miriam Hoffmann my office and temporarily laboratory colleague for the always funny and friendly conversations. Lennart Hofer, thank you for all your helpful ideas and the many enjoyable hours in the lab.

Simon Walber and Nicholas Jäck we will forever remain Team Rosini. Thank you very much for the many conversations and your open and friendly manner, which made my daily lab routine so much sweeter.

I would also like to thank my friends outside the university who have supported me throughout this work.

Finally, I would like to thank my family. Without your continuous support this work would not have been possible. I would especially like to thank my brother, Michael Steinfort, for the many conversations on evenings after the lab, where you listened to me for hours, built me up and motivated me. To my mother, Gabriele Steinfort, and my father, Dr. Frank Steinfort, I thank you for the countless phone calls, your visits and your constant support throughout the whole time of my doctoral thesis. Thank you also for always trying to understand what was bothering me in the lab, for keeping your fingers crossed for my experiments and that I was always able to rely on you 100 %.

8. Appendix

8.1 List of Tables

8.2 List of Figures

8.3 List of Abbreviations

AB	Aziridine Bromoacetic acid
ABP	Aziridine Bromopropionic acid
Alloc	allyloxy carbonyl
BCC	butyl biscyclocarbonate
Boc	tert-butyloxycarbonyl
d	doublet
DBU	1,8-Diazabicyclo[5.4.0]undec-7-ene
DCM	dichloromethane
DIPEA	*N*-diisopropylethylamine
DMF	*N,N*,dimethylformamide
DMSO	dimethylsulfoxide
DMSO-d_6	deuterated dimethyl sulfoxide
DNA	deoxyribonucleic acid
D_2O	deuterium oxide
EDS	succinylated 2,2'-(ethylenedi-oxy)bis(ethylamine)
e. g.	exempli gratia (for example
Eq	equivalent
ESI	electrospray ionization
ESI-MS	electrospray ionization mass spectrometry
et al.	et alii (and others)
Fmoc	fluorenyl methoxycarbonyl
GCBr	Glycerol Carbonate Bromoacetic acid
GCEA	Glycerol Carbonate Ethylene Amine
GCI	Glycerol Carbonate Sodium Iodide
GCT	Glycerol Carbonate Tosyl chloride
Gly	Glycine
HMD	hexamethylendiamine
HPLC	high-performance liquid chromatography
Hz	hertz
LiOTf	lithium trifluoromethanesulfonate

m	multiplet
mAU	milli absorption units
m/z	mass-to-charge ratio
NMP	*N*-methyl-2-pyrrolidone
NMR	Nuclear magnetic resonance
PB	Pyrrolidine Bromoacetic acid
PBP	Pyrrolidine Bromopropionic acid
pent	pentet
Phe	Phenylalanine
ppm	parts per million
PyBOP	benzotriazol-1-yloxytripyrrolidinophosphonium hexafluorophosphate
q	quartet
quin	quintet
R_f	retention factor
RP-HPLC	reverse phase high-performance liquid chromatography
RT	room temperature
s	singlet
t	triplet
TBAB	tetrabutylammonium bromide
TBAI	tetrabutylammonium iodide
TBD	1,5,7-Triazabicyclo[4.4.0]dec-5-en
TDS	Triple bond − Diethylenetriamine − Succinic acid
TEA	triethylamine
THF	Tetrahydrofuran
TFA	trifluoroacetic acid
TIPS	triisopropylsilane
t_R	retention time
UV-Vis	ultraviolet and visible spectroscopy
Vol.-%	volume percent

8.3 Analytics

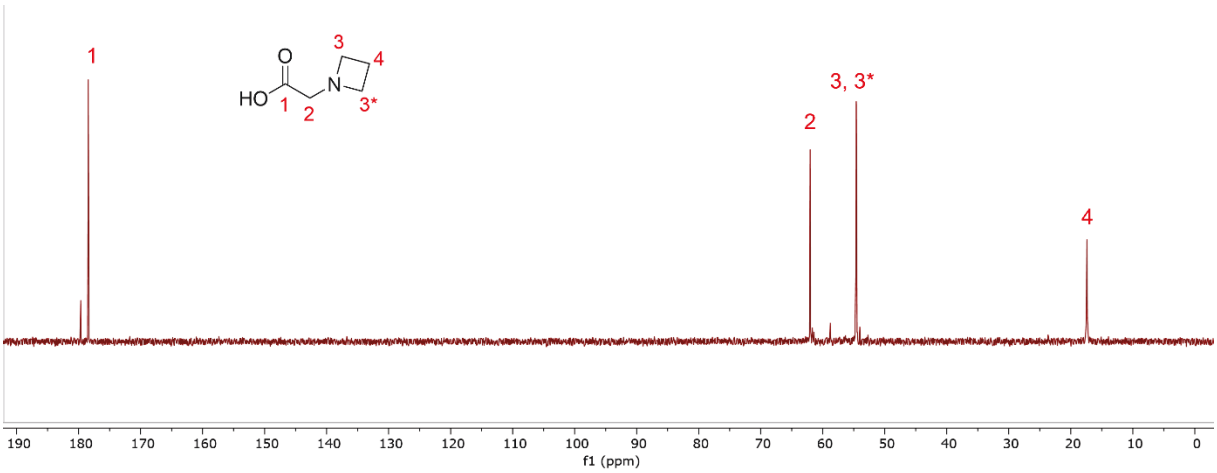

Figure 70: 75 MHz ^{13}C-NMR of the AB building block in D_2O.[128]

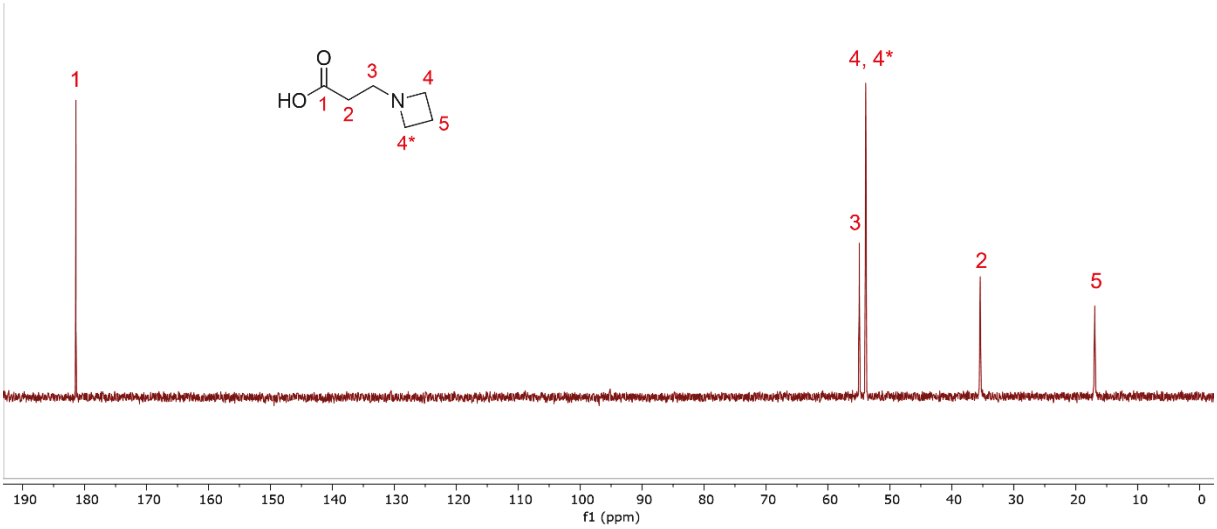

Figure 71: 75 MHz ^{13}C-NMR of the ABP building block in D_2O.[128]

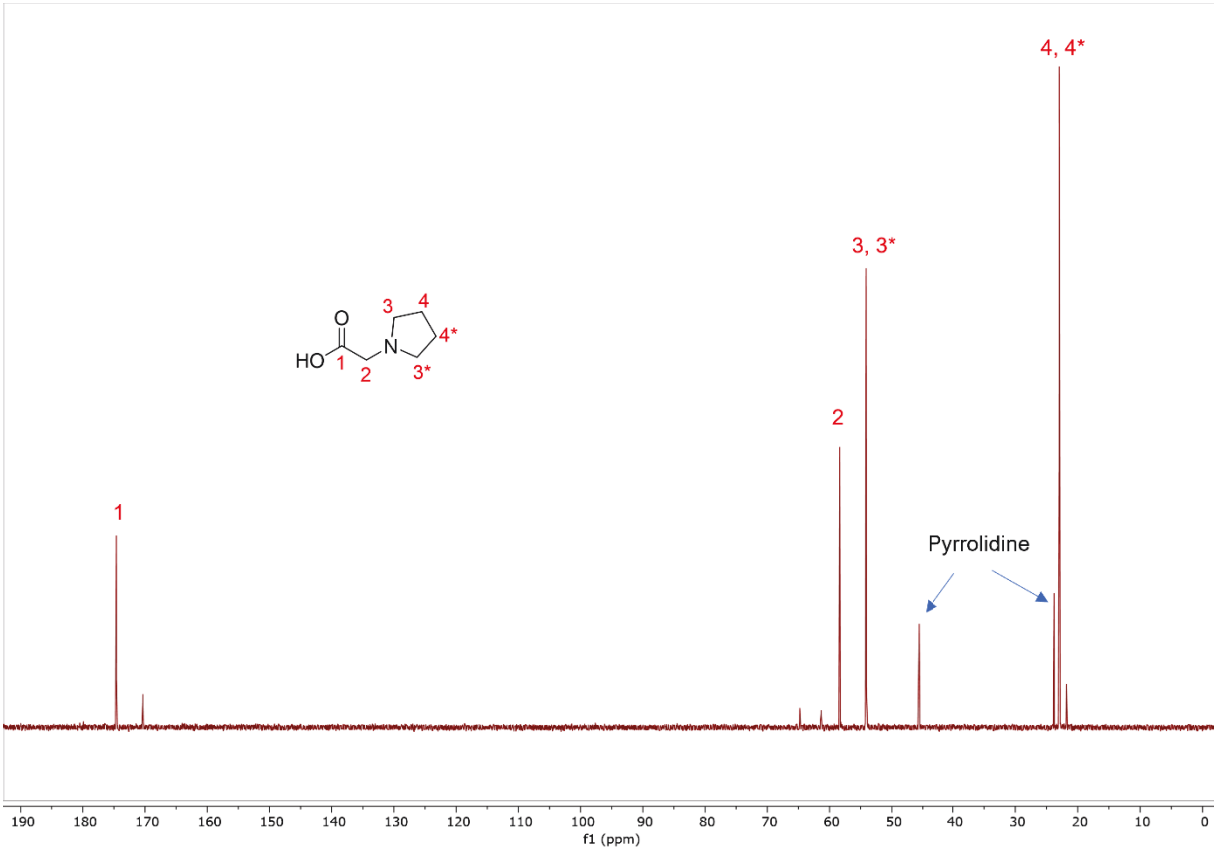

Figure 72: 150 MHz ^{13}C-NMR of the PB building block in D_2O.[128]

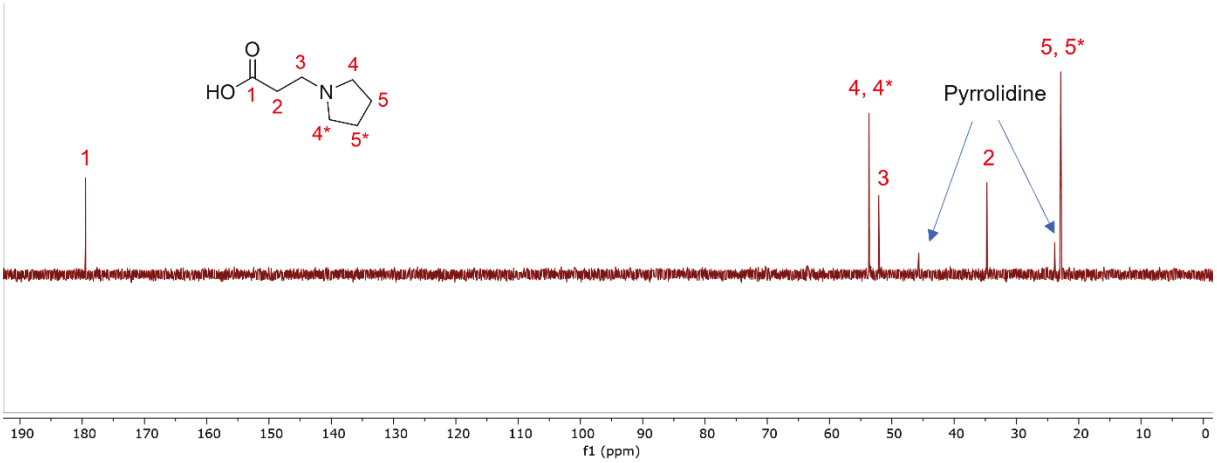

Figure 73: 150 MHz ^{13}C-NMR of the PBP building block in D_2O.[128]

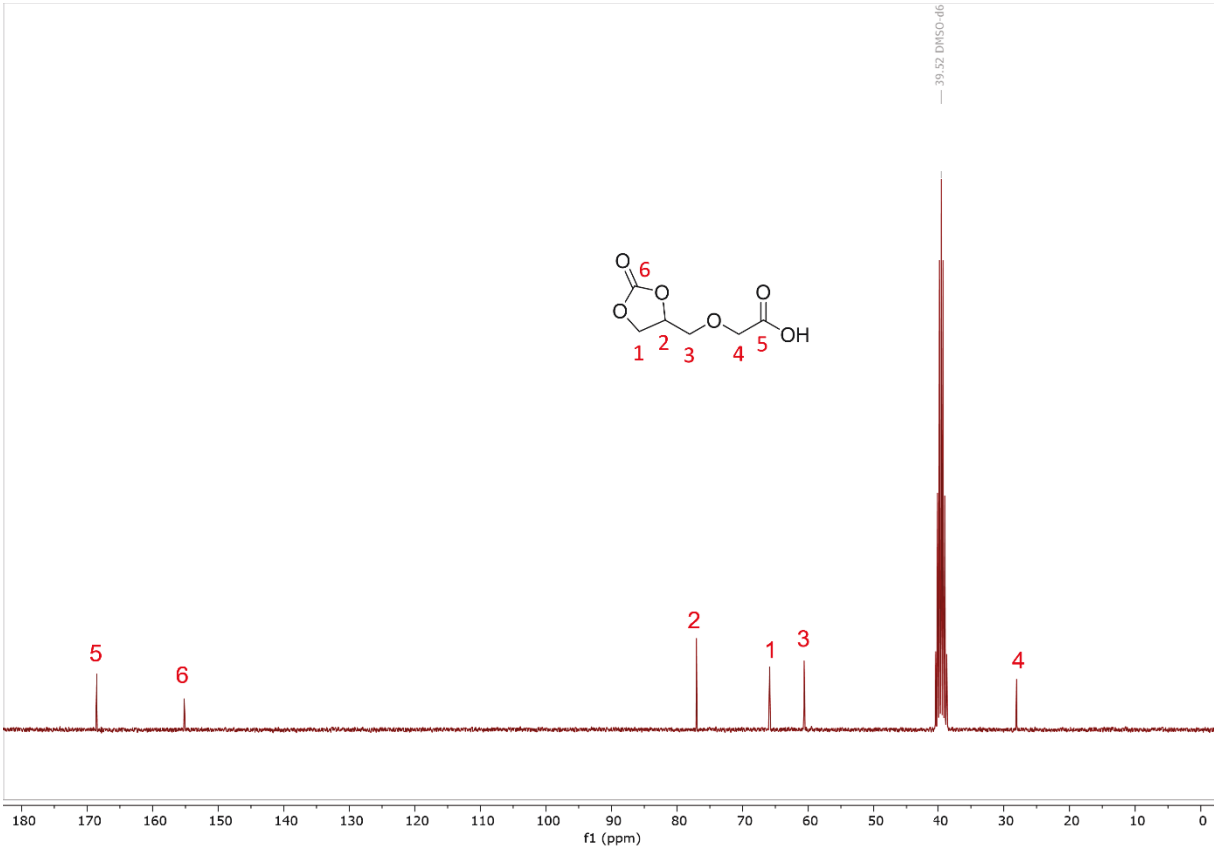

Figure 74: 75 MHz ^{13}C-NMR of the GCBr building block in DMSO-d_6.

Mass Spectrum SmartFormula Report

Analysis Info

Analysis Name	D:\Data\Spektren 2021\HAR21HR000026.d	Acquisition Date	1/28/2021 4:05:12 PM
Method	tune_low_new.m	Operator	Peter Tommes
Sample Name	Steinfort RS_GC_Final in CH3CN/H2O (CH3OH)	Instrument	maXis 288882.20213
Comment			

Acquisition Parameter

Source Type	ESI	Ion Polarity	Positive	Set Nebulizer	0.3 Bar
Focus	Not active	Set Capillary	4000 V	Set Dry Heater	180 °C
Scan Begin	50 m/z	Set End Plate Offset	-500 V	Set Dry Gas	4.0 l/min
Scan End	1500 m/z	Set Collision Cell RF	600.0 Vpp	Set Divert Valve	Source

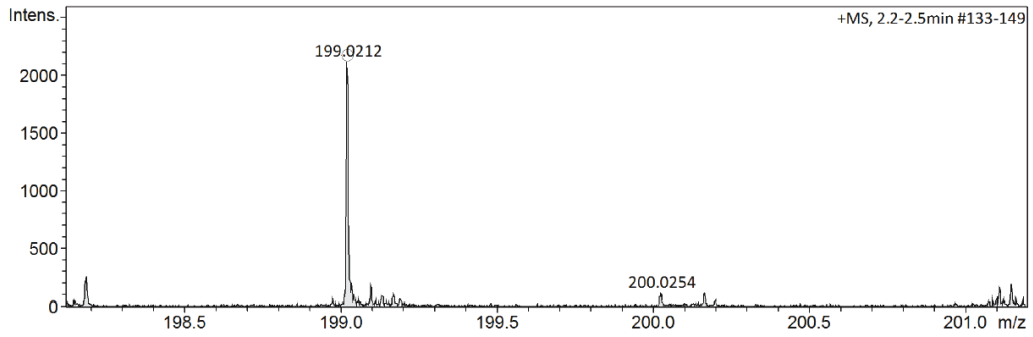

Meas. m/z	#	Ion Formula	m/z	err [ppm]	mSigma	# mSigma	Score	rdb	e⁻ Conf	N-Rule
199.0212	1	C6H8NaO6	199.0213	0.6	11.0	1	100.00	2.5	even	ok

Figure 75: HR-ESI of the GCBr building block.

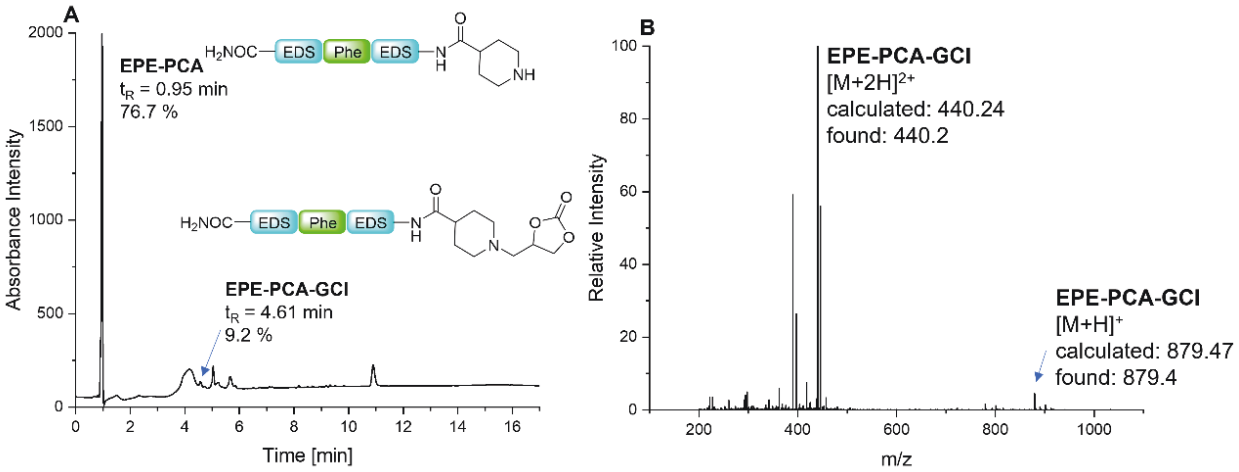

Figure 76: A: RP-HPLC chromatogram (Gradient 5-95 vol.-% - MeCN in H_2O (0.1 vol.-% formic acid, run time 17 min) of the oligomer EPE-PCA-GCI. B: HPLC-ESI-MS of EPE-PCA-GCI at t = 4.61 min (gradient of 5 to 95 vol.-% acetonitrile in water containing 0.1 vol.-% formic acid, run time 17 min).

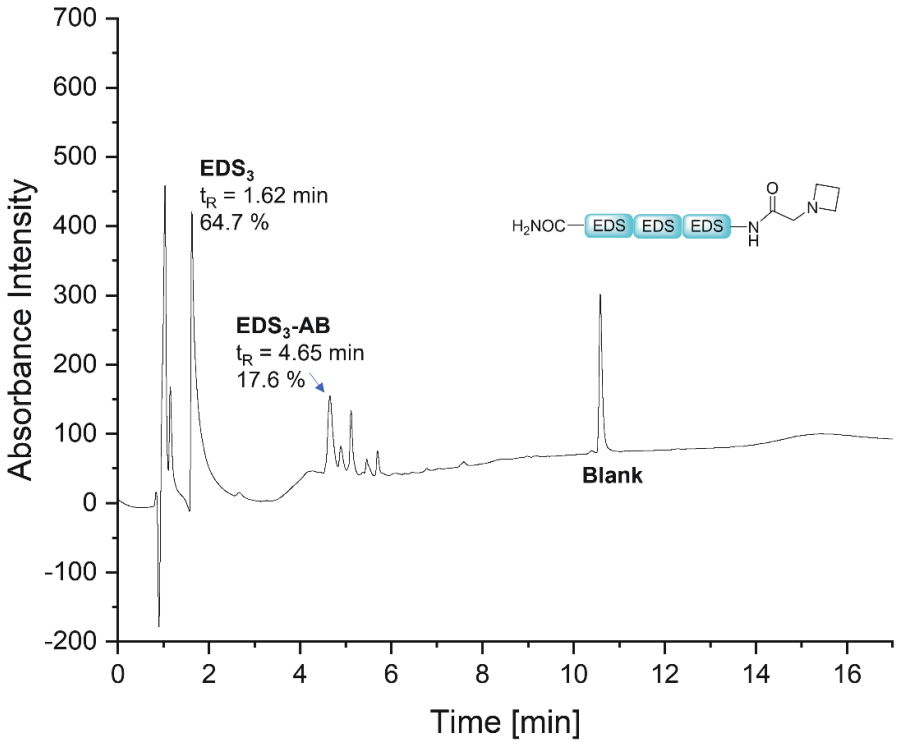

Figure 77: RP-HPLC chromatogram (Gradient 5-95 vol.-% - MeCN in H_2O (0.1 vol.-% formic acid, run time 17 min) of EDS_3-AB.

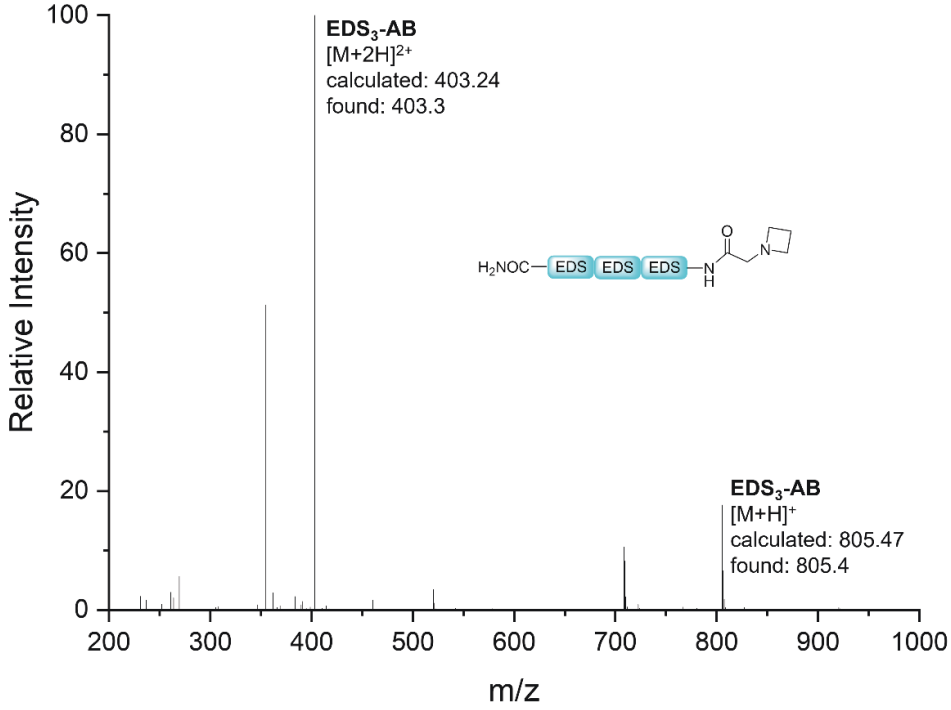

Figure 78: HPLC-ESI-MS of EDS_3-AB at t = 4.65 min (gradient of 5 to 95 vol.-% acetonitrile in water containing 0.1 vol.-% formic acid, run time 17 min) which corresponds to the RP-HPLC spectrum in Figure 77.

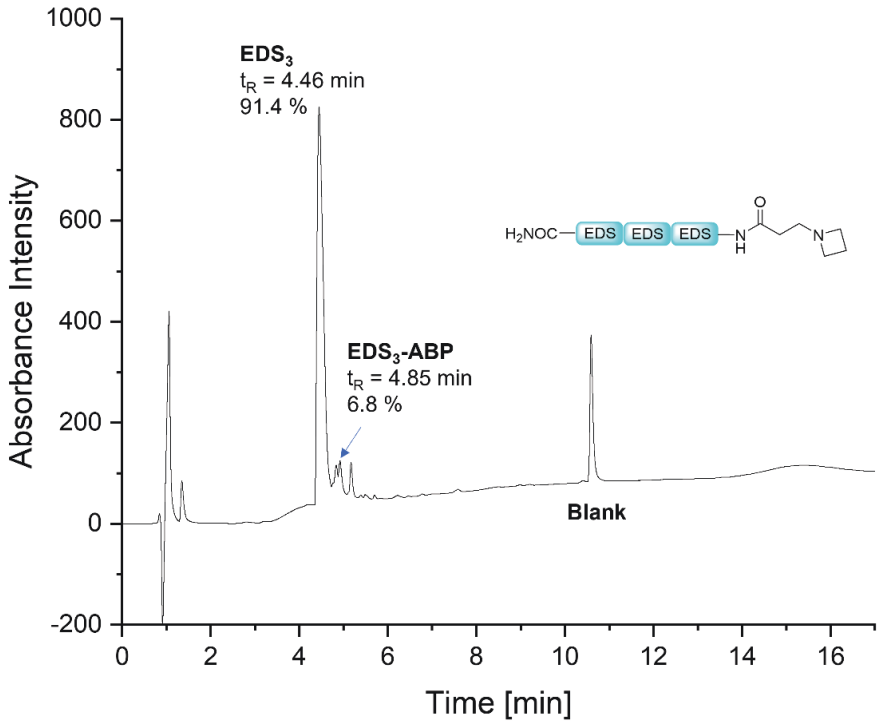

Figure 79: RP-HPLC chromatogram (Gradient 5-95 vol.-% - MeCN in H_2O (0.1 vol.-% formic acid, run time 17 min) of EDS_3-ABP.

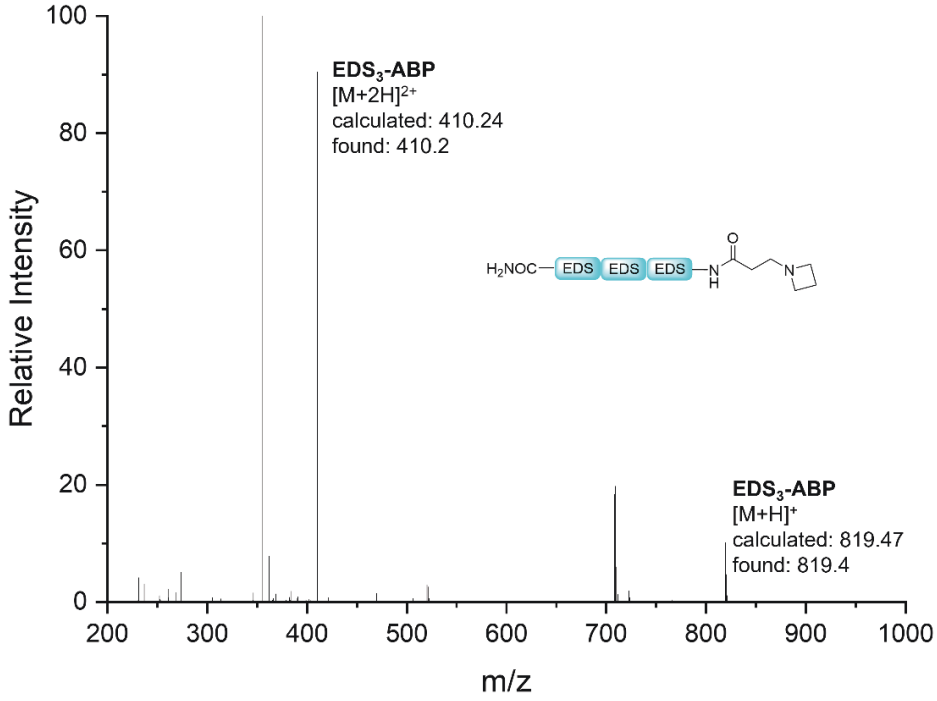

Figure 80: HPLC-ESI-MS of EDS_3-ABP at t = 4.85 min (gradient of 5 to 95 vol.-% acetonitrile in water containing 0.1 vol.-% formic acid, run time 17 min) which corresponds to the RP-HPLC spectrum in Figure 79.

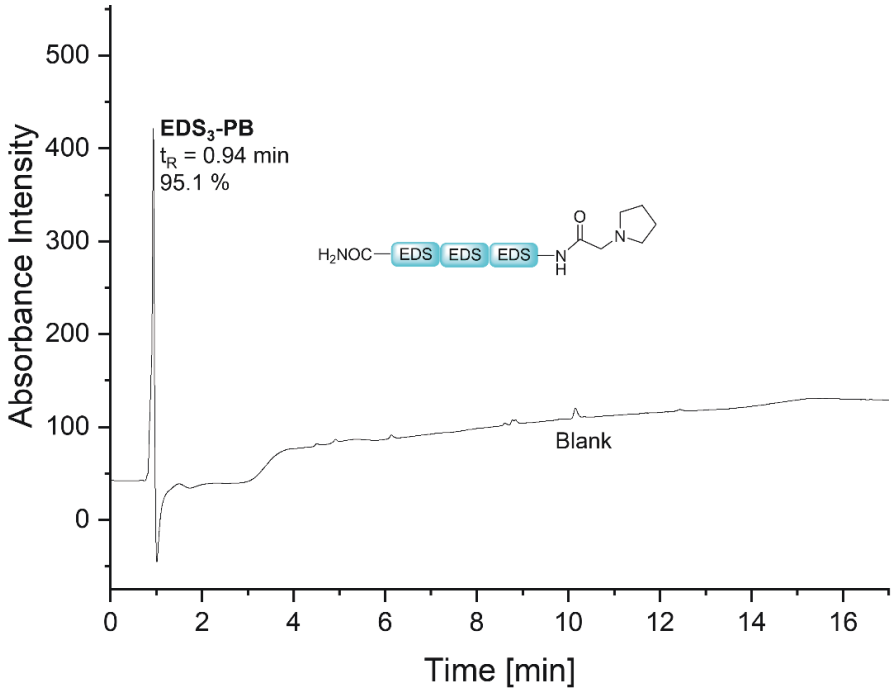

Figure 81: RP-HPLC chromatogram (Gradient 5-95 vol.-% - MeCN in H_2O (0.1 vol.-% formic acid, run time 17 min) of EDS_3-PB.

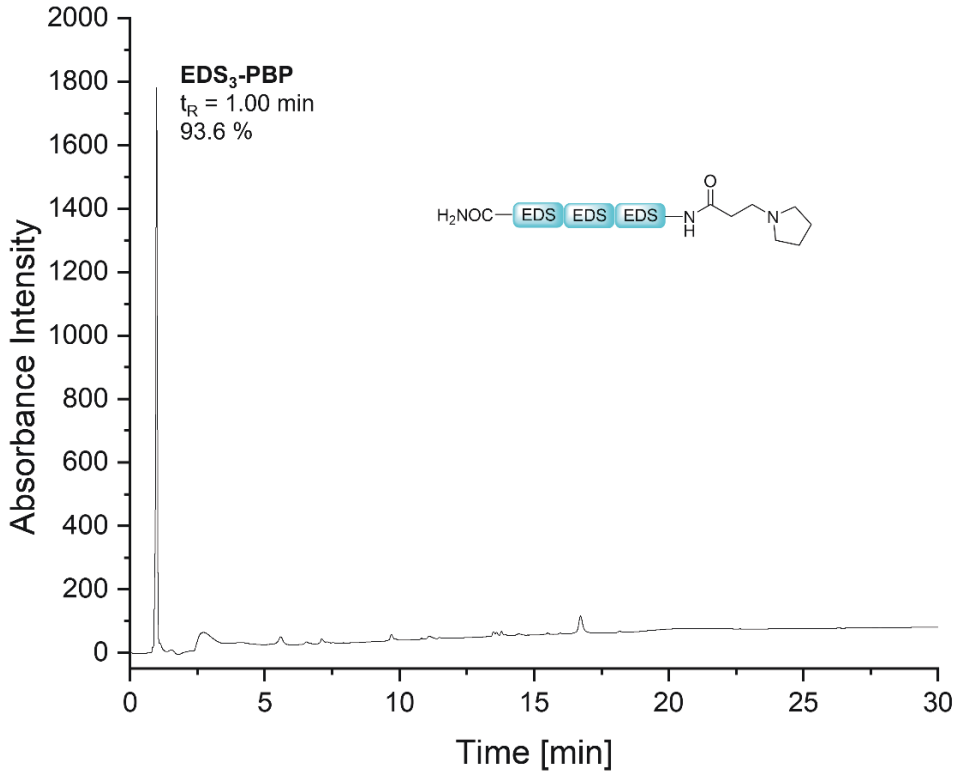

Figure 82: RP-HPLC chromatogram (Gradient 5-95 vol.-% - MeCN in H_2O (0.1 vol.-% formic acid, run time 30 min) of EDS_3-PBP.

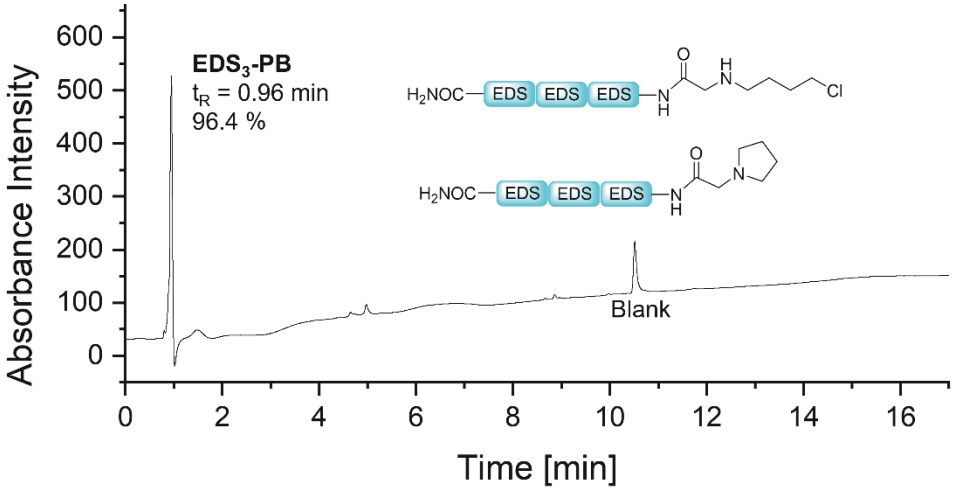

Figure 83: RP-HPLC chromatogram (Gradient 5-95 vol.-% - MeCN in H_2O (0.1 vol.-% formic acid, run time 17 min) of the oligomer EDS_3-PB-Fmoc-Cl after deprotection.

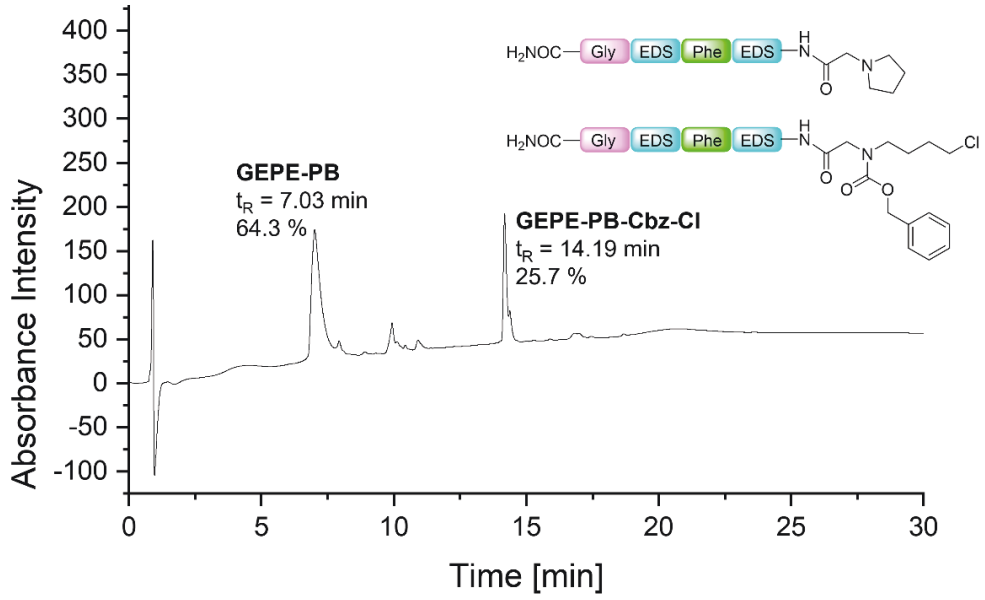

Figure 84: RP-HPLC chromatogram (Gradient 5-95 vol.-% - MeCN in H_2O (0.1 vol.-% formic acid, run time 17 min) of GEPE-PB-Cbz-Cl.